

Hedgehog-Interacting Protein (Hhip)

as a candidate Foxn1 target in the thymus

Chen Xiangzhen Hannah

Jesus College

University of Oxford

A thesis submitted for the degree of DPhil in Paediatrics

Abstract

The thymus is a primary lymphoid organ that supports the development of functional T cells through its unique stromal architecture. The most important and abundant component of this microenvironment are thymic epithelial cells, or TECs. TEC development, function and maintenance are critically dependent on the expression of the master transcription factor Foxn1. The Hedgehog-Interacting Protein (Hhip) was identified as a novel candidate target of Foxn1-mediated gene expression. Hhip is an inhibitor of Hedgehog (Hh) signalling, an embryonic developmental pathway which is also vital for normal T cell development.

I first provided evidence that Foxn1 indirectly modulated the Hh signalling pathway via *hhip*. To identify a role for Hhip in thymus biology, I investigated the consequences of a constitutive deficiency for *hhip* expression in embryonic and neonatal mice, and demonstrated that loss of *hhip* resulted in an upregulation of Hh signalling via the coreceptors Gas1 and Boc, affecting the relative frequencies of cortical and medullary TECs in a dose-dependent manner and favouring medullary TEC development. I also generated a novel transgenic mouse model with a targeted loss of *hhip* in Foxn1-expressing cells, to specifically delineate the role of Hhip in TECs. This approach additionally circumvented the limitation of neonatal lethality in constitutive *hhip*-deficient mice. TEC-targeted loss of *hhip* expression not only impacted TEC sublineage decisions, but also affected the ability of TECs to perform positive thymocyte selection, resulting in the generation of T cells with reduced TCR signal strength which were less responsive to mitogenic stimuli. In aggregate, the experimental data here presents the first evidence that Hhip plays an important role in regulating TEC differentiation and function.

Acknowledgements

I would like to extend my sincere gratitude to my supervisor, Prof Georg Holländer. His kindness, wisdom and inspiration have been invaluable, and I will always be grateful for his unwavering support. Many thanks also go to Dr Andy Bassett, for his infinite Crispr knowledge and unlimited patience.

It takes a village – and so I would like to acknowledge the past and present members of the Holländer group for all the coffee and chocolate, but in particular Mary, Stefano and Wei, just for being all-round stellar human beings. In addition, the work in this thesis would not have been possible without the generosity and expertise of a great number of people, including but not limited to Tiago Luis, Rain Lau, Kathrin Jansen and the BMS staff.

Finally, to my father, for whom no words will do justice. To my mother, too, who I know is watching from above.

Table of Contents

Abstract ---------- i
Acknowledgements ---------- ii
Table of Contents ---------- iii

1: Introduction ---------- 1
1.1 Immune system 1
1.1.1 Innate immunity 1
1.1.2 Adaptive immunity 2
1.2 Thymus 5
1.2.1 T cell development 6
1.2.2 TEC development 10
1.3 Foxn1 13
1.3.1 Known molecular mechanisms upstream and downstream of Foxn1 15
1.3.2 Foxn1 transcriptional regulation in TECs 17
1.4 Hedgehog signalling 18
1.4.1 Hh signalling mechanism 19
1.4.2 Hh signalling in the thymus 22
1.4.3 Hhip 24
1.5 Hypothesis and aims 26
2: Materials and Methods ---------- 27
2.1 Mice 27
2.1.1 C57BL/6 27
2.1.2 B6.SJL.CD45.1 27
2.1.3 $Hhip^{tm1Amc/J}$ 28
2.1.4 $Foxn1^{Cre}$ 28
2.1.5 $Hhip^{lox/lox}$ 28
2.1.6 GBS-GFP 29
2.1.7 Timed matings 29
2.2 General reagents 30
2.3 Genotyping 31
2.3.1 Isolation and amplification of genomic DNA 31
2.3.2 Agarose gel electrophoresis 32
2.4 Molecular biology 33
2.4.1 RNA extraction and cDNA synthesis 33
2.4.2 qPCR 34
2.4.3 CRISPR/Cas9 synthetic guide RNA (sgRNA) design and cloning 34
2.5 Microbiology 37
2.5.1 Preparation of competent DH5α cells 37
2.5.2 Cell transformation 37
2.5.3 Plasmid preparation 37
2.6 *In vitro* experiments 38
2.6.1 Cell lines preparation 38
2.6.2 Experimental transfection 38
2.6.3 Fetal Thymic Organ Culture (FTOC) 39
2.6.4 Stimulation assay 40
2.7 Organ preparation and cell isolation 40
2.7.1 TEC isolation 40
2.7.2 T cell isolation 41
2.7.3 Haematopoietic progenitor isolation 41

2.8 Transplantation studies 41
2.8.1 Fetal liver transplant 41
2.8.2 Thymus transplant 42
2.9 Flow cytometry 43
2.9.1 Antibody staining 43
2.9.2 FACS analysis and sorting 44
2.10 Imaging 45
2.10.1 Sample processing 45
2.10.2 Cytospin preparation 46
2.10.3 Haematoxylin and Eosin (H&E) staining 46
2.10.4 Immunohistochemistry 46
2.10.5 Microscopy 47
2.11 Generation of Hhip$^{lox/lox}$ 47
2.11.1 Transfection for generation of mouse model 47
2.11.2 Screening 48
2.11.3 Preparation of ES cells for blastocyst injection 48
2.11.4 Breeding 49
2.11.5 Transgenic mouse generation 49
2.12 Pseudo-bulk sequencing 50
2.13 Statistical analysis 50
3: Identification of *Hhip* as a Novel Foxn1 Target in TECs ---------- 52
3.1 Preliminary evidence positioning *hhip* downstream of Foxn1 52
3.2 Hh signalling genes are expressed by both TECs and T cells 54
3.3 Confirmation of *hhip* as a direct Foxn1 binding target 57
4: Shh signalling mediated by Hhip is relevant in cTECs and forms a feedback loop with Foxn1 ---------- 59
4.1 Modulating Hh signalling affects thymocyte development at E18.5 within 4 days 59
4.1.1 Increased Shh signalling causes delayed maturation of single positive CD4 T cells 62
4.1.2 Addition of rHhip at E18.5 is insufficient to alter thymocyte development 64
4.1.3 Blocking of Shh binding by 5E1 does not affect thymocyte development and appears functionally distinct from rHhip 67
4.1.4 Inhibiting Hh signalling downstream using selective Gli inhibitors severely affects normal thymocyte maturation 68
4.2 Hhip regulates TEC differentiation and MHC-II expression 74
4.3 rHhip and rShh modulate Hh signalling as expected by Gli transcription 77
4.4 Preventing Foxn1 from binding to *hhip* regulatory sequences decreases *hhip* transcription and alters Hh signalling 83
4.4.1 Overexpression of Foxn1 does not upregulate *hhip* 84
4.5 rShh causes upregulation of *foxn1* 87
5: Constitutive Loss of *Hhip* Affects Thymus Development and Function - 91
5.1 Genetic loss of *hhip* affects TEC development and MHC-II expression 91
5.1.1 Addition of rHhip at E18.5 is sufficient to rescue a *hhip*-deficiency 93
5.1.2 Reduced *hhip* expression results in persistent changes in TEC development 95
5.1.3 Hhip-mediated Hh signalling changes are modulated by Gas1 and Boc 99
5.1.4 Loss of *hhip* impairs gene expression 102
5.2 Complete loss of *hhip* affects early T cell development 108
5.2.1 T cell defect in neonates is transient and is not sustained after FTOC culture 115
5.2.2 *Hhip* heterozygosity does not affect adult thymopoiesis 118
5.3 *Hhip*-deficiency in TECs accounts for changes in cTEC/mTEC ratios 119

5.4 Hhip-/- TECs can support development of healthy progenitors but not in the same manner as a WT thymus 123
5.5 *Hhip*-deficient thymocytes migrate to the periphery 135
5.6 Hhip-/- thymocytes have intrinsic altered expression of markers 138
5.6.1 Increased TCRβ expression is sustained in peripheral Hhip-/- T cells 150
5.6.2 Crosstalk from Hhip-/- thymocytes does not affect integrity of postnatal WT TECs 152
5.7 A *hhip*-deficiency does not affect the lymphoid committed precursor 153
6: A Mouse Model Exhibiting TEC-Targeted Loss of *Hhip* ---------- 159
6.1 Overall gene targeting strategy 159
6.1.1 sgRNA design 160
6.1.2 Homology construct 162
6.1.3 Transfection 163
6.1.4 Screening 164
6.2 *In vitro* Cre transfection 166
6.3 Chimeras 168
6.4 $Hhip^{lox/lox}$ 171
6.4.1 The TEC compartment in $Hhip^{lox/lox}$ mice is not distinguishable from WT 171
6.4.2 Thymocyte development in $Hhip^{lox/lox}$ mice is comparable to WT 173
6.4.3 Peripheral T cell compartment of $Hhip^{lox/lox}$ mice is comparable to WT 175
6.5 $Foxn1^{Cre+/-}Hhip^{flox/flox}$ 177
6.5.1 TEC differentiation in $Hhip^{flox/flox}$ mice is altered 178
6.5.2 Normal thymocyte frequencies are observed in $Hhip^{flox/flox}$ mice 181
6.5.3 Thymocyte selection in $Hhip^{flox/flox}$ mice is non-lineage specific 184
6.5.4 $Hhip^{flox/flox}$ negative selection allows T cells with lower TCR signal strength to survive 191
6.6 Neonatal $Hhip^{flox/flox}$ TECs display normal MHC expression 195
6.6.1 Neonatal $Hhip^{flox/flox}$ thymocytes are phenotypically less mature 197
6.7 Fewer $Hhip^{flox/flox}$ T cells exit the thymus, but in normal proportions 202
6.7.1 $Hhip^{flox/flox}$ CD4 naïve cells are less responsive to T cell stimulation 203
7: Discussion ---------- 207

References ---------- 218
Supplementary ---------- 255

1: Introduction

1.1 Immune system

The immune system is the body's defense mechanism that protects against infection and disease. It comprises an elaborate network of cells, tissues and organs that are collectively able to recognise and react against foreign pathogens, mounting an appropriate response to eliminate these harmful factors. The immune system can be broadly differentiated into two categories, innate or adaptive immunity, based on speed and specificity of response.

1.1.1 Innate immunity

The innate immune system provides an initial rapid line of defence against infection. This includes mechanical barriers such as the body's surfaces, which are designed to prevent pathogens from entering the body. If a microbe manages to bypass this physical barrier, contact with the epithelial surface triggers a cellular response via production of factors such as chemokines and cytokines, resulting in signalling cascades to recruit circulating white blood cells like phagocytes (encompassing macrophages, neutrophils, dendritic cells) and natural killer (NK) cells (Akira, S. *et al.*, 2006). These cells possess pattern recognition receptors (PRRs) on their cell surface, which can recognise and interact with pathogen-associated molecular patterns (PAMPs), conserved structures unique to certain groups of microbes. Binding of these cognate ligands to PRRs activates the immune cells to engulf and destroy the invaders immediately (Akira, S. & Takeda, K., 2004). Alongside, the complement system is also activated, consisting of plasma proteins circulating in the blood that collectively comprise the classical, alternative, and lectin pathways. The classical complement pathway is initiated by a

molecule known as C1q, which binds directly to pathogen surfaces and antibody-antigen complexes, while the lectin pathway is initiated by binding of a protein known as the mannan-binding lectin to bacteria and viruses (Whaley, K. & Schwaeble, W., 1997; Peterson, S. *et al*., 2001). Binding leads to an activation cascade, resulting in the generation of a protease called the C3 convertase. Concurrently, the alternative pathway can also be activated by spontaneous hydrolysis of C3 (Müller-Eberhard, H. & Schreiber, R., 1980). Downstream activity of the C3 convertase subsequently marks pathogens for destruction, stimulates and recruits phagocytes, as well as catalyses the assembly of the membrane attack complex on the cell membrane of pathogens, causing membrane lysis and cell death to eliminate the harmful organisms (Rus, H. *et al*., 2005; Shin, M. *et al*., 1996; Podack, E., 1984).

The different processes of the innate immune system are extremely effective but are not specific to a particular pathogen. The innate immune system therefore curbs the spread of most common microorganisms, often within mere hours. However, this system is not infallible, and it is thus complemented by adaptive immunity, a slower but highly sophisticated system present only in vertebrates.

1.1.2 Adaptive immunity

In contrast to the innate immune system, adaptive immunity differs by its utilisation of a concept known as immunological memory, where the body remembers initial encounters with a pathogen and is subsequently able to initiate an enhanced and highly specific response upon repeat encounters. The adaptive immune response is primarily mediated by a subset of white blood cells known as lymphocytes, of which the two major classes are thymus-derived (T) and bursa-derived (B) cells. As

a population, T cells express billions of unique T cell receptors (TCRs) on their cell surface that each individually distinguishes a specific sequence and structure, and are thus collectively capable of recognising a huge array of protein sequences (Davis, M. & Bjorkman, P., 1988; Pasqual, N. *et al*., 2002). Mature T cells can be further differentiated based on their typically mutually exclusive cell surface expression of either the CD4 or CD8 glycoproteins, where CD4 and CD8 T cells perform different immunological functions. The protein peptides that T cells recognise, termed antigens, are presented on cell surfaces in the context of major histocompatibility complex (MHC) molecules (Ploegh, H. *et al*., 1981). All nucleated cells express MHC class I (MHC-I) molecules, which are recognised by CD8 T cells. Specialised cells including professional antigen-presenting cells (APCs) also express MHC class II (MHC-II), recognised primarily by CD4 T cells (Gay, D. *et al*., 1987; Butz, E. & Bevan, M., 1998). MHC-I molecules generally present antigens generated by the degradation of cytosolic proteins, while MHC-II molecules present peptides derived from extracellular proteins (Rock, K. *et al*., 1994; Santambrogio, L. *et al*., 1999). Upon infection, if a pathogen carrying an MHC-I presented antigen comes into contact with a CD8 T cell bearing a receptor specific for that antigen, binding of the receptor to the antigen triggers the clonal expansion of that particular CD8 T lymphocyte population. These CD8 cells then become activated and acquire effector functions that allow them to effectively eliminate pathogens. These include indirect mechanisms such as the production of cytotoxins and cytokines to recruit macrophages and trigger the caspase cascade, initiating programmed cell death (Medema, J. *et al*., 1997; Gurlo, T. & von Grafenstein, J., 2003). CD8 T cells may also directly initiate the apoptosis pathway by expression of Fas ligand, which binds to the cell death surface receptor Fas on invading cells (Kagi, D. *et al*., 1994), or secrete the lethal pore-forming molecule Perforin as well as granzymes to stimulate

target cell death (Peters, P. *et al.*, 1991). This is a hallmark of cellular adaptive immunity, where expansion of the T cell population specific to the pathogen in question initiates a widespread immune response.

Like T cells, B cells also express unique and clonally specific antigen receptors (BCRs). BCRs are membrane-bound antibodies that allow specific antigen recognition in the absence of MHC molecules. Binding of an antigen to the corresponding BCR causes internalisation of the complex, where the antigen is processed into peptides and re-presented on the surface by MHC-II molecules (pMHC-II) (Lanzavecchia, A., 1985). These pMHC-II complexes are recognised by antigen-specific CD4 helper T (T_H) cells, which in turn activate these B cells to clonally expand and stimulate further production of antibodies (Owens, T. *et al.*, 1997; Smith, K. *et al.*, 2000). The antibodies bind specifically to the pathogen, preventing them from attacking host cells and marking them for clearance by phagocytes in a process known as opsonisation (Hutchinson, I. & Zola, H., 1978), as well as activating the complement cascade to trigger cell death (Rossbacher, J. & Shlomchik, M., 2003). B cells thus coordinate the humoral adaptive immune response, as antibodies can diffuse via the circulatory system to extracellular fluids, complementing the T cell-mediated cellular response.

The effectiveness of the immune system relies on its ability to selectively harness the mechanisms provided by B cells and CD8 T cells, mounting the most suitable response appropriate for the specific type of infectious agent. This is largely mediated by CD4 T cells, which differentiate and acquire specific roles depending on the nature of the pathogenic response and its environment. For example, the response to intracellular bacteria creates a pro-inflammatory environment with high

levels of the cytokines interleukin-12 (IL12) and interferon-γ (IFN-γ). These mediators cause naïve CD4 cells to differentiate into T helper 1 (T_{H1}) cells able to further secrete IFN-γ, which in turn activates CD8 T cells and macrophages (Trinchieri, G. *et al.*, 2003; Bach, E. *et al.*, 1995). In contrast, when attacked by extracellular pathogens or during an allergic reaction, high levels of interleukin-4 (IL4) and interleukin-2 (IL2) are secreted by activated T cells, in particular T helper 2 (T_{H2}) cells, and this induces further T_{H2} differentiation (Kopf, M. *et al.,* 1993; Cote-Sierra, J. *et al.*, 2004; Seder, R. *et al.*, 1994). In response, B cells are activated, secreting antigen-specific antibodies that among other effector mechanisms can also stimulate mast cells to initiate what is known as an allergic response (Le Gros, G. *et al.*, 1990; Noelle, R. *et al.*, 1984). Other subsets of CD4 cells can also be generated depending on the cytokine environment, such as follicular helper (T_{FH}), T helper 17 (T_{H17}) or induced regulatory T cells (iT_{reg}), which induce various distinct downstream processes, further dictating the specificity of the immune response.

T cells play a central role in ensuring the overall homeostasis and efficacy of the immune system. A sophisticated system is thus required to ensure that T cells develop correctly, retaining the dangerous ability to effectively attack foreign pathogens without accidentally attacking an individual's own cells. This important system exists in the form of the thymus, a specialised immune organ vital for successful development and bespoke selection of T cells.

1.2 Thymus

The thymus is a primary lymphoid organ critically responsible in vertebrates for the generation of a functionally competent population of T cells. This unique lymphopoietic capacity is enabled by its stromal components, comprising an array

of different cell types of which thymic epithelial cells (TECs) are of primary functional importance (Lobach, D. & Haynes, B., 1987). TECs form a three-dimensional cellular network constituting the thymic epithelial microenvironment and can be categorised into two distinct sublineages, cortical (cTEC) and medullary (mTEC). As indicated by their names, cTECs and mTECs segregate into physically discrete compartments, and possess unique structural, antigenic and functional characteristics. Specifically, these compartments serve as discrete functional regions conducive for the individual steps of thymocyte maturation. cTECs primarily occupy the outer aspects of the thymus, including a subcapsular zone. mTECs reside in the inner regions forming a separate compartment, the medulla. The area at the interphase of the cortex and medulla is termed the cortico-medullary junction (CMJ), facilitating the entry of blood-borne thymocyte progenitors and controlling the emigration of mature lymphocytes (Lind, E. *et al*., 2001; Mori, K. *et al*., 2007; Pearse, G., 2006). Crosstalk between TECs and developing T cells, or thymocytes, is indispensible for the normal maturation and selection of thymocytes into functionally competent T cells (de la Hera, A. *et al*., 1989).

1.2.1 T cell development

Haematopoietic precursors from the bone marrow begin as pluripotent stem cells capable of generating different blood cell lineages. Of this population, a subset becomes committed lymphoid-primed multipotent progenitors (LMPPs) that give rise to the lymphoid T and B lineages (Kondo, M. *et al*., 1997; Adolfsson, J. *et al*., 2005). Immature T cell precursors deriving from LMPPs enter the developed thymus via blood vessels located in the CMJ. This process is facilitated by a subset of thymic endothelial cells that express P-selectin, allowing the interaction with P-selectin glycoprotein ligand 1 (PSGL-1) expressed on these haematopoietic

progenitors, initiating an adhesion cascade (Lind, E. *et al.*, 2001, Rossi, F. *et al.*, 2005). At this stage, the progenitors do not yet express the characteristic T cell surface markers CD4 and CD8, and are therefore termed “double-negative” (DN). The expression of additional cell surface markers such as CD44, CD25 and CD117 (c-Kit) identifies progressive maturational stages in the murine model, each with a unique developmental potential. Immature DN stage 1 (DN1) thymocyte precursors ($CD44^+CD25^-$) move from the CMJ towards the subcapsular zone and are exposed to Delta-like ligand 4 (Dll4) expressed on cTECs. Engagement of Dll4 with the Notch ligand expressed on thymocytes activates downstream signals responsible for the cells’ commitment to a T cell fate, inducing the process of T cell receptor (TCR) rearrangement, consisting of α, β, γ and δ loci. This is mediated by the lymphoid cell-specific recombination-activating genes Rag1 and Rag2 (Oettinger, M. *et al.*, 1990; Godfrey, D. *et al.*, 1994). An inframe rearrangement of the TCRβ locus leads to cell differentiation and assembly of the pre-TCR complex, where the TCRβ subunit associates with the pre-TCRα chain (Zamisch, M. *et al.*, 2005; Kishi, H. *et al.*, 1991). Gain of CD25 expression marks the transition to the DN2 phenotype ($CD44^+CD25^+$) that is followed by a loss of CD44 expression, designated DN3 ($CD44^-CD25^+$), a stage that is fully committed to the T cell lineage (von Boehmer, H. & Fehling, H., 1997). Successful pre-TCR signalling initiates TCRα rearrangement and allows DN3 cells to progress via the DN4 ($CD44^-CD25^-$) stage to a phenotype marked by the concomitant expression of CD4 and CD8, called “double-positive” (DP) (Mallick, C. *et al.*, 1993; Irving, B. *et al.*, 1998) Pre-TCR signalling occurs cell-autonomously by self-oligomerisation, which signifies the completion of TCRβ chain gene rearrangement, and is essential for T cell development (von Boehmer, H. *et al.*, 1999; Yamasaki, S. *et al.*, 2006). In some mouse strains, a transition population of $CD4^-CD8^+$ cells can be found between the

DN stages and DP phenotype, called immature CD8 (iCD8) cells (Hugo, P. *et al.*, 1990). TCRβ expression initiates rearrangement of the TCRα chain requiring again the activity of both Rag genes, and fully commits cells to an αβ T lineage. In the absence of a correctly assembled pre-TCR, apoptosis results (von Boehmer, H. *et al.*, 1999). Alternatively, progenitors which do not express the pre-TCR complex correctly do not initiate TCRα rearrangement and may instead rearrange their TCR γ and δ loci, moving to the periphery as γδ T cells without progressing to the DP stage (Prinz, I. *et al.*, 2006; Ciofani, M. & Zúñiga-Pflücker, J., 2010).

Once the TCRα chain is successfully rearranged, it pairs with the existing TCRβ chain and these are expressed together initially at low levels on DP cells as the TCR complex (Goldrath, A. & Bevan, M., 1999). cTECs enforce the process of positive selection which requires the presentation of self-peptides bound to major histocompatibility complexes (pMHC). αβ TCR^+ DP thymocytes need to bind either pMHC-II or pMHC-I complexes with a minimum level of affinity to receive appropriate survival signals to further their differentiation into $CD4^+CD8^-$ or $CD4^-CD8^+$ cells respectively, known as “single-positive” (SP) thymocytes. Cells that fail to engage with any pMHC with appropriate affinity lack these survival signals and consequently undergo apoptosis as a consequence of “T cell neglect” (Bendelac, A. *et al.*, 1992; Brändle, D. *et al.*, 1994; Goldrath, A. *et al.*, 1999).

The small proportion of thymocytes that survive the TCR-based selection in the cortex downregulate their CD4 and CD8 expression slightly, giving rise to an intermediate $CD4^+CD8^{low}$ population, regardless of their lineage specification (Brugnera, E. *et al.*, 2000). Concurrently after TCR engagement, they upregulate the expression of the chemokine receptor Ccr7 and become responsive to the

ligands Ccl19 and Ccl21, which are produced by mTECs and attract thymocytes to migrate to the medulla (Ueno, T. *et al*., 2004). mTECs express a broad repertoire of self-peptides, in part due to the capacity of a subpopulation of these cells that express the autoimmune regulator Aire (Anderson, M. *et al*., 2002). This transcriptional facilitator allows the promiscuous expression of tissue restricted antigens. Collectively, the population of mTECs represents an almost complete molecular repertoire of each individual's antigenic individuality (Derbinski, J. *et al*., 2001; Sansom, S. *et al*., 2014). mTECs also instruct thymocytes with moderate TCR affinities to adopt a regulatory T cell (T_{reg}) fate, establishing them as effectors of a dominant form of T cell tolerance (Lin, J. *et al*., 2016). However, SP thymocytes are eliminated by a mechanism referred to as negative selection should they display high affinity TCRs for any self antigens presented by mTECs and thus have the potential to be autoreactive (Sant'Angelo, D. & Janeway, C., 2002). A significant first wave of negative selection also occurs in the cortex, where a large fraction of cells are eliminated (McCaughtry, T. *et al*., 2008; Hu, D. *et al*., 2015; Stritesky, G. *et al*., 2013). This cortical negative selection is facilitated at least in part by dendritic cells in the cortex (McCaughtry, T. *et al*., 2008). SP cells that survive both positive and negative selection, thus expressing a suitable TCR affinity will complete their differentiation program (Daniels, M. *et al*., 2006; Mckeithan, T, 1995). The maturation of SP thymocytes can be followed by the markers CD62L, CD69, CD24 and Qa2, where newly generated SP cells are usually $CD62L^{low}CD69^{hi}CD24^{hi}Qa2^{low}$, while mature cells are $CD62L^{hi}CD69^{low}CD24^{low}Qa2^{hi}$ (Takahama, Y. *et al*., 2006). After approximately 10-12 days in the medulla, mature SP T cells exit to the periphery to become effector T cells (T_{eff}) (Egerton, M. *et al*., 1990). This phenomenon of sequential positive and negative selection thus

produces a functionally competent T cell repertoire tolerant to self antigens yet reactive against foreign antigens.

1.2.2 TEC development

TECs are essential for the generation of functional T cells, and are tightly regulated by a variety of molecules and signalling pathways, as well as by reciprocal interactions with thymocytes. The thymus and parathyroid develop during embryogenesis in mice from the third pharyngeal pouch, and in humans from both the third and fourth pharyngeal pouches, which are transient embryonic structures. In the murine model, during embryonic development, the Sonic Hedgehog (Shh) and Bone Morphogenic Protein (BMP) signalling pathways regulate embryonic patterning and modulate the formation of the third pharyngeal pouch (Bleul, C. & Boehm, T., 2005; Bain, V. *et al*., 2016; Moore-Scott, B. & Manley, N., 2005). At around embryonic day (E) 9, preliminary organ patterning genes such as *hoxa3* (Manley, N., & Capecchi, M., 1995), *pax1* (Wallin J. *et al*., 1996), *pax9* (Peters, H. *et al*., 1998), *eya1*, *six1/4* (Zou D. *et al*., 2006) and *tbx1* (Jerome, L., & Papaioannou, V., 2001) regulate the initial outgrowth of the thymic epithelial anlage. Here, immature bipotent TEC progenitors which express the epithelial marker Plet-1 early in development arise from the endoderm into the thymic region (Depreter, M. *et al*., 2008; Rossi, S. *et al*., 2006). Following, the transcription factor Foxn1 is expressed in these cells around E11.25, and marks the region of the prospective thymus, while the parathyroid region is designated by Gcm2 (Gordon, J. *et al*., 2001). Foxn1 is the first marker that demonstrates commitment to the TEC fate (reviewed in Holländer, G. *et al*., 2006). The thymus and parathyroid glands then begin to descend separately by E12.5, forming anatomically individual organs.

At this time, Foxn1 also begins to direct the differentiation of the immature progenitors into functional epithelia which eventually attain either a cortical or medullary phenotype, often characterised by expression of the cell surface marker Ly51 or reactivity to the ulex europaeus agglutinin I (UEA-1) lectin respectively. Expression of the keratins (K) 8 or 5 can also be used to distinguish cTECs and mTECs (Nowell, C. *et al*., 2011). While cTECs and mTECs can be demarcated as early as E13.5, the thymic epithelial microenvironment is composed during murine embryogenesis mostly by cTECs. The proportion of mTECs begins to increase substantially from around E17.5 and reaches its peak around 4 weeks of age (Gray, D. *et al*., 2006; van Vliet. *et al*., 1985). Expression of MHC-II is acquired by TECs at the embryonic stage, allowing them to perform their functions as APCs. At the embryonic stage, all TECs are MHC-II positive, where $Ly51^{+}$ cTECs express high levels of MHC-II while UEA-1^{+} mTECs are MHC-II^{int} to MHC-II^{hi}. Over time, expression levels of MHC-II change differentially during the early postnatal period. cTECs downregulate MHC-II expression, instead expressing low to moderate levels of MHC-II. Within the mTEC compartment, MHC-II^{hi} cells persist but MHC-II^{int} cells remain till around 2 weeks of age, after which a MHC-II^{low} population emerges, such that adult mTECs can be differentiated as immature ($mTEC^{low}$) or mature ($mTEC^{hi}$), which correlates with cell surface levels of the marker CD80 (Yang, S. *et al*., 2006). $mTEC^{low}$ ($CD80^{-}MHC\text{-}II^{low}$) express a smaller set of TRAs, while $mTEC^{hi}$ ($CD80^{hi}MHC\text{-}II^{hi}$) express the autoimmune regulator Aire and thus a much larger and more diverse array of TRAs (Derbinski, J. *et al*., 2005). mTEC development is also supported by other factors such as the receptor activator of nuclear factor kappa-B ligand (RANKL), which promotes the differentiation and expansion of mTECs to a mature phenotype both during fetal and postnatal stages of development and maintenance respectively (Rossi, S. *et al*., 2007; Akiyama, T. *et*

al., 2008; Akiyama, N. *et al*., 2016). Fibroblast growth factors 7 and 10, which signal via the receptor Fgfr2IIIb, are also essential for the expansion of both cortical and medullary epithelia that have adopted a TEC fate (Revest, J. *et al*., 2001).

Both cTECs and mTECs arise during fetal development from a common bipotent progenitor (Plet-1^{+}EpCAM^{+}K5^{+}K8^{+}) capable of regenerating a fully functional cortical and medullary thymic epithelium (Gill, J. *et al*., 2002; Rossi, S. *et al*., 2006). However, the choice of progression to either the cTEC or mTEC differentiation programs is poorly defined. TECs proliferate rapidly, coinciding with the colonisation of the thymus by T cell progenitors, and it appears cortical and medullary development require reciprocal interactions with committed T cells, although it has also been shown that progenitors can develop into both cTEC and mTEC lineages without lymphostromal interactions (Gray, D. *et al*., 2006; Holländer, G. *et al*., 1995; Shores, E. *et al*., 1991; Jenkinson, W. *et al*., 2005). mTECs can arise from mTEC-lineage restricted progenitors which are Claudin (Cld) 3 and 4 positive (Hamazaki, Y. *et al*., 2007), as well as from bipotent progenitors that express traditionally cTEC-specific molecules such as the proteasomal subunit β5t (Ohigashi, I. *et al*., 2013; Baik, S. *et al*., 2013; Ulyanchenko, S. *et al*., 2016; Rodewald, H. *et al*., 2001; Rossi, S. *et al*., 2006). This suggests that mTECs pass through a cTEC-like program before becoming mTECs (Ohigashi, I. *et al*., 2015). cTECs too may differentiate from the common progenitor, or from a cTEC-specific CD205^{+}CD40^{-} progenitor population (Shakib, S. *et al*., 2009). However, while what determines lineage fate choice is unclear, the ability of TEC progenitors to differentiate and attain full functionality is absolutely dependent on the expression of Foxn1. This transcriptional factor commits thymic epithelia to a TEC fate and serves subsequently as the single most important regulator in TEC development,

essential for the proliferation, maturation, maintenance and function of these cells (Chen, L. *et al*., 2009; Cheng, L. *et al*., 2010; Corbeaux, T. *et al*., 2010; Bleul, C. *et al*., 2006; Žuklys, S. *et al*., 2016).

1.3 Foxn1

Forkhead box N1 (Foxn1) is part of a large and functionally diverse family of transcription factors defined by the structural feature of a forkhead DNA binding domain (Jackson, B. *et al*., 2010). Foxn1 is significant both in the skin (Mecklenburg, L. *et al*., 2001) and in the thymus (Pantelouris, E. & Hair, J., 1970; Frank, J. *et al*., 1999; Nehls, M. *et al*., 1994). In the skin, Foxn1 is found in keratinocytes during the early stages of terminal differentiation, and loss of Foxn1 results in defective follicular differentiation and thus a hairless phenotype (Prowse D. *et al*., 1999; Lee, D. *et al*., 1999). In the thymus, transcripts for *foxn1* are first detected in the mouse around E11.25 to 11.5 (Balciunaite, G. *et al*., 2002) and are detected in the different epithelial lineages throughout fetal life (Gordon J. *et al*., 2001) and in the postnatal thymus (Blackburn, C. *et al*., 1996). In humans where Foxn1 is equally essential for the normal development of skin appendages and the thymus (Frank, J. *et al*., 1999), Foxn1 transcripts are detected as early as the mid-sixth week of gestation throughout the thymus domain of the third pharyngeal pouch (Farley, A. *et al*., 2013). Foxn1 is expressed in TECs in a cell-autonomous manner, where it is both necessary and sufficient throughout life to direct the differentiation of precursors to phenotypically mature and functional competent TECs (Bleul, C. *et al*., 2006; Žuklys, S. *et al*., 2016; Cheng, J. *et al*., 2010). Consequently, an absence of *foxn1* causes the nude phenotype in mice (Flanagan, S., 1966) and in humans a comparable condition marked by alopecia universalis, nail dystrophies and athymia, causing a specific form of severe combined

immunodeficiency (SCID) marked by the absence of T cells (Frank, J. *et al*., 1999, Palamaro *et al*., 2014). It is, however, of note that with progressive age Foxn1 protein cannot be uniformly detected in all TECs for reasons yet to be elucidated (Rode, I*. et* al., 2015) despite continuous expression of some of its well-defined target genes (Itoi, M. *et al*., 2007).

The gene dosage and age sensitive expression of *foxn1* in the individual TEC lineages maintains not only the cells' postnatal integrity and homeostasis, but also influences the overall thymic architecture (Chen, L. *et al*., 2009; Ruan, L. *et al*., 2014), highlighting Foxn1's role in maintaining the thymic epithelial scaffold. Foxn1 appears to decline in expression over time, correlating with the well-documented age-related involution of the thymus (dos Santos Reis, M. *et al*., 2015; Rode, I. *et al*., 2015). Indeed, insufficient Foxn1 expression during postnatal life has been correlated with accelerated thymic aging (Cheng, L. *et al*., 2010; Sun, L. *et al*., 2010; Guo, J. *et al*., 2012). This may suggest that the amount of Foxn1 required for TEC maintenance is reduced once the thymus has reached a certain growth, but a minimum level of expression of Foxn1 is nonetheless absolutely necessary for normal TEC function.

The cellular consequences of *foxn1* loss of function mutations have been described in detail in the mouse, where the absence of Foxn1 transcriptional activity precludes normal TEC differentiation, resulting in an early arrest in thymic organogenesis with the formation of a cystic primordium incapable of attracting a normal number of lymphoid precursors which are then not committed to the T cell lineage and fail to differentiate normally beyond a DN1 stage (Nowell, C. *et al*., 2011; Nehls, M. *et al*., 1994; Pantelouris, E. & Hair, J., 1970). Additionally,

deliberate ablation of *foxn1* at developmental stages beyond the formation of the thymus primordium consistently results in a loss of regular thymic function, further demonstrating its essential nature for TECs (Corbeaux, T. *et al*., 2010). For example, conditional disruption of *foxn1* separately either in mTECs or cTECs results in thymic atrophy concurrent with a loss of regular thymopoiesis (Guo, J. *et al*., 2011; Žuklys, S. *et al*., 2016). Using a conceptually inverse approach, it has conversely been demonstrated that enforced Foxn1 expression in nude mice after arrest of their thymus organogenesis rescues TEC development and function (Bleul, C. *et al*., 2006). Furthermore, TEC-specific overexpression of *foxn1* can limit the decline of thymopoiesis (Zook, E. *et al*., 2011) and, more recently, seemingly reverse the age-related involution of the mouse thymus, although the precise temporal control is important (Ruan, L. *et al*., 2014). These experiments reveal that a TEC developmental block due to Foxn1 deficiency can be corrected even at a time later than the developmental stage at which Foxn1 expression is normally detected, and collectively validate the direct impact of Foxn1 on TEC development.

1.3.1 Known molecular mechanisms upstream and downstream of Foxn1

Foxn1 expression in the thymus is most notedly regulated upstream by two well-known developmental signalling pathways, Wingless (Wnt) and BMP, and to a certain extent Shh (Blaciunaite, G. *et al*., 2002; Bleul, C. & Boehm, T., 2005; Bain, V. *et al*., 2016). Wnt signals are transduced via the binding of secreted Wnt glycoproteins to cell surface receptors including the Frizzled (Fz) receptor and the low-density lipoprotein receptors (LRP) 5 and 6 which serve as co-receptors. Upon ligand binding to the cognate receptor complex, β-catenin is stabilised consequent to activation of the canonical Wnt signalling pathway, and translocates to the nucleus where a complex with Lef/Tcf family members is formed to initiate

transcription. Wnt proteins may directly control Foxn1 expression via this canonical pathway, in particular Wnts 1, 4, 5a and 5b (Blaciunaite, G. *et al*., 2002; Mulroy, T. *et al*., 2002; Hu, Bing. *et al*., 2010). Engagement of BMP signalling constitutes another pathway by which Foxn1 expression is regulated as its absence reverts thymic epithelia to a basal state of foregut epithelium (Soza-Ried, C. *et al*., 2008; Bleul, C. & Boehm, T., 2005). Finally, Shh expression in the third pharyngeal pouch may partially regulate *foxn1*, possibly via the downstream transcription factor Tbx1 (Bain, V. *et al*., 2016; Moore-Scott, B. & Manley, N., 2005).

Foxn1 itself modulates the transcription of a number of essential thymic genes, regulating processes that influence both TECs and T cells. One major signalling pathway positively regulated by Foxn1 is the Notch pathway, required for early T cell development (Pui, J. *et al*., 1999). Foxn1 is upstream of *notch1* (Cai, J. *et al*., 2009), and controls the expression of Notch ligands Delta-like ligand (Dll) 1 and 4, where Dll4 is the nonredundant Notch1 ligand during intrathymic T cell commitment at the haematopoietic progenitor stage (Tsukamoto, N. *et al*., 2005; Koch, U. *et al*., 2008). This regulatory network is a complex feedback loop, as *wnt5a* is a target of Notch (Hu, B. *et al*., 2010), yet Wnts directly regulate *foxn1*. Dll4, along with stem cell factor (SCF) and the chemokines Cxcl12 and Ccl25, are haematopoietic factors which work in synergy to facilitate thymopoiesis (Calderón, L. & Boehm, T., 2012). Ccl25 stimulates the migration and colonisation of thymocytes, following which Cxcl12 functions in a Notch-dependent Dll4-directed manner to induce differentiation of DN3 thymocytes (Vicari, A. *et al*., 1997; Janas, M. *et al*., 2010). This is supported by SCF at a regulatory growth checkpoint, where SCF inhibits differentiation into DP cells while allowing DN progenitor proliferation in a dose-dependent manner (Wang, H. *et al*., 2006). Foxn1 has been shown to regulate,

likely in a direct fashion, the expression of these critical factors, where haematopoietic activity in the thymic epithelium is repressed in *foxn1*-deficient mice (Nowell, C. *et al*., 2011; Calderón, L. & Boehm, T., 2012). This is particularly relevant for Dll4 and Ccl25, which together suffice to drive thymocyte development to the DP stage (Calderón, L. & Boehm, T., 2012). Other molecules include CD40, MHC-II and Cathepsin L, required for activation of antigen presenting cells, presentation of peptides and proteolytic cleavage of peptides respectively, and are thus crucial in thymocyte development and T cell selection (Galy, A. & Spits, H., 1992; Nakagawa, T. *et al*., 1998). All three markers are downregulated during loss of *foxn1*, although the mechanisms or pathways by which this is achieved are not understood (Nowell, C. *et al*., 2011). However, this supports that Foxn1 crucially regulates genes important for TEC function, which are in turn necessary for the normal selection and maturation of thymocytes.

1.3.2 Foxn1 transcriptional regulation in TECs

In addition to genes relevant for thymocyte development, Foxn1 is also essential for the expression of genes that influence TEC differentiation, proliferation and maintenance. Foxn1 cooperates in conjunction with the transcription factor Hoxa3 to regulate *pax1*, where single *pax1* mutants fail to support TEC differentiation adequately, despite the fact that initial formation of the thymic primordium as controlled by Hoxa3 initially occurs in a Foxn1-independent fashion (Nowell, C. *et al*., 2011; Su, D. *et al*., 2001). Foxn1 also functions in tandem with the transcription factor p63, a primary regulator of epithelial progenitor cell proliferation in the thymus, to enable TEC proliferation, where *p63*-positive cells do not develop normally in *foxn1*-deficient mice. While *p63*-null TECs do express *foxn1*, they nonetheless display proliferation defects (Senoo, M. *et al*., 2007; Burnley, P. *et al*.,

2013). As such, it is unclear if Foxn1 directly regulates *p63*, although both are necessary for normal TEC proliferation. In zebrafish, *foxn1* is found upstream of DNA replication licensing factor (*mcm2*) and cell division cycle associated 7 (*cdca7*), two loci responsible for gene replication in the context of cell proliferation. Foxn1 directly regulates *mcm2* in zebrafish TECs, and dictates TEC proliferation as well as the cells' maintenance and structural organisation. However, this has not as yet been verified in mice or humans (Ma, D. *et al*., 2012).

Recently, target genes directly regulated by Foxn1 have been identified that are significant in T cell development as well as TEC function, including *psmb11*, which encodes the proteasome component β5t and is important for accurate positive selection of CD8 T cells (Ripen, A. *et al*., 2011; Žuklys, S. *et al*., 2016). One of these targets was the Hedgehog-Interacting Protein (Hhip) (Žuklys, S. *et al*., 2016). This gene is part of the Shh signalling pathway, a pathway critical for parathyroid patterning and thus thymus fate, as well as T cell development (Bain, V. *et al*., 2016; Figueiredo, M. *et al*., 2016; Crompton, T. *et al*., 2007).

1.4 Hedgehog signalling

The Hedgehog (Hh) signalling pathway is a highly conserved developmental pathway that regulates important events during embryogenesis including patterning, cell proliferation, fate decisions and survival (Weed, M. *et al*., 1997; Ingham, P. & McMahon, A., 2001; Duman-Scheel, M. *et al*., 2002). In vertebrates, the Hh ligand family consists of Sonic (Shh), Indian (Ihh) and Desert (Dhh). Ihh and Dhh are expressed in a small number of tissues and affect several early cell developmental processes including differentiation, proliferation and maturation (reviewed in Ingham, P. & McMahon, A., 2001). However, Dhh is most significant in

the testi, where it primarily controls gonad development and spermatogenesis (Yao, H. *et al*., 2002; Bitgood, M. *et al*., 1996). Ihh controls chondrocyte and perichondrial differentiation, thus significantly impacting bone development (Clark, A. *et al*., 2000; Karp, S. *et al*., 2000). In contrast, Shh is broadly expressed and thus the most extensively studied Hh family member. It affects almost every embryonic stage of development and also impacts on the adult stage, including left-right, dorso-ventral, and anterior-posterior patterning (Martí, E. *et al*., 1995; Pagán-Westphal, S. & Tabin, C., 1998). During organogenesis, Shh is predominantly or exclusively expressed by most epithelial components, while target genes are often expressed in various cell types (Gritli-Linde, A. *et al*., 2001). All the Hh ligands have non-redundant roles due to their differential expression patterns. However, due to extensive sequence homology (>90%), particularly between Shh and Ihh, the latter may function in a partially overlapping manner with Shh in certain tissue types (Astorga, J. & Carlsson, P., 2007; Ramalho-Santos, M. *et al*., 2000; Zhang, X. *et al*., 2001).

1.4.1 Hh signalling mechanism

Hh proteins are first produced as pro-proteins and enter the secretory pathway upon sequence signal cleavage. They are subsequently modified, undergoing both cholesterol coupling at their C-terminal end as well as palmitoylation at their N-terminal end, which enhance solubility and allow the molecules' dispersion within the cell membrane (Peters, C. *et al*., 2004; Chen, M. *et al*., 2004). Indeed, Hh is able to travel up to 300 μm in the vertebrate limb bud, a process that is partially enabled by the transporter Dispatched (Disp) (Kawakami, T. *et al*., 2002). Conversely, Hh can also be retained and accumulated at the membrane (Tukachinsky, H. *et al*., 2012). These biophysical properties create the flexibility for

Hh ligands to act both in autocrine and paracrine fashions, and to perform over both short and long ranges, creating spatial and temporal morphogen gradients to dictate specific cellular responses (Yang, Y. *et al*., 1997; Harfe, B. *et al*., 2004).

Mechanistically, Hh signals via its receptor Patched (Ptch1), which in the absence of Hh constitutively represses the transducing molecule Smoothened (Smo) usually by limiting its entry into the primary cilium, a protruding microtubule-like organelle expressed by most vertebrate cells with the notable exception of differentiated myeloid and lymphoid cells (Rohatgi, R. *et al*., 2007; Wheatley, D., 1995). Upon the binding of Hh to Ptch1, the complex is internalised and releases the inhibition of Smo, subsequently allowing Smo to translocate into the primary cilium (Denef, N. *et al*., 2000). Sufficient accumulation of Smo activates the Hh pathway by engaging downstream Gli transcription factors Gli1, Gli2 and Gli3 (Kim, J. *et al*., 2009). Without Smo activity, Gli1 is not expressed and Gli2 and Gli3 are proteolytically processed to a repressive form, designated Gli^{R}. Activation of Smo however induces expression of Gli1 and the processing of Gli2 and Gli3 into transcriptionally active forms (Gli^{A}). Physiologically, Gli3 acts predominantly as a repressor, while Gli1 and Gli2 perform activator functions, with Gli2 contributing the majority of Gli^{A} activity (Méthot, N. & Basler, K., 1999; Ohlmeyer, J. & Kalderon, D., 1998; Lee, J. *et al*., 1997; Aza-Blanc, P. *et al*., 1997; Bai, C. *et al*., 2002). However, Gli2 and Gli3 share certain overlapping functions as demonstrated in $Gli2^{-/-}Gli3^{-/-}$ double knockout transgenic mice (McDermott, A. *et al*., 2005; Buttitta, L. *et al*., 2003). Both Gli^{A} and Gli^{R} enter the nucleus where they either promote or inhibit gene transcription respectively. The overall effect of Hh signalling is thus regulated at the most basic level by the delicate balance of Gli^{A} and Gli^{R} activity. This balance is further influenced by the transmembrane proteins CAM-related/Downregulated by

Oncogenes (Cdo) and Brother of Cdo (Boc), as well as the GPI-linked protein Growth Arrest-Specific 1 (Gas1). These proteins bind to Ptch1 independently, forming co-receptor complexes that promote Shh signalling (Izzi, L. *et al.*, 2011; Tenzen, T. *et al.*, 2006). While the precise mechanism of how signalling is enhanced by Gas1, Boc and Cdo is unclear, it is possible that these molecules stabilise the Ptch1 complex or alternatively allow it to accumulate, thus facilitating Hh-mediated signalling.

Hh signalling exerts an additional dynamic level of regulation upon itself in the form of an autoregulatory loop, a phenomenon commonly observed with complex signalling systems. All three Gli factors are able to enhance their own expression in a positive feedback loop. Paradoxically, Gli transcription also activates the repressor Ptch1. This results in an upregulation of Ptch1 at the site of Hh production, allowing the repressor to limit the Hh signal and its range within the tissue (Nakano, Y. *et al.*, 1989). In addition to Ptch1, the vertebrate homolog Ptch2 and the negative inhibitor Hhip are also positively upregulated by Hh signalling, establishing a feedback mechanism that restricts the magnitude and location of the Hh signal (Jeong, J. & McMahon, A., 2005; Motoyama, J. *et al.*, 1998; Chuang, P. & McMahon, A., 1999). Molecules that typically positively enhance the Hh signal, such as the co-receptor Gas1, are downregulated in parallel (Lee, C. *et al.*, 2001). Hh signalling can also upregulate itself by controlling the modification of pathway members such as Smo, where Hh inhibits ubiquitination of Smo to allow its cell surface accumulation and consequent pathway activation (Li, S. *et al.*, 2012). In addition to ligand concentration, the duration of exposure to Hh also changes levels of Hh signalling and thus the final biological impact (Scherz, P. *et al.*, 2007; Dessaud, E. *et al.*, 2007). Finally, Hh can also induce the ubiquitination and

degradation of Gli to limit the duration of its signal (Di Marcotullio, L. *et al*., 2007; Zhang, Q. *et al*., 2006). In aggregate, the intricate positive and negative transcriptional feedback loops along with the existence of both Gli^A and Gli^R forms allow Hh signalling to function almost as a switch, whereby Gli transcription attains a signalling-sufficient concentration only in the presence of a threshold amount of Hh signal, upon which cell fate is determined (Lai, K. *et al*., 2004).

1.4.2 Hh signalling in the thymus

Hh signalling is active both in the embryonic and adult thymus, where most major components of the Hh signalling pathway including Ptch1, Smo and the Gli transcription factors are expressed in the thymus (Sacedón, R. *et al*., 2003, Outram, S. *et al*., 2000). Human TECs express all three Hh ligands in epithelial cells distributed across the thymus, although a larger proportion of Shh-expressing TECs can be found in the subcapsular, medullary and cortico-medullary junction regions (Sacedón, R. *et al*., 2003). In the murine model, Shh is expressed in TECs but Ihh is found in blood vessels instead, and *dhh* mRNA is not detectable (Outram, S. *et al*., 2000). While there is limited data regarding the role of Dhh in T cell development, possibly due to the low to non-existent levels present in the thymus, Dhh negatively regulates erythrocyte differentiation, indicating a level of regulatory control in haematopoiesis since the population of the common myeloid progenitor (CMP) in the bone marrow is increased in *dhh*-deficient mice (Lau, C. *et al*., 2012).

Both Shh and Ihh exert an important influence on intrathymic T cell development (Outram, S. *et al*., 2007). Ihh is highly expressed in DP thymocytes, and positively regulates thymocyte differentiation along with the DN-DP transition. As such, the secretion of Ihh by DP thymocytes is able to restrict proliferation of their own

progenitors, thus acting as a feedback mechanism. This effect has been suggested to be a result of paracrine Ihh signalling from a different cell type such as TECs, but based on the expression profile of Ihh, most likely occurs in a homotypic fashion between thymocytes at different stages of their development, rather than between TECs and thymocytes. The extent and direction of regulation may however depend on whether a threshold concentration of Ihh is attained within the tissue (Outram, S. *et al*., 2009).

Shh is essential not only for the transition of thymocytes through separate differentiation stages but also for the selection of the TCR repertoire (Shah, D. *et al*., 2004; Rowbotham, N. *et al*., 2007; Hager-Theodorides, A. *et al*., 2009). Shh promotes the differentiation, proliferation and survival of early thymic progenitors (ETPs), and is essential for the differentiation of DN1 thymocytes to the DN2 stage. Shh also provides survival signals for DN4 cells to transit to the DP differentiation stage, thus revealing a continuous role for Shh thymocyte development before pre-TCR signalling is initiated (Shah, D. *et al*., 2004; El Andaloussi, A. *et al*., 2006). In contrast, pre-TCR signalling does not require Hh. However, Shh signalling negatively regulates aspects of TCR signalling strength, thus influencing antigen receptor repertoire selection. Both positive and negative selection are affected by Shh signalling, resulting in a decreased DP-CD4 transition (Rowbotham, N. *et al*., 2007). Once thymocytes have developed into mature T cells, Shh may continue to contribute to CD4 T cell proliferation (Lowrey, J. *et al*., 2002). In summary, Shh signalling intersects with all aspects of T cell development and maintenance. Given that Shh is expressed by TECs, normal thymocyte development may be regulated at least in part by this molecule and its downstream signalling pathway.

Alongside its influence on thymocyte development, Shh signalling regulates patterning of the vertebrate pharyngeal pouches between the pharyngeal arches during development. Shh signalling in the pouch endoderm and neighbouring epithelium restricts expression of the parathyroid marker Gcm2 and is thus considered to control parathyroid specification (Grevellec, A. *et al.*, 2011, Moore-Scott, B. & Manley, N., 2005). In the absence of Shh, Foxn1 is expressed throughout the pouch. This observation may result from a direct suppression of *foxn1* expression via Tbx1, a target of Shh-regulated gene expression. Thus, Shh may indirectly influence TEC fate commitment (Bain, V. *et al.*, 2016; Reeh, K. *et al.*, 2014). Shh signalling has also been recently shown to affect TEC cellularity, with mTECs being particularly affected, since *shh*-null mice display decreased relative percentages of total mTECs and $Aire^{+}mTEC^{hi}$ (Saldaña, J. *et al.*, 2016). Taken together, Shh-mediated signals significantly impact on T cell development via the regulation of thymus organogenesis, TEC integrity and thymocyte development.

1.4.3 Hhip

The Hedgehog-Interacting Protein (Hhip) is a structural decoy inhibitor that sequesters Hh ligands and thus negatively regulates Hh signalling (Ingham, P. & McMahon, A., 2001). Loss of Hhip increases Hh signalling and severely impairs the development of epithelial organs including the pancreas, stomach, and lung (Chuang, P. *et al.*, 2003; Kawahira, H. *et al.*, 2003). Hhip also modulates Fgf-mediated signalling in respiratory epithelia, where activation of Hhip is required to sustain Fgf10 expression in the lungs (Chuang, P. *et al.*, 2003). This is of particular relevance for thymic development since Fgf10 has a recognised role in TEC growth both pre- and postnatally (Revest, J. *et al.*, 2001). Notably, comparable studies on the role of Hhip in the thymus have not been reported.

Hhip and Ptch1 both bind to and inhibit Hh ligands, and compete for binding at the same pseudo-active binding groove in Shh, albeit via different chemical interactions (Bosanac, I. *et al*., 2009). However, Hhip is the only Hh pathway inhibitor that directly binds to Shh at nanomolar affinity. There is at least a partially different functional requirement in embryonic models, excluding a complete redundancy of these pathway modulators (Bosanac, I. *et al*., 2009; Hebrok, M. *et al*., 2000; Goodrich, L. *et al*., 1997). Like Ptch1, Hhip is upregulated by Shh signalling as part of an overall negative feedback loop, but unlike Ptch1, Hhip is not as efficiently internalised (Incardona, J. *et al*., 2000; Jeong, J. & McMahon, A., 2005). Hh inhibition by Hhip was therefore postulated to occur via sequestration of Hh at the cell surface, preventing paracrine signalling by hindering the movement of Hh (Jeong, J. & McMahon, A., 2005). More recent evidence however now suggests that Shh signalling results in the internalisation and degradation of Hhip in the cilium in a Smo-dependent cell autonomous manner, while allowing Hhip to continue to act non-cell autonomously (Pampliega, O. *et al*., 2013; Kwong, L. *et al*., 2014). Biochemical studies also demonstrate that Hhip is a secreted molecule that can also be retained at the cell surface by interactions with heparan sulfate (Holtz, A. *et al*., 2015). As such, Hhip is often found expressed in cells adjacent or in close proximity to Hh-expressing cells (Chuang, P. & McMahon A., 2005). Taken together, these findings favour the notion that Hhip modulates long range or paracrine Hh signalling, rather than acting in an autocrine manner.

Hhip-deficient mice succumb to respiratory failure soon after birth, contributing to a lack of a detailed mechanistic understanding of Hhip's role in thymus organogenesis and function. High expression of *hhip* and *smo* combined with low expression of *ptch1* in TECs (Sansom, S. *et al*., 2014) suggests that Hhip may be a

key modulator of Hh signalling in these cells and could thus control TEC and T cell development indirectly. With the new knowledge implicating Hhip to be positioned downstream of Foxn1-mediated gene transcription, it is of interest to investigate the role of Hhip in the context of the thymus and in particular TEC biology.

1.5 Hypothesis and aims

The master transcription factor Foxn1 and the Hh signalling pathway are fundamentally indispensible for regular thymus organogenesis. I postulate that an important downstream effector molecule regulated by Foxn1 could be the candidate target Hhip, given its established role as an inhibitor of Hh signalling. My key hypothesis is thus that Foxn1-regulated expression of Hhip is relevant for normal TEC development and function.

My research objectives are:

i. To establish a genetic mouse model that can be used to investigate a TEC-restricted loss of Hhip

i. To identify a role for Hhip in TEC development and function

ii. To evaluate if Hhip expression by TECs is required for normal T cell development

2: Materials and Methods

2.1 Mice

Animal work was conducted in accordance with UK Home Office regulations. Mice colonies were maintained at University of Oxford biomedical science facilities unless otherwise stated. All experiments were conducted with littermate controls, denoted as wild-type (WT). Wild-type mice represent a normal, conventional phenotype typical of a non-genetically manipulated background consistent with the appropriate mouse strain. All control mice were age-matched and adult mice were matched for sex in all experiments. Both sexes were used at equal frequencies. Mice were culled using Schedule 1 methods and all procedures performed via specified methods on the relevant project license.

2.1.1 C57BL/6

C57BL/6J black inbred wild-type mice and C57BL/6BrdCrHsd-Tyr^{c} albino wild-type mice, which have a mutation in the tyrosinase gene, were obtained from Harlan Laboratories for breeding. C57BL/6 mice for fetal thymic organ culture (FTOC) experiments and other phenotyping were purchased from the in-house colony maintained by the University of Oxford.

2.1.2 B6.SJL.CD45.1

B6.SJL.CD45.1 congenic mice for transplantation experiments were obtained from the in-house colony maintained by the University of Oxford. These mice have a conventional C57BL/6 genetic background but carry the differential CD45.1 allele, as opposed to CD45.2 in regular wild-type C57BL/6 inbred mice.

2.1.3 Hhip$^{tm1Amc/J}$

Hhip$^{tm1Amc/J}$ mice were obtained from The Jackson Laboratory. These were generated by Andrew McMahon via disruption of exon 1 of the endogenous *hhip* gene using a beta-galactosidase (*lacZ*) and PGK-neo cassette, resulting in null expression (Chuang, P. & McMahon, A., 2003). Heterozygous mice (Hhip+/-) are viable while homozygous mice (Hhip-/-) die shortly after birth due to respiratory failure. Mice were originally maintained on a mixed C57BL/6, Swiss-Webster and 129 genetic background, but were subsequently backcrossed onto the C57BL/6 background for 5 generations.

2.1.4 Foxn1^{Cre}

Foxn1^{Cre} mice were generated by Saulius Žuklys as P1 artificial chromosome (PAC) transgenic animals (Žuklys S. *et al.*, 2009). The coding sequence for iCre was inserted into a Foxn1 PAC clone and injected into the pronuclei of fertilised B6D2F1 oocytes, establishing the transgenic line B6;D2-Tg(Foxn1-Cre)8Ghr. This line was maintained as a heterozygous Foxn1$^{Cre+/-}$ colony on a C57BL/6 background as homozygous Foxn1^{Cre} mice are infertile. Foxn1$^{Cre+/-}$ mice were bred to Hhip$^{lox/lox}$ mice to generate mice conditionally deficient for *hhip* expression in Foxn1-expressing cells.

2.1.5 Hhip$^{lox/lox}$

Hhip$^{lox/lox}$ mice were created using Crispr/Cas9 technology. C57BL/6N JM8.F6 ES cells were transfected with plasmid constructs containing sequences for the Cas9 endonuclease and synthetic guide RNAs (sgRNAs) targeting either side of *hhip* exon 2, along with a homology construct containing the *hhip* exon 2 sequence flanked by loxP sites to allow homologous integration of loxP sites around exon 2,

creating a conditional $Hhip^{lox}$ allele. Successfully targeted ES cells were injected into the blastocysts of albino C57BL/6BrdCrHsd-Tyr^{c} mice and chimeras were selected by coat colour and confirmed by genotyping. Chimeras were propagated via *in vitro* fertilisation to test for germline transmission. Offspring that successfully integrated the mutation were bred to $Foxn1^{Cre+/-}$ mice until homozygosity for the $Hhip^{lox}$ allele. Presence of the correctly targeted *hhip* allele is denoted as $Hhip^{lox}$, while alleles that have had *hhip* exon 2 successfully excised by $Foxn1^{Cre}$ and thus have null expression of *hhip* in Foxn1-expressing cells are distinguished as $Hhip^{flox}$.

2.1.6 GBS-GFP

GBS-GFP mice were a kind gift from Tessa Crompton from University College London (UCL), UK. These were originally generated by James Briscoe, where fragments of a FoxA2 enhancer containing a binding site for the Gli transcription factors were cloned upstream of the *hsp69* minimal promoter and eGFP, forming the 8GBS-gsp58-eGFP transgene which was subsequently subcloned into mice (Balaskas, N. *et al*., 2012). Hh signalling via Gli transcriptional activity can thus be monitored via GFP expression. Mice were maintained, time mated and sacrificed at UCL facilities. Mice were genotyped for presence of the transgene by taking blood samples and measuring GFP expression by flow cytometry.

2.1.7 Timed matings

Mating pairs were set up overnight and females checked for vaginal plugs the next morning. Plug-positive females were designated to be at gestational age E0.5.

2.2 General reagents

Several standard buffers and media were used in different experiments and made in-house (Tables 2.1, 2.2). All concentrations listed are final concentrations.

Table 2.1: Standard buffers

Buffer	Ingredients	Company	Concentration
Annealing Buffer (2X)	Tris	Merck	200 mM
	EDTA	Sigma	2 mM
	NaCl	VWR	100 mM
Fluorescence-Activated Cell Sorting (FACS) Buffer	Phosphate-Buffered Saline (PBS)	Gibco	1X
	Fetal Calf Serum (FCS)	Sigma	2%
Liberase Digestion Buffer	PBS	Gibco	1X
	Liberase	Roche	2.5 mg/ml
	DNase	Roche	10 mg/ml
Lysis Buffer	Tris	Merck	100 mM
	Ethylenediaminetetraacetic acid (EDTA)	Sigma	5 mM
	Sodium Dodecyl Sulfate (SDS)	Sigma	0.2%
	Sodium Chloride (NaCl)	VWR	200 mM
	Proteinase K	Roche	100 µg/ml
Magnetic-Activated Cell Sorting (MACS) Buffer	PBS	Gibco	1X
	EDTA	Sigma	5 mM
	Filtered Bovine Serum Albumin (BSA)	Sigma	0.2%
Red Blood Cell (RBC) Lysis Buffer	Ammonium Chloride (NH_4Cl)	Sigma	0.8%
	EDTA	Sigma	0.1 mM
	Potassium Bicarbonate ($KHCO_3$)	Gibco	1 g/l
Tris-EDTA (TE) Buffer	Tris	Merck	10 mM
	EDTA	Sigma	1 mM

Table 2.2: Standard medias

Media	Ingredients	Company	Concentration
1C6 Media	Iscove's Modified Dulbecco's Medium (IMDM) + GlutaMax	Gibco	1X
	Heat-Inactivated FCS (FCS-HI)	HyClone	10%
	Penicillin-Streptomycin (Pen-Strep)	Sigma	1X
Fetal Thymic Organ Culture (FTOC) Media	IMDM + GlutaMax	Gibco	1X
	Heat-Inactivated FCS (FCS-HI)	HyClone	10%
	Pen-Strep	Sigma	1X
ES Cell Media	BHK-21 Glasgow Minimum Essential Medium (GMEM)	Gibco	1X
	Glutamine	Gibco	1X
	Sodium Pyruvate MEM	Gibco	1 mM
	Non-Essential Amino Acids	Gibco	1X
	FCS-HI	HyClone	10%
	Lif	Gibco	1X
	2-Mercaptoethanol	Sigma	100 µM
OP9-DL1 Media	Alpha-Minimum Essential Media (Alpha-MEM)	Sigma	1X
	FCS-HI	HyClone	20%
	Pen-Strep	Sigma	1X
TEC Media	IMDM	Gibco	1X
	2-Mercaptoethanol	Sigma	50 µM
	Primatone RL/UF	Sigma	0.3 mg/ml
	FCS	Sigma	2%
T Cell Media	RPMI	Sigma	1X
	FCS	Sigma	10%
	Pen-Strep	Sigma	1X
	2-Mercaptoethanol	Sigma	50 µM

2.3 Genotyping

2.3.1 Isolation and amplification of genomic DNA

Tissue samples from ear clips (adult mice) or tail snips (embryos and newborn mice) were lysed for a minimum of 4 hours in 600 µl lysis buffer incubated at 55°C. Remaining debris was pelleted and removed, and genomic DNA precipitated with

600 µl isopropanol (VWR) and washed with 500 µl 70% ethanol (VWR). The supernatant was discarded and the DNA pellet resuspended in 50 µl TE buffer.

Following, genomic DNA was amplified by polymerase chain reaction (PCR) in a thermocycler (Applied Biosystems) under the conditions listed below (Table 2.3). 1 µl of DNA was used in each 25 µl reaction mix containing 200 µM deoxynucleotides (dNTPs) (Sigma), 0.2 µM each of the relevant forward and reverse primers (Tabie S1 in Supplementary), 1X Taq buffer and 0.02 u/µl Taq polymerase (Sigma). The amplification temperature (T_a) was designated as the lowest melting temperature (T_m) of the primer pair used minus 5 (T_m - 5°C).

Table 2.3: Thermocycler conditions for standard genotyping PCR

Step	**Cycles**	**Temperature**	**Duration**
1	1	94°C	4 min
2	34	94°C	30 sec
		T_a	40 sec
		72°C	1 min
3	1	72°C	10 min
4	1	4°C	Hold

2.3.2 Agarose gel electrophoresis

Agarose gels were prepared with UltraPure Agarose (Invitrogen), 1X Tris-Borate-EDTA (TBE) buffer (Sigma) and 1:20000 GelRed dye (Biotium), at a concentration of agarose dependent on the expected PCR product size. 10 µl of amplified PCR product for each genotyping sample was mixed 5:1 with 6X gel loading dye (Thermo Fisher Scientific), loaded into wells and run in a gel tank. The 1 kb Plus DNA ladder (NEB) was used as a comparison to determine the size of the PCR product. Gels were visualised using the Gel Doc XR+ system (Bio-Rad).

2.4 Molecular biology

2.4.1 RNA extraction and cDNA synthesis

RNA isolation was performed using the RNeasy Micro kit (Qiagen) following manufacturer's recommendations. Briefly, cells were lysed and homogenised by centrifugation in the QIAshredder column (Qiagen) or vortexing. An equal volume of 70% ethanol was added to promote binding and the sample subsequently loaded onto the RNeasy MinElute spin columns (Qiagen). Cell lysates were subject to several washing steps and treated with RNase-free DNase (Qiagen) to remove genomic DNA. RNA samples were eluted in 12 µl and used immediately or stored at -20°C until subsequent use. RNA concentrations and quality were measured using the NanoDrop instrument (Thermo Scientific).

cDNA for experiments on Hhip$^{tm1Amc/J}$ mice were synthesised using Superscript III reverse transcriptase (Invitrogen) with 4 µl RNA per 20 µl reaction. A 13 µl sample was prepared containing 4 µl RNA, 1 µl 10mM dNTPs, 1 µl 50 ng/µl random hexamers (Sigma) and 7 µl sterile nuclease-free water (Ambion), and heated to 65°C in a thermocycler for 5 min. Samples were then chilled on ice and a second mix added containing 4 µl 5X First-Strand buffer, 1 µl 0.1M Dithiothreitol (DTT), 1 µl SuperScript III reverse transcriptase and 1 µl RNaseOUT recombinant RNase inhibitor (Invitrogen). This was mixed gently and incubated at 25°C for 5 min and 50°C for 30 min, then inactivated by heating at 70°C for 15 min. Finally, samples were treated with 1 µl RNase H (NEB) for 20 min at 37°C before being used or stored at -20°C.

cDNA for experiments on all other mice and cell lines were synthesised with the SensiFAST cDNA kit (Bioline). RNA, 4 µl 5X TransAmp Buffer, 1 µl reverse

transcriptase (Bioline) and up to 20 µl nuclease-free water were mixed gently and incubated in a thermocycler for 10 min at 25°C, 15 min at 42°C and 5 min at 85°C. Samples were used immediately or stored at -20°C.

2.4.2 qPCR

qPCR experiments were conducted using the SensiMix SYBR Hi-Rox Kit (Bioline) in the StepOnePlus Real-Time PCR system (Applied Biosystems). 1-3 µl of template cDNA were used per 10 µl reactions containing 1X SensiMix SYBR (Bioline) and 100 nM of each relevant primer pair (Tabie S1 in Supplementary). Reactions were run as per manufacturer's recommendations (Table 2.4). Expression levels of each gene was normalised against *gapdh* expression and calculated as $2^{-\Delta CT}$ to demonstrate fold change.

Table 2.4: Thermocycler conditions for qPCR

Step	Procedure	Cycles	Temperature	Duration
1	Polymerase Activation	1	95°C	10 min
2	Amplification	40-50	95°C	15 sec
			60°C	15 sec
			72°C	15 sec
3	Melt Curve	Variable	60-95°C	Variable

2.4.3 CRISPR/Cas9 synthetic guide RNA (sgRNA) design and cloning

sgRNA sequences were designed and verified for potential off-target effects using the CRISPR Design website (Massachusetts Institute of Technology). Synthetic guide RNAs (sgRNAs) for the $Hhip^{lox/lox}$ mice were produced in conjunction with Andrew Bassett (University of Oxford), and tested for cleavage efficiency in the N2A cell line using High Resolution Melt Analysis (HRMA), discussed in Chapter 6.

Table 2.5: sgRNA sequences

Name	Sequence	Cloned Into	Purpose
sgRNA2	CTGGGCCGGCTATATATTAGAGG	PX459	Transgenic Mouse
sgRNA4	TACGATTCAATATATGCTCTGGG	PX459	Transgenic Mouse
BS1	GCCCCTAACCCAACAGACGCTGG	PX330-eGFP, PX459-Ruby	*In Vitro*
BS2	GCGGGGCGGCGGGACGCTCTTGG	PX330-eGFP, PX459-Ruby	*In Vitro*
BS3	GAGCAGCAAGGGCAGGACGCGGG	PX330-eGFP, PX459-Ruby	*In Vitro*
TSS or NS Site	AGAGGAGACCTCAGCATCCTCGG	PX330-eGFP	*In Vitro*
CS	CCTGAAAGAGATGTCCTGGATGG	PX330-eGFP	*In Vitro*

The sequences in Table 2.5 above as well as their complementary reverse sequences were synthesized as oligonucleotides (Sigma), including appropriate overhangs (5'– CACC, 3'– CAAA) to allow for subsequent plasmid cloning. 5 µl of each 100 µM forward and reverse oligonucleotides was mixed with 10 µl of annealing buffer and allowed to anneal in the thermocycler (Table 2.6).

Table 2.6: Thermocycler conditions for annealing program

Step	Cycles	Temperature	Duration
1	1	98°C	1 min
2	99	98-88°C	5 sec, decrease 0.1°C/cycle
3	99	88-78°C	10 sec, decrease 0.1°C/cycle
4	99	78-68°C	10 sec, decrease 0.1°C/cycle
5	99	68-58°C	10 sec, decrease 0.1°C/cycle
6	99	58-48°C	10 sec, decrease 0.1°C/cycle
7	99	48-38°C	10 sec, decrease 0.1°C/cycle
8	99	38-18°C	1 sec, decrease 0.2°C/cycle
9	99	18°C	Hold

Annealed oligonucleotides were phosphorylated by incubation of 1 µl annealed oligonucleotides, 1 µl 10X T4 DNA ligase buffer (Roche), T4 Polynucleotide Kinase

(NEB) and 7 µl nuclease-free water at 37°C for 30 min. Subsequently, the phosphorylated mixture was diluted 10X in nuclease-free water and used immediately or frozen at -20°C.

The plasmid vectors PX459, modified PX330-eGFP and PX458-Ruby (Addgene) were kind gifts from Andrew Bassett, Joey Riepsaame and Philip Hublitz (University of Oxford) respectively. PX459 contains a puromycin resistance cassette, while PX330-eGFP and PX459-Ruby contain eGFP and Ruby fluorescent selection markers respectively. Plasmid vectors were linearised by incubating 2 µg vector, 5 µl 10X T4 DNA ligase buffer, 2 µl BbsI (NEB) and nuclease-free water to a total of 50 µl at 37°C for 2 hours. Digested vectors were then purified using the QIAquick PCR purification kit (Qiagen) according to manufacturer's protocol, where samples were allowed to bind to a column and then washed. Purified samples were eluted in 30 µl Buffer EB (Qiagen).

Finally, phosphorylated oligonucleotides were cloned into the linearised vectors. 1 µl purified linearised vector, 2 µl diluted oligonucleotides, 1 µl T4 DNA ligase buffer, 4 µl nuclease-free water and 1 µl T4 DNA ligase (Roche) were incubated at 18°C for 2 hours. 2 µl of this mixture was then transformed into 50 µl of competent DH5α cells, which were either prepared in-house as detailed below or purchased from Thermo Fisher Scientific. Cloned plasmid DNA were analysed for concentration and purity using the Nanodrop, then sent for sequencing in-house to confirm accuracy. Primers for sequencing were either designed in-house or known sequences from the relevant plasmid backbone were used (Tabie S1 in Supplementary).

2.5 Microbiology

2.5.1 Preparation of competent DH5α cells

Single colonies of DH5α cells were grown on Luria Broth (LB) agar (Fisher Scientific) plates overnight at 37°C. Each single colony was then grown in liquid culture of 20 ml LB (Fisher Scientific) until reaching an optical density of approximately 0.4 as measured by the Spectrostar spectrophotometer (VWR). Following which, cells were centrifuged, supernatant discarded and cell pellets resuspended in 0.1 M $MgCl_2$ (Sigma). Cells were chilled for 10 min, pelleted again and resuspended in 0.1 M $CaCl_2$ (Sigma). After cooling on ice for another 10-30 min, cells were centrifuged and resuspended in 1 ml 0.1 M $CaCl_2$. Competent cells were used at this stage or frozen at -80°C until further use.

2.5.2 Cell transformation

1-2 µl of plasmid was pipetted into 50 µl competent DH5α cells. Samples were left on ice for 40 min, heat shocked for 1 min in a 42°C water bath and allowed to cool on ice for a further 5 min. 200 µl Super Optimal broth with Catabolite repression (SOC) medium (Thermo Fisher Scientific) at room temperature was added and incubated for 30 min at 37°C. 100 µl of the mixture was plated onto an LB agar plate containing 1X ampicillin (Sigma). Plates were allowed to incubate overnight at 37°C. Single colonies were picked the next day and cultured in 10 ml LB with 1X ampicillin for 6-8 hours. At this point, liquid cultures were either frozen at -80°C to create long-term glycerol (Sigma) stocks or used in miniprep or maxiprep protocols.

2.5.3 Plasmid preparation

To purify plasmids, Plasmid Mini or Maxi Kits (Qiagen) were used as per manufacturer's protocols depending on the amount of plasmid required. Briefly,

plasmids were grown in liquid culture and centrifuged to obtain bacterial cell pellets. Supernatants were discarded and pellets resuspended in several wash buffers. Plasmid DNA was eluted either by centrifugation or using Qiagen tips. DNA was then precipitated using isopropanol and washed with 70% ethanol. Pellets were air dried and resuspended in Buffer EB or TE buffer.

2.6 *In vitro* experiments

2.6.1 Cell lines preparation

Cells were frozen, thawed, passaged and expanded using standard tissue cultured techniques in a sterile Class II laminar flow hood. Cells were passaged at 90-95% confluency and counted using a haemocytometer (Neubauer) and Trypan blue (Thermo Fisher Scientific) to distinguish dead cells. Cells were harvested by incubation with 0.25% Trypsin-EDTA (Gibco) for 10 min at 37°C. cTEC 1.2 and mTEC 2.3 cell lines were cultured with TEC media, the mTEC 1C6 cell line with 1C6 media, and ES cells with ES cell media. All wells, dishes and flasks used for culture of ES cells were gelatinised by coating with 0.1% gelatin (Sigma) for at least 15 min and the excess aspirated.

2.6.2 Experimental transfection

Cells were seeded at 50-60% confluency in 6-well plates (Corning) and allowed to grow overnight. Cells were transfected with the plasmid(s) of interest within 24 hours of plating as per manufacturer's recommendations using 7.5 µl Lipofectamine 3000 (Thermo Fisher Scientific) per well. Cells were cultured for 48 hours from the time of transfection. Following this, cells were trypsinised with 0.25% Trypsin-EDTA (Gibco) for 10 min, washed and collected as a single cell suspension for analysis on the BD FACS Aria III (BD Biosciences). Successfully transfected cells were

selected on the basis of GFP or Ruby expression and sorted into eppendorf tubes containing FCS. Sorted cells were then pelleted and stored in Buffer RLT (Qiagen) at -20°C until further use.

2.6.3 Fetal Thymic Organ Culture (FTOC)

Embryos were gently dissected from the uterine horn of the sacrificed mother, removed from the amniotic sacks and washed in 1X PBS with 10% FCS-HI. Tail snips were taken from embryos for genotyping. Whole thymic lobes were then dissected from embryos and gently cleaned. 12-well plates (Corning) were loaded with 2 ml FTOC media in each well and polycarbonate filter membranes (Whatman) gently placed on the surface of the media and allowed to float. Thymic lobes were cultured on the membranes as *in vitro* hanging drop cultures for 4 or 7 days in an incubator at 37°C with 10% CO_2. Recombinant Mouse Sonic Hedgehog, N-Terminus (R&D Systems) was reconstituted to 100 mg/ml in 1X PBS and 0.1% BSA, and used in select experiments at 0.5, 0.25 and 0.05 µg/ml final concentrations in FTOC media. Recombinant Mouse Hhip (R&D Systems) was prepared as a 100 mg/ml solution in 1X PBS and used in select experiments at 0.1 or 1 µg/ml final concentration in FTOC media. The 5E1 anti-Shh monoclonal antibody in supernatant form (DSHB) was used in several experiments at a final concentration of 5 µg/ml in FTOC media, while GANT61 (Abcam), a selective Gli1 and Gli2 small molecule inhibitor, was dissolved in DMSO to a concentration of 10 mM and used in specified experiments at a final concentration of 10 µM in the FTOC media.

2.6.4 Stimulation assay

96-well flat bottom plates were coated with a range of concentrations of purified anti-mouse CD3 antibody at 4°C overnight, then washed with 1X PBS to remove excess antibody. Immediately before staining, 1 µl CellTrace CFSE dye (Invitrogen) was predissolved into 18 µl DMSO (Invitrogen), and diluted into 10 ml PBS to get a 10 µM working solution. Naïve peripheral CD4 T cells were sorted in FCS-HI and resuspended in PBS at a concentration of 1 mil/ml. Cells were stained in equal volume with the CellTrace CFSE dye (Invitrogen) working solution to get a final concentration of 5 µM, and incubated at 37°C for 20 min. The solution was quenched using FACS buffer, and CFSE-stained cells resuspended in T cell media with 1 µg/ml purified anti-mouse CD28 antibody at 1 mil/ml. 200 000 cells were plated per well and cultured in an incubator at 37°C with 10% CO_2. After 3 days, cells were analysed by flow cytometry. Cell proliferation was analysed using the FlowJo Cell Cycle Proliferation platform.

2.7 Organ preparation and cell isolation

2.7.1 TEC isolation

Thymi were isolated and cleaned of residual fat and connective tissue. Thymi were then exposed to sequential enzymatic digestion by incubation at 37°C in Liberase digestion buffer. Briefly, 2 ml of digestion buffer was added to each sample and thymi gently disrupted by pipetting. This was incubated for 10 min, after which the supernatant was collected. This step was then repeated 2 more times, with 1 ml of fresh digestion buffer each time. When digesting embryonic thymi, only 500 µl of digestion buffer was used per sample. The supernatant was collected into a 50 ml Falcon tube (Corning) containing 40 ml of cold FACS buffer, then centrifuged and the resulting cell pellet resuspended to achieve a single cell suspension.

Adult TECs were incubated with α-CD45 beads (Miltenyi Biotec) at a concentration of 5 x 10^6 µl per 10 x 10^6 cells for 15 min at 4°C. Following, cells were washed with FACS buffer, incubated with 100 µg/ml DNase I (Roche) and filtered through a 30 µm filter (Millipore). Cells were then resuspended at a concentration of 100 mil/ml in FACS buffer and depleted for CD45 expression using the *"depletes"* program on the AutoMACS separator (Miltenyi Biotec).

2.7.2 T cell isolation

T cells were obtained by gently squashing the thymi, spleen or lymph nodes between 2 frosted glass slides (Thermo Scientific) to release thymocytes. Splenocytes were incubated 4:1 with RBC lysis buffer for 5 min at room temperature to remove erythrocytes. Cells were then washed with cold FACS buffer and filtered through a 70 µm filter (Millipore) before washing followed by resuspension as a single cell suspension.

2.7.3 Haematopoietic progenitor isolation

Haematopoietic progenitors were obtained by crushing the femurs and tibiae using a mortar and pestle until the bones turned white. Cell suspensions collected were washed with FACS buffer and filtered through a 70 µm filter (Millipore).

2.8 Transplantation studies

2.8.1 Fetal liver transplant

Hhip$^{tm1Amc/J}$ heterozygous mice were time mated to obtain embryos at E14.5. Fetal livers were dissected from embryos and gently squashed between frosted glass slides (Thermo Scientific) and filtered through a 70 µm cell strainer (Greiner) to obtain a single cell suspension in IMDM with 50% FCS-HI. Cells were spun down,

resuspended in sterile 1X dPBS with 0.02% BSA and kept on ice until injection. Recipient B6.SJL.CD45.1 male mice at 6-7 weeks of age were irradiated with a lethal dose of 1000-1100 rad split 4 hours apart to deplete haematopoietic cells. Mice were injected intraperitoneally or intravenously with 3-4 million Hhip-/- or WT fetal liver cell suspensions. Mice were monitored twice daily for 16 days and thrice weekly thereafter. Recipient mice were culled after 5 weeks and analysed.

2.8.2 Thymus transplant

Hhip$^{tm1Amc/J}$ heterozygous mice were time mated to obtain embryos at E18.5. Tail snips were taken for genotyping and thymi were isolated from embryos and grown as FTOC for 1 day. The next day, recipient B6.SJL.CD45.1 male mice between 11-12 weeks of age were anaesthetised by subcutaneously administering equal parts 1 mg/ml Domitor (Vetoquinol) and 100 mg/ml Ketamidor (Chanelle) prepared by animal weight, followed by an equal volume of the analgesic Buprecare (Animalcare) at 0.3 mg/ml. When mice were fully anaesthetised, 2 whole WT or Hhip-/- embryonic thymic lobes were transplanted under the renal capsule of the left kidney of recipient mice using aseptic surgery. Surgery was kindly performed by Tiago Luis (University of Oxford). Vicryl Rapide (Johnson & Johnson) dissolvable sutures were used. Post-surgery, mice were administered 5 mg/ml of the anaesthetic reversal drug Antisedan (Vetoquinol) in a dose volume equal to the amount of Dormitor given and 500 µl PBS (Gibco) to prevent dehydration. Mice were monitored until reflexes had returned fully, then daily for 8 days and twice weekly thereafter. Recipient mice were culled and analysed after 6 weeks.

2.9 Flow cytometry

2.9.1 Antibody staining

A number of antibodies were used to differentiate specific cell types and populations for phenotypic analysis. The antibodies listed below (Table 2.7) were used for flow cytometry.

Table 2.7: FACS antibodies

Antibody	Clone	Isotype	Conjugate	Source
Aire	5H12	Rat IgG2c, κ	Alexa Fluor 488	eBioscience
B220	RA3-6B2	Rat IgG2a, κ	PE	BioLegend
CCR7	4B12	Rat LOU/M IgG2a	BV421, BV605, PE	BD Biosciences
CD117	2B8	Rat IgG2b, κ	PE Cy5	BioLegend
CD11b	M1/70	Rat IgG2b, κ	Biotin	BioLegend
CD11c	N418	Armenian Hamster IgG	Biotin	BioLegend
CD19	1D3	Rat IgG2a, κ	Biotin	eBioscience
CD205	205yekta	Rat IgG2a, κ	PE efluor610	BioLegend
CD24	M1/69	Rat IgG2b, κ	APC, FITC	BioLegend
CD25	PC61.5	Rat IgG1, l	BV605, efluor450	eBioscience
CD28	37.51	Syrian Hamster IgG	-	BioLegend
CD31	390	Rat IgG2a, κ	Biotin	BioLegend
CD3ε	145-2C11	Armenian Hamster IgG	-	BioLegend
CD3ε	17A2	Rat IgG2b, κ	-	BioLegend
CD3ε	145-2C11	Armenian Hamster IgG	PerCP Cy5.5	eBioscience
CD4	RM4-5	Rat IgG2a, κ	APC Cy7, PE Texas Red	BioLegend
CD44	IM7	Rat IgG2b, κ	PE Cy7, PE efluor610	eBioscience
CD45	30-F11	Rat IgG2b, κ	Alexa Fluor 700	BioLegend
CD45.1	A20	Mouse IgG2a, κ	BV510	BioLegend
CD45.2	104	Mouse IgG2a, κ	BV510	BioLegend
CD49b	DX5	Rat IgM, κ	Biotin	BioLegend
CD5	53-7.3	Rat IgG2a, κ	PE Cy5, PerCP Cy5.5	BioLegend
CD62L	MEL-14	Rat IgG2a, κ	PE Cy7	BioLegend
CD69	H1.2F3	Armenian	PE Cy5, PE Cy7	BioLegend

		Hamster IgG		
CD80	16-10A1	Armenian Hamster IgG	PE Cy5	BioLegend
CD86	GL-1	Rat IgG2a, κ	PE Cy7	BioLegend
CD8a	53-6.7	Rat IgG2a, κ	Alexa Fluor 700	BioLegend
Epcam	G8.8	Rat IgG2a, κ	PerCP Cy5.5	BioLegend
F4/80	BM8	Rat IgG2a, κ	Biotin	BioLegend
Fc Block (Mouse)	2.4G2	Rat IgG2b, κ	-	BD Biosciences
FoxP3	FJK-16s	Rat IgG2a, κ	PE efluor610	eBioscience
Gr-1	RB6-8C5	Rat IgG2b, κ	Biotin	BioLegend
Helios	22F6	Armenian Hamster IgG	BV421	BioLegend
I-A/I-E	M5/114. 15.2	Rat IgG2b, κ	FITC, BV421	BioLegend
Ki67	16A8	Rat IgG2a, κ	Alexa Fluor 647, Alexa Fluor 700	BioLegend
Ly51	6C3	Rat IgG2a, κ	PE	BioLegend
MHC-I	28-14-8	Mouse IgG2a, κ	PE	eBioscience
NK1.1	PK136	Mouse IgG2a, κ	Biotin	BioLegend
PD-1	29F.1A12	Rat IgG2a, κ	APC	BioLegend
Qa-2	695H1-9-9	Mouse IgG2a, κ	Biotin	BioLegend
Strept avidin	-	-	APC, APC Cy7, BV605, PerCP Cy5.5	BioLegend
TCRβ	H57-597	Rat IgG2b, κ	APC Cy7, FITC, PE	eBioscience
TCRγδ	GL3	Armenian Hamster IgG	Biotin	eBioscience
Ter119	TER-119	Rat IgG2b, κ	Biotin	BioLegend

The UEA-1 lectin (Vector Laboratories) labelled in-house with Cy5, Live/Dead Fixable Aqua stain kit (Thermo Fisher Scientific) and DAPI (Thermo Fisher Scientific) were also used.

Where appropriate, the Live/Dead Aqua stain was conducted for 30 min at room temperature in the dark, where 1 µl of the stain was added to a total sample volume of up to 5 million cells in 1 ml. Extracellular antibody stainings were conducted for 20 min at 4°C in the dark. Concentrations of antibodies used were based on titrated

volumes, and range between 0.25-1.5 µg/100 µl (of up to 5 million cells). Fc Block was used for splenocytes. For intracellular antibody stainings, samples were first stained for cell-surfaced molecules, then fixed and permeabilised using reagents from the Foxp3 staining buffer set (eBioscience) as per manufacturer's recommendations for a minimum of 1/2 hour at 4°C in the dark. Cells were then stained with specific intracellular antibodies for 1-2 hours at 4°C in the dark. When necessary, 1 µl of DAPI per 100 µl of sample volume was added to the sample tube and gently vortexed just before analysis.

2.9.2 FACS analysis and sorting

The BD FACS Aria III (BD Biosciences) was used both for phenotypic analysis as well as cell sorting. Samples were resuspended in between 0.2 to 1 ml of FACS buffer and vortexed gently before loading onto the machine. Cells were sorted into eppendorf tubes pre-wet and coated with FCS. Sorting was conducted using the 4-way purity mask, with a routine purity of ≥99%.

2.10 Imaging

2.10.1 Sample processing

Relevant organs were freshly isolated and any excess fat, blood or connective tissue removed. Organs were immersed in OCT compound (Tissue-Tek) and frozen in cryomolds (Leica) using dry ice and isopropanol (Fluka). Frozen samples were stored at -20°C. When required, frozen tissue blocks were sectioned at 6 or 8 µm with a cryostat (Leica) and collected onto charged SuperFrost Plus precleaned microscope slides (VWR) and stored at -20°C after drying.

2.10.2 Cytospin preparation

Superfrost microscope glass slides (Thermo Fisher Scientific) were soaked in a cleaning solution of 0.25 g/ml NaOH and 95% ethanol for 2 h, then rinsed extensively with distilled H_2O without letting slides dry out. Slides were then incubated with a 1X poly-d-lysine (Sigma) solution in a plastic container with gentle agitation for 30 min. Following, slides were allowed to dry completely at 37°C and stored in a cool, dry and dust-free environment until ready for use.

10000 sorted cells were resuspended in 100 µl 1X PBS (Gibco). Filter cards (Shandon) were pre-wet with PBS by centrifuging in the Cytospin centrifuge (Shandon). Cells were loaded onto pre-wet poly-d-lysine or Superfrost Plus microscope slides by centrifugation and allowed to air dry. In some cases, 1000 cells were sorted directly onto poly-d-lysine coated slides. Cell spots were delineated using a PapPen (Abcam) before being stored at -20°C.

2.10.5 Haematoxylin and Eosin (H&E) staining

Slides were stained in filtered haematoxylin (Sigma) for 1 min then rinsed with running ddH_2O. Slides were then stained with eosin (Thermo Scientific) for 2 min and rinsed. Stained slides were then sequentially dehydrated with an ascending series of ethanol concentrations (70, 80, 90 and 100%) for 30 sec each. Slides were allowed to dry completely before mounting with Hydromount (National Diagnostics). Coverslips were sealed with clear nail polish (Various).

2.10.6 Immunohistochemistry

Slides were fixed and permeabilised with acetone at -20°C for between 30-60 min. For Foxn1 staining, slides were fixed in 10% formalin solution (Sigma Aldrich) for

15 min and permeabilised with 0.01% Triton X-100 (Sigma) for 1 hour at room temperature, then blocked with 10% donkey serum (Sigma) for 1 hour at room temperature. Slides were subsequently stained with primary antibodies in blocking solution, washed twice with 1X PBS, and stained with secondary antibodies at 1:1000 dilution for 1 hour in 1X PBS. Slides were washed twice in 1X PBS before mounting with Duolink *In Situ* Mounting Medium with DAPI (Sigma). Coverslips were sealed with clear nail polish (Various). Slides were allowed to dry for at least 20 min before analysis. The primary antibodies rabbit anti-mouse Foxn1 (kind gift from Manami Itoi, Meiji University of Integrated Medicine) and goat anti-mouse Hhip (R&D systems), were used at 1:200 dilution overnight. The rat anti-mouse Keratin (K) 8 (TROMA-1) or K8-biotin antibodies (DSHB) were used at 1:500 for 1 hour. Secondary antibodies used include Streptavidin-FITC and Streptavidin-APC Cy7 (BioLegend), donkey anti-goat AF488, donkey anti-rat AF555 and donkey anti-rabbit AF647 (Thermo Fisher).

2.10.7 Microscopy

IHC stainings were visualised using the Floid Cell Imaging Station (Thermo Fisher Scientific) or the DeltaVision Elite (GE Healthcare). H&E stainings were visualised using the ICC50 HD microscope (Leica). Images were edited for colour contrast where appropriate and size bars calculated using Adobe Photoshop (Adobe).

2.11 Generation of Hhip$^{lox/lox}$

2.11.1 Transfection for generation of mouse model

sgRNAs for the Hhip$^{lox/lox}$ model were cloned into PX459 plasmids. 2.5 µg of both PX459-sgRNA plasmids and 2.5 µg of the circular homology construct were electroporated into C57BL/6N JM8.F6 ES cells using the Neon transfection system

(Life Technologies) at 3×1400 V for 10 ms. Cells were then plated at low density on mitotically inactivated mouse embryonic fibroblasts. After 24 hours, cells were selected using puromycin-containing media (1.75 μg/ml) for a period of 48 hours and then were cultured for a further 5 days without selection. Individual colonies that survived were isolated and expanded in 96-well plates.

2.11.2 Screening

To duplicate 96-well plates with single ES cell clones, ES cells were split at 70-80% confluency into identical positions on 2 separate 96-well round bottom plates. One feeder plate was used for continued growth and the other plate used for DNA screening. After splitting, plates were incubated at 37°C. The next day, media was changed and plates frozen or used to synthesise DNA. For DNA preparation, plates were washed twice with 1X PBS and incubated with lysis buffer overnight. Digested material was washed and DNA eluted with isopropanol and 70% ethanol.

DNA was amplified using Taq polymerase using the standard genotyping protocol. DNA products expected above 2 kb in size were amplified using the SequalPrep Long PCR Kit (Thermo Fisher Scientific) or Phusion Hot Start Flex DNA Polymerase (NEB) following manufacturer's protocol. Amplified DNA was then analysed on an agarose gel.

2.11.3 Preparation of ES cells for blastocyst injection

ES cell clones identified to contain the correctly recombined *hhip* locus were thawed onto feeder layer coated tissue culture plates and cultured for 2 days until well defined colonies were visible. On the day of injection, cells were trypsinised to obtain a single-cell suspension.

3 week old albino C57BL/6J female mice were superovulated and mated with albino C57BL/6J male mice. Embryos were flushed from the uteri of successfully mated mice on day 3.5 of pregnancy and cultivated for 2-3 hours until the majority of obtained embryos were at the expanded blastocyst stage. ES cell suspensions were then injected into the cystic cavity of individual blastocysts. Following injection, the blastocysts were further cultivated to allow the collapsed blastocysts to recover from the injection and to re-expand. Successfully injected blastocysts then implanted into the uteri of 2.5 day pseudo-pregnant foster CD1 mice, which were prepared by mating 6 week old CD1 mice with vasectomised CD1 male mice.

2.11.4 Breeding

Male mice with a reasonably high percentage of chimerism were mated with albino C57BL/6 female mice to propagate germ line transmission. Sperm was harvested from one high percentage chimera (90%) and used for *in vitro* fertilisation of C57BL/6 donor eggs. Successfully fertilised embryos were implanted into pseudo-pregnant foster CD1 mice.

2.11.6 Transgenic mouse generation

Production of PX459-sgRNAs was carried out by Andrew Bassett (Genome Engineering, University of Oxford). ES cell transfections, blastocyst injections and mouse preparations were conducted by Ben Davies and colleagues (Transgenics Core, University of Oxford). *In vitro* fertilisation and subsequent implantations were conducted by Jackie Sloane-Stanley and colleagues (Transgenic Group, Weatherall Institute of Molecular Medicine).

2.12 Pseudo-bulk sequencing

mTECs and cTECs from E18.5 WT and Hhip-/- mice were sorted for sequencing analysis. Three biological replicates of 200 cells each were sorted for each condition into 96-well V-bottom plates (Eppendorf) containing 2 µl lysis buffer (0.2% Triton-X (Sigma) and 0.5U RNase Inhibitor (Takara)), and frozen at -80°C immediately. Samples were prepared using the Smart-seq2/NexteraXT non-stranded protocol (Picelli, S. *et al.*, 2014). Paired end sequencing (75 bp read length) using the HiSeq4000 platform (Illumina) was conducted for prepared libraries over one lane of a flow cell (Oxford Genomics Centre). QC metrics were generated by the FastQC package and all samples passed QC. Read alignment, quantification and post-mapping QC was performed using pipeline_scrnaseq.py (https://github.com/snsansom/scseq) (Kathrin Jansen, University of Oxford). Briefly, sequence reads were mapped using hisat2 (Kim, D. *et al.*, 2015) using a two-pass strategy and the number of reads mapping to gene models quantitated with the featureCounts program (http://bioinf.wehi.edu.au/featureCounts/). Per-gene Fragments Per Kilobase of transcript per Million mapped reads (FPKM) values were estimated using Cufflinks (Trapnell, C. *et al.*, 2010), and read counts were converted to upper-quartile normalised Transcripts Per Million (TPM) values using Salmon (Patro, R. *et al.*, 2017).

2.13 Statistical analysis

Bar graphs show mean values and error bars represent standard error of mean, calculated by the software Prism (Graphpad). Statistical analysis was conducted using Prism or SPSS (IBM). Probability values were calculated with student's t-test (unpaired, two-tailed, normal distribution) unless otherwise stated. Significance is represented as * $p < .05$; ** $p < .01$; *** $p < .001$. Where appropriate, a one tailed,

non-gaussian, paired t-test was used to analyse experiments when 1 thymi lobe was treated with a compound and the other lobe from the same biological sample used as a untreated control. Bonferroni correction was applied in select cases for qPCR experiments with multiple testing.

3: Identification of *Hhip* as a Novel Foxn1 Target in TECs

Despite clear evidence that Foxn1 is a master regulator of TEC differentiation and function, detailed knowledge beyond Foxn1 acting as a transcription factor was limited as only a few specific target genes were known that were transcriptionally regulated by Foxn1. Recent molecular studies from my research group have yielded a list of candidate genes whose expression are lost upon deletion of Foxn1 activity, thus implying these loci to be positively regulated (either directly or indirectly) by Foxn1 (Žuklys, S. *et al*., 2016). Given the paramount importance of Hh signalling in organ development, I set out to identify molecules within this pathway that might be controlled by Foxn1 in their expression and could therefore be direct targets of Foxn1-mediated transcriptional control.

3.1 Preliminary evidence positioning *hhip* downstream of Foxn1

Chromatin immunoprecipitation sequencing (ChIP-seq) analysis was used to identify potential genes which could be bound by Foxn1. This identified a 5-nucleotide Foxn1 consensus binding motif of GACGC (Žuklys, S. *et al*., 2016) (3.1A), almost identical to a previously published 4-nucleotide sequence (ACGC) identified by electrophoretic mobility shift assay (Schlake, T. *et al*., 1997). ChIP-seq data was compared against RNA sequencing data obtained from mouse models with a complete absence of *foxn1,* in which a hypomorphic variant of Foxn1 was expressed mono-allelically, or where Foxn1 was postnatally ablated in cTECs (Žuklys, S. *et al*., 2016). These studies revealed a preliminary list of candidate genes (Table S2 in Supplementary) that had a Foxn1 ChIP-seq binding peak near their transcriptional start site (TSS) and were significantly downregulated in TECs upon loss of *foxn1* when compared to WT cells, as verified by EdgeR, DESeq and

Cuffdiff programs. Hence, these candidate genes were likely directly regulated by Foxn1. Several genes in this list had previously been demonstrated as likely targets of Foxn1-controlled transcription and were important for thymus function, such as *dll4*, *ccl25* and *cd83* (Tsukamoto, N. *et al*., 2005; Nowell, C. *et al*., 2011; Fujimoto, Y. *et al*., 2002). The list also contained, however, 28 high confidence candidate genes that had thus far not been put in context of thymus organogenesis. For many of these sequences, little functional information was known.

To evaluate if these above mentioned high confidence genes were expressed in Foxn1-expressing cells at reasonable levels which could allow for further experimental work, adult wild-type (WT) C57BL/6 TECs were sorted and analysed for mRNA expression using qPCR (3.1B). All candidate genes were detectable in both cTECs and mTECs, albeit at varying levels. A detailed literature review was conducted in par to contextualise if any of these genes were likely to play a functional role in the thymus. Certain genes had not yet been directly studied in the thymus, but showed great potential for a putative role in regulating T cell development, such as *mreg*, which controls homeostasis of cathepsin D, where cathepsin D-deficient mice display apoptosis of lymphoid cells in the thymus (Frost, L. *et al*., 2013; Benes, P. *et al*., 2008), or *hes6*, a part of the Notch signalling pathway which as discussed previously is essential for T cell lineage commitment (Pissarra, L. *et al*., 2000). Another gene in this list was *hhip*, an inhibitor of Hh signalling, a pathway known to be significant for both proper T cell development and thymus organogenesis. Importantly, unlike many of the other candidate genes, there were no known homologs of *hhip* which could potentially compensate for a loss-of-function setting. This positioned *hhip* as an excellent candidate for investigation. mRNA transcripts of *hhip* were expressed at clearly detectable levels

in both cTECs and mTECs. Expression levels were within a similar range to that of *foxn1* (3.1B). Foxn1 ChIP-seq data (Žuklys, S. *et al.*, 2016) revealed in the context of the *hhip* locus a single significant peak near the transcriptional start site (TSS) with an irreproducible discovery rate (IDR) of <0.05 within 5 kilobases (kb) upstream and 100 basepairs (bp) downstream (3.1C). RNA-seq analysis demonstrated that *hhip* was expressed at 26.3 fpkm in WT cTECs, but this expression was reduced to 8.03 fpkm when Foxn1 was conditionally ablated in cTECs, resulting in a differential log2 fold change of 1.71 (p=0.0002) (3.1D). Although this fold change was modest in comparison to some of the other high confidence target genes (Žuklys, S. *et al.*, 2016), it nonetheless positioned the *hhip* gene as downstream of Foxn1.

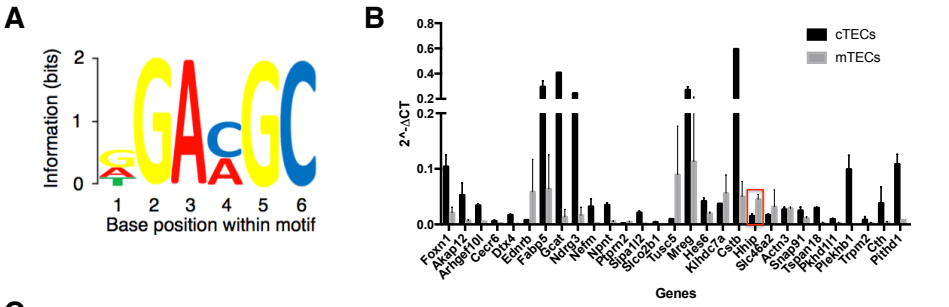

Gene	WT (fpkm)	KO (fpkm)	Log2	Test Statistic	p	Direction	Foxn1 ChIP-Seq Peak
Hhip	26.3032	8.02743	1.71223	3.35412	0.0002	WT>KO	Yes

Figure 3.1: Initial selection of *hhip* as candidate of interest based on ChIP-seq and RNA-seq data
(A) MEME-ChIP-derived Foxn1 binding site motif GAC/AGC for TSS-associated peak, reproduced with permission from Žuklys, S. *et al.*, 2016. **(B)** qPCR analysis of candidate Foxn1 targets, *foxn1*, and *hhip* expression in primary TECs sorted from 2 week old C57BL/6 WT mice. TECs were sorted as CD45-Epcam+ live single cells, and further distinguished as cTECs or mTECs by Ly51 and UEA-1 expression. Values are normalised to *gapdh* expression. 2 independent experiments were conducted with technical triplicates and pooled. **(C)** Foxn1 ChIP-seq data shows clear peak in red box near transcriptional start site of *hhip,* shown on the reverse strand in blue. **(D)** Bioinformatics analysis of RNA-seq data shows expression of *hhip* in primary cTECs from1 week old C57BL/6 WT mice (denoted as WT) compared to cTECs from a mouse model where exons 7 and 8 of the *foxn1* locus have been deleted in a doxycyclin-induced manner (denoted as KO), fold change of the two (log2), and the statistical validity (p).

3.2 Hh signalling genes are expressed by both TECs and T cells

Hhip expression was further verified both *ex vivo* and *in vitro* to confirm its relevance in the context of thymus biology. *Hhip* and other integral members of the

Hh signalling pathway were expressed in primary adult TECs sorted from WT C57BL/6 mice at 2 and 4 weeks of age (3.2A, 3.2B). The expression levels of individual genes required for Hh signalling pathway gene as tested by qPCR correlated with RNA-seq data from 1 week old WT mice (Sansom, S*. et al*., 2014). Basic regression analysis gave an R^2 value of 0.927 for the Hh genes in cTECs and 0.794 in mTECs. All Hh genes except the ligand Shh were expressed in T cells, albeit at much lower levels compared to TECs (3.2C). In particular, *hhip* was expressed highly in TECs concurrent with the detection of *foxn1*, which is not expressed by T cells (3.2D). Transcripts for *hhip* and the three Hh ligands were also confirmed in embryonic thymic cells isolated at distinct gestational ages to establish the suitability of investigating a loss of Hh signalling in early thymic development. *Hhip* mRNA was robustly expressed in embryonic TECs (3.2E). Transcripts for the Hh ligands *shh*, *ihh* and *dhh* were also detected in TECs but at lower copy numbers. *Ihh*-specific mRNA was barely detectable. Of note, *hhip* transcripts were not found in embryonic T cells (3.2F). These results are in line with published data demonstrating that Hh signalling occurs in the thymus, corroborating the involvement of Hh signalling machinery in TEC and T cell developmental biology (reviewed in Crompton, T. *et al*., 2007). Furthermore, the presence of *hhip* transcripts in TECs is in concordance with the claim that *hhip* is a candidate target of Foxn1. *Hhip* was also expressed in the murine cortical cell line cTEC1.2, but lowly in medullary mTEC2.3 and mTEC1C6 cells (3.2G). Finally, Hhip protein expression was confirmed in primary TECs by immunohistochemistry of frozen thymus sections. Here, Hhip was sparsely distributed throughout the thymic cortex and medulla of 4 week old WT mice (3.2H). No preferential localisation of Hhip was observed by eye within the thymic architecture.

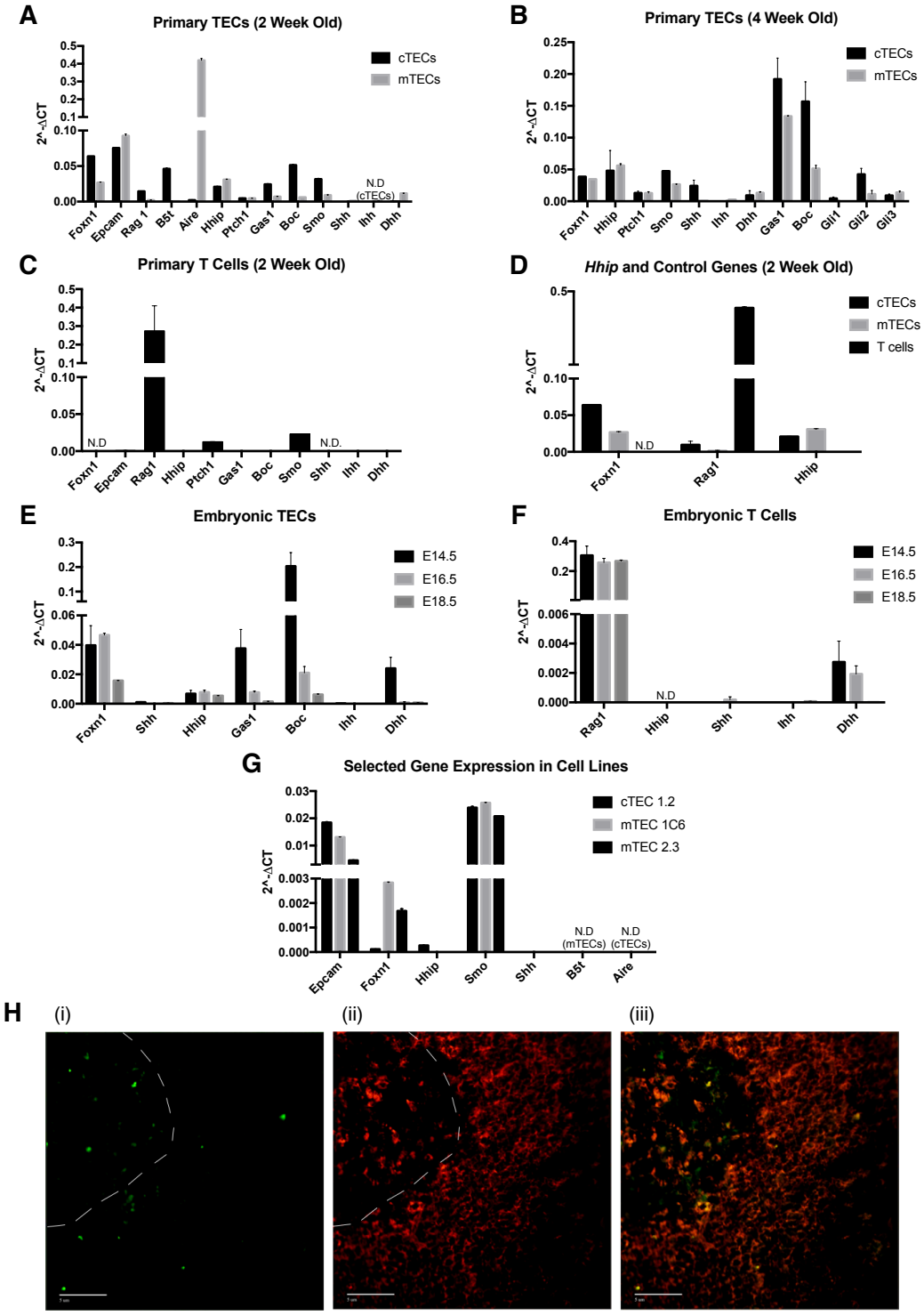

Figure 3.2: Expression of Hh genes in the adult and embryonic primary TECs, T cells and TEC cell lines
qPCR shows expression of integral members of the Hh signalling pathway in **(A)** 2 week old and **(B)** 4 week old WT C57BL/6 sorted TECs. **(C)** Expression of Hh signalling genes in 2 week old WT C57BL/6 T cells. T cells were sorted as CD45+Lin-Epcam- live single cells. **(D)** *Hhip* and control genes' expression in TECs and T cells. *Hhip* and Hh signalling members in **(E)** embryonic WT TECs and **(F)** embryonic WT T cells at various developmental stages. *Foxn1* and *rag1* are shown as internal controls. **(G)** Gene expression in murine cell lines. *Epcam, foxn1, b5t (psmb11)* and *aire* are shown as TEC control genes. 2-ΔCT values are normalised to *gapdh* expression. **(H)** Immunohistochemistry (IHC) staining of 6 um 4 week old WT C57BL/6 frozen thymus sections using a 60X objective, with (i) Hhip and (ii) K8, showing (iii) expression of Hhip protein in both the thymic cortex and medulla. White dotted lines demarcate the cortex and medulla.

3.3 Confirmation of *hhip* as a direct Foxn1 binding target

Three consensus binding motifs, referred to as BS1, BS2, and BS3, were identified within the Foxn1 ChIP-seq peak near the *hhip* TSS (3.3A). Using Crispr/Cas9 technology, synthetic guide RNAs (sgRNAs) were designed to specifically target and cleave these sites. sgRNAs for each site were chosen based on their MIT design algorithm (http://crispr.mit.edu) results, where selected guides were predicted to have no off-target effects and induce cleavage within the motif, resulting in indel insertion during cell-directed non-homologous end joining repair and thus disruption of the specific binding motif (Bassett, A. *et al.*, 2013). These sgRNAs were transfected in a PX330 plasmid vector (Cong, L. *et al.*, 2013) into the cTEC1.2 cell line for 48 hours. Compared to either vehicle control (an empty plasmid vector containing only Cas9 mRNA but no sgRNA) or sequence control (an sgRNA targeting a non-significant sequence upstream of the TSS, designated NS Site), *hhip* expression was significantly reduced when any of the three binding sites were ablated (3.3B). These results suggest that compromising the ability of Foxn1 to bind to any of its binding motifs upstream of the TSS interferes with *hhip* expression, and therefore directly demonstrate that *hhip* is a Foxn1 target gene.

A

```
ATGAGAGGCT GTGTGAGAAG CTGCAGCCGC CGGCAGAGGA GACCTCAGCA  50
TCCTCGGGAG CCCAGCGCCA ACCCTGCCTC CGCCCGGCCC GCTGCCACCA  100
CCGCCGCCCT TTCGGTTCCT GCTACTGTCT CACCTAAACA ACTCCCATTC  150
AGCGGACAAG CGAAGTTCTA TGACTCTCTT CTCCTCTCCT TCCTCCTCTT  200
CTTCCAACTC CTTCTCCTCC CACTTCCCAA CCGCTGTGGA AAGCCCCTAA  250
CCCAACAGAC GCTGGCAAGG CTGCGGACAA GTGTCATCTG CACTTTATCT  300
TGCTGCTCCT ACTGCCCTAA GGCAAAGTTG CATAGCTCTA CATCTTTCTT  350
TCCCAGCCAC CTCCCTCTGC CCCCAAGAGC GTCCCGCCGC CCCGCAGCAC  400
TCTCCTGGAG CTGCGCCCTA GTGCCCCTGC TGGGCAGTGG CCTTTCCCCC  450
ACCCCATCCT CCCGCGTCCT GCCCTTGCTG CTCCGGGCAG ACG

BS1: Position 258-262
BS2: Position 379-403
BS3: Position 464-468
```

B **Levels of *Hhip* Upon Crispr Knockdown of Foxn1 Binding Sites in cTEC1.2**

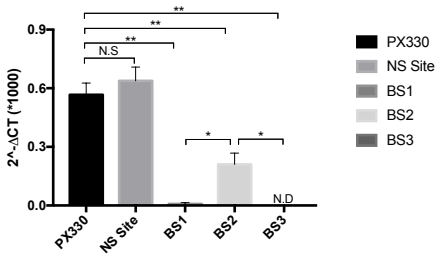

Figure 3.3: Ablation of Foxn1 binding sites affects *hhip* expression
(A) Foxn1 binding motifs (GACGC) were identified within the TSS-associated Foxn1 ChIP-seq peak of *hhip*, where the first nucleotide within this peak on the reverse strand was denoted as position 0. **(B)** Binding sites BS1, BS2 and BS3 were targeted using Crispr/Cas9 design and cleaved in the cTEC1.2 cell line by transfection for 48 hours. The empty plasmid vector PX330 was used as a control, as well as an sgRNA targeting a non-significant site (NS Site). 2 independent experiments were conducted and pooled, and values normalised to *gapdh* expression. P-values were determined by student's t test where * $p < .05$; ** $p < .01$.

This preliminary data, together with a detailed literature survey corroborated a very likely role of Hhip in thymus biology and underscored the relevance of studying the role of *hhip* in thymus organogenesis and function.

4: Shh signalling mediated by Hhip is relevant in cTECs and forms a feedback loop with Foxn1

Hh signalling modulates various aspects of thymocyte development in the embryonic thymi (reviewed in Barbarulo, A. *et al.*, 2016). This contention has primarily been established using genetic mouse models displaying reduced Hh signalling, following the loss of expression of key elements of the Hh pathway such as Shh, Smo, and Ptch1. However, loss of Hhip has not been directly investigated. I sought firstly to characterise the direct effects of Hh signalling on TEC and T cell development and delineate the role of Hhip in this context, and secondly to understand the relationship between Foxn1, Hhip and the Hh signalling pathway. For this purpose, two *in vitro* experimental models were used, namely the fetal thymic organ culture (FTOC) system and TEC cell lines. Both systems allow convenient *ex vivo* experimental manipulation, enabling the study of thymus biology when Hh signalling is exogenously altered.

4.1 Modulating Hh signalling affects thymocyte development at E18.5 within 4 days

As Hhip is an inhibitor of Hh signalling, loss of *hhip* should result in a phenotype consistent with increased Hh signalling. The E18.5 embryonic thymi contains distinct cTEC and mTEC populations and has been seeded with haematopoietic progenitors, allowing analysis of both TEC and thymocyte development. E18.5 WT C57BL/6 thymi were cultured as FTOC in the presence of 0.5 µg/ml recombinant Shh (rShh) protein. This concentration has previously been carefully established to be effective to influence lymphoid development in E14.5 and E17.5 WT thymi

(Outram, S. *et al.*, 2000). FTOC revealed after 4 and 7 days that addition of rShh reduced the production of mature CD4 T cells (see Supplementary for full gating strategy). Correspondingly, more DP thymocytes accumulated (4.1A, 4.1B), a finding consistent with results reported in the literature (Rowbotham, N. *et al.*, 2007). These changes were more prominent after 7 days of culture. However, while thymic cellularity was comparable between treated and untreated cultures, cell numbers of lymphocytes recovered from FTOC treated for 7 days were significantly lower than that of 4 days ($1.85 \pm 0.3 * 10^6$ vs $0.53 \pm 0.1 * 10^6$ in the non-manipulated WT setting), despite the similar presence of an altered CD4 phenotype (4.1C). This is an acknowledged disadvantage of the *ex vivo* culture system and not likely a reflection of rShh toxicity (Takahama, Y., 2000). All further FTOC experiments with E18.5 thymi were therefore restricted to a 4 day culture period to ensure consistency and robustness of the experimental conditions.

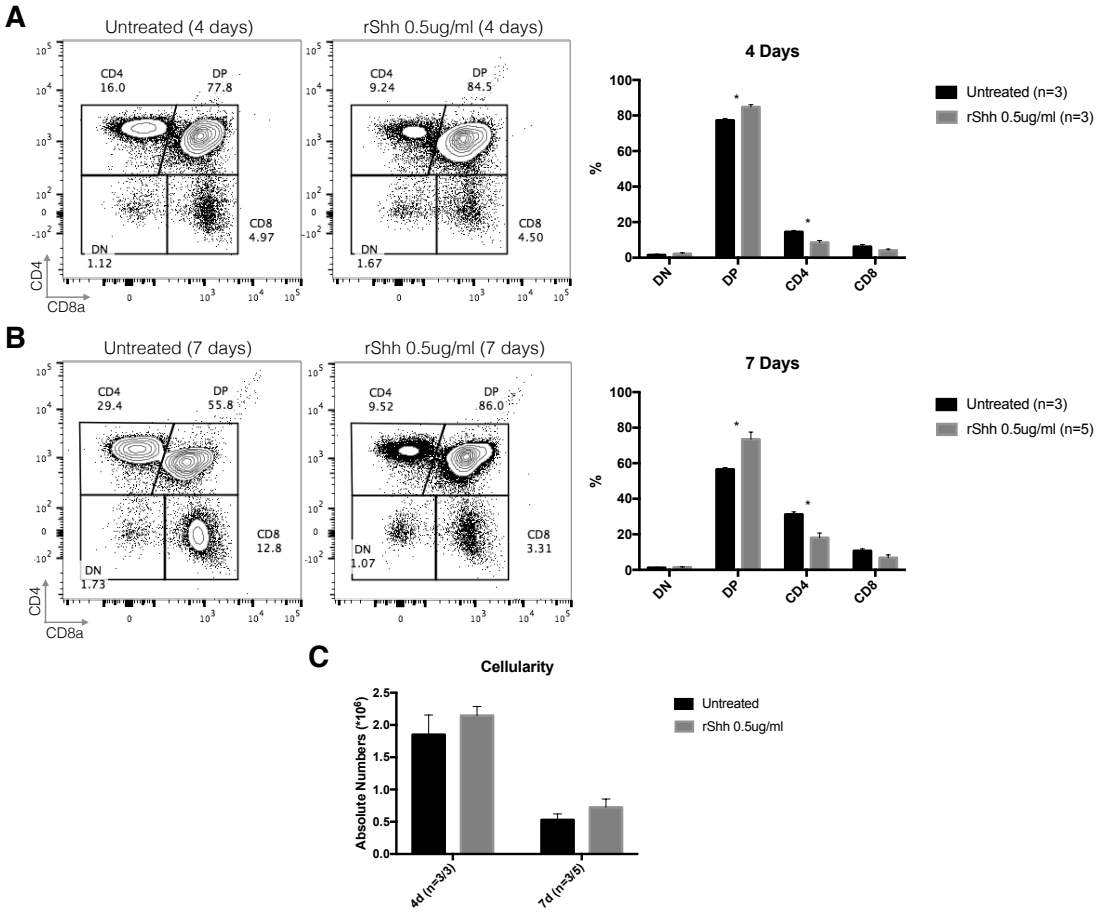

Figure 4.1: FTOC culture for 4 days gives similar phenotype and more cells compared to 7 day culture
Thymi from WT C57BL/6 E18.5 embryos were isolated and grown as FTOC. rShh protein was added to the FTOC culture media of half the samples, while the other half received normal unmodified media (Untreated) for either **(A)** 4 days or **(B)** 7 days. Total live Lin- single T cells were gated and divided into thymocyte subpopulations by CD4 and CD8a expression. **(C)** Absolute cell numbers recovered after processing of the thymi were counted before FACS analysis. FACS plots show representative samples of each condition. Graphs shown are from a single experiment and are representative of at least 2 independent experiments. P-values were determined by student's t test where * p < .05. Total experimental size: 4 days WT n=11, rShh n=11; 7 days WT n=6, rShh n=8.

4.1.1 Increased Shh signalling causes delayed maturation of single positive CD4 T cells

Further analysis of T cells from WT E18.5 FTOC in the presence of 0.5 µg/ml rShh did not reveal any changes in the overall frequencies of cells in each DN stage (4.2A, 4.2B), although more cells with a DN2 phenotype seemed to progress to DN3 (85.6 ± 1.9% vs 64.9 ± 4.8%) upon exposure to exogenous rShh signalling (4.2C). This finding is in agreement with a previous observation that Shh signalling accelerates the differentiation and survival of thymocytes in the absence of pre-TCR signalling (El Andaloussi, A. *et al.*, 2006). The maturational progression to the

DN3 stage coincided with an upregulation of CD5, in keeping with Shh's role as a negative regulator of signalling via the pre-TCR (Azzam, H. *et al.*, 1998; Rowbotham, N. *et al.*, 2009). Consistent with these changes, the geometric mean fluorescence intensity (gMFI) of TCRβ on DN3 cells was increased in parallel (4.2D).

Despite the accelerated progression of DN cells, further maturation of thymocytes into $TCR\beta^{+}$ single positive T cells appeared impaired, as an increased proportion of immature $TCR\beta^{low}CD5^{low}$ thymocytes (18.9 ± 0.7% vs 25.1 ± 2.1%) was observed, accompanied by a decrease in frequencies of more mature $TCRB^{hi}CD5^{hi}$ cells (22.1 ± 0.7% vs 11.3 ± 1.0%) (4.2E). Analysis of the single positive lineages revealed that increased Shh signalling resulted in a CD4-specific maturational defect. While the proportion of mature CD8 (mCD8) cells ($CD8a^{+}TCR\beta^{+}$) was reduced in treated cultures as compared to untreated controls as a proportion of the total CD8 population (83.0 ± 4.5% vs 65.8 ± 6.3%), this difference was not statistically significant when related to the overall T cell cellularity of the FTOC (4.10 ± 0.9% vs 3.47 ± 0.8%) (4.2A, 4.2F). In contrast, newly single positive CD4 cells ($CD4^{+}CD25^{-}CD69^{hi}CD24^{hi}$), hereafter referred to as immature CD4 (iCD4), were increased as a proportion of total CD4 T cells (4.2F). The frequency of the most mature CD4 population ($CD4^{+}CD25^{-}CD69^{low}CD24^{low}$), hereafter referred to as mCD4, was decreased both relative to the CD4 compartment (61.5 ± 1.9% vs 34.5 ± 6.8%) and as a percentage of total T cells (8.63 ± 0.6% vs 3.01 ± 0.9%) (4.2A, 4.2F). These results confirmed the importance of Shh in maintaining regular T cell development, and provided a reference point to understand how a loss of Hhip could potentially influence Hh signalling in the thymus.

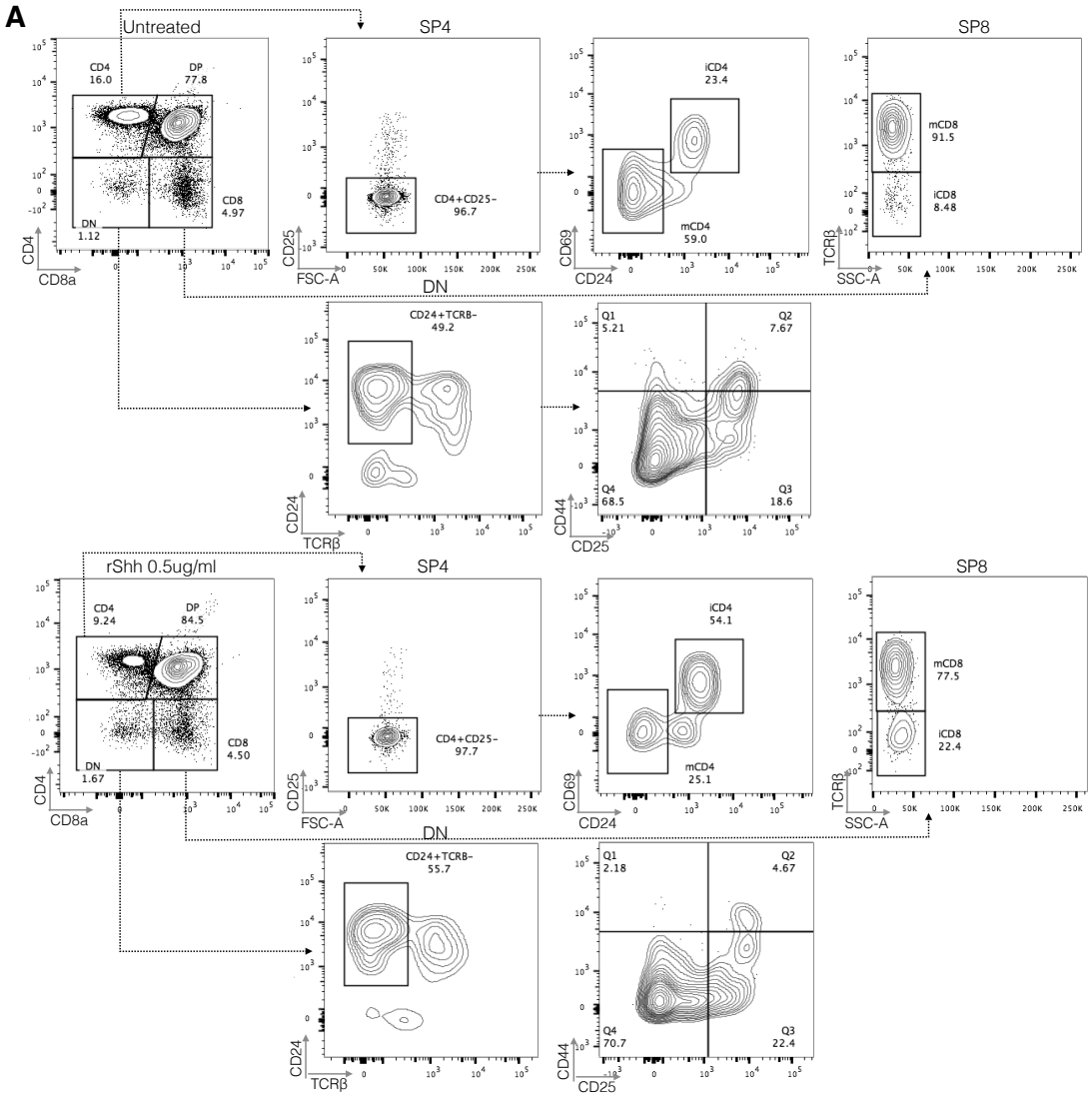

Figure 4.2: Addition of rShh to E18.5 FTOC results in decreased maturation of mCD4 T cells
(A) Development of individual thymocyte subpopulations in E18.5 FTOC was assessed for effects of exposure to rShh protein, compared to untreated. CD25- SP CD4 cells were gated and identified as iCD4 (CD69hiCD24hi) and mCD4 (CD69lowCD24low). SP CD8 cells were identified as mCD8 (TCRβ+) and iCD8 (TCRβ-). True DN (CD24+TCRβ-) cells were divided into stages by CD44 and CD25 expression.

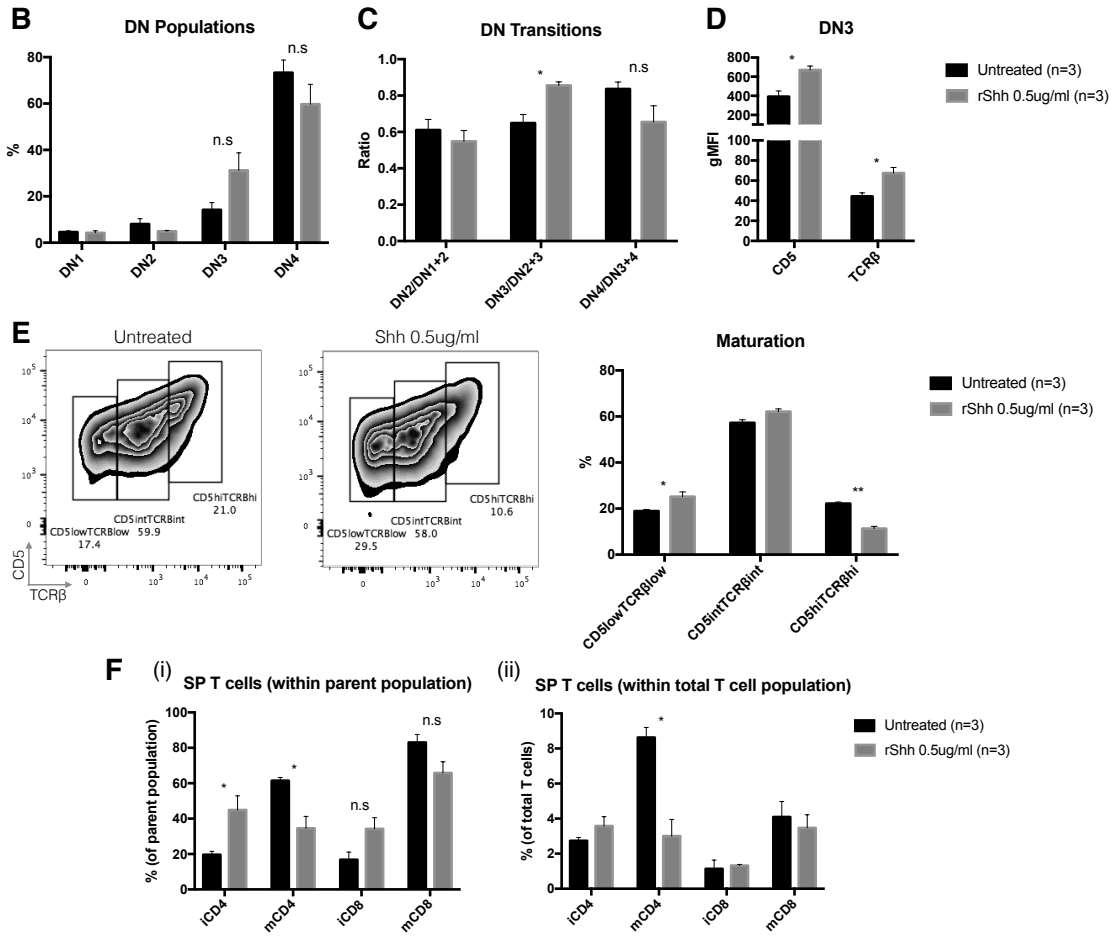

Figure 4.2: Addition of rShh to E18.5 FTOC results in decreased maturation of mCD4 T cells
(continuation) **(B)** The total DN population was gated as live CD4-CD8-Lin-CD24+TCRβ- single cells, and frequencies of DN cells in the DN1 (CD44+CD25-), DN2 (CD44+CD25+), DN3 (CD44-CD25+) and DN4 (CD44-CD25-) stages are shown. **(C)** Transitions between each DN stage were calculated by taking the frequency of cells in each stage, and dividing it by the total frequency of cells in that stage and the previous e.g DN2/DN1+2, and so on. **(D)** Cell surface concentrations represented by geometric mean fluorescence of CD5 and TCRβ are shown for the DN3 population. **(E)** Total Lin- single T cells were assessed for untreated and rShh conditions for CD5 and TCRβ expression to analyse maturation. **(F)** Immature and mature single positive T cell subpopulations, previously gated in (A), as a frequency (i) of the parent SP CD4 or CD8 populations, or (ii) of total T cells. Experiment shown is representative of at least 3 independent experiments. P-values were determined by student's t test where * $p < .05$, ** $p < .01$. Total experimental size: WT n=11, rShh n=11.

4.1.2 Addition of rHhip at E18.5 is insufficient to alter thymocyte development

FTOC with E18.5 WT thymi were next exposed to a maximal concentration of recombinant Hhip protein (rHhip) at 1.0 µg/ml (Saldaña, J. *et al.*, 2016) to evaluate whether an excess of Hhip would inhibit endogenous Hh signalling and result in a phenotype opposite to that observed when rShh was added. The presence of rHhip for 4 days of culture did not alter the overall T cell phenotypic profile (4.3A, 4.3C) or cellularity (4.3B). While the relative percentages of iCD4 and mCD4 T cells seemed slightly altered (4.3A), this was not statistically significant (4.3D). However, rHhip

appeared to accelerate maturation as assessed by TCRβ and CD5 expression, where the relative percentage of TCRβ^{hi}CD5^{hi} cells increased from 16.6 ± 1.1% to 20.4 ± 0.6% (4.3E). This alteration was accompanied by increased cell surface detection of TCRβ, CD5 and the cellular activation marker CD69 on all mature single positive T cell subpopulations (4.3F, 4.3G).

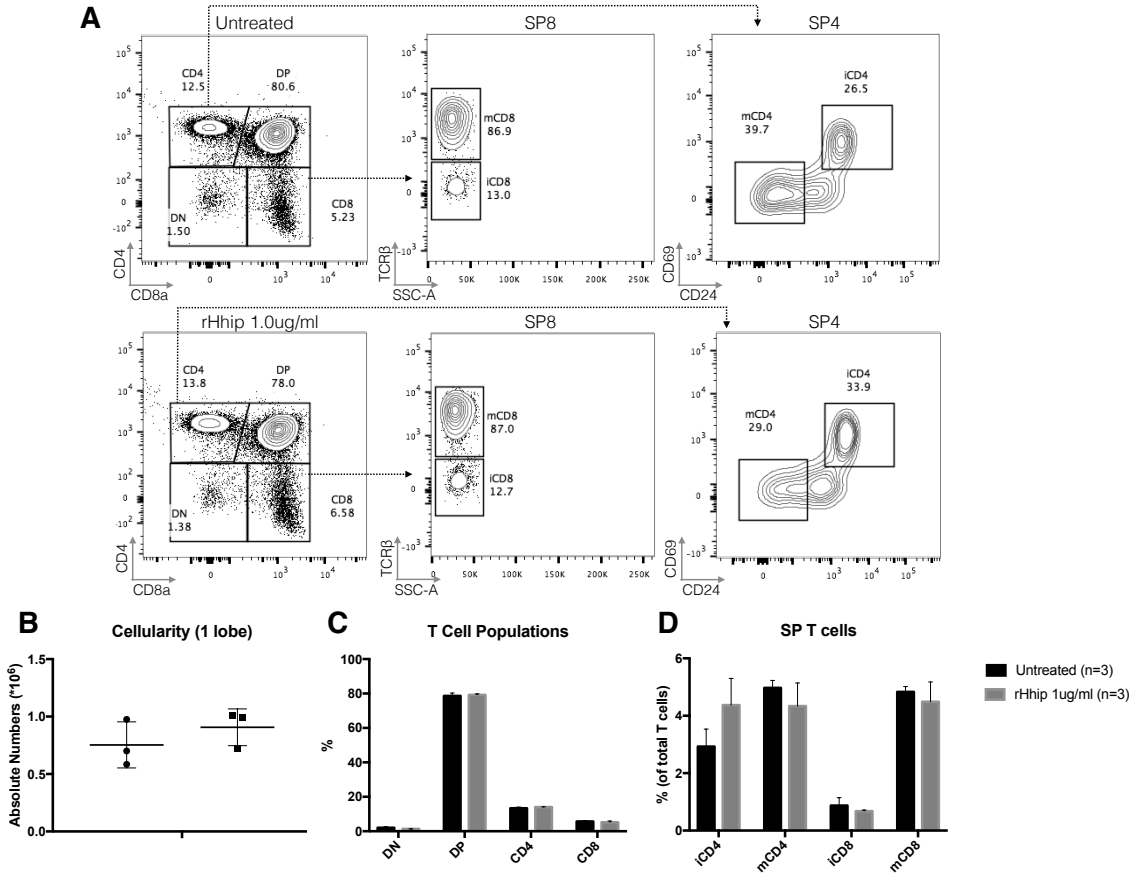

Figure 4.3: rHhip culture does not affect overall thymocyte profile but impacts TCRβ and CD5 expression
(A) Representative FACS plots show profiles of CD4 and CD8 T cells in E18.5 FTOC either treated with rHhip or untreated. **(B)** Overall cellularity, **(C)** frequencies of T cell thymocyte subpopulations and **(D)** proportions of immature and mature CD4 and CD8 subpopulations as a proportion of total T cells are shown.

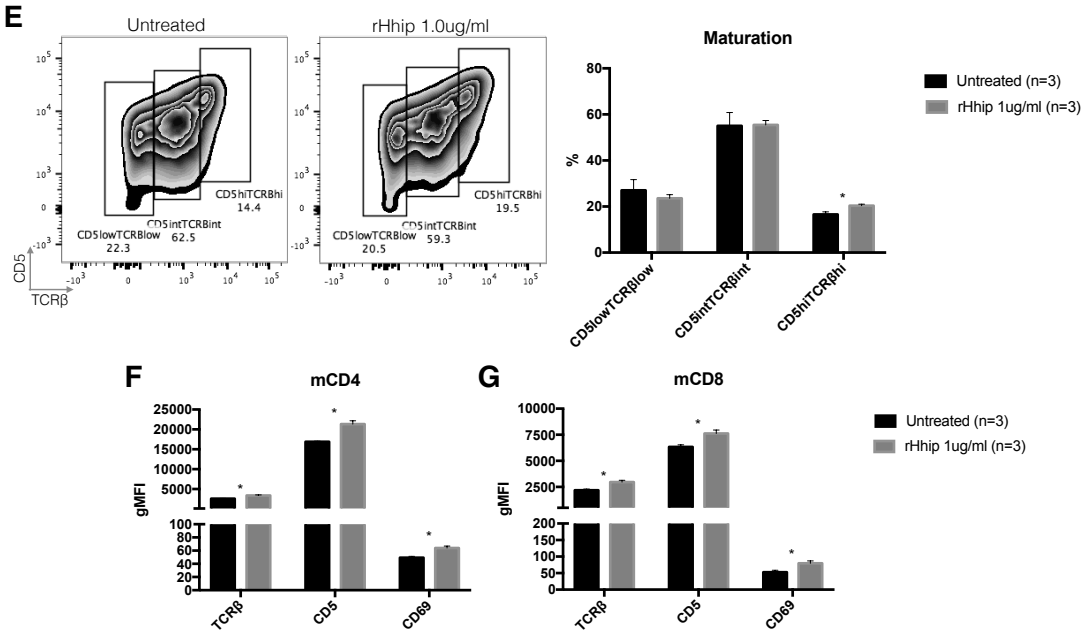

Figure 4.3: rHhip culture does not affect overall thymocyte profile but impacts TCRβ and CD5 expression (continuation) **(E)** Frequencies of total T cells expressing varying levels of CD5 and TCRβ are shown. Geometric mean levels of TCRβ, CD5 and CD69 are shown for **(F)** mCD4 and **(G)** mCD8 T cells. P-values were determined by student's t test where * $p < .05$. Experiment shown is representative of 2 independent experiments. Total experimental size: WT n=6, rHhip n=6.

Expression of the cell surface markers CD5, CD69 and TCRβ usually parallel the response to TCR signalling and may indicate changes in thymocyte selection, although this is traditionally studied on DP cells and not single positive T cells (Yamashita, I. *et al.*, 1993; Tarakhovsky, A. *et al.*, 1995). The lack of differences in frequencies of individual T cell populations in the presence of rHhip may suggest that Hh signals need to be limited below a certain level to ensure normal thymocyte development, as shown by the aberrant thymocyte development observed in the rShh-supplemented FTOC. Decreases in signal intensities beyond such a threshold, for example in the presence of rHhip, are therefore unlikely to drastically affect overall T cell differentiation, at least as observed in the E18.5 FTOC. Alternatively, these observations could relate to an artefact of the chosen FTOC culture length, whereby Hh inhibition might require more time to take effect. Nonetheless, the results suggest a possible role for Hhip in regulating the normal maturation and TCR signalling of thymocytes.

4.1.3 Blocking of Shh binding by 5E1 does not affect thymocyte development and appears functionally distinct from rHhip

In order to establish if Hhip's sole thymic function is to limit Hh signalling by sequestration, WT E18.5 thymi were cultured in the presence of 5E1, an anti-Shh antibody. Despite binding to the same pseudo-active groove of Shh as Hhip, 5E1 does not functionally coordinate the pseudo-active site unlike Hhip, instead physically occupying the site and preventing downstream Shh signalling (Maun, H. *et al.*, 2010). Similar to rHhip, 5E1 did not alter the overall T cell profile at a concentration of 5 µg/ml, which was previously shown to be effective for the neutralisation of Shh protein (Outram, S. *et al.*, 2000) (4.4A). However, unlike rHhip, changes in TCRβ and CD5 cell surface concentrations were not detected, both in terms of frequencies of positive cells (4.4B) as well as gMFI levels (data not shown). This could imply a potential functional role for Hhip in the thymus aside from simply obstructing Shh availability.

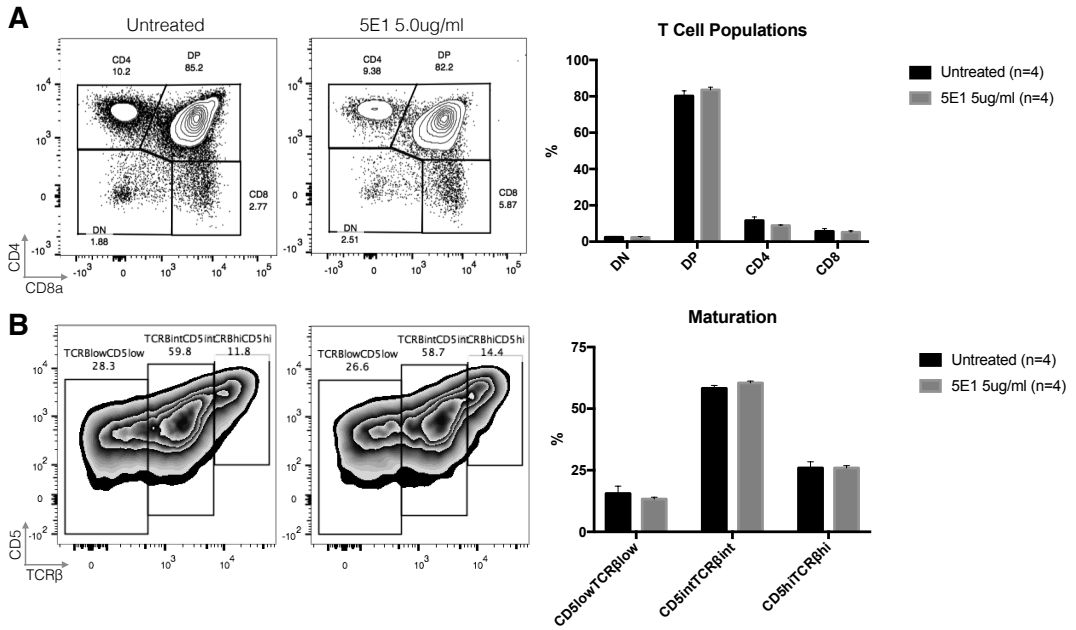

Figure 4.4: 5E1 impacts neither development nor maturation of thymocytes in E18.5 FTOC
(A) FACS plots and statistics of live single Lin- T cell subpopulations representative of 2 independent experiments probing the effect of Hh inhibition with 5E1. **(B)** TCRβ and CD5 expression profiles of total T cells are shown. Total experimental size: WT n=7, 5E1 n=7.

4.1.4 Inhibiting Hh signalling downstream using selective Gli inhibitors severely affects normal thymocyte maturation

The increased availability of rHhip or 5E1 may not necessarily equate to complete inhibition of downstream Hh signalling, given the complexity of the pathway where Hh and its corresponding signalling machinery are not always expressed within the same cell, and Hh is able to move across relatively long distances (Chuang, P. & McMahon A., 2005; Callejo, A. *et al.*, 2006). Allowing rHhip and 5E1 to freely diffuse in the FTOC culture media might also have been inadequate for the inhibitors to successfully enter the thymi and migrate to where Hh was located. To probe whether this contention is correct, GANT61, a selective inhibitor targeting the 2 primary transcriptional activators of the Hh signalling pathway, Gli1 and Gli2, was cultured with E18.5 WT thymi. The presence of 10 μM GANT61 resulted in a significant increase in the DN population (1.6 ± 0.2% to 3.76 ± 0.5%). Consequently, a significant reduction of single positive CD4 T cells (11.9 ± 1.1 % vs 6.91 ± 1.5%) was also observed (4.5B, 4.5C). Both iCD4 and mCD4 frequencies were reduced, while an intermediate CD4 population ($CD4^{+}CD25^{-}CD69^{low}CD24^{int}$), referred to as semi-mature CD4 (smCD4), was increased relative to iCD4 and mCD4, but not as a proportion of total T cells (4.5C). The population of mCD8 thymocytes was also reduced (3.39 ± 0.5% vs 1.81 ± 0.4%) in the presence of GANT61 (4.5C). In addition, significantly lower expression of TCRβ was observed for all single positive T cell populations, whereas CD24 expression was increased, a marker for immature T cells. CD69 and CD5 gMFI levels were downregulated on several single positive T cell populations (4.5D, 4.5E). This reduction was accompanied by a change in the frequencies of TCRβ and CD5-positive cells, resulting in an increased frequency of immature $CD5^{low}TCR\beta^{low}$ thymocytes in the FTOC exposed to GANT61. The cell surface density of TCRβ also changed in

GANT61-supplemented cultures, requiring bespoke flow cytometry analysis gates (4.5F).

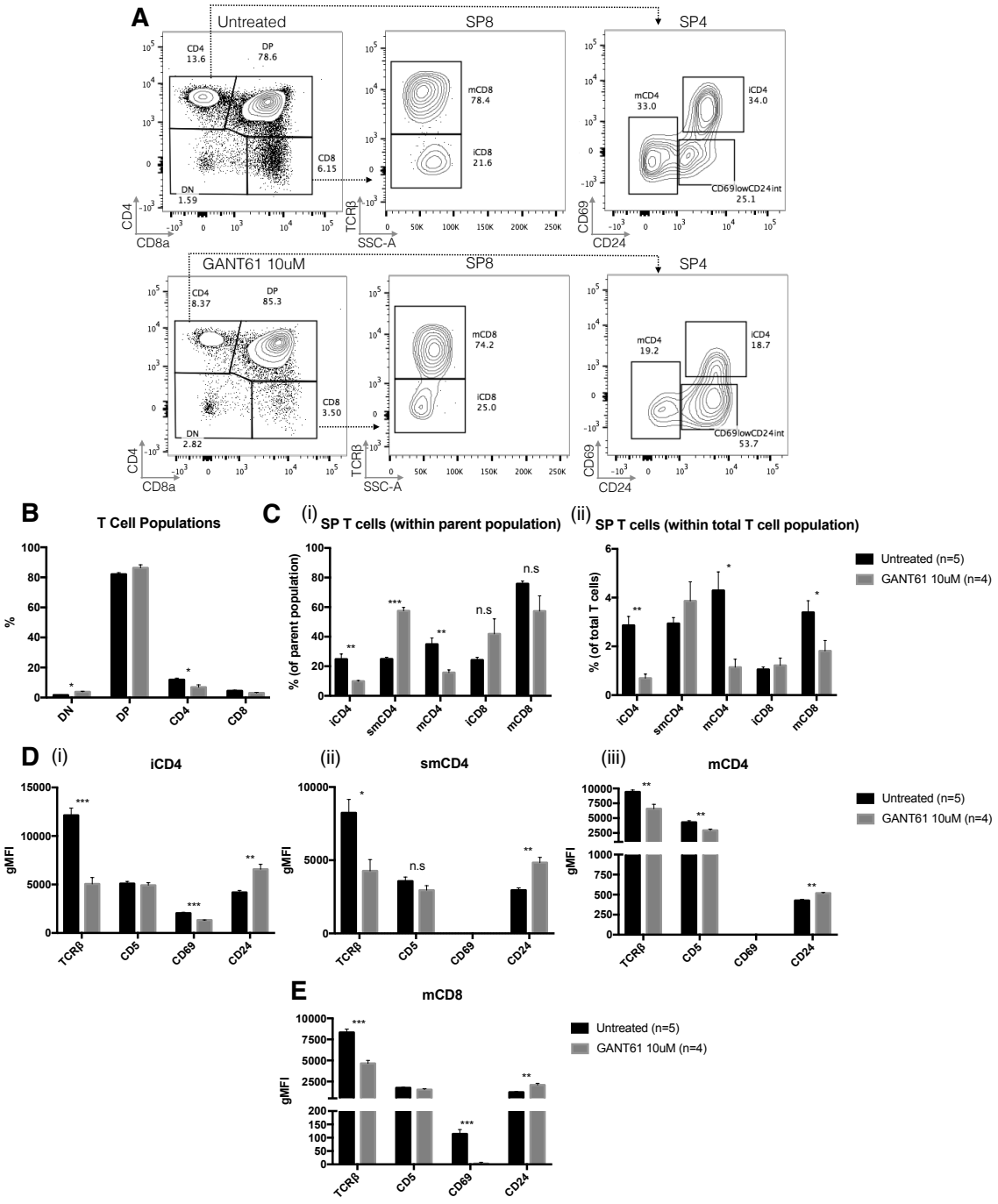

Figure 4.5: GANT61 negatively affects single positive T cell development and maturation
(A) Thymocyte subpopulations were compared between untreated E18.5 FTOC and FTOC treated with the Gli inhibitor GANT61. **(B)** Frequencies of thymocyte subpopulations are shown for each condition. **(C)** Frequencies of immature, semi-mature and mature CD4 and CD8 subpopulations are shown (i) as a frequency of the parent CD4 or CD8 population, and (ii) as a percentage of total T cells. **(D)** Expression of TCRβ, CD5, CD69 and CD24 were assessed for (i) iCD4, (ii) smCD4 and (iii) mCD4, as well as **(E)** mCD8 populations.

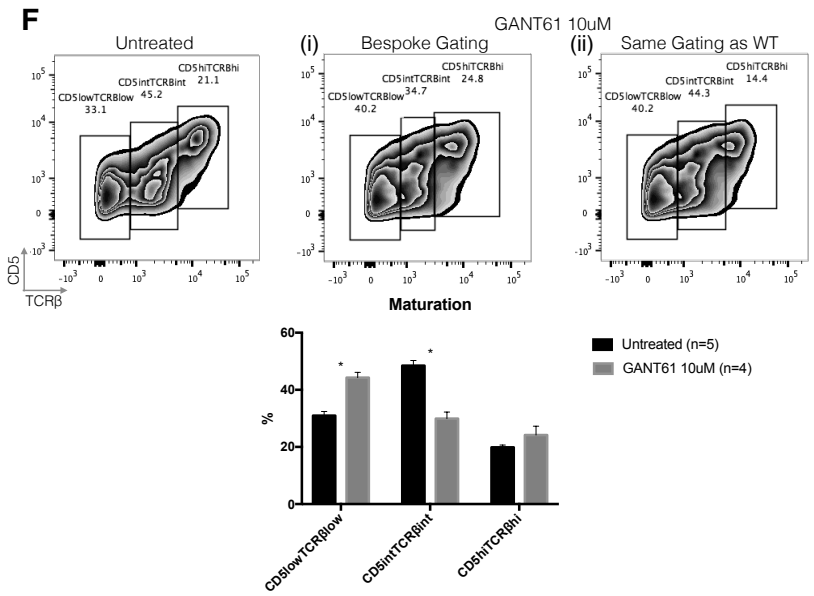

Figure 4.5: GANT61 negatively affects single positive T cell development and maturation
(continuation) **(F)** Frequencies of TCRβ and CD5-expressing Lin- live single T cells are shown for both untreated and GANT61 conditions. Two gating strategies were used, (i) a bespoke gating strategy where the three visually distinct cell populations are gated, and (ii) the same gating strategy used for untreated cells. Both yielded statistically different results from WT. Statistics here demonstrate frequencies obtained using the bespoke gates. Experiment shown is representative of 2 independent experiments. P-values were determined by student's t test where * $p < .05$, ** $p < .01$, *** $p < .001$. Total experimental size: WT n=7, GANT61 n=7.

Changes in TCRβ, CD5 and CD69 expression may reflect defects in the process of TCR engagement and positive selection, where the presence of more $TCR\beta^{low}CD5^{low}CD69^{low}$ cells for example could represent an inability of thymocytes to successful interact with pMHC complexes presented by TECs (Hu, Q. *et al.*, 2012). These markers were therefore used to distinguish thymocytes into sequential stages of maturational progression (4.6A). The frequencies of immature thymocytes with a pre-selection phenotype ($TCR\beta^{low}CD69^{-}$) were increased in cultures supplemented with GANT61 (30.3 ± 1.5% vs 43.1 ± 1.8%). Alongside, the percentages of mature thymocytes with a post-selection phenotype ($TCR\beta^{hi}CD69^{hi}$ and $TCR\beta^{hi}CD69^{low}$) were significantly decreased (4.6A, 4.6B). Examination of the CD4/CD8 profile in each selection stage revealed that pre-selection thymocytes were able to progress along in the maturation process and be positively selected, consequently engaging their TCR ($TCR\beta^{int}CD69^{-}$ and $TCR\beta^{int}CD69^{+}$) (4.6A, 4.6C). However, after selection had occurred, fewer single positive CD4 and CD8 T cells

were generated in the presence of GANT61 (4.6A, 4.6D). The CD4/CD8 ratio remained unchanged during the maturational progression, implying that lineage commitment was unaffected (4.6E).

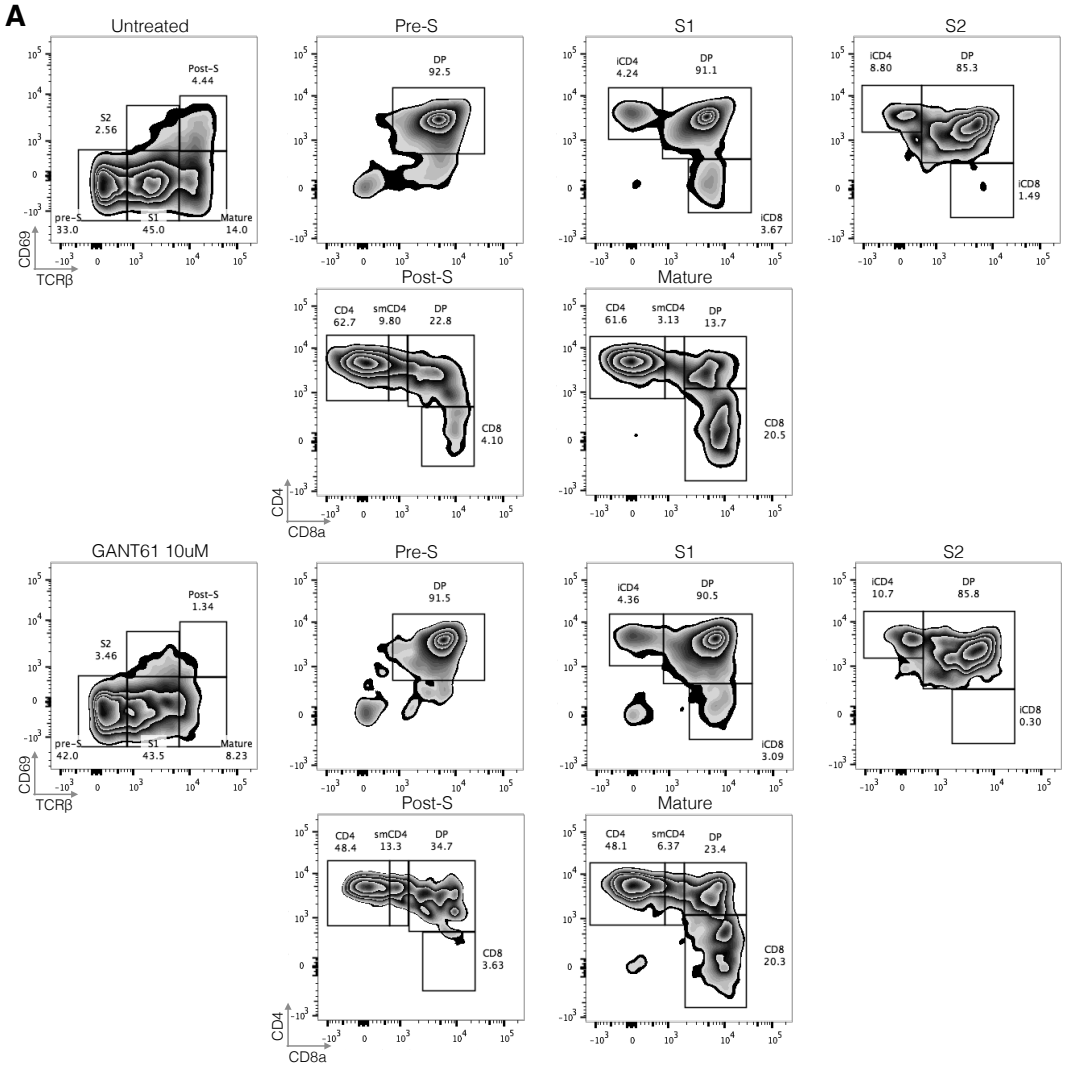

Figure 4.6: GANT61 results in aberrant exit of thymocytes post positive selection
(A) Representative FACS plots showing CD4/CD8 T cell profile of Lin- live single cells at individual, successive stages of positive selection according to differential TCRβ and CD69 expression. Cells that have not yet been selected are defined as CD69-TCRβ- (Pre-S), cells undergoing selection are CD69lowTCRβint (S1) and CD69+TCRβint (S2), and cells that have been selected are CD69hiTCRβhi (Post-S). Mature cells are defined as CD69lowTCRβhi.

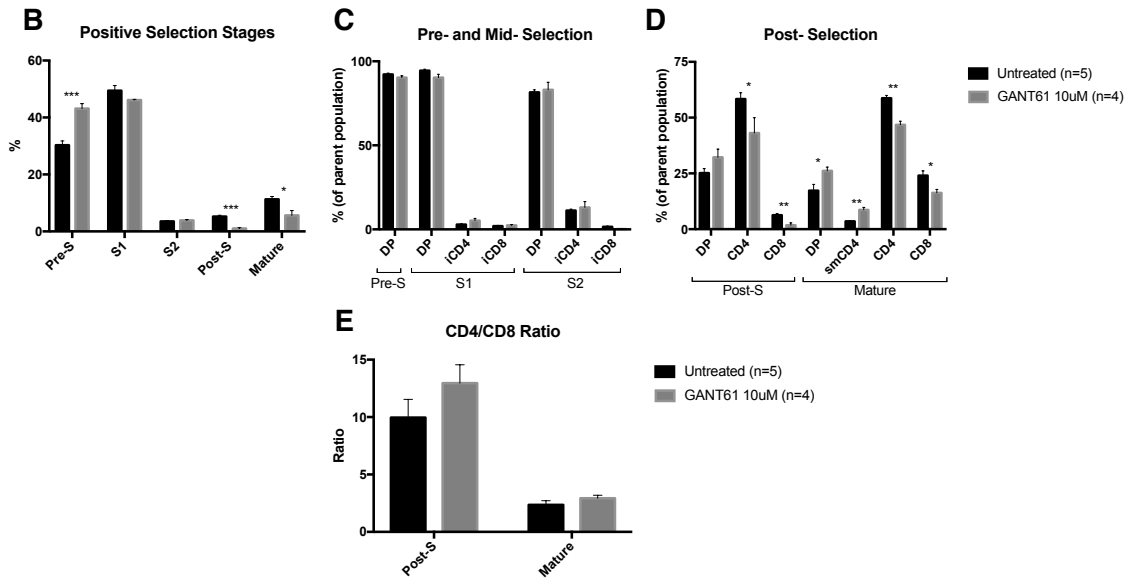

Figure 4.6: GANT61 results in aberrant exit of thymocytes post positive selection
(continuation) **(B)** Frequencies of total cells in each selection stage are shown for both the untreated and GANT61-treated conditions, gated on total Lin- live T cells. Frequencies of individual thymocyte subpopulations in each selection stage are shown for **(C)** pre-selection (Pre-S) and mid-selection (S1 and S2) stages, as well as **(D)** post-selection (Post-S and Mature) stages. **(E)** CD4/CD8 ratios of T cells in the post selection stages were calculated by dividing the frequencies of total CD4 cells over CD8 cells in each stage. P-values were determined by student's t test where * $p < .05$, ** $p < .01$, *** $p < .001$. Experiment shown is representative of 2 independent experiments.

Given that GANT61 inhibits Gli transcription, these results propose that a loss of intracellular Hh signal transduction negatively impacts thymocyte maturation and positive selection. A comparable phenotype was observed, however, when Hh signalling was increased in FTOC (by addition of rShh), which also reduced the frequency of mCD4 cells. One explanation for this overt discrepancy may be that the outcome of Hh signalling is tightly regulated by complex autoregulatory loops. In the rShh experiment, it is possible that addition of rShh stimulated the endogenous pathway in the thymi to compensate quickly for the exogenous pharmacological signal, resulting in an overall downregulation of downstream Hh events. Conversely, while Gli3 usually acts as a repressor *in vivo* in the thymic stroma (Hager-Theodorides, A. *et al.*, 2009), in the *ex vivo* experiment where Gli1 and Gli2 transcription was inhibited by exposure to GANT61, the pathway could have been induced to regulate the processing of Gli3 differently to favour the activator form, thus positively regulating the endogenous Hh signal, a mechanism

which has been demonstrated in other organs such as the limbs (Wang, C. *et al.*, 2007). A more likely explanation could be that normal thymocyte selection and maturation is dependent on a very specific and narrow range of Hh signalling input. Changes to the amount of signalling, such as either too much or too little Hh signal, may result in a comparable loss of regular thymocyte development. However, this interpretation would be inconsistent with the phenotype observed in FTOC supplemented with rHhip, where sequestration of Hh and thus reduction of signalling did not impact the frequencies of thymocyte subpopulations, conditional on the assumption that the concentration of rHhip added was sufficient to inhibit all available Hh ligands. Thus, Hhip may have a unique function in the thymus which includes a non-Hh related effect, but this is at present not supported by evidence.

The *in vitro* data thus far, regardless of the experimental system's limitations, suggests that Hhip is required for regular thymocyte maturation via functional modulation of the Hh signalling pathway, particularly given the unique phenotype observed upon addition of rHhip that was not recapitulated with 5E1. The data also provides a good characterisation of the events that take place in the thymus as a direct result of Hh signalling, which may be more difficult to identify precisely in conventional transgenic models where loss of function of a single gene affects not only cells in the thymus, but many other organs as well, which can have a carry-on systemic effect. A constitutive loss of Shh signalling is most well established for its role in multiple stages of thymocyte development ranging from early DN thymocyte proliferation and differentiation to the selection of TCR-positive cells (reviewed in Crompton, T. *et al.*, 2007). Some evidence has also demonstrated that activation of thymocyte-intrinsic Hh signalling can affect the differentiation of DP cells to the single positive stage (Furmanski, A. *et al.*, 2012). The results here confirm that

positive selection and maturation beyond the DP stage constitute two additional and equally important aspects of Hh signalling in the thymus.

4.2 Hhip regulates TEC differentiation and MHC-II expression

Foxn1 and Shh are expressed in the thymus exclusively by TECs, whereas Hhip is preferentially but not uniquely expressed by these cells, as *hhip* transcripts are found in extremely low but detectable levels in T cells (3.2D). As such, TECs were analysed to evaluate whether the changes in T cell development consequent to altered Hh availability were directly effected by alterations in TEC biology (see Supplementary for full gating strategy). E18.5 FTOC were therefore supplemented with reagents to exogeously modulate Hh signalling. Neither the addition of rShh or GANT61 changed the relative frequencies of cortical or medullary TECs after 4 days (4.7A, 4.7C). In contrast, the addition of rHhip resulted in a statistically significant change in the frequencies of individual TEC subpopulations, with an increase in cTEC frequencies (88.0 ± 1.5% vs 93.5 ± 1.2%) and a corresponding decrease in mTECs (11.0 ± 1.4% vs 6.19 ± 1.1%) (4.7B). While reproducible, these changes were relatively mild.

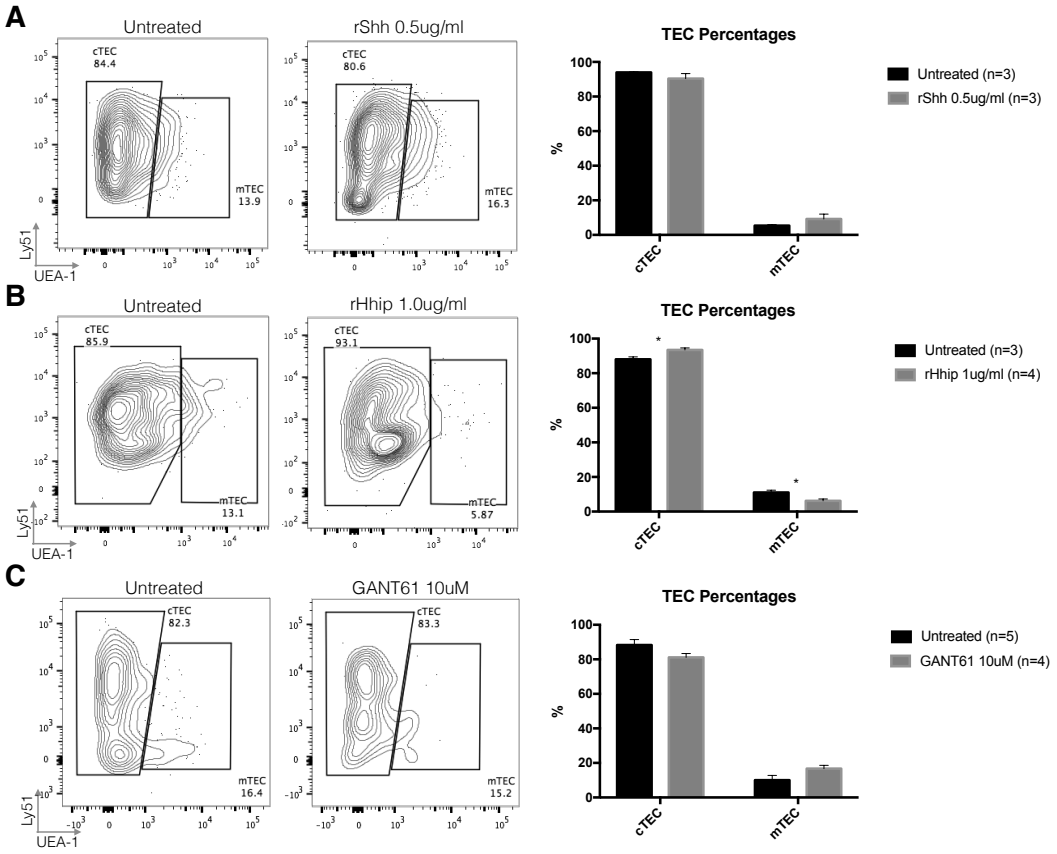

Figure 4.7: rHhip affects cortical and medullary TEC frequencies
Representative FACS plots and statistics showing the cTEC/mTEC distribution, distinguished by Ly51 and UEA-1, upon addition of **(A)** rShh, **(B)** rHhip or **(C)** GANT61. Percentages relate to the total TEC population (CD45-Epcam+ live single cells). P-values were determined by student's t test where * $p < .05$. At least 2 independent experiments were conducted for each condition. Total experimental size: rShh n=11, WT n=11; rHhip n=7, WT n=7; GANT61 n=7, WT n=7.

Shh signalling did, however, affect TEC biology independent of the relative frequencies of cortical and medullary fractions, reducing the proportion of MHC-II highly expressing cells (68.4 ± 2.2% vs 57.4 ± 2.9%). In contrast, inhibition of Shh signalling via GANT61 increased this proportion from 80.1 ± 5.7% to 97.4 ± 0.7% (4.8A). Within MHC-II positive TECs, supplementing rHhip increased cell surface concentrations of this molecule on mTECs as measured by gMFI, whereas rShh and GANT61 had no such effect (4.8B, 4.8C, 4.8D).

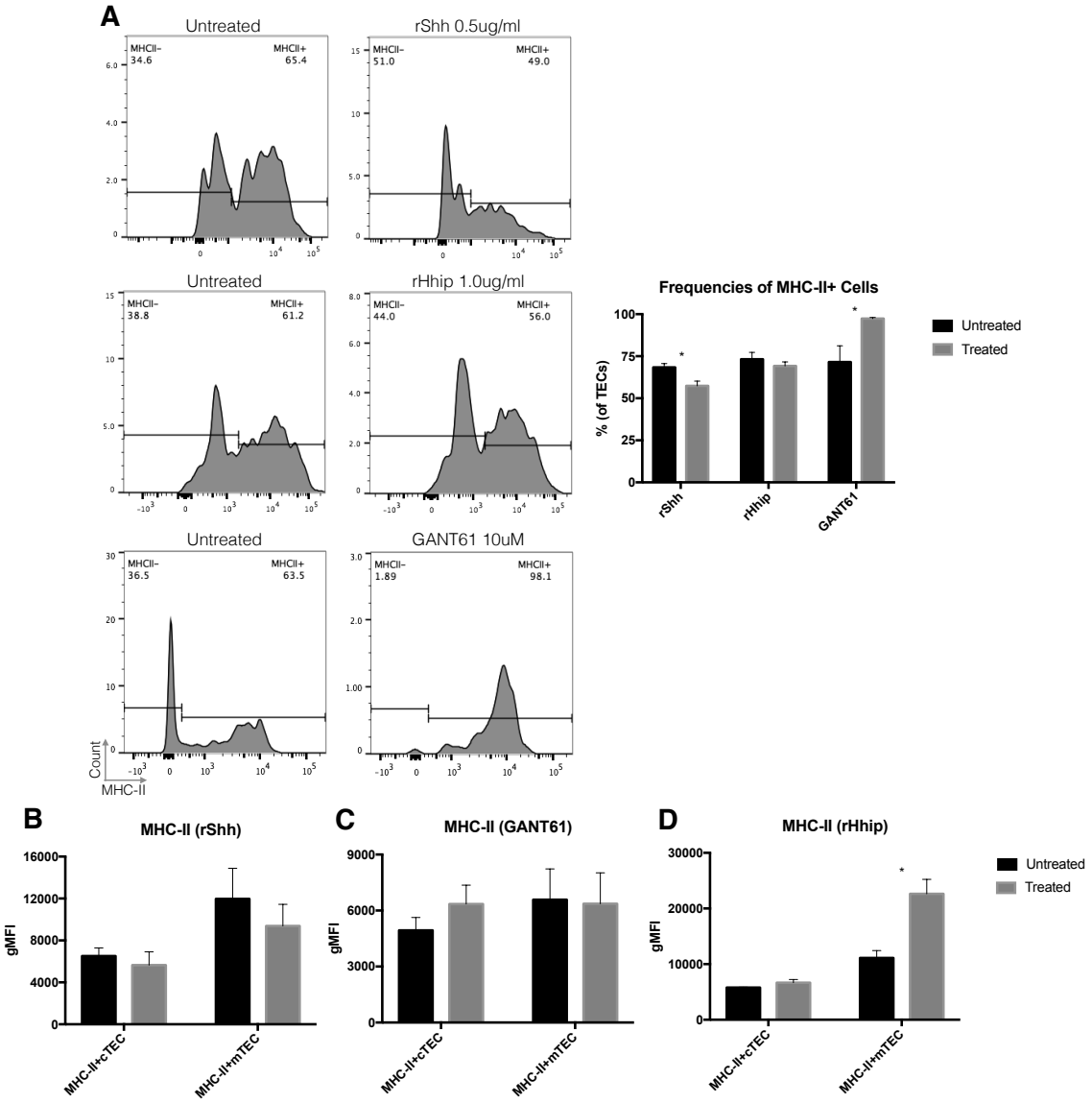

Figure 4.8: Stimulation and inhibition of Shh signalling affect frequencies of MHC-II+ TECs
(A) Representative FACS histograms and statistics show cells that express high levels of MHC-II, defined as MHC-II +, within the total TEC (live single CD45-Epcam+CD31- cells) population upon addition of rShh, rHhip or GANT61. Gate positions were drawn based on CD45+Epcam- cells as a negative control, which are largely MHC-II-. **(B)** Expression levels as assessed by geometric mean fluorescence intensities for cTECs (MHC-II+Ly51+UEA-1-) and mTECs (MHC-II+Ly51-UEA-1+) are shown for **(B)** rShh, **(C)** GANT61 and **(D)** rHhip. P-values were determined by student's t test where * $p < .05$. At least 2 independent experiments were conducted for each condition. Total experimental size: rShh n=11, WT n=11; rHhip n=7, WT n=7; GANT61 n=7, WT n=7.

These results identify a role for Hhip in regulating TEC differentiation and MHC-II expression changes, that are likely linked to alterations of TEC function. However, these changes are inconsistent with the contention that Hhip blocks Hh signalling, as the data from FTOC exposed to either rShh or GANT61 indicates that Shh signalling negatively regulates the expression of MHC-II on developing cells, but does not influence the ratio of cTECs to mTECs. This is also in contrast to recently

published data claiming that Shh regulates TEC differentiation, where loss of Shh resulted in alterations of TEC frequencies (Saldaña, J. *et al*., 2016). However, those published findings were shown via a loss-of-function experiment using Shh-deficient embryos, rather than gain-of-function, and supports that a minimum threshold level of Shh signalling is required for proper TEC differentiation, as theorised earlier for thymocyte development. When this requirement is not met, either in the Shh-deficient setting or when rHhip is added, abnormal TEC differentiation occurs. In contrast, when Shh availability is increased, the downstream signalling pathway may establish an auto-regulatory adaptation to maintain normal TEC differentiation. This mechanism would explain why an addition of rShh did not result in a change in TEC ratios. However, this scenario does not explain the different outcomes consequent to addition of GANT61 and rHhip in FTOC, which were both expected to inhibit Hh signalling, although both inhibitors upregulated MHC-II expression albeit in different manners. Blocking Hh signalling at the receptor level in contrast to inhibiting downstream transcription may therefore translate into distinct outcomes. This would argue for a functionally distinct role for Hhip in controlling mTEC differentiation, as evidenced by influencing the cells' ability to express MHC-II.

4.3 rHhip and rShh modulate Hh signalling as expected by Gli transcription

The conclusions above on the role of Hhip and Hh signalling in the thymus are all dependent on the assumption that addition of rShh or rHhip to FTOC increases or decreases Hh signalling respectively. To confirm this, thymi from E18.5 GBS-GFP embryos were analysed, where levels of GFP expression in these reporter mice are regulated by the binding of Gli transcription factors, thus providing a useful quantitative measure of Gli transcription and consequently Hh signalling (Balaskas,

N. *et al*., 2012). A small blood sample from each embryo was taken and genotyped based on GFP reporter expression, where positivity indicated presence of the GBS-GFP transgene regardless of the absolute expression level. One lobe from each embryo was cultured under normal conditions in the absence of any extrinsic factors that might modulate Hh signalling, while the other lobe was exposed to either 0.5 µg/ml rShh or 1.0 µg/ml rHhip, allowing an intra-individual analysis of altered Shh signalling and controlling for the variability of reporter gene penetrance.

Addition of rHhip resulted in a reduced frequency of GFP^+ cTECs in all samples. In contrast, the response to rHhip in mTECs was variable (4.9A). On the other hand, exposure of GBS-GFP E18.5 thymic lobes to rShh increased the frequencies of GFP^+ mTECs but did not alter the frequencies of GFP^+ cTECs (4.9B).

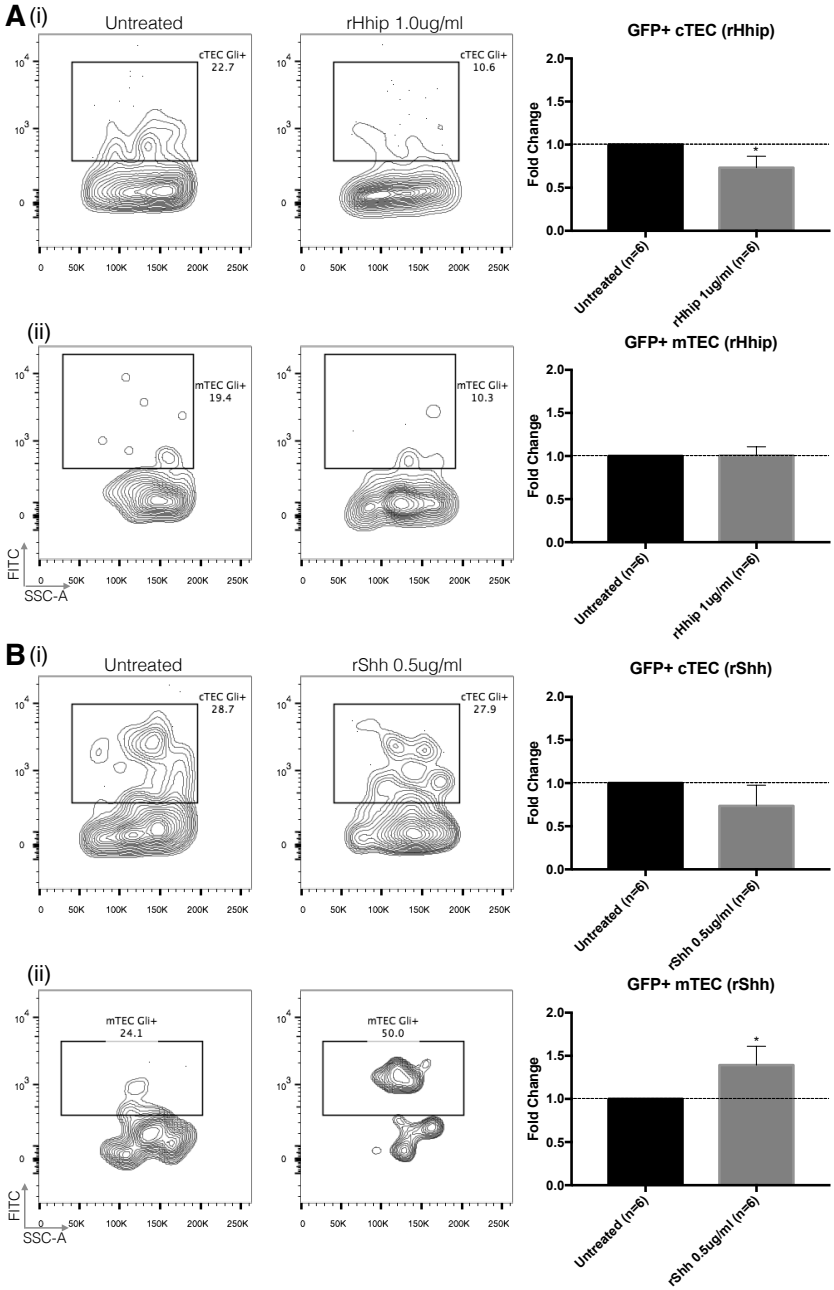

Figure 4.9: Alterations in Hh signalling are reflected by changes in the frequency of reporter-positive TECs
Representative FACS plots and statistics showing percentage of GFP+ cells within (i) cTEC or (ii) mTEC populations, upon addition of **(A)** rHhip or **(B)** rShh to GBS-GFP E18.5 thymi grown as FTOCs for 4 days. Paired samples were used, where lobes from each GBS-GFP thymi were separated and cultured separately, one as the untreated control and the other treated with rShh/rHhip in media. Gates were drawn based on the untreated cTEC population. The percentages of GFP+ cTECs and mTECs in the untreated lobe of each paired sample were normalised as 1, and the percentages of GFP+ cells in the treated lobe calculated relative to the untreated control, giving relative fold change values. Statistics were pooled from 2 independent experiments and significance was calculated using the non-parametric Wilcoxon matched-pairs signed rank test. Total experimental size: rHhip n=6, WT n=6; rShh n=6, WT n=6.

Addition of rHhip decreased Gli activity as measured by the gMFI of GFP in cTECs, in keeping with a reduction in frequency of GFP^+ cTECs. However, gMFI levels of GFP were not affected within the GFP^+ cTEC population, demonstrating that the presence of rHhip in FTOC reduced the numbers of cells that induced Hh signalling

but not the extent of Gli-mediated transcription in each of the responding cells (4.10A). A comparable result was observed in mTECs exposed to rShh, as Gli activity was marginally increased in the total mTEC population but not the GFP^+ mTECs (4.10B). The presence of rShh resulted in increased cell surface expression of MHC-II on GFP^+ mTECs, whereas an opposite change was observed in the presence of rHhip (4.10C). However, these numerical differences were not statistically significant due to the small sample size. Nonetheless, these findings are nevertheless useful as the trends were consistent. The experiment with GBS-GFP thymic lobes demonstrated the expected response of TECs to rShh and rHhip, promoting and inhibiting Hh signalling respectively. The increased availability of exogenous rShh and rHhip appears to induce more cells to initiate or abrogate Hh signalling, but does not influence the amount of signal transduced in each individual cell. This partially addresses why modulating the amount of signal transcribed in each cell using GANT61 produced a different effect from increasing or restricting the availability of the Hh signal, such as by addition of rShh or rHhip.

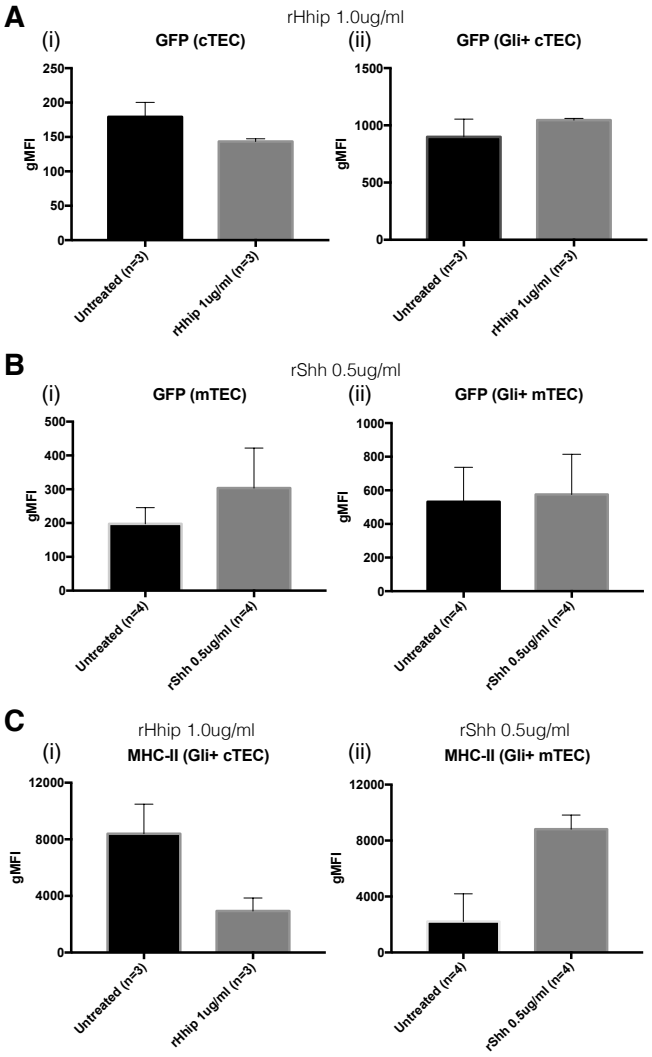

Figure 4.10: Addition of rShh or rHhip affect frequencies of GFP+ cells but not the amount of Gli transcription
(A) Graphs show expression of Gli measured by geometric mean fluorescence intensities of GFP in the (i) total cTEC population and (ii) the GFP+ cTEC population in the GBS-GFP untreated lobe and the treated (rHhip) lobe. **(B)** Expression of Gli as before, but in the (i) total mTEC population and (ii) GFP+ mTEC population in the untreated and rShh-treated lobes. **(C)** Expression of MHC-II in the Gli+ TEC compartment with (i) addition of rHhip and (ii) addition of rShh. Differences were not significant between untreated and treated paired samples as assessed by a one-tailed parametric paired t-test. 2 independent experiments were conducted, but statistics shown above are from 1 single experiment. Total experimental size: rHhip n=6, WT n=6; rShh n=6, WT n=6.

Results from the TEC experiments clearly suggest that Hh signalling preferentially favours mTEC development. This conclusion is supported by the literature where a loss of Shh signalling reduces mTEC percentages (Saldaña, J. *et al.*, 2016). One possible mechanism to explain this result is autocrine regulation of the common progenitor by Hh signalling to adopt either the cTEC or mTEC differentiation program, which would explain why changes in Gli transcription were primarily seen only in one TEC subpopulation. If regular Hh signalling preferentially directs TEC

progenitors to an mTEC fate, addition of rHhip (thus downregulating Hh signalling) would allow more progenitors to adopt a cTEC phenotype, consequently increasing cTEC frequencies. These new cTECs would then display reduced Hh signalling, consistent with the observed decreased Gli activity within these cTECs. Conversely, when rShh is added, progenitors adopt an mTEC fate and the increased Hh signalling is detected in the mTEC compartment. Given however that mTEC frequencies were not increased when rShh was added to WT FTOC, further work has to be conducted to validate if there is indeed some kind of threshold requirement for Hh signalling in TEC development beyond which increased Hh signalling as represented by rShh has no effect on relative TEC frequencies, or if other downstream factors are responsible.

Taken together with the thymocyte data, the results imply that the principle role of Shh in the thymus is to signal in a paracrine fashion from TECs to T cells to influence thymocyte development, where a tightly regulated level of Shh signalling is required for normal CD4 development and any alterations in ligand availability change the efficiency of single positive CD4 T cell maturation. In parallel, Hh signalling also affects TEC biology. Here, Hhip may have a unique role in negatively regulating the availability of Hh ligands in TECs, thus operating in an autocrine fashion. The transcriptional changes resultant from exposure of FTOC to rHhip via the culture media may require more time to phenotypically affect TECs and their function than was provided in the *in vitro* system employed, and as such was not reflected in terms of an altered thymocyte development profile. The regulation of MHC-II expression together with the altered expression of TCRβ and CD5 in the rHhip-supplemented FTOC also suggest that TCR signalling may be influenced by Hhip, which is crucial for proper TEC selection and function and the

generation of normal and functionally competent T cells. Given the contention that *hhip* is a target of Foxn1 in TECs, these results support the notion that Hhip may be most relevant in TEC differentiation or function and any impact on T cells may be indirect via altered TEC function. This needs to be further elucidated using a more appropriate experimental model, such as a physiological *in vivo* model with a genetic loss-of-function of *hhip.*

4.4 Preventing Foxn1 from binding to *hhip* regulatory sequences decreases *hhip* transcription and alters Hh signalling

I next investigated whether Foxn1 directly controls *hhip* expression in TECs under a non-physiological setting, and whether cTECs and mTECs would be differentially affected by Foxn1 regulation. Using Crispr/Cas9 technology, sgRNAs were designed to target and cleave Foxn1 binding motifs (GACGC) within the Foxn1 ChIP-seq peak at the *hhip* transcriptional start site, previously defined as BS1, BS2 and BS3. An sgRNA targeting an irrelevant genomic sequence upstream of the *hhip* transcriptional start site was used as a negative control, referred to as TSS (Table 2.5). These were transfected individually into a cTEC cell line and *hhip* expression measured after 48 hours by qPCR. As shown previously in Chapter 3, *hhip* expression was significantly compromised following the disruption of BS1, BS2 or BS3 (3.3B). An sgRNA targeting the coding sequence of *hhip* exon 2, referred to as CS, was designed as a positive control, given that disruption of the exon sequence may cause frameshift mutations and negatively impact gene expression (4.11A, Table 2.5). Transfection of CS resulted in decreased levels of *hhip* mRNA, similar to when the binding sites were targeted, suggesting that removal of Foxn1 binding sites and thus disturbance of Foxn1 regulation has a severe impact comparable to that of disturbing the *hhip* coding sequence (4.11B). Concurrent to a

decrease of *hhip*-specific mRNA, transcripts encoding the transducer *smo* and the downstream repressor *gli3* were diminished when the Foxn1 bindings sites were ablated, whereas expression of the downstream activator *gli1* and the Hh receptor *ptch1* were increased. This was consistent with enhanced Hh availability and signalling resulting from a loss of Hhip (4.11C).

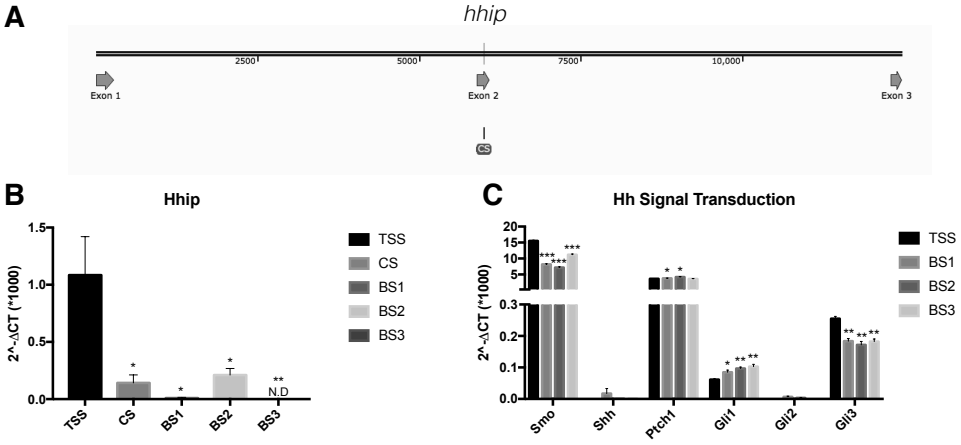

Figure 4.11: Ablation of Foxn1 binding sites affects *hhip* expression and expression of Hh pathway members
(A) Design of an sgRNA sequence (CS), highlighted in blue, to target the coding sequence of *hhip* exon 2, where the reverse strand of *hhip* is shown above. **(B)** Expression of *hhip* as measured by qPCR when either a non-significant upstream site (TSS), the coding sequence (CS) or the Foxn1 binding sites (BS1, BS2, BS3) were cleaved using the Crispr/Cas9 system. **(C)** Expression of key elements of the Hh pathway when *hhip* expression is reduced, compared to the control transfected with TSS. 2 independent experiments were conducted and pooled, and values normalised to *gapdh* expression. P-values were determined by student's t test where * $p < .05$, ** $p < .01$, *** $p < .001$.

4.4.1 Overexpression of Foxn1 does not upregulate *hhip*

Next, overexpression of Foxn1 was assessed to see if *hhip* expression would be affected in the presence of increased amounts of Foxn1. The cTEC1.2 cell line was transfected with a murine Foxn1 plasmid and analysed after various time points. Transfection for 24 or 48 hours both resulted in a significant increase of *foxn1* RNA copy numbers (4.12A), which correlated with an upregulation of the established Foxn1 targets *dll4* and *ccl25* (4.12B), thus demonstrating that Foxn1 protein must have been expressed. Contrary to expectations, transcripts for *hhip* and the transducing molecule *smo* were downregulated (4.12B). *Gli1* and *ptch1* mRNA were increased, similar to conditions in which *hhip* expression was reduced consequent to deleting the gene's Foxn1 binding sites (4.12C). To eliminate the

possibility that Foxn1 may regulate *hhip* indirectly via Gli1 or Ptch1, ChIP-seq and RNA-seq data were carefully re-evaluated. However, evidence could not be found to suggest either the presence of a Foxn1 binding motif or Foxn1-regulated transcription of either of these two genes, or indeed any of the key Hh signalling pathway molecules (Žuklys, S. *et al*., 2016). Rather, *gli1* and *ptch1* upregulation are more appropriately explained by the increased availability of Hh-mediated signalling arising from the reduced expression of *hhip*. Given the unexpected lack of increase of *hhip* transcripts in response to Foxn1 plasmid transfection, immunohistochemistry (IHC) experiments were conducted to confirm if transfection of the Foxn1 plasmid resulted in protein production. IHC demonstrated clear fluorescence confirming successful production of Foxn1 protein in the transfected cTEC1.2 cell line, similar to primary TEC cells which were used as a positive comparison, but in contrast to the untransfected cTEC1.2 negative control where minimal fluorescence was detected and the majority of any fluorescent signal detected appeared to be weak background noise in the cytoplasm (4.12D).

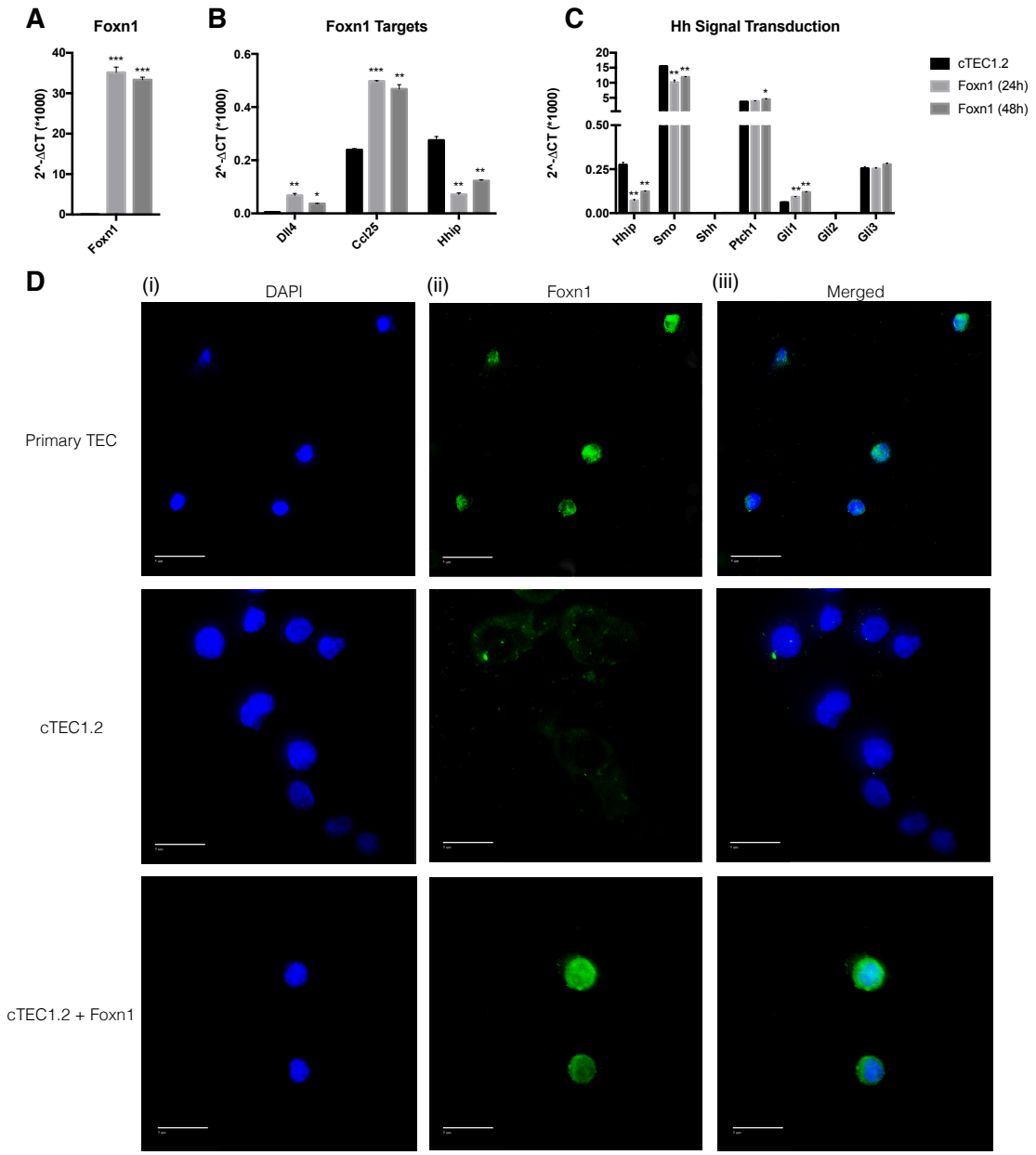

Figure 4.12: Foxn1 plasmid is successfully transfected but does not translate entirely into nuclear protein
(A) *Foxn1* transcripts in cTEC1.2 after transfection with the plasmid for either 24 or 48 hours, compared to the untransfected control treated only with Lipofectamine. **(B)** Expression of the Foxn1 downstream targets *dll4, ccl25* and *hhip.* **(C)** Expression of Hh pathway genes after transfection of Foxn1 as assessed by qPCR. 2 independent experiments were conducted and pooled, and values normalised to *gapdh* expression. P-values were determined by student's t test where * $p < .05$, ** $p < .01$, *** $p < .001$, where asterisks above each condition represent a statistical significance in comparison to the cTEC1.2 control. **(D)** (i) Foxn1 expression in green (AF488) in primary TECs from 6 week old WT C57BL/6 mice as shown by IHC as a positive control with nuclear expression demonstrated by DAPI in blue. (ii) IHC of untransfected cTEC1.2, and (iii) IHC of cTEC1.2 transfected with Foxn1 plasmid for 48 hours. Representative pictures are shown. At least 2 independent experiments were conducted with consistent results.

mRNA expression of *shh* was extremely low in the cTEC1.2 cell line despite evident activation of the Hh pathway as supported by the increased expression of *gli1* and *ptch1*. To rule out the possibility that Foxn1 failed to upregulate *hhip* due to an absence of critical components of the Hh pathway, Foxn1 was next transfected

into cTEC1.2 in the presence of rShh (0.5 µg/ml). Again, *hhip* expression was not increased (data not shown), but Foxn1-specific transcripts were detected in the presence of rShh, although this increase was not statistically significant (4.13A). To investigate if *foxn1* expression was affected by Shh, 2 different doses of rShh were added to cTEC1.2 culture for 48 hours. Upregulation of *foxn1* expression was observed when either 0.05 µg/ml or 0.5 µg/ml rShh were added (4.13B). Interestingly, when Foxn1 binding sites upstream of the hhip gene were targeted, mRNA levels of *foxn1* were also increased concurrent to the decrease in *hhip* expression (4.13C).

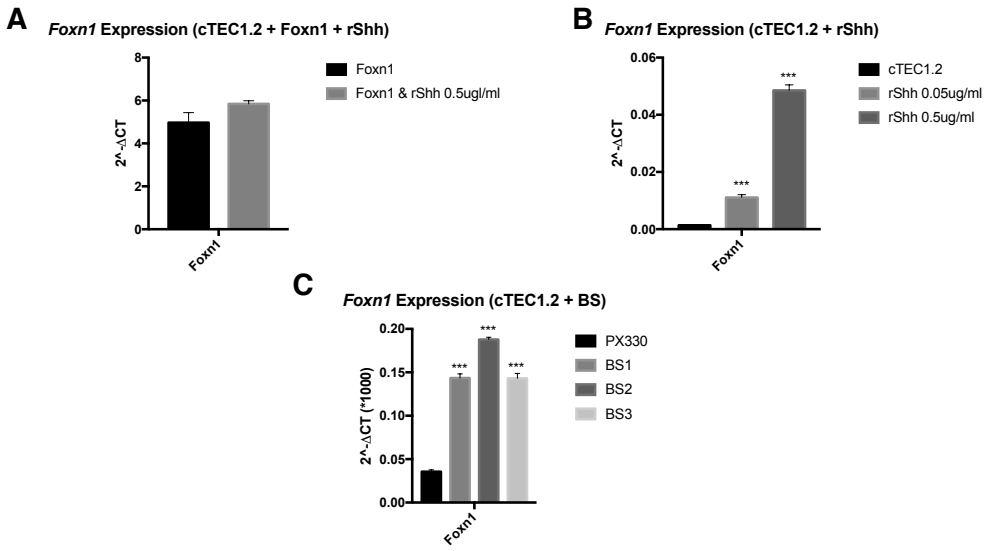

Figure 4.13: Changes in Hh signalling increase *foxn1* expression
(A) cTEC1.2 was either transfected with Foxn1 plasmid alone for 48 hours, or transfected along with rShh in the culture media for 48 hours. **(B)** cTEC1.2 was cultured with varying concentrations of rShh protein in the culture media for 48 hours, compared to an untreated culture grown with normal media. **(C)** Foxn1 transcript levels were assessed by qPCR upon transfection of cTEC1.2 with Crispr/Cas9 sgRNAs targeting Foxn1 binding sites within the *hhip* gene (BS1, BS2, BS3) for 48 hours, compared to empty vehicle control (PX330). 2 independent experiments were conducted and pooled, and values normalised to *gapdh* expression. P-values were determined by student's t test where * $p < .05$, ** $p < .01$, *** $p < .001$. Asterisks above each condition represent a statistical significance in comparison to the control condition (either cTEC1.2 or empty vehicle control).

4.5 rShh causes upregulation of *foxn1*

To confirm that the increase in *foxn1* transcripts was a consequence of heightened Hh signalling events, changes in RNA copy numbers for essential molecules of the Hh signalling pathway were evaluated by qPCR in cTEC1.2 cultured in the presence of rShh (0.5 µg/ml). Transcripts of *smo* were reduced under these

experimental conditions, but the expression of other genes including *hhip* remained unchanged (4.14A). A comparable result was observed in FTOC (4.14B). The consequence of higher *foxn1* mRNA copy numbers was next assessed by probing the expression of downstream Foxn1 targets. rShh via upregulation of Foxn1 promoted the expression of the Foxn1 downstream targets *dll4* in cTECs (4.14C). Transcripts of *foxn1* were fewer in mTECs upon addition of rShh (4.14D), but the paucity of these cells in the E18.5 thymus after 4 days of organ culture may account for this reduction to likely be a technical artefact, not least as the standard error was very high. To clarify whether Hh signalling exerts a differential role in cTECs when compared to mTECs, both cortical (cTEC1.2) and medullary (mTEC2.3) TEC cell lines were exposed for 2 days to either rShh or rHhip. Under these conditions, cTEC1.2 cells displayed an increase in *foxn1* transcripts upon exposure to rShh, which was not observed when culturing these cells with rHhip (4.14E, 4.14G). mTEC2.3 cells did not show changes in the expression of *foxn1*, control genes, downstream targets or Hh pathway genes (4.14E, 4.14F, 4.14G, 4.14H).

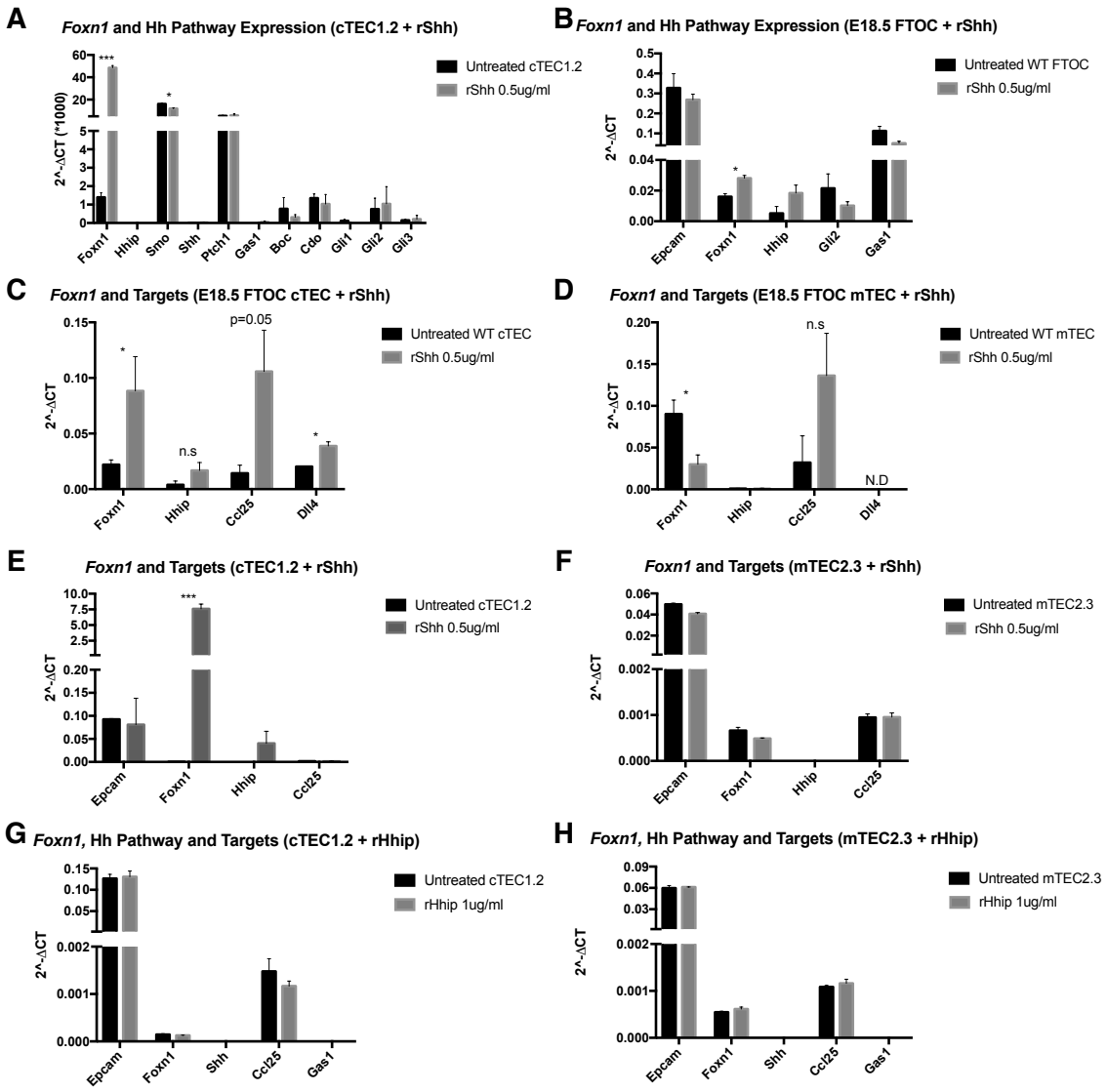

Figure 4.14: rShh influences Foxn1 expression as assessed by target genes
(A) Expression of Foxn1 and Hh signalling gene transcripts upon culture of cTEC1.2 with rShh in the culture media for 48 hours, compared to cTEC1.2 cultured with untreated media. *Foxn1* mRNA levels were assessed in **(B)** total TECs isolated from E18.5 WT FTOC grown for 4 days, as well as in the **(C)** cTEC (Ly51+UEA-1-) and **(D)** mTEC (Ly51-UEA-1+) populations. rShh was added to the culture media of either the **(E)** cTEC1.2 or **(F)** mTEC2.3 cell lines for 2 days and expression of *foxn1*, the Foxn1 targets *hhip* and *ccl25*, and the control gene *epcam* assessed by qPCR. Expression of select genes upon exposure to rHhip in **(G)** cTEC1.2 or **(H)** mTEC2.3 culture media for 2 days was examined. *Epcam* was used as a control gene as *epcam* expression is not known to be affected by Foxn1 or Hh signalling. Values are normalised to *gapdh* expression. P-values were determined by student's t test where * $p < .05$, ** $p < .01$, *** $p < .001$. Asterisks above each condition represent statistical significance in comparison to the untreated control.

None of the Hh signalling pathway genes with the exception of *smo* displayed any expression changes in the cultures with rShh. This could indicate that the concentration of rShh used was insufficient to fully activate the Hh pathway. However, this would strongly suggest that *foxn1* is regulated directly by Shh or a via Hh pathway-extrinsic mechanism, rather than as a downstream consequence of increased Hh signalling. There is currently no published evidence directly linking

Shh and Foxn1, although an indirect negative regulation has been observed via the transcription factor Tbx1, and ectopic activation of Shh during embryonic patterning prevents *foxn1* expression from expanding into the pharyngeal endoderm (Bain, V. *et al*., 2016; Reeh, K. *et al*., 2014).

These results present the first evidence that *foxn1* may be positively regulated by Shh. As *hhip* is downstream of Foxn1, this suggests a potential feedback loop where Foxn1 can control its own expression by upregulating *hhip* to inhibit Shh signalling. While the overexpression of *foxn1* mRNA in cell lines was unsuccessful to upregulate *hhip*, the inhibition of Foxn1 binding resulting in a subsequent loss of *hhip* expression clearly showed that *hhip* is directly downstream of Foxn1. It is however possible that Foxn1 regulates another downstream target that in turn also affects the expression of *hhip,* which may not be present in the cell lines. This is unlikely to be a member of the Hh pathway as assessed by the qPCR results, but could be a different gene that can only be detected by a genome-wide screen. A search for Foxn1 binding sites in the transcriptional start site region of the major Hh pathway members (*gli1, gli3, gli3, ptch1, smo, shh*) was conducted but no evidence was found. Another possibility to explain the results is that additional physiological cues are required for Foxn1 to regulate certain target genes, which may not be present in an *in vitro* culture. Future experiments should be conducted using a more representative *in vivo* setting. However, in order to understand how and why Foxn1 regulates certain genes, it is necessary to first fully appreciate the role of these genes in the context of thymus development and function. The *in vitro* experiments above have been beneficial in setting out a framework of the key elements in the thymus that Hhip and the Hh signalling pathway modulate, and the role of Hhip will now be further explored in an *in vivo* setting in the following chapters.

5: Constitutive Loss of *Hhip* Affects Thymus Development and Function

In vitro analyses are often limited as phenotypes observed may not be fully representative of a true physiological setting. Mice conventionally deficient for *hhip* ($Hhip^{tm1Amc/J}$) were therefore studied to evaluate how a global genetic loss of *hhip* expression would affect normal thymic organogenesis and function. Having established that *hhip* is a downstream target of Foxn1, the primary aim was to assess if TEC phenotype and function, and consequently T cell development were altered in mice homozygous for a loss of *hhip* expression (designated Hhip-/-). These mice possess a null allele due to replacement of *hhip* exon 1 and lack Hhip activity (Chuang, P. *et al*., 2003). While they look superficially normal at birth, they display clear mutations of the lungs and endochondral skeleton, and are thus neonatal lethal due to respiratory failure. The thymus has not been studied in these mice. As such, embryonic and newborn Hhip-/- mice were investigated.

5.1 Genetic loss of *hhip* affects TEC development and MHC-II expression

Thymi with either a complete or partial loss of *hhip* expression, represented by the homozygous (Hhip-/-) and heterozygous (Hhip+/-) genotypes respectively, did not appear visually different from WT in terms of size or shape. The correct genotypes were confirmed by PCR (5.1A). Thymic cellularity was comparable between the different genotypes when processed by enzymatic digestion with Liberase (5.1B), although there was significant variation between individual samples due to the unpredictability of the exact time when mice were born. However, TEC frequencies and absolute numbers were comparable between all genotypes (5.1C). Hhip+/- and

Hhip-/- thymi displayed altered cTEC to mTEC ratios, where the Hhip+/- thymi displayed a significantly higher frequency of mTECs and correspondingly less cTECs (68.0 ± 3.8%) in comparison to WT thymi (79.1 ± 4.4%). This difference was further compounded in the Hhip-/- mouse where only 54.6 ± 5.0% TECs had a cTEC phenotype (5.1D). Frequencies of MHC-II positive TECs were similar between genotypes, but Hhip-/- TECs expressed lower cell surface concentrations of MHC-II as assessed by geometric mean fluorescence intensity (5.1E). These observations suggest that Hhip influences TEC sublineage choice and phenotype.

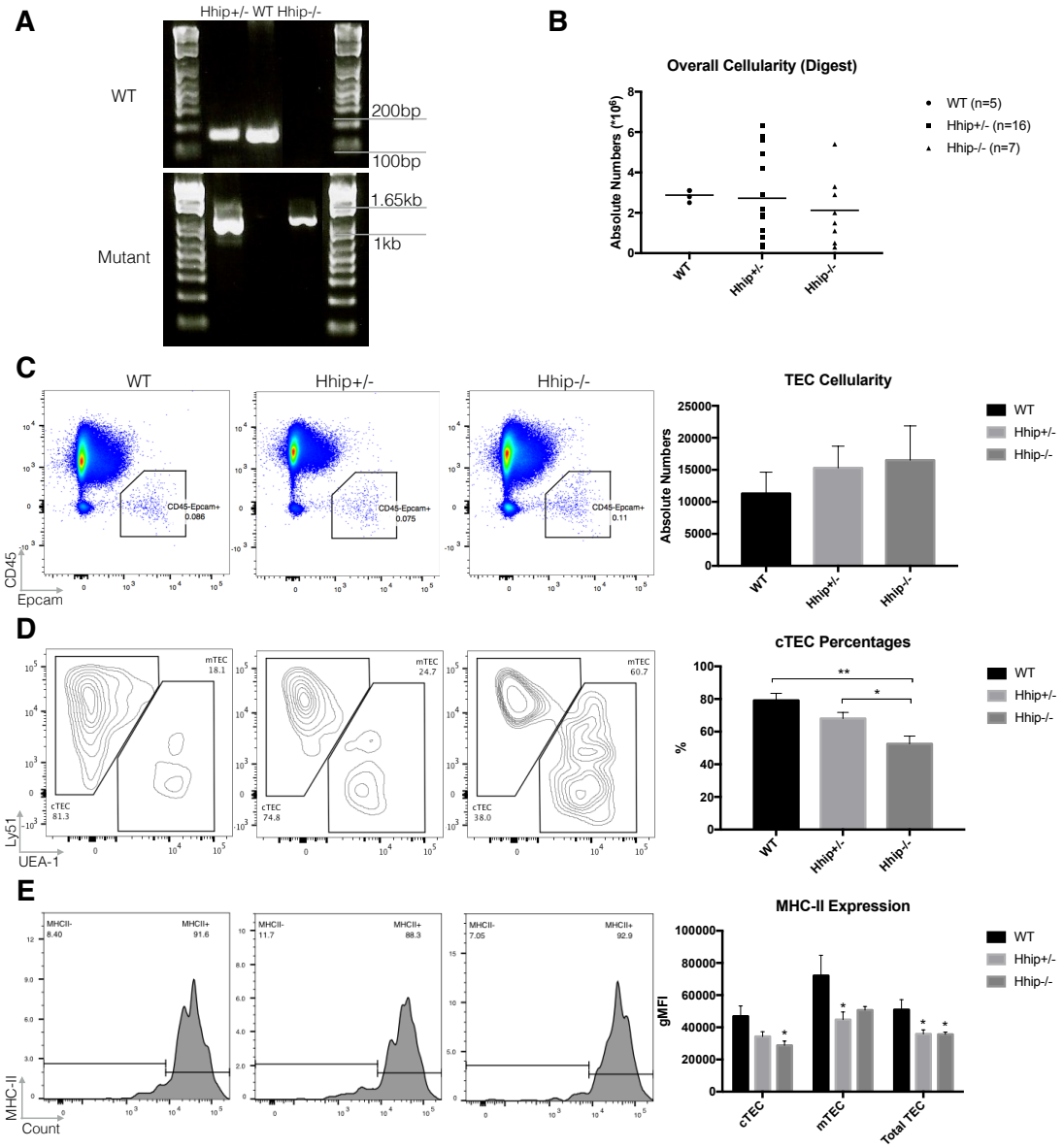

Figure 5.1: Loss of *hhip* expression alters TEC lineage differentiation and MHC-II expression
(A) Representative genotyping results of WT, Hhip+/- and Hhip-/- neonates, showing the WT allele PCR product of 150 bp, and the mutant allele product of 1 kb. Hhip+/- mice had both alleles and thus amplified both PCR products. A 1kb+ ladder was run on the agarose gel as comparison. **(A)** Thymus cellularity using Liberase enzymatic digest. **(C)** Representative FACS plots showing percentages of live single CD45-Epcam+CD31- cells. Graph shows absolute TEC numbers, calculated from overall cell yield. **(D)** cTEC/mTEC frequencies, gated on MHC-II+CD45-Epcam +CD31- live single cells. **(E)** Frequencies of MHC-II+ total TECs shown in FACS plots and geometric mean fluorescence intensities of MHC-II shown in graph. Graphs shown are from a single experiment, statistics are pooled across all experiments. At least 3 independent experiments were conducted. P-values were determined by student's t test where * $p < .05$, ** $p < .01$. Total experimental size: WT n=7, Hhip+/- n=16, Hhip-/- n=7.

5.1.1 Addition of rHhip at E18.5 is sufficient to rescue a *hhip*-deficiency

As Hhip-/- mice die soon after birth, TECs could not be analysed after this age. To extend the analysis to a slightly more developed stage, Hhip-/- thymi were isolated at E18.5 and cultured for 4 days as FTOC, allowing TECs to continue to develop to a more mature phenotype, albeit under *ex vivo* conditions. Similar trends in

cellularity (5.2A), relative frequencies of the individual TEC lineages (5.2B) and MHC-II cell surface levels (5.2C) were observed in E18.5 FTOC when compared to neonatal mice. To investigate if a non-specific supplement of Hhip protein would be able to alter the TEC phenotype in Hhip-/- thymi to become comparable to WT, E18.5 Hhip-/- FTOC were cultured in the presence of rHhip (1.0 µg/ml) for 4 days. Addition of exogenous rHhip was sufficient to reverse the *hhip*-deficient phenotype such that cTEC ratios in Hhip-/- + rHhip cultures (84.3 ± 1.5%) were comparable to WT at 81.1 ± 2.2% (5.2D, 5.2E). rHhip supplement also affected MHC-II expression, such that MHC-II cell surface levels in rescued Hhip-/- cultures were indistinguishable from WT (5.2F). This demonstrated that the TEC phenotype seen in *hhip*-deficient genotypes was a direct consequence of a loss of *hhip*, and that the presence (and absence) of Hhip is sufficient to alter TEC development regardless of where the Hhip protein originates from, suggesting a cell non-autonomous role for Hhip.

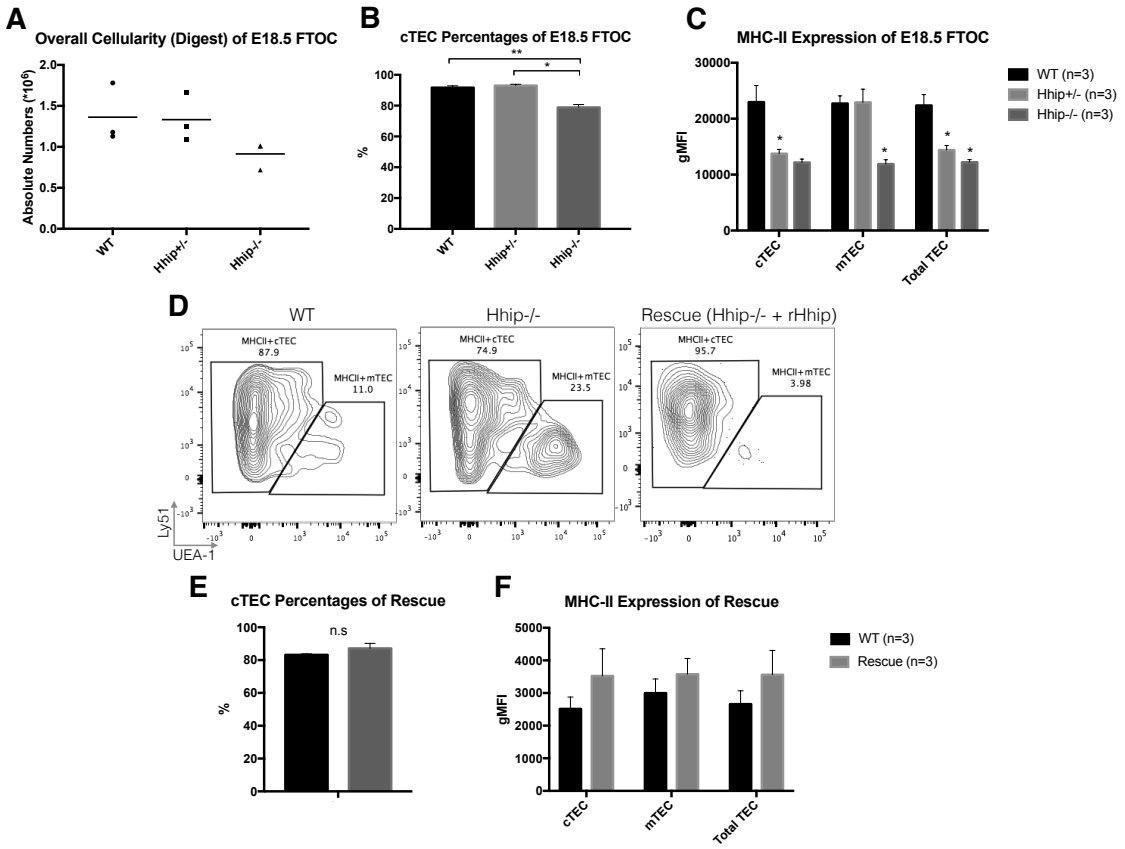

Figure 5.2: Supplementing rHhip in FTOC is sufficient to rescue the Hhip-/- TEC phenotype
(A) Total cellularity of E18.5 FTOC grown for 4 days, processed by Liberase enzymatic digestion. **(B)** TEC distribution and **(C)** MHC-II expression for indicated mouse strains. **(D)** Representative FACS plots showing frequencies of live single CD31-CD45-Epcam+MHC-II+ cTECs and mTECs in WT, Hhip-/-, as well as Hhip-/- FTOC where rHhip (1 ug/ml) was added to the culture media, designated Rescue. **(E)** cTEC percentages and **(F)** MHC-II expression of Rescue are shown in comparison to WT. Graphs shown are from a single experiment, statistics are pooled across 2 experiments. At least 3 independent experiments were conducted. P-values were determined by student's t test where * $p < .05$, ** $p < .01$. Total experimental size: WT n=14, Hhip+/- n=12, Hhip-/- n=6, Rescue n=5.

5.1.2 Reduced *hhip* expression results in persistent changes in TEC development

Although thymus organogenesis is completed early during postnatal life, TECs are continually replaced throughout adult life, albeit at a slower turnover rate. To determine the role of Hhip on the requirement for continuous TEC replacement, adult Hhip+/- mice were next analysed at different postnatal ages to see if any defects were sustained post-early development. TEC cellularity was comparable between WT and Hhip+/- mice at all time points investigated (5.3A). The architectural organisation of the thymus was comparable for WT and Hhip+/- mice, with distinct cortical and medullary areas of similar size and no apparent

aberrations observed by haematoxylin and eosin (H&E) stains of tissues from 4 and 12 week old mice (5.3B).

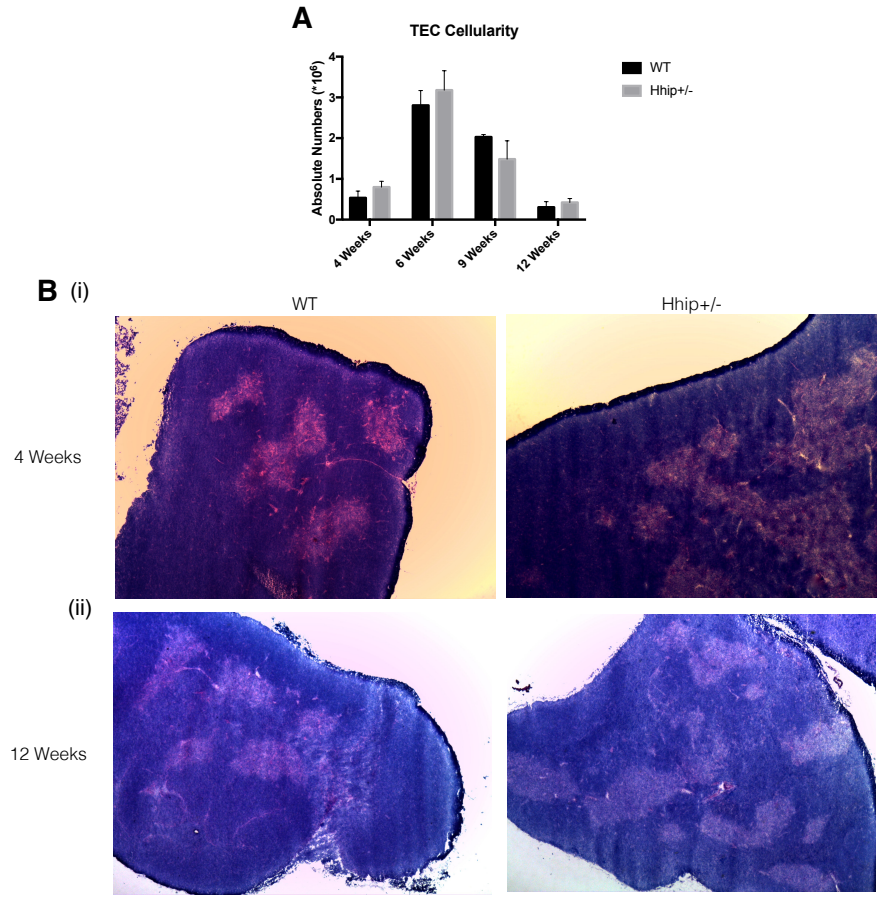

Figure 5.3: Cell numbers and general morphology in adult Hhip+/- thymi are comparable with WT
(A) Absolute TEC numbers (CD45-Epcam+ live single cells) of adult WT and Hhip+/- thymi at indicated ages. **(B)** Haematoxylin and Eosin (H&E) staining of WT and Hhip+/- thymic tissue of (i) 4 week and (ii) 12 week old mice. Images were visualised at 4X magnification. Statistics are pooled across all experiments, where at least 2 independent experiments were conducted for each time point. Total experimental size: 4 weeks WT n=6, Hhip+/- n=9; 6 weeks WT n=7, Hhip+/- n=6; 9 weeks WT n=6, Hhip+/- n=6; 12 weeks WT n=6, Hhip+/- n=5. Statistical significance was determined by student's t test.

Independent of total TEC cellularity, frequencies of the two TEC lineages were different between WT and Hhip+/- adult mice (5.4A, 5.4C). At 4 weeks of age, the frequency of Hhip+/- cTECs was increased compared to WT cTECs (7.23 ± 1.2% vs 4.88 ± 1.0%), in contrast to the results observed in neonatal mice. With progressive age, this difference tapered off and WT and Hhip+/- cTECs and mTECs displayed similar frequencies in 6 week old mice (WT 15.5 ± 3.6%, Hhip+/- 13.5 ± 2.0%). At 9 weeks of age, Hhip+/- mice now had fewer cTECs (15.4 ± 1.5% vs 21.7 ± 2.9%), and this difference persisted in 12 week old mice (WT 46.7 ± 4.5,

Hhip+/- 30.9 ± 4.9%). Contrary to neonatal mice, the cell surface expression of MHC-II was not affected, and the differentiation from immature mTEC^{low} (MHC-II^{int}) to mature mTEC^{hi} (MHC-II^{hi}) was unchanged in Hhip+/- animals (5.4B. 5.4C, 5.4D). In previous *in vitro* data as well as in newborn mice, changes in MHC-II expression and TEC frequencies appeared to be closely linked, but here appear to be mutually exclusive. These results are not completely comparable given the difference in experimental models and conditions used. However, it is conceivable that MHC-II expression may be more sensitive to Hh signalling at an earlier developmental stage, and may be developmentally regulated. In the adult mouse, MHC-II expression in the different TEC subpopulations is fairly stable, where MHC-II can be used as a marker particularly in mTECs to differentiate maturity. In contrast, at earlier ages, MHC-II levels display more variation and may reflect changes in development (Yang, S. *et al*., 2006). The changes in MHC-II expression seen in Hhip-/- newborn TECs as compared to WT may therefore be a product of Hh signalling changes consequent to loss of *hhip* altering early conventional TEC development.

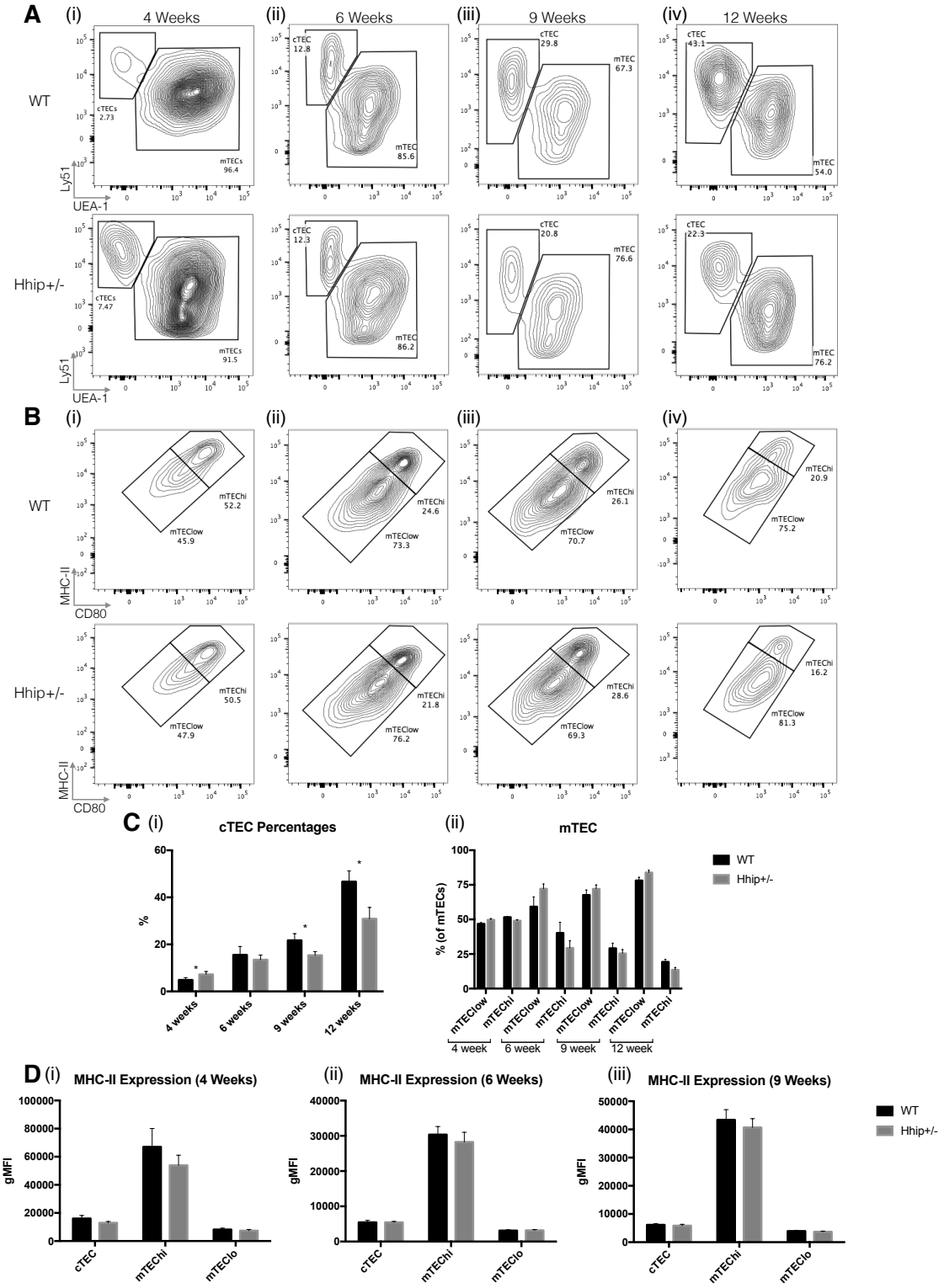

Figure 5.4: *Hhip* heterozygosity in adult mice changes TEC frequencies but not MHC-II expression
(A) Representative FACS plots show cTEC and mTEC frequencies in (i) 4, (ii) 6, (iii) 9, and (iv) 12 week old WT and Hhip+/- mice. **(B)** mTEChi and mTEClow cells as distinguished by MHC-II and CD80 expression, where mTECs were previously gated as CD45-Epcam+Ly51-UEA-1+. **(C)** (i) cTEC percentages and (ii) mTEChi and mTEClow frequencies. **(D)** MHC-II levels represented by geometric mean of TECs at (i) 4, (ii) 6 and (iii) 9 weeks of age. Graphs shown are from a single experiment, statistics are pooled across all experiments. P-values were determined by student's t test where * $p < .05$. Total experimental size: 4 weeks WT n=6, Hhip+/- n=9; 6 weeks WT n=7, Hhip+/- n=6; 9 weeks WT n=6, Hhip+/- n=6; 12 weeks WT n=6, Hhip+/- n=5.

5.1.3 Hhip-mediated Hh signalling changes are modulated by Gas1 and Boc

To evaluate the downstream consequence of a loss of *hhip* on Hh signalling molecules, most of which are expressed in a feedback loop, Hhip+/- cTECs and mTECs from mice at 4, 6 and 9 weeks of age were isolated and the expression of key Hh signalling components compared against WT. Expression of the positive co-receptors Gas1 and Boc, the Hh receptor Ptch1 and the downstream transcription factor Gli2 were impacted (5.5A, 5.5B, 5.5C). Changes in *gas1* copy numbers correlated positively with the frequencies of cTECs in 4 week old mice, where there were more Hhip+/- cTECs which also expressed higher levels of Gas1, while Hhip+/- mTECs expressed less Gas1 (5.5D). In keeping with this observation, Gas1 expression was comparable between genotypes in cTECs and mTECs isolated from 6 week old mice. Finally, at 9 weeks of age, where there were now more Hhip+/- mTECs as compared to WT, Gas1 expression in these mTECs had also increased, along with levels of Boc (5.5E). Importantly, *hhip* mRNA copy numbers remained comparable between WT and Hhip+/- TECs, demonstrating a compensatory mechanism that allowed regular *hhip* expression independent of gene copy number (5.5A, 5.5B, 5.5C). To evaluate if the mRNA expression changes of *gas1* and *boc* observed were a direct consequence of reduced Hhip, *hhip* expression was targeted in the cTEC1.2 line. When two of the previously identified Foxn1 binding motifs (3.3A) were ablated in combination, reducing the expression of *hhip* (3.3B), *gas1*, *boc* and *gli2* expression were upregulated (5.5F). As Gli2 is a primary transcriptional activator of Shh signals in the mouse (Pan, Y. *et al.*, 2006; Ding, Q. *et al.*, 1998; Sasaki, H. *et al.*, 1999), loss of one *hhip* allele did indeed result in increased Hh signalling. Taken together, the observations above confirmed that a decrease in *hhip* gene copy number directly affects Hh signalling despite no overt change in *hhip* mRNA presence, mediated by Gas1 and Boc.

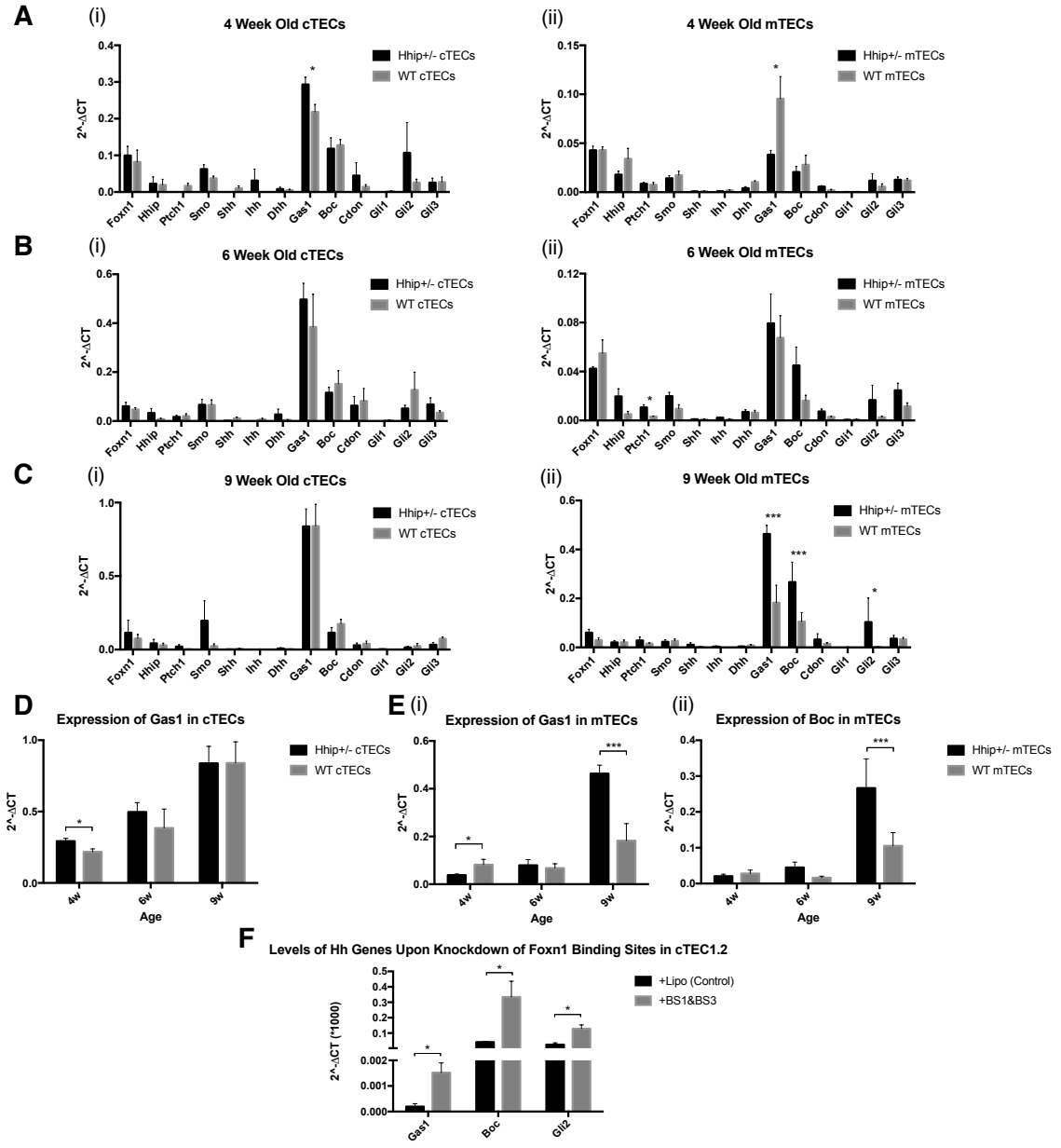

Figure 5.5: Changes in Hh signalling in TECs as a result of *hhip* heterozygosity are mediated by Gas1 and Boc
Expression levels of effector molecules of the Hh signalling pathway in cTECs and mTECs of **(A)** 4, **(B)** 6 and **(C)** 9 week old WT and Hhip+/- mice. Expression of **(D)** *gas1* in cTECs and **(E)** (i) *gas1* and (ii) *boc* in mTECs. **(F)** Loss of previously defined Foxn1 binding sites BS1 and BS3 near the *hhip* translational start site using Crispr/Cas9 targeting in the cTEC1.2 cell line after 48 hours. Significant changes in expression of *gas1*, *boc* and *gli2* are shown. Values are normalised to *gapdh* expression. P-values were determined by student's t test where * p < .05, ** p < .01, *** p < . 001 and Bonferroni correction was applied.

This result is unexpected as expression of the two positive regulators *gas1* and *boc* is characteristically downregulated as an autoregulatory response to Hh signalling (Lee, C. *et al.,* 2001; Tenzen, T. *et al.*, 2006). The results also displayed no significant differences in *hhip* mRNA levels in Hhip+/- TECs as compared to WT. As *hhip* itself is a positive target of Hh signalling, the increased Hh signalling under

heterozygous Hhip+/- conditions could have upregulated *hhip* expression via a previously documented feedback loop (Chuang, P. & McMahon, A., 1999).

Parallel to an increase in thymus size, TEC numbers proliferate rapidly during the first 4 weeks of life, coinciding with a particularly strong expansion of cells with an mTEC phenotype. In mice older than 4 weeks of age, thymic involution is initiated, affecting the mTEC population preferentially such that the mTEC/cTEC ratio is reduced (Gray, D. *et al*., 2006). Early in thymus development, Hh signalling likely favours mTEC development, as the frequencies of these cells are increased in neonatal mice homozygously deficient for *hhip.* In the Hhip+/- thymus, the compensatory mechanism to boost *hhip* expression to normal levels (as represented by comparable numbers of *hhip* transcripts in Hhip+/- and WT TECs) may potentially inhibit Hh signalling to a level lower than WT, thus resulting in comparatively reduced mTEC frequencies. Once involution is initiated after 4 weeks of age, the phase of mTEC expansion is replaced by homeostatic maintenance and eventual contraction of the mTEC population, which may require less Hh signalling. The changes in TEC frequencies could thus be a reflection of stage specific sensitivity to Hh signals and autoregulation. In addition, *foxn1* expression is regulated differentially between cTECs and mTECs upon thymic involution, with reduced transcription in cTECs (O'Neill, K. *et al*., 2016). In keeping with *hhip* as a target of Foxn1, comparatively reduced levels of *foxn1* in cTECs with age could possibly result in reduced expression of *hhip* in any cTEC-like bipotent progenitors, increasing Hh signalling. In Hhip+/- mice, this could potentially further promote an mTEC fate and promote mTEC expansion with age as seen in the data above.

5.1.4 Loss of *hhip* impairs gene expression

Transcriptional changes in Hhip-/- mice were investigated to assess the molecular consequences in different TEC subpopulations in the complete absence of *hhip* expression. To this end, cTECs and mTECs were isolated from E18.5 WT and Hhip-/- thymi as biological replicates of 200 cells each. mRNA was generated using the Smart-seq2 protocol (Picelli, S. *et al.*, 2014) and the products sequenced. Under these conditions, 200 cells are considered sufficient to yield a transcriptomic signature representative of bulk RNA measurements (Marinov, G. *et al.*, 2014). Upper-quartile normalised transcripts per million (TPM) values for each genotype and cell type were analysed and compared.

Table 5.1: Gene expression of control genes in WT and Hhip-/- E18.5 TECs

Gene	WT cTEC (tpm)	Hhip-/- cTEC (tpm)	WT mTEC (tpm)	Hhip-/- mTEC (tpm)	cTEC log2 FC	mTEC log2 FC
Gapdh	1862.7	2125.3	2668.4	2396.9	0.190	-0.155
Actb	1789.0	1610.6	3305.6	2458.1	-0.152	-0.427
Foxn1	78.8	59.6	35.5	47.6	-0.403	0.423
Enpep	11.9	17.9	0	2.47	0.589	NA
H2-k1	590.7	592.5	858.1	1269.7	0.00439	0.565
H2-ab1	7106.2	5917.7	8833.3	12892.5	-0.264	0.546

All biological replicates passed quality check (QC) metrics. Expression of the housekeeping genes *gapdh* and *actb* were used as internal positive controls, and demonstrated high expression levels with robust TPM values. Log_2 fold change (FC) values were calculated between WT and Hhip-/- mTECs and cTECs. Significant changes between individual samples were not observed, consistent with the notion that an absence of Hhip should not affect the expression of housekeeping genes. All TECs expressed *foxn1*, *h2-k1* (MHC-I) and *h2-ab1* (MHC-II), and cTECs expressed *enpep* (Ly51), while mTECs expressed none (WT) or

very low levels (Hhip-/-), verifying that cTECs and mTECs were correctly differentiated during the sorting process.

Table 5.2: Gene expression of Hh signalling genes in WT and Hhip-/- E18.5 TECs

Gene	WT cTEC (tpm)	Hhip-/- cTEC (tpm)	WT mTEC (tpm)	Hhip-/- mTEC (tpm)	cTEC log2 FC	mTEC log2 FC
Hhip	2.29	0.217	1.98	0.105	-3.40	-4.24
Shh	0.820	0.0333	0	0	-4.62	NA
Ihh	0	0	0	0	NA	NA
Dhh	0.0467	0.0367	0.325	4.23	-0.348	3.70
Smo	12.1	12.8	6.82	5.30	0.0796	-0.364
Ptch1	3.31	1.84	2.45	3.26	-0.849	0.412
Ptch2	8.25	0.0633	0.0950	0.28	-7.02	1.56
Disp1	6.36	1.98	8.63	10.1	-1.69	0.228
Disp2	0.980	0	0.175	0.765	NA	2.13
Gas1	1.55	5.797	0.185	0.0550	1.90	-1.75
Boc	14.1	7.95	2.55	1.44	-0.821	-0.827
Cdon	0.343	1.15	0.415	0.645	1.74	0.636
Gli1	0.867	0	0.910	0	NA	NA
Gli2	8.48	5.10	0	0.860	-0.732	NA
Gli3	9.07	5.33	2.59	3.94	-0.766	0.603
Kif7	3.43	0	0	0.165	NA	NA
Sufu	5.56	3.77	1.85	4.33	-0.766	0.603

Hhip transcripts were reduced in both Hhip-/- cTECs and mTECs when compared to WT epithelia. Hence, disruption of the *hhip* locus resulted in reduced mRNA expression. Consequently, it is unlikely that Hhip-/- TECs express normal full-length Hhip protein. The loss of *hhip* transcripts in Hhip-/- mice also verified that a compensatory mechanism was likely present in heterozygous animals, as Hhip+/- mice did not demonstrate reduced *hhip* transcripts by qPCR analysis. Expression of gene products related to Hh signalling was next investigated. Transcripts of the ligand *ihh* were not found in TECs. A $\log_2$ FC of -4.62 for *shh* expression was found between WT and Hhip-/- cTECs, indicating an almost 25-fold decrease. In contrast, *shh* transcripts were not detected in mTECs under these conditions. A possible explanation for this discrepancy may be that the “pseudo-bulk” sequencing

conditions with only 200 cells were suboptimal to detect *shh* expression. *Dhh* transcripts were detected both in cTECs and mTECs. This result is opposite to published data in the literature (Outram, S. *et al.*, 2000), but corroborates with a PCR-based detection of *dhh* in TECs isolated from embryos, and 2 week and 4 week old mice (3.2), suggesting that this is unlikely to be due to a technical error. Hence, a potential involvement of Dhh in TEC differentiation should therefore not be precluded, not least as Hhip-/- mTECs display a $\log_2$ FC increase of 3.7 in *dhh* transcripts compared to WT epithelia.

Transcripts for canonical members of the Hh signalling pathway could be detected in cTECs and mTECs with the notable exception of *gli2* and *kif7*, which were not found in WT mTECs. Transcripts for several genes were differentially expressed by at least two fold when comparing WT and Hhip-/- TECs, including *ptch2, disp1*, *disp2, gas1* and *cdon*. Loss of *hhip* expression resulted in increased *gas1* expression in Hhip-/- cTECs, confirming that a loss of Hhip directly upregulated *gas1* transcription as previously demonstrated by qPCR. However, the overall changes in expression of Hh signalling molecules as deduced from the gene expression results were inconclusive. TPM values were relatively low for many transcripts, particularly the Hh ligands, revealing different expression patterns between cTECs and mTECs. Hence, these data did not support the conclusion that Hh signalling may have been uniformly affected by the loss of regular *hhip* expression. Moreover, most E18.5 TECs are still immature and as a population may contain a large proportion of cells still in transition to a more mature phenotype and cell stage. In conclusion, the precise consequences of a loss of *hhip* expression would be best studied in adult TEC populations where the biological impact of changes in Shh signalling can be defined with more clarity. Instead, the

sequencing data was also used for a genome-wide screen to identify genes whose expression are significantly affected consequent to a loss of Hhip.

Table 5.3: Gene expression of relevant genes identified in WT and Hhip-/- TECs

Gene	WT cTEC (tpm)	Hhip-/- cTEC (tpm)	WT mTEC (tpm)	Hhip-/- mTEC (tpm)	cTEC log2 FC	mTEC log2 FC
Ly75	24.6	23.8	5.68	4.26	-0.0477	-0.415
Tnfrsf11a	2.67	4.88	23.3	110.3	0.870	2.25
Ccl7	24.6	561.7	0.0450	21.1	4.52	8.87
Ccr6	0.0467	0.0367	0.0450	12.0	-0.348	8.06
Ccr7	35.5	0.0700	247.0	310.0	-8.99	0.327
Sox17	0.0333	0	29.3	0.110	NA	-8.06
Sox6	7.82	0.480	12.2	0.265	-4.03	-5.53
Wnt2	0	0	5.65	0.160	NA	-5.14
Hoxa1	0.0800	8.489	0	0.335	6.73	NA
Fgf7	1.683	2.09	0.0850	3.74	0.310	5.46

Over 700 genes were identified whose gene expression was significantly (log_2 FC value >5 or <-5) different between WT and Hhip-/- TECs. Several of these genes had been previously studied in the context of thymus organogenesis and function or have a known interaction with the Hh signalling pathway, and a select list is presented above in Table 5.3. Genes whose differential expression pattern did not meet the log_2 FC threshold of -5/5 included *ly75* (CD205) and *tnfrsf11a* (RANK), which are known markers of the TEC progenitor population (Baik S. *et al.*, 2013). *Ly75* was expressed highly in cTECs and lower in mTECs, and *tnfrsf11a* was expressed lowly in cTECs and highly in mTECs. Expression of these 2 markers in both cTEC and mTEC populations correlated with the suggestion that these early TEC populations contained not only committed cells but also bipotent progenitors. The increased expression of *tnfrsf11a* in Hhip-/- mTECs (log_2 FC 2.25) also strongly supported the notion that the loss of Hhip promotes mTEC differentiation, as RANK signals positively regulate mTEC development (Akiyama, T. *et al.*, 2008).

Transcripts for chemokines and their receptors, including *ccl7*, *ccr6* and *ccr7,* were found differentially expressed between WT and Hhip-/- TECs. *Ccr6* is important for the migration and differentiation of DN1 early thymocyte progenitors (Bunting, M. *et al*., 2014), and is significantly upregulated in Hhip-/- mTECs as compared to WT. *Ccl7* is important in the periphery for T_{H2} immune responses and is constitutively expressed in the thymus (Horikawa, T. *et al*., 2002; Vestergaard, C. *et al*., 2004), and was drastically upregulated in both Hhip-/- cTECs and mTECs. *Ccr7* levels were expressed at high levels in WT cTECs and decreased in Hhip-/-, although CCR7 is usually found on the cell surface of thymocytes (Kim, C. *et al*., 1998). These molecules are important in normal T cell development and function, and the observed changes in their expression provide an indication that a loss of *hhip* expression does not merely affect TEC phenotype, but likely alters TEC function as well. Alongside, changes in expression were observed in genes such as *fgf7,* which impacts on TEC differentiation and function (Revest, J. *et al*., 2001; Rossi, S. *et al*., 2007). *Fgf7* expression was increased in Hhip-/- mTECs, consistent with the observation that loss of *hhip* favoured mTEC differentiation, as provision of recombinant Fgf7 in WT mice promotes mTEC expansion (Erickson, M. *et al*., 2002). Expression of the transcription factor *hoxa1* was also more than 100-fold upregulated in Hhip-/- cTECs. Mice constitutively deficient in *hoxa1* expression display a hypoplastic thymus, demonstrating the importance of Hoxa1 in thymus organogenesis (Makki, N. *& Capecchi, M. et al*., 2012). These changes in the transcription profile of Hhip-/- mice indicate that a change in Hh signalling may indeed impact, either directly or indirectly, on TEC development and function.

Loss of *hhip* expression also altered the copy numbers of transcripts encoding the Sox transcription factors *sox17* and *sox6*. Sox6 is from a group of sex-determining

transcription factors, and is known to promote chondrogenesis and erythropoesis (Smits, P. *et al*., 2001; Dumitriu, B. *et al*., 2006), similar to Dhh's involvement in testis development and erythrocyte differentiation (Lau, C. *et al*., 2012) and Ihh in chondrocyte differentiation (Vortkamp, A. *et al*., 1996). Sox17 is important for the maintenance of fetal haematopoietic stem cells (Kim, I. *et al*., 2007). These provide an example of how a loss of *hhip* resulting in alterations in Hh signalling could effect transcriptional changes of genes important in Hh-modulated processes. These downstream changes also extend to molecules involved in other signalling pathways. For example, *fgf7* expression was affected as shown above, and Hhip is a known modulator of the Fgf signalling pathway (Chuang, P. *et al*., 2003; Kawahira, H. *et al*., 2003). *Wnt2*, a ligand in the Wnt signalling pathway crucial for embryonic development (reviewed in Croce, J. & McClay, D., 2008) was downregulated in Hhip-/- mTECs. These signalling mechanisms are all crucial for cell fate and embryonic patterning (reviewed in Perrimon, N. *et al*., 2012), a primary biological role of Hh signalling. However, as these signalling pathways often work in tandem in an intricate network, changes in the expression of these molecules supports that a loss of *hhip* expression likely modulates Hh signalling in TECs, and that the downstream transcriptional changes in other pathways may potentially be the result of Hh signalling changes. Hhip, Wnt2, and Fgf signalling have been well documented in the lung mesenchyme, wherein signalling may occur in a paracrine manner to the epithelium, affecting other signalling molecules such as Bmp4 (Yin, Y. *et al*., 2008; Bellusci, S. *et al*., 1997; Hrycaj, S. *et al*., 2015; Goss, A. *et al*., 2011). It is therefore conceivable that the phenotype seen in Hhip-/- TECs is partially caused by interactions with mesenchymal cells in and surrounding the thymus, as expression of *hhip* is also lacking in these cells in mice with a constitutive *hhip*-deficiency.

Genome-wide transcriptomic changes arising from the constitutive loss of a gene are exceedingly complex and therefore mostly preclude an unequivocal conclusion about which pathways or molecules are affected as a direct consequence of this genetic alterations. Nevertheless, the sequencing results present three points here for further consideration. First, the loss of *hhip* expression significantly alters the downstream expression of Hh signalling molecules including *gas1*, and genes broadly important in TEC differentiation and function as well as specific mTEC differentiation, reinforcing the importance of Hhip in TECs. Second, Hh signalling in TECs may be effected by other ligands than only Shh, and the potential role of Dhh in particular, if any, should be considered in the future. Finally, a constitutive loss of *hhip* will affect many different cell types that may be either directly or indirectly involved in the organogenesis, differentiation, function and maintenance of the thymus at any point in time. Changes in TEC biology may therefore be the result of cell-intrinsic and/or cell-extrinsic alterations, the latter highlighting a crosstalk between different cell lineages, a phenomenon well described in the thymus. Further chapters will focus on clarifying the TEC-specific cell-intrinsic role of Hhip.

5.2 Complete loss of *hhip* affects early T cell development

Neonatal thymocytes were next analysed to investigate whether a constitutive loss of *hhip* affected T cell development. Thymocyte cellularity was comparable for newborn WT, Hhip+/- and Hhip-/- mice (5.6A), and the individual thymocyte subpopulation frequencies of Hhip+/- mice were comparable to those of WT animals (5.6B). The frequency of total DN cells was comparable between WT and Hhip-/- thymi (5.6B). The transitional capacity of cells in each DN developmental stage was calculated by dividing the frequencies of cells with a specific developmental phenotype by the combined total of cells in said population and its

immediate precursors, for example DN2 divided by DN1 + DN2. This allowed an assessment of how many cells had successfully progressed from the previous stage. Based on these calculations, although frequencies of cells in each of the various DN stages were not significantly different between genotypes (5.6C, 5.6D), less Hhip-/- DN1 cells successfully progressed to the DN2 phenotype (5.6D), suggesting a slight delay in development. In addition, loss of *hhip* expression reduced the frequencies of single positive T cells (5.6B), where frequencies of CD4 cells were decreased to 0.714 ± 0.07% compared to WT (1.44 ± 0.2%). The frequency of iCD8 cells was significantly increased in Hhip-/- mice (Hhip-/- 3.56 ± 0.4%, WT 2.43 ± 0.2%), and mCD8 thymocytes also seemed slightly increased, although this was not significant (Hhip-/- 0.114 ± 0.04%, WT 0.0646 ± 0.03%) (5.6E). Consequently, the CD4/CD8 ratio was significantly decreased in Hhip-/- mice in comparison to WT animals (5.6E). However, the mCD8 population is barely detectable at this early postnatal stage and large variance in the cells' detection make any reliable quantification difficult.

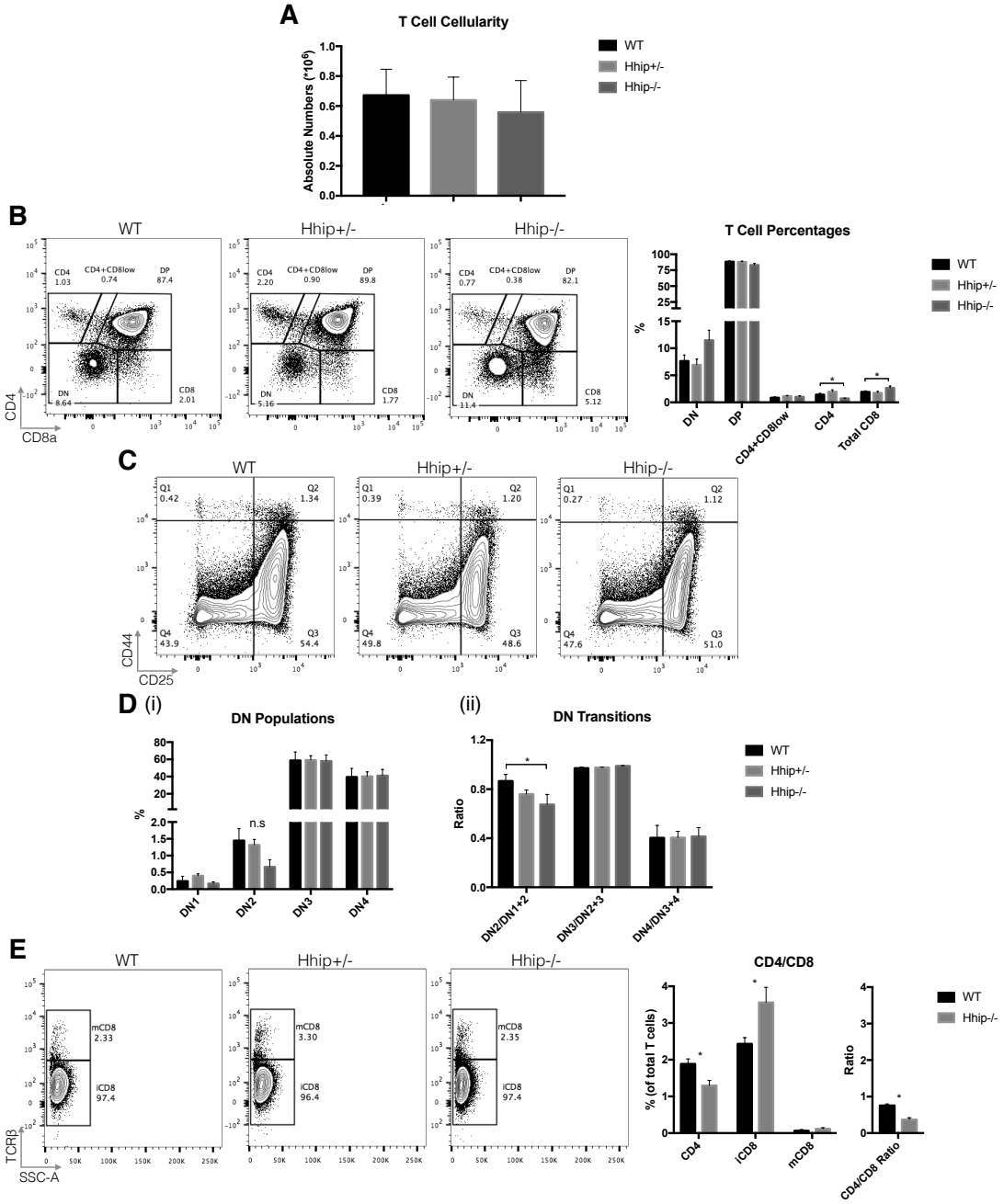

Figure 5.6: Absence of Hhip affects single positive T cell development
(A) Absolute T cell numbers, calculated based on live Lin- single T cells yielded from mechanical disruption of thymi, of WT, Hhip+/- and Hhip-/- neonates. **(B)** Representative FACS plots and frequencies of individual thymocyte subpopulations. **(C)** DN stages were distinguished by CD44 and CD25 expression where **(D)** (i) DN1 is represented as CD44+CD25-, DN2 as CD44+CD25+, DN3 as CD44-CD25+ and DN4 as CD44-CD25-. (ii) DN transitions were calculated by taking frequencies of cells in the population of interest, divided by the total frequencies of cells in that population and the one preceding e.g DN2/DN1+DN2. **(E)** The CD8 population was further divided into iCD8 and mCD8, defined as CD8a+TCRβ- and CD8a+TCRβ+ respectively. Frequencies of iCD8, mCD8 and CD4 cells are shown as a proportion of total Lin- single T cells. The CD4/CD8 ratio was calculated as total CD4 frequencies divided by total CD8. Graphs shown are from a single experiment, statistics are pooled across all experiments. At least 3 independent experiments were conducted. P-values were determined by student's t test where * $p < .05$. Total experimental size: WT n=11, Hhip+/- n=20, Hhip-/- n=14.

Normal maturation was impaired in Hhip-/- thymocytes, where the proportion of immature $CD5^{low}TCR\beta^{low}$ cells was significantly increased from 39.6 ± 0.7% in WT to 44.8 ± 1.6% in Hhip-/- (5.7A), implying that comparatively more thymocytes in

the Hhip-/- mouse had not yet signalled via their TCR, a necessary step to receive survival signals and mature further. CCR7 and CD69 expression was next assessed to follow the progression of thymocytes moving from the cortex to medulla. Cells that do not express CCR7 are located in the cortex, and these cells can be further distinguished by their expression of CD69, as immature cells that have not undergone positive selection do not express CD69, whereas cells that have upregulated CD69 have likely just encountered TCR ligands, hence the increased expression of CD69 as a cell activation marker (Ueno, T. *et al.*, 2004). The $CCR7^{-}CD69^{+}$ population was increased in Hhip-/- mice (6.88 ± 0.6%) as compared to WT with 5.15 ± 0.2% (5.7B, 5.7C). The distribution of thymocytes with this phenotype was altered, with significantly reduced frequencies of CD4 cells observed in Hhip-/- mice was compared to WT (5.7C). After positive selection takes place, cells upregulate CCR7 in response to signals from the medulla, thus adopting a $CCR7^{+}CD69^{+}$ phenotype (5.7B). However, these cells are nascent in the young mouse and may not represent a true population, thus further statistical analysis was excluded.

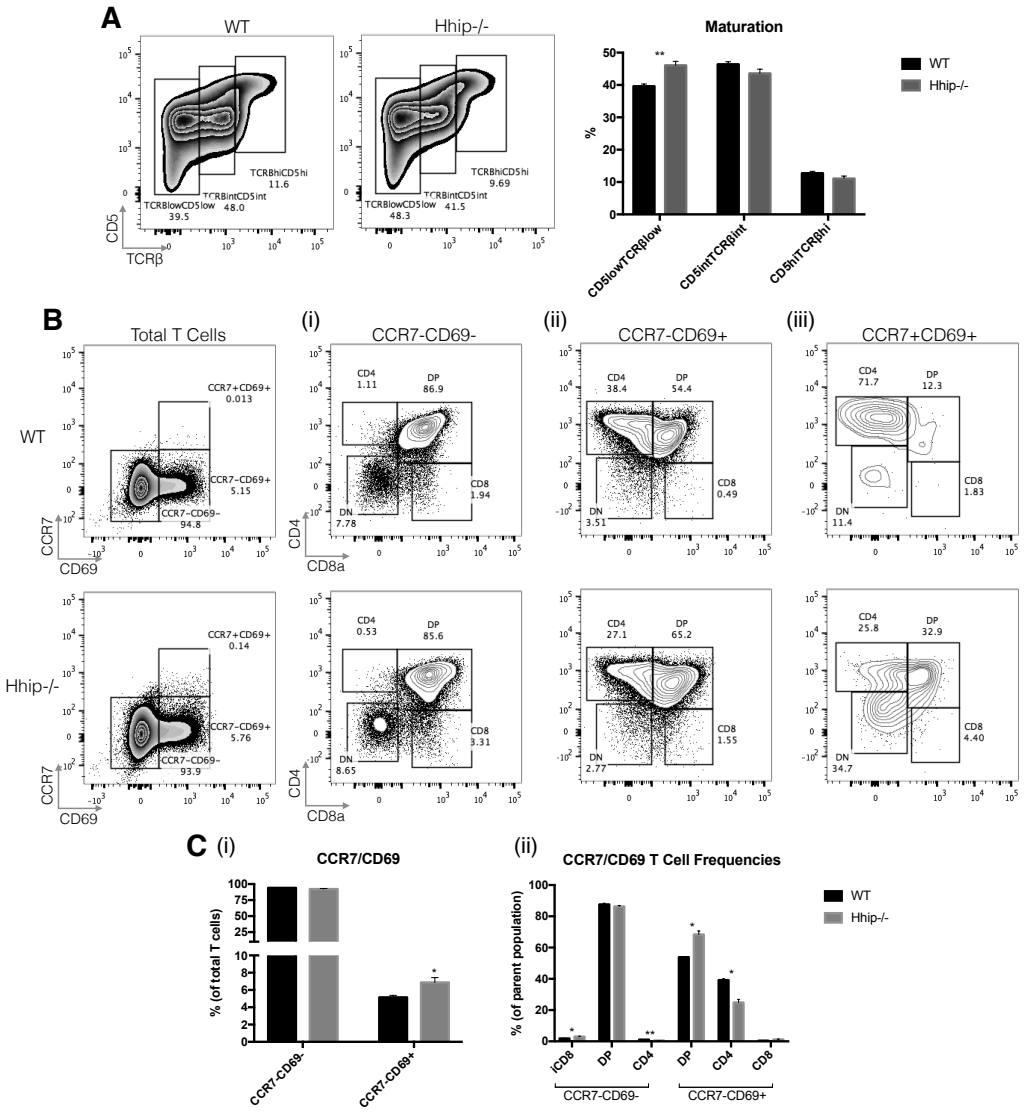

Figure 5.7: Complete loss of *hhip* affects maturation of CD4 T cells
(A) Maturation as assessed by CD5 and TCRβ expression in WT and Hhip-/- neonates. **(B)** (i) CCR7-CD69-, (ii) CCR7-CD69+ and (iii) CCR7+CD69+ live single Lin- T cells, and the frequencies of thymocytes based on CD4 and CD8a expression analysed in each compartment. **(C)** (i) Frequencies of total T cells with either a CCR7-CD69- or CCR7-CD69+ phenotype. (ii) Distribution of individual thymocyte subpopulations with these phenotypes, where the parent population refers to either CCR7-CD69- or CCR7-CD69+ total T cells.

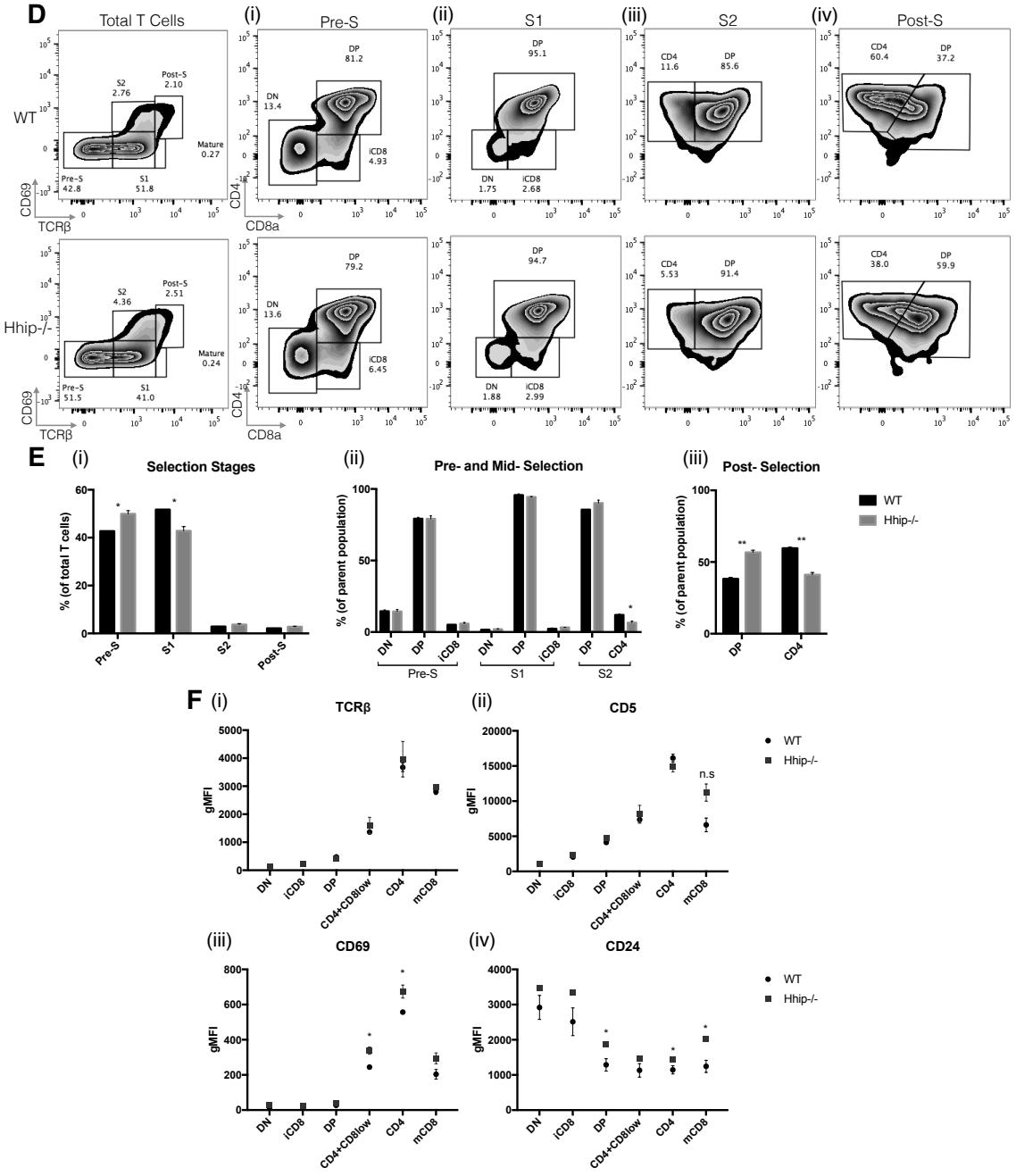

Figure 5.7: Complete loss of *hhip* affects maturation of CD4 T cells
(continuation) **(D)** Representative FACS plots showing live Lin- single T cells divided into different selection stages as defined by TCRβ and CD69 expression, and the corresponding thymocyte profile in each stage, namely (i) CD69-TCRβ- (Pre-S), (ii) CD69-TCRβint (S1), (iii) CD69+TCRβint (S2) and (iv) CD69hiTCRβhi (Post-S). The mature stage was excluded due to low cell numbers. **(E)** (i) Frequencies of total cells in each selection stage. (ii) Distribution of individual thymocyte subpopulations in the pre- and mid- selection stages (Pre-S, S1, S2) and (iii) post-selection (Post-S) stage. **(F)** Expression of (i) TCRβ, (ii) CD5, (iii) CD69 and (iv) CD24 of individual thymocyte subpopulations. Graphs shown are from a single experiment where WT n=3, Hhip-/- n=3, and is representative of 2 independent experiments. P-values were determined by student's t test where * $p < .05$, ** $p < .01$.

Positive selection is a crucial component of the thymocyte maturation process and is effected by cTECs in the cortex, while negative selection largely occurs in the medulla. To specifically evaluate the dynamics of thymocyte selection in Hhip-/- mice as compared to WT given the delayed maturation observed, cells were

analysed for the sequential upregulation of TCRβ and concurrent changes in CD69 expression. The frequency of $CD69^{-}TCR\beta^{-}$ thymocytes i.e cells that had not yet engaged in the selection process (Pre-S) were increased in Hhip-/- mice. However, cells at the subsequent developmental stage, marked by the $CD69^{-}TCR\beta^{int}$ phenotype (designated S1) were less abundant, indicating a partial developmental block in the initiation of selection. The CD4 compartment was reduced in Hhip-/- mice in the late stage of selection (S2), as well as immediately post-selection (Post-S) (5.7D, 5.7E). Cells presenting with a $CD69^{low}TCR\beta^{hi}$ phenotype, which usually constitutes the most mature population, were very low in numbers and thus excluded from analysis. TCRβ and CD5 expression were not significantly different in any of the T cell subpopulations between WT and Hhip-/-. However, CD69 expression was increased in Hhip-/- $CD4^{+}CD8^{low}$ and CD4 populations, and CD24 was increased in Hhip-/- DP, CD4 and mCD8 populations (5.7F).

The data suggests that a deficiency of *hhip* affects the generation of CD4 T cells, consistent with increased Hh signalling and the earlier *in vitro* experiments (4.1, 4.2). Hhip-/- thymocytes are unable to develop in the same manner as WT thymocytes, as evidenced by the increased proportion of $CD5^{low}TCR\beta^{low}$ immature cells and corresponding decreased frequencies of CD4 mature cells, and brings to light a potential developmental defect. However, as the overall frequencies of DN and DP subpopulations in Hhip-/- mice are similar to WT animals, and the thymocyte subpopulation profile of immature populations in pre-selection stages are comparable, loss of Hhip may primarily impair selection of cells during the later stages of development. Post-selection single positive T cells in the Hhip-/- thymus also presented with an altered, less mature phenotype represented by high CD69 and CD24 expression, in contrast to mature WT single positive T cells that

traditionally downregulate both CD69 and CD24 before exiting the thymus. This could therefore indicate a defect in the selection process that allows a less competent and functional population of T cells to survive.

5.2.1 T cell defect in neonates is transient and is not sustained after FTOC

WT, Hhip+/- and Hhip-/- E18.5 FTOC displayed comparable T cell frequencies after 4 days of culture (5.8A). The percentage of $CD5^{hi}TCR\beta^{hi}$ cells was reduced in Hhip-/- mice when compared to WT (17.1 ± 0.3% vs 21.3 ± 1.0%) (5.8B), although frequencies of individual thymocyte subpopulations in each stage of selection, as defined according to their CD69 and TCRβ expression profile, were comparable (5.8C). This indicated that the initial developmental defect seen in neonatal mice where CD4 frequencies were reduced in Hhip-/- animals was likely a delay and not a partial block, as this could be overcome after 4 days of culture.

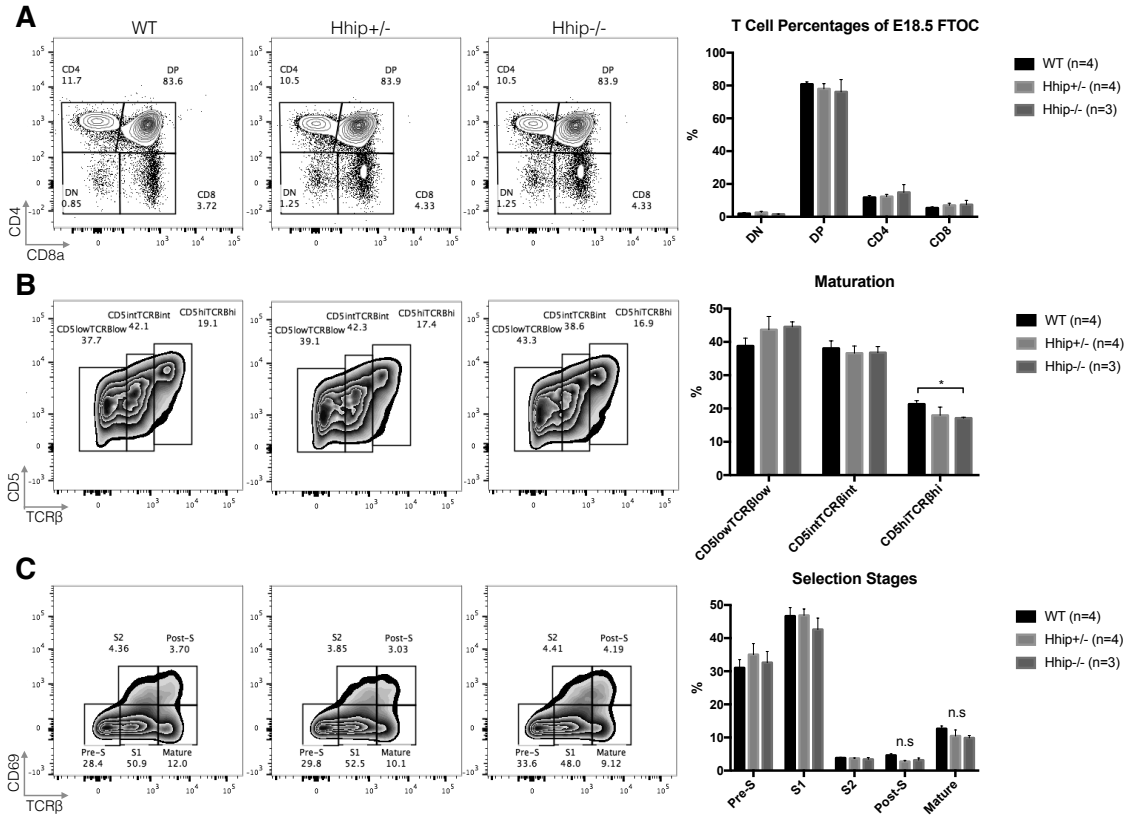

Figure 5.8: Regular frequencies of thymocyte subpopulations are observed after FTOC
(A) Representative FACS plots and statistics of individual thymocyte subpopulation frequencies after E18.5 thymi of WT, Hhip+/- and Hhip-/- genotypes have been cultured as FTOC for 4 days. **(B)** Maturation is assessed by the proportions of live single Lin- T cells expressing various levels of CD5 and TCRβ. **(C)** Selection stages of total T cells are defined by CD69 and TCRβ expression. Graphs shown are from a single experiment and is representative of at least 2 independent experiments, Statistics are pooled from 2 experiments. P-values were determined by student's t test where * $p < .05$. Total experimental size: WT n=6, Hhip+/- n=8, Hhip-/- n=5.

E18.5 Hhip-/- thymi were next cultured with 1.0 µg/ml rHhip in the FTOC media to evaluate if overexpression of Hhip would have any effect on thymocyte development, in particular with regards to TCRβ and CD5 expression, which are consistently altered in Hhip-/- mice. T cell frequencies were unchanged by exposure to rHhip as compared to WT (5.9A). Addition of rHhip reduced the proportion of immature $CD5^{low}TCR\beta^{low}$ cells (WT 29.5 ± 0.1%, rHhip 22.3 ± 2.2%) and instead produced a larger fraction of mature $CD5^{hi}TCR\beta^{hi}$ cells at 37.6 ± 2.3% compared to only 15.6 ± 2.9% in WT (5.9B). Fewer cells had a $CD69^{-}TCR\beta^{-}$ pre-selection phenotype, although the distribution of individual thymocyte subpopulations within this stage was comparable to WT (5.9C, 5.9D). While more cells were $CD5^{hi}TCR\beta^{hi}$, TCRβ and CD5 cell surface levels on each individual

thymocyte subpopulation as assessed by geometric mean fluorescence intensity were unaffected (5.9E).

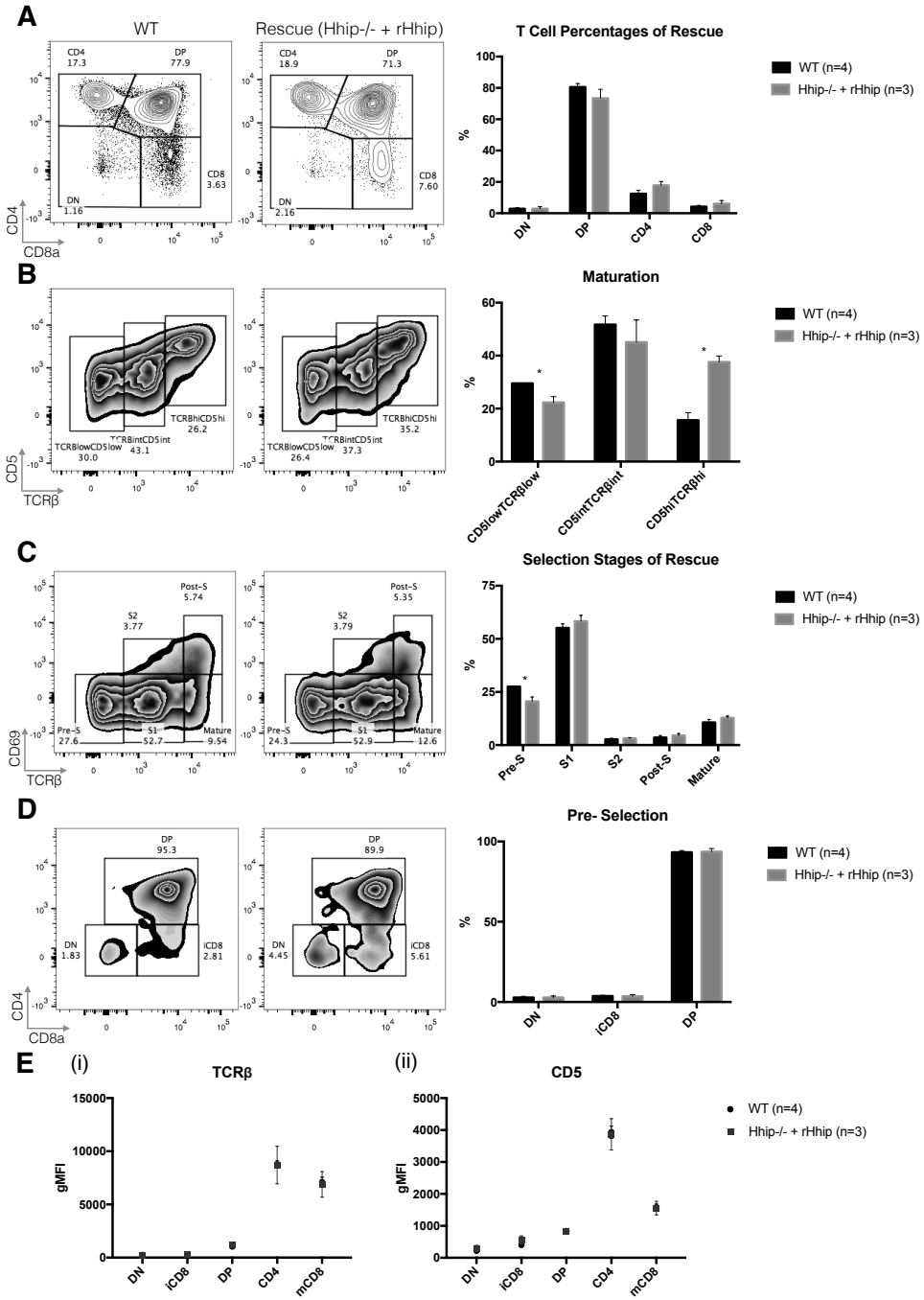

Figure 5.9: Supplement of rHhip changes frequencies of CD5 and TCRβ-expressing Hhip-/- cells
(A) Thymocyte profiles of E18.5 WT and Hhip-/- cultures supplemented with rHhip in the FTOC media. **(B)** CD5 and TCRβ low, intermediate and high-expressing live single Lin- T cells upon addition of rHhip. **(C)** Selection stages of total T cells defined by CD69 and TCRβ expression, and **(D)** the distribution of individual thymocyte subpopulations in the pre-selection CD69-TCRβ- stage. **(E)** (i) TCRβ and (ii) CD5 expression by geometric mean fluorescence intensity in all thymocyte populations. 2 independent experiments were conducted and statistics are pooled. P-values were determined by student's t test where * $p < .05$.

These results confirm that the reduced CD4 frequencies observed in Hhip-/- neonates reflected an early developmental defect that could be corrected with time.

Consequently, the Hhip-/- thymi is able to support the production of thymocyte precursors to mature T cells. Altered T cell frequencies seen in the neonates may therefore reflect a slight delay in one of the developmental stages rather than a complete block or deficiency preventing normal mature T cells from developing. Hhip also plays a role, whether by affecting Hh signalling or via a direct mechanism, in facilitating the correct maturation of T cells that have engaged and signalled correctly via their TCR. The precise mechanism will need to be further elucidated to determine whether Hhip affects the ability of T cells to signal via their TCR and upregulate TCRβ and CD5 expression, or if it affects the ability of TECs to successfully engage with thymocytes' TCR. Importantly, as rHhip was added freely in the media, and could affect any cell within the thymus, the phenotype observed could be a consequence of a combination of the two. The cell type-specific role of Hhip thus has to be delineated further.

5.2.2 *Hhip* heterozygosity does not affect adult thymopoiesis

Although Hhip+/- neonates did not show any defects in thymocyte development, adult Hhip+/- TEC frequencies were altered, thus an impact on T cell development by the altered Hhip+/- TEC environment could not be precluded. As such, Hhip+/- adult T cells were examined for phenotypic differences. Thymocyte cellularity was largely unaffected by the loss of a single *hhip* allele (5.10A). An extensive phenotypic analysis of the different thymocyte subpopulations revealed comparable frequencies between WT and Hhip+/- mice at 4, 6 and 9 weeks of life (5.10B, 5.10C), as well as expression levels of common cell surface markers. These findings were expected as when previously analysed for the TEC compartment, Hhip+/- mice did not display obvious defects in thymopoiesis and a compensatory mechanism had been previously noted in adult TECs, where loss of one *hhip* allele

did not reduce *hhip* mRNA transcripts. This data demonstrated that a partial loss of *hhip* does not impair overall T cell development.

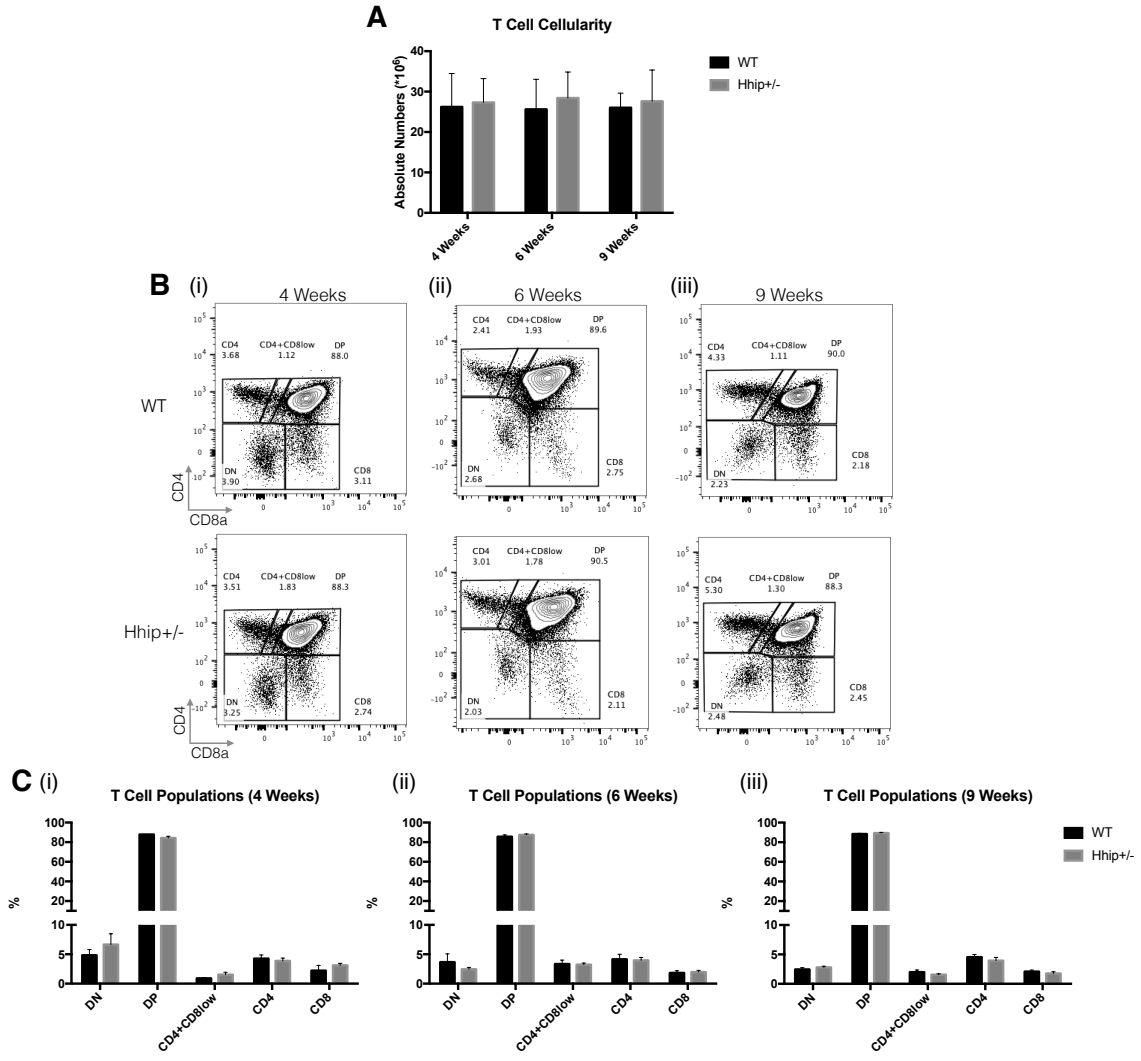

Figure 5.10: T cell development of adult Hhip+/- mice is equivalent to WT
(A) Overall cellularity of T cells at indicated ages comparing between WT and Hhip+/- mice. **(B)** Representative FACS plots and **(C)** statistics of thymocyte subpopulations from WT and Hhip+/- animals of (i) 4, (ii) 6 and (iii) 9 weeks of age. At least 2 independent experiments were conducted for each age, graphs shown are from a single experiment. Statistics are pooled and statistical significance was determined using the student's t test. Total experimental size: 4 weeks WT n=6, Hhip+/- n=7; 6 weeks WT n=6, Hhip+/- n=7; 9 weeks WT n=6, Hhip+/- n=6.

5.3 *Hhip*-deficiency in TECs accounts for changes in cTEC/mTEC ratios

Constitutive Hhip-/- mice uniformly lack *hhip* expression. This therefore precludes an identification of the specific cell type responsible for the thymus phenotype observed in these mice. To investigate whether a loss of *hhip* expression restricted to TECs and other non-haematopoietic thymic stromal cells account for the phenotype observed in systemically Hhip-deficient mice, thymus transplant

experiments were conducted. For this purpose, E18.5 thymic lobes isolated from either WT or Hhip-/- donor embryos were transplanted under the kidney capsules of syngeneic healthy adult mice. These experimental conditions allowed the verification of whether the thymic stromal phenotype of Hhip-deficient TECs would persist in the presence of Hhip-sufficient thymocytes and haematopoietic stromal cells. Moreover, these experiments also addressed whether Hhip-/- TECs could support regular differentiation of WT thymocyte progenitors, which would specify if the maturational defects observed in Hhip-/- thymocytes were thymocyte-intrinsic or due to an insufficient TEC microenvironment. Host and donor cells could be distinguished by different CD45 alleles, where the donor WT and Hhip-/- strain has a CD45.2 allele, while the host B6.SJl.CD45.1 mice have a CD45.1 allele.

Transplanted Hhip-/- thymic lobes had increased total cellularity when compared to grafted WT lobes, but the absolute numbers of TECs were not significantly different between genotypes (5.11A, 5.11B). The TEC phenotype observed previously in the constitutive *hhip*-deficient mice was maintained in the grafts, with fewer cTECs detected in lobes grafted from Hhip-deficient embryos compared to WT transplants (8.05 ± 1.9% vs 23.1 ± 6.2%) (5.11C). Within the cTEC compartment, frequencies of MHC-II^{hi} cells were increased in *hhip*-deficient epithelia from 50.6 ± 0.6% to 76.2 ± 8.9%. Similarly, cTECs with an MHC-I^{hi} phenotype were more abundant in comparison to Hhip-proficient epithelia (90.6 ± 4.5% vs 67.0 ± 3.2%) (5.11D, 5.11E). This change in frequencies of MHC-I^{hi} and MHC-II^{hi} cTECs was further paralleled by a higher cell surface concentration of MHC-I on these cells (5.11E).

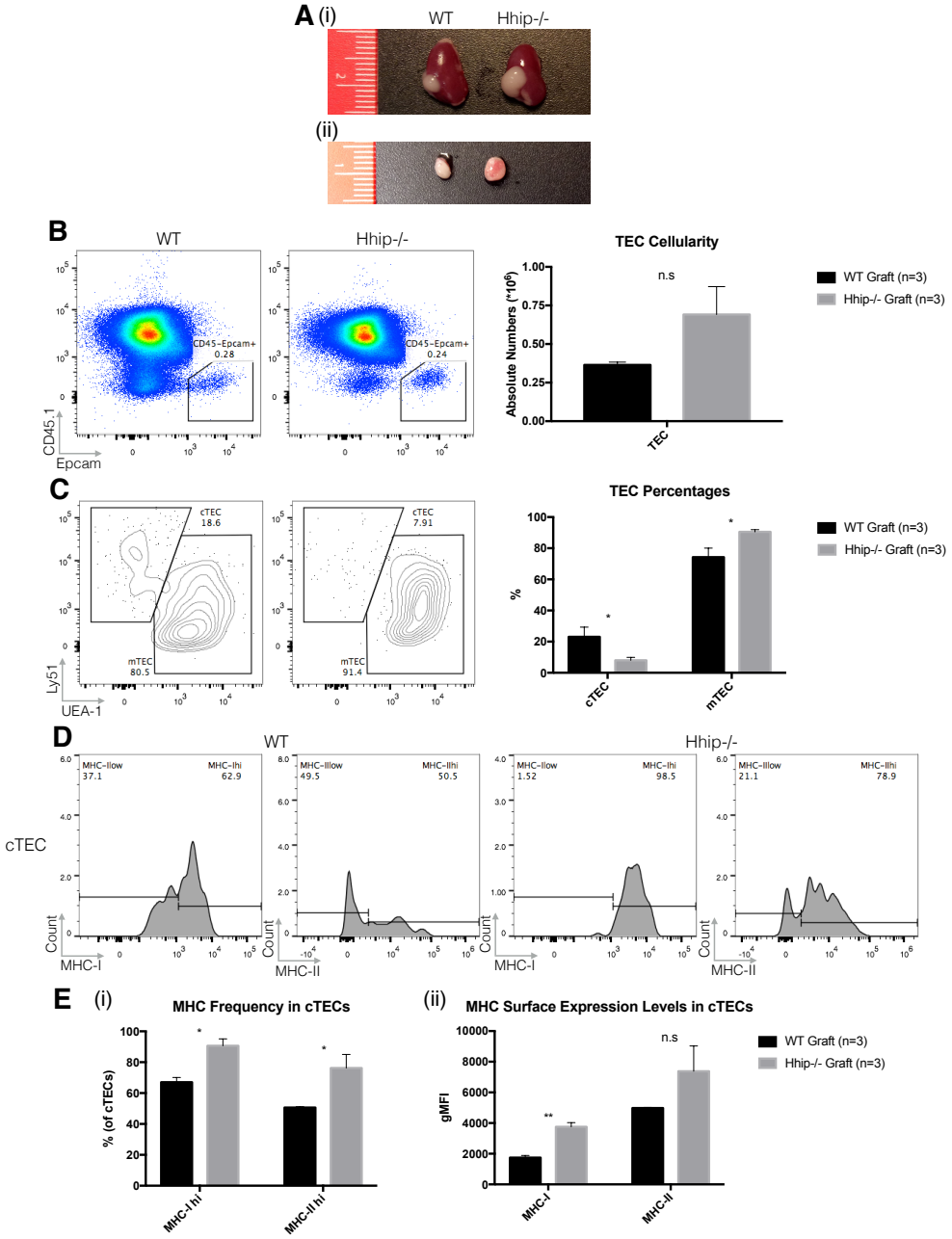

Figure 5.11: Hhip-/- TECs remain different from WT after being transplanted into a normal healthy environment **(A)** (i) Representative images of transplanted E18.5 WT and Hhip-/- thymic lobes grafted under the host kidney capsule after 6 weeks, and (ii) single lobes removed from under the capsule. **(B)** Frequencies and absolute numbers of CD45-Epcam+ live single TECs. **(C)** cTEC/mTEC distribution based on Ly51 and UEA-1 expression. **(D)** MHC-I and MHC-II expression on cTECs. **(E)** (i) Frequencies of MHC-I and MHC-II highly expressing cTECs, and (ii) cell surface expression of both MHC-I and MHC-II in cTECs. 2 independent experiments were conducted, graphs and statistics shown are from a single experiment. P-values were determined by student's t test where * p < .05, ** p < .01. Total experimental size: WT n=5, Hhip-/- n=5.

Subpopulations of mTECs in the grafts was next analysed. Frequencies of mTEC^{low}, mTEC^{hi} and MHC-II^{+}Aire^{+} populations were similar as a proportion of total mTECs (5.12A, 5.12D). Frequencies of cells that expressed high levels of MHC were increased in the mTEC^{low} population, but not in the mTEC^{hi} population, which

were already gated on MHC-II^{hi} cells (5.12B, 5.12C). This suggested that although mTEC^{low} cells as a population express low to intermediate levels of MHC-II, a larger proportion of mTEC^{low} cells in the Hhip-/- graft expressed higher levels of MHC as compared to the WT graft, independent of CD80 cell surface expression. Similar to the cTEC population, MHC-I cell surface concentrations were higher among both mTEC^{low} and mTEC^{hi} populations of *hhip*-deficient epithelia (5.12D).

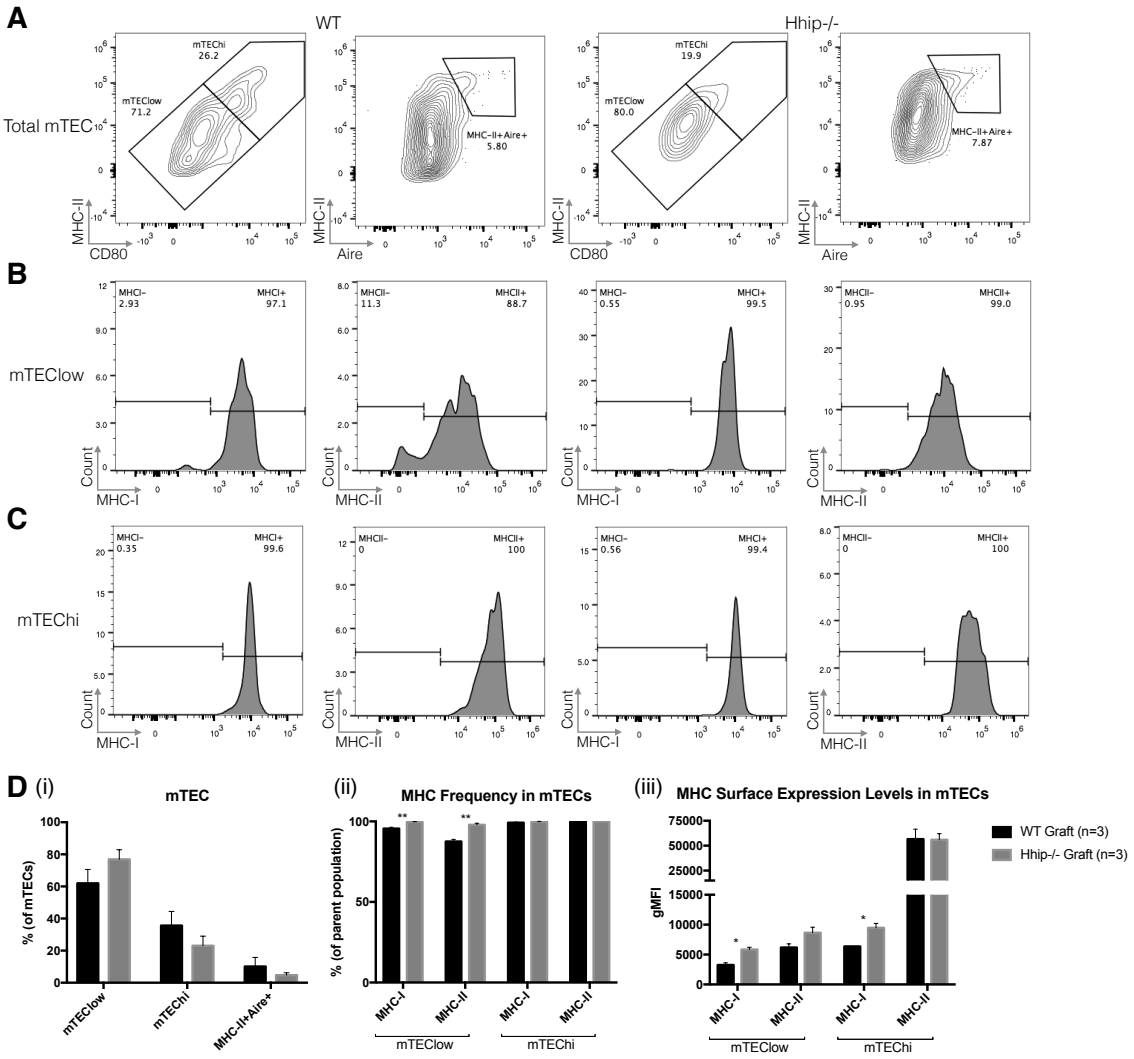

Figure 5.12: Hhip-/- mTEC populations are equivalent in frequency but express higher levels of MHC
(A) Representative FACS plots showing distribution of mTEChi and mTEClow cells based on MHC-II and CD80 expression, as well as mature MHC-II+Aire+ frequencies, for WT and Hhip-/- E18.5 thymi grafted under the kidney capsule of adult hosts for 6 weeks. Frequencies of **(B)** mTEClow and **(C)** mTEChi cells that express high levels of MHC-I and MHC-II, represented as MHC-I+ and MHC-II+ in the FACS plots. **(D)** (i) Frequencies of different mTEC subpopulations. (ii) Frequencies of MHC-I+ and MHC-II+ cells in the mTEClow population. (iii) Cell surface expression of MHC-I and MHC-II in mTEC subpopulations. Total mTECs were gated as CD45-Epcam+Ly51-UEA-1+ live single cells. P-values were determined by student's t test where * $p < .05$, ** $p < .01$. Plots and statistics are representative of 2 independent experiments.

Altered TEC ratios were sustained in the pseudo-adult Hhip-/- thymus, confirming a clear requirement for Hhip in the maintenance of normal cTEC and mTEC frequencies. More cTECs and $mTEC^{low}$ cells in the Hhip-/- transplant also expressed higher cell surface levels of MHC-I and MHC-II, which was not previously observed in neonatal Hhip-/- or adult Hhip+/- mice. This phenotype may have an impact on the cells' ability as antigen-presenting cells, and this aspect will be investigated in greater detail below.

5.4 Hhip-/- TECs can support development of healthy progenitors but not in the same manner as a WT thymus

Analyses of thymocytes were gated specifically on recipient-derived $CD45.1^+$ Hhip-proficient cells to exclude any intrinsic *hhip*-deficiency. WT and Hhip-/- grafts showed a comparable thymocyte profile (5.13A). Specifically, early stage development of recipient DN cells in the Hhip-/- graft was normal (5.13B, 5.13C). The frequencies of DP and CD8 cells were comparable (5.13A), and the maturation of single positive CD4 cells was unaffected (5.13D). However, cell surface concentrations of TCRβ and CD5 were reduced on mature thymocyte populations (5.13E).

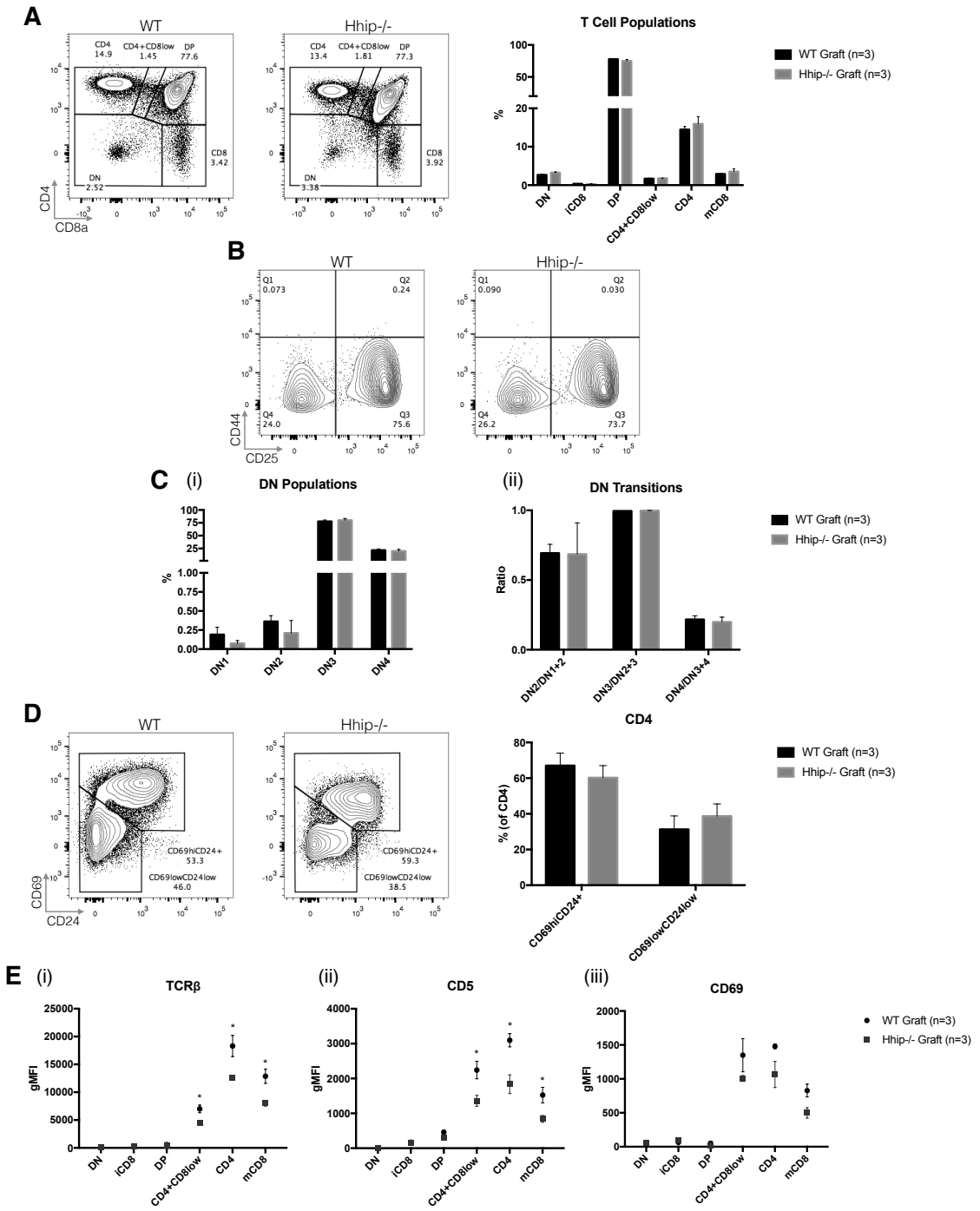

Figure 5.13: T cell frequencies in the WT and Hhip-/- thymus grafts are equivalent
(A) Representative FACS plots and statistics show CD45.1 (recipient-derived) T cell populations in transplanted WT or Hhip-/- thymi after 6 weeks. **(B)** DN developmental stages are distinguished using CD44 and CD25 expression, and **(C)** (i) frequencies of DN cells in each stage are shown, (ii) DN transitions were calculated by taking the frequency of cells in the population of interest, divided by the frequencies of cells in that population and the one immediately preceding, e.g DN2/DN1+DN2. **(D)** Maturity of CD4 cells was distinguished by CD69 and CD24 expression. **(E)** Expression levels of (i) TCRβ, (ii) CD5 and (iii) CD69 in individual thymocyte subpopulations of WT and Hhip-/- grafts. P-values were determined by student's t test where * p < .05. Plots and statistics are representative of 2 independent experiments.

Using the cell surface markers CCR7, CD69, Qa2 and MHC-I, maturational development of recipient T cells in the grafted thymi was further analysed. As previously elaborated, CCR7 and CD69 distinguish cells in the cortex and medulla,

while expression of Qa2 and MHC-I can be used to further specify the maturity of thymocytes (Mingueneau, M. *et al*., 2013; Xing, Y. *et al*., 2016; Kishimoto, H. & Sprent, J., 1997). The transplanted Hhip-/- thymus harboured fewer recipient-derived thymocytes with a $CCR7^{-}CD69^{-}Qa2^{-}MHC\text{-}I^{low}$ phenotype (WT 84.2 ± 0.5%, Hhip-/- 80.4 ± 0.3%). These cells represent immature thymocytes that have not yet undergone selection. In contrast, there were more thymocytes detected in the Hhip-/- graft with a $CCR7^{+}CD69^{-}Qa2^{+}MHC\text{-}I^{+}$ phenotype (1.92 ± 0.1% vs 1.07 ± 0.1%), which represent thymocytes in the medulla with a post-selection phenotype (5.14A, 5.14B). This suggests that more thymocytes survive the selection process in the absence of *hhip* expression by non-haematopoietic thymic stromal cells. Hence, this defect is entirely stromal dependent. However, the grafting experiments revealed a contradiction when compared to the conventional Hhip-/- mice, where fewer selected CD4 cells were observed in neonatal Hhip-/- mice but not in the graft. This discrepancy is however in keeping with the previously described explanation that a Hhip-deficiency may affect TECs and T cells differentially.

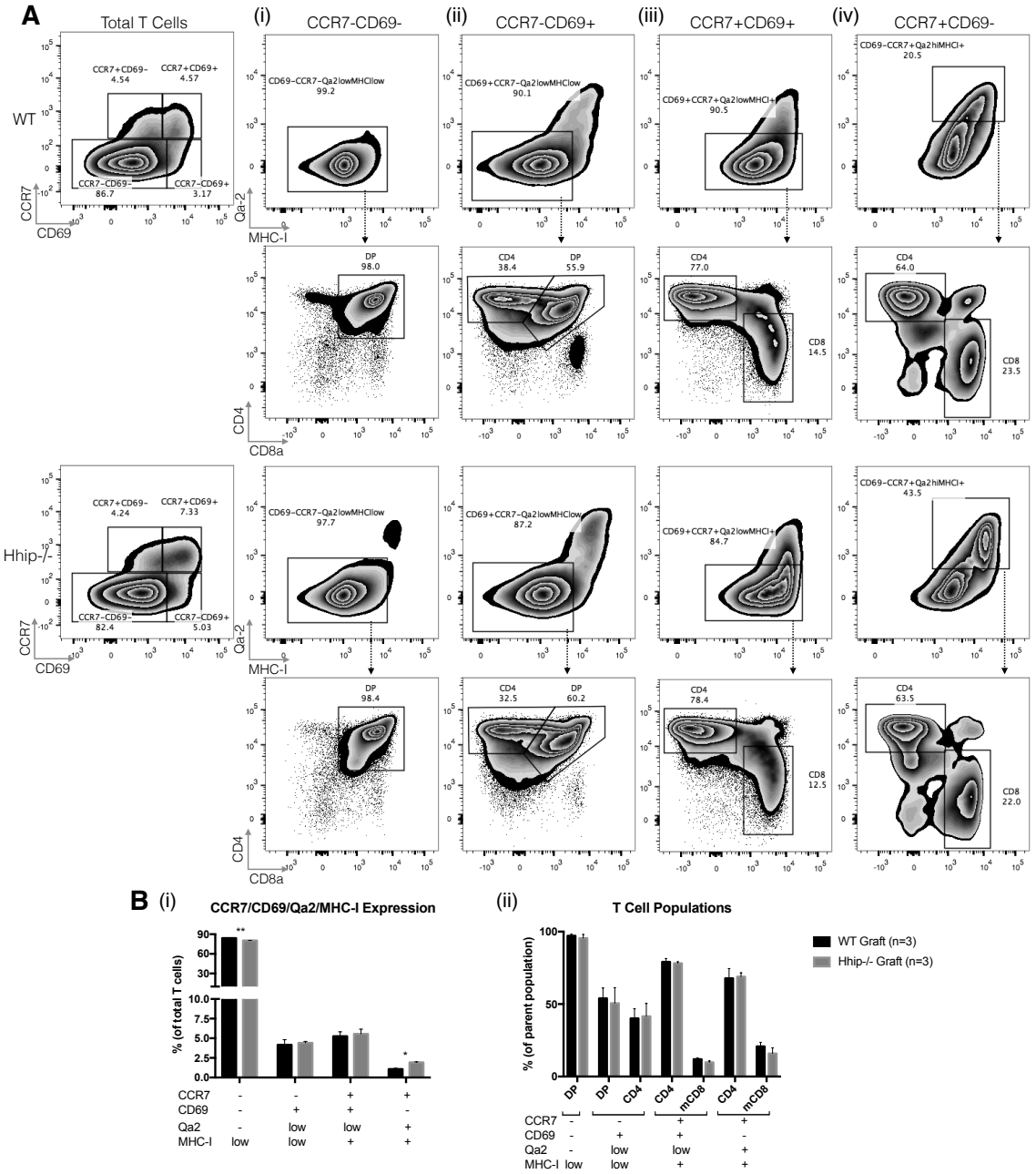

Figure 5.14: Thymocytes developing in the Hhip-/- thymus graft show accelerated positive selection
(A) Representative FACS plots show CD45.1 donor thymocytes split into selection stages based on CCR7 and CD69 expression. The (i) CCR7-CD69-, (ii) CCR7-CD69+, (iii) CCR7+CD69+ and (iv) CCR7+CD69- stages are shown sequentially and further gated based on Qa2 and MHC-I expression, and the thymocyte profile in that stage is shown below. **(B)** (i) Frequencies of total live single CD45.1 Lin- T cells with each selection phenotype. (ii) Distribution of individual thymocyte subpopulations within each stage, where the parent population refers to T cells with that selection phenotype. P-values were determined by student's t test where * $p < .05$, ** $p < .01$. Plots and statistics are representative of 2 independent experiments.

The ratio of CD4 and CD8 single positive TCRβ$^+$ thymocytes was comparable for recipient cells from both thymus grafts (5.15A). In the adult mouse, the maturational progression of early DP thymocytes to fully mature CD4 and CD8 single positive thymic T cells can be separated into distinct stages for either lineage (5.15B). In

CD4 development, TCRβ^{+} DP thymocytes in the cortex express CD69 as a consequence of activation upon MHC-II engagement of their complete antigen receptor, and downregulate CD8a expression to attain a CCR7^{-} TCRβ^{int}CD24^{hi}CD69^{hi} phenotype (stage A). Committed to the CD4 lineage, these cells subsequently upregulate their TCR complex on the cell surface, gaining CCR7 expression (stage B) and later increased MHC-I expression (stage C). The following steps in the cells' maturation are characterised by sequential downregulation of the activation marker CD24 (stage D) and upregulation of Qa2 (stage E). Thymocyte development in the Hhip-/- microenvironment displayed, when compared to WT stromal conditions, a significantly higher proportion of cells with a fully mature phenotype (stage E) (5.15C, 5.15D). Other relevant differences in thymocyte progression were, however, not observed in the Hhip-/- stromal environment. This suggests that more CD4 cells have possibly survived the selection process within a Hhip-/- thymic stroma as compared to a WT setting.

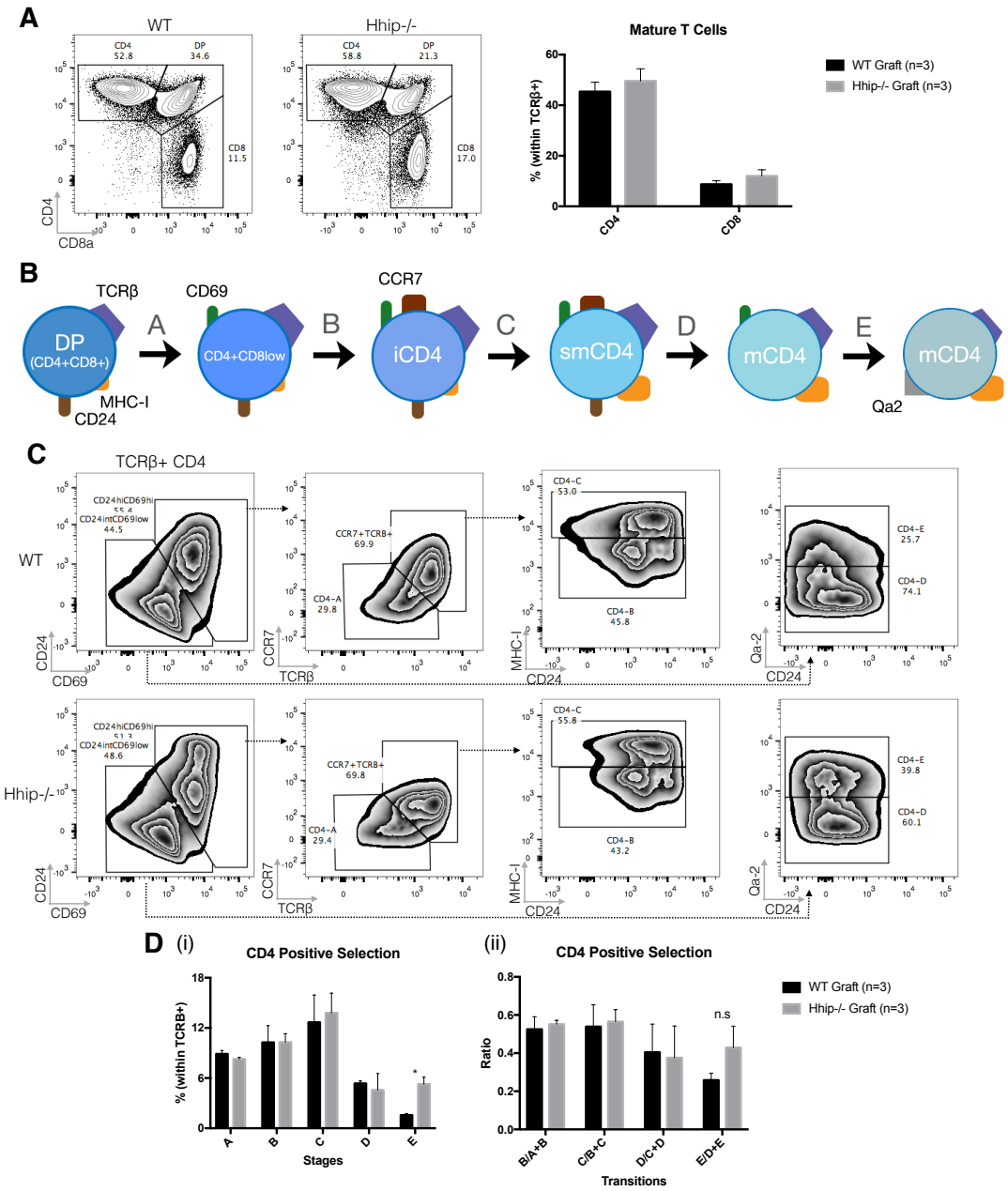

Figure 5.15: Positive selection in the Hhip-/- grafted thymus allows more CD4 cells to survive
(A) Representative FACS plots of mature TCRβ+ recipient-derived thymocytes in WT and Hhip-/- E18.5 transplanted thymic lobes after 6 weeks. **(B)** Figurative schematic of CD4 positive selection stages. **(C)** TCRβ+ CD4 cells were divided into positive selection stages using CD24, CD69, CCR7, TCRβ, Qa2 and MHC-I expression. **(D)** (i) Frequencies of live single Lin- TCRβ+ T cells in each selection stage. (ii) The ability of cells to progress through each stage was calculated by taking the frequency of cells in the stage of interest, divided by the total frequency of cells in that stage and the one immediately preceding, e.g B/A+B. P-values were determined by student's t test where * p < . 05. FACS plots and statistics are representative of 2 independent experiments.

Intrathymic differentiation of DP thymocytes to phenotypically mature single positive CD8 T cells can be divided into 6 individual stages (5.16A). Unlike the CD4 lineage, early CD8 lineage commitment can already be observed within the TCRβ^{+}DP population, where cells about to undergo positive selection display slightly elevated levels of TCRβ and CCR7 (stage A). Transition to the next developmental stage is

marked by an upregulation of cell surface MHC-I (stage B). Subsequent to this stage, CD8-lineage committed thymocytes lose CD4 expression whilst maintaining TCRβ and CD8a expression, as well as upregulate CD69 in response to TCR engagement (stage C). Following selection, they downregulate CD69 expression (stage D) (Ross, J. *et al*., 2014). Continued maturation is marked by upregulation of the marker Qa-2 (stage E), and CD24 is downregulated in the most mature subpopulation just about to exit the thymus (stage F). Within the Hhip-/- thymic stromal environment, the transition to downregulate CD24 expression was affected, resulting in an accumulation of thymocytes in stage E of their development (5.16B, 5.16C). Similar to the CD4 lineage, it appears that more CD8 cells have survived positive selection via the engagement of their TCR with pMHC complexes presented by the Hhip-/- thymic stroma, as demonstrated by the increased frequency of mature cells in stage E, a post-selection stage. However, not all of these cells go on to successfully acquire a fully mature phenotype, marked by downregulation of CD24. This could indicate that the Hhip-/- stroma is unable to support normal late stage maturation of thymocytes, or that a mechanism such as negative selection is in place to eliminate any additional cells that aberrantly survived positive selection.

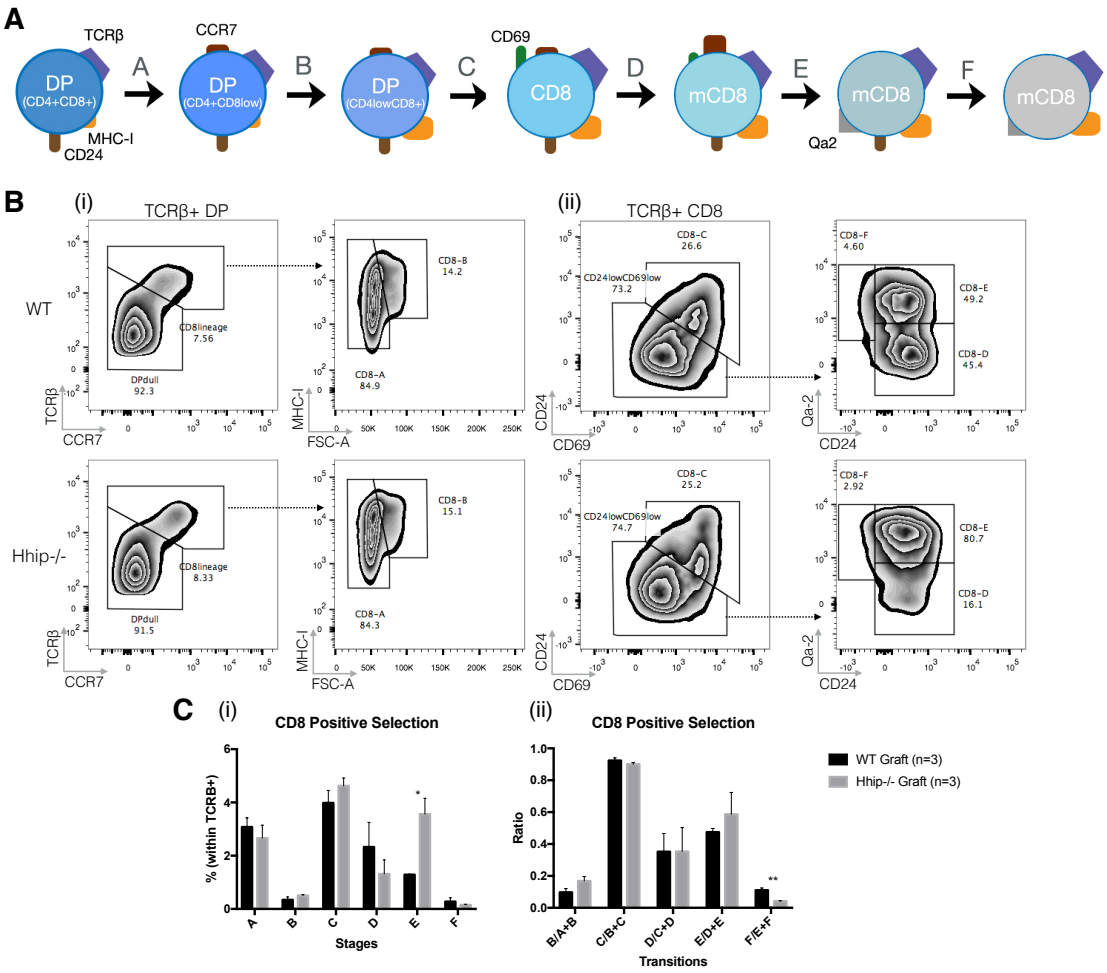

Figure 5.16: Positive selection of CD8 cells is impaired in the Hhip-/- thymus
(A) Figurative schematic of CD8 positive selection stages. **(B)** (i) Early committed recipient-derived CD8 cells of WT and Hhip-/- thymus grafts are gated from the TCRβ+ DP population, followed by (ii) more mature cells within the TCRβ+ CD8 compartment. These are divided into selection stages based on TCRβ, CCR7, MHC-I, CD24, Qa2 and CD69 expression. **(C)** (i) Frequencies of live single Lin- TCRβ+ T cells in each selection stage. (ii) The ability of cells to progress through each stage was calculated by taking the frequency of cells in the stage of interest, divided by the total frequency of cells in that stage and the one immediately preceding, e.g B/A+B. P-values were determined by student's t test where * $p < .05$, ** $p < .01$. FACS plots and statistics are representative of 2 independent experiments.

Negative selection is important in the thymus to eliminate thymocytes that interact with pMHC complexes via their TCR with too high affinity, which may lead to autoreactivity in the periphery. It also acts as a checkpoint for any cells that have aberrantly survived positive selection despite not interacting correctly with TEC-presented antigen complexes, as engagement via the TCR is also required in negative selection. The concomitant cell surface expression of a transcription factor, Helios, and PD-1, an inhibitory receptor, identify cortical thymocytes that have been negatively selected as part of the first wave of thymocyte selection (Daley, S. *et al.*, 2013). In this first cortical wave of selection, the CD4 and CD8

lineages cannot be accurately distinguished as the majority of thymocytes here are DP cells. FoxP3^{+} cells were excluded from analysis as these often express high levels of Helios (Hu, D. *et al.*, 2015). The frequency of Helios^{+}PD-1^{+} among CCR7^{-} CD24^{+} thymocytes in the cortex was comparable for the two tissues examined (5.17A). However, expression levels of CD24 and CD69 were mildly elevated in CCR7^{-}CD24^{+}Helios^{+}PD-1^{+} thymocytes, suggesting that more immature cells were being negatively selected in the cortex of the Hhip-/- thymus (5.17B). The second wave of negative selection occurs in the medulla, where thymocytes express CCR7 and are either CD24 positive or negative, depending on the extent of their maturity. Expression of Helios among these cells identifies thymocytes subject to apoptosis as a mechanism of maintaining T cell tolerance. Here, the frequency of cells undergoing negative selection was equivalent for both groups of thymic grafts (5.17B).

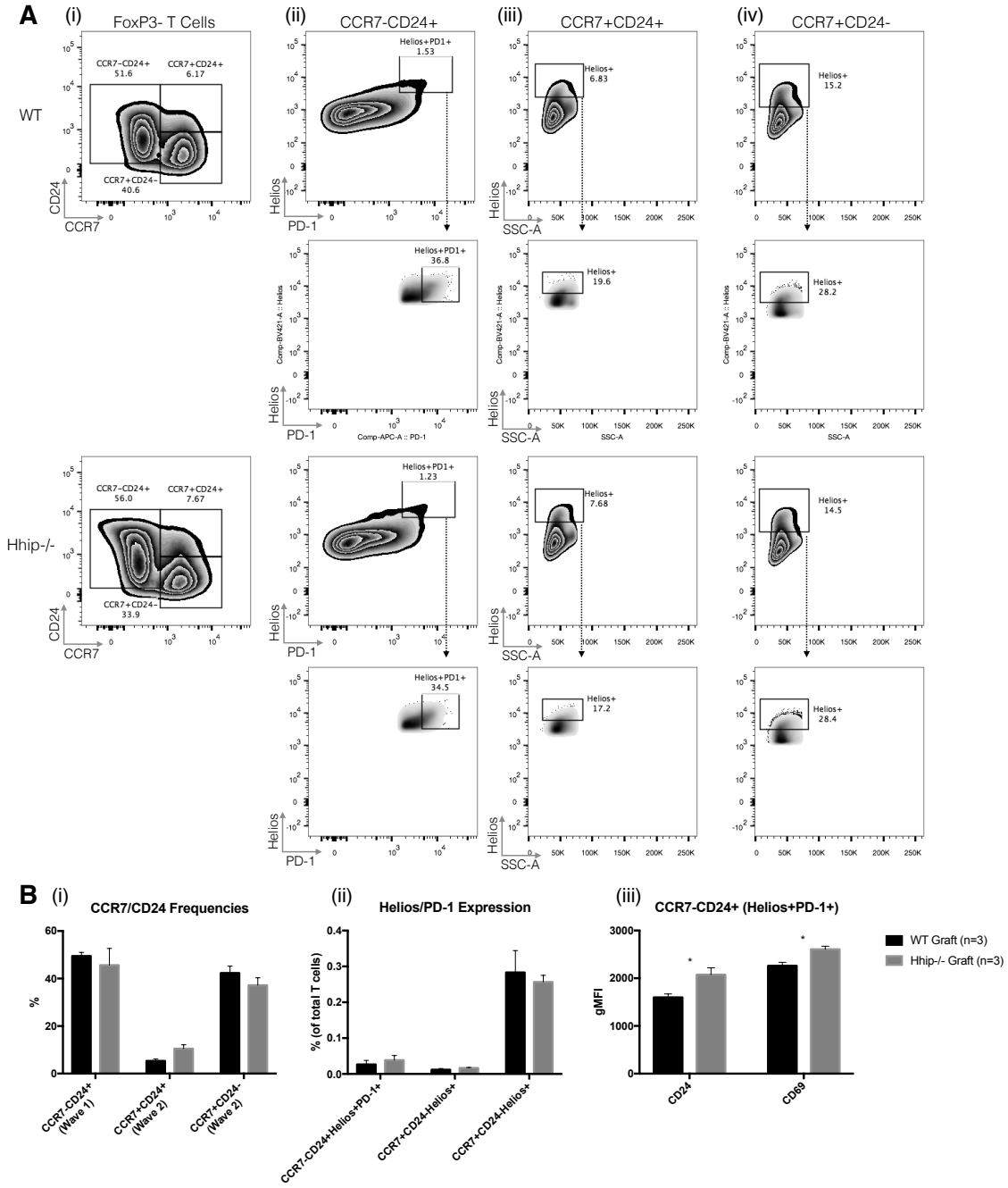

Figure 5.17: Thymocytes in WT and Hhip-/- grafts have different cell surface marker expression
(A) (i) Recipient-derived FoxP3- thymocytes from WT and Hhip-/- E18.5 thymic grafts are divided into cortex and medullary locations by CCR7 and CD24 expression, and the fraction of cells undergoing negative selection defined by (ii) Helios and PD-1 expression in the cortex (wave 1), or (iii) (iv) Helios positivity only for cells in the medulla (wave 2). A "pre-gate" is first drawn to identify positive cells, following which a density plot is used to identify highly expressing cells. **(B)** (i) Frequencies of cells in each location. (ii) Frequencies of cells undergoing negative selection. (iii) Statistically significant differences in surface expression of CD24 and CD69 are shown for the CCR7-CD24+ cell fraction undergoing negative selection. P-values were determined by student's t test where * $p < .05$. FACS plots and statistics are representative of 2 independent experiments.

Wave 2 of negative selection was analysed separately for the two T cell lineages, and this analysis revealed reduced frequencies of mature CD69^{low} CD4 and CD8 cells undergoing negative selection in the Hhip-/- graft (5.18A, 5.18B). This would suggest that *hhip*-deficient mTECs have a defect in negative selection and do not

correctly effect negative selection on mature cells; however, when distinguished by CCR7 and CD24 expression, the overall frequencies of cells being negatively selected in the medulla were comparable to WT (5.17B). In addition, $CD69^{low}$ mature cells should develop from their $CD69^{hi}$ counterparts, which are selected normally in the Hhip-/- grafts (5.18B). These observations could instead indicate an overall maturational issue, where the *hhip*-deficient epithelia does not facilitate regular maturation of thymocytes, resulting in impaired loss and acquisition of relevant cell surface markers such as CD69 and CD24 which are used here to distinguish maturity and define selection stages. The observation that single positive thymocytes in the Hhip-/- graft expressed lower cell surface levels of CD5 (5.13E) also correlates with the reduced frequencies of mature $Helios^{+}$ cells, since cells that have a lower TCR signalling affinity are not likely to be negatively selected. This could be a carry-on effect from a defect in positive selection that allows cells that have not engaged properly with their TCR and have low signalling affinity to survive. It is of note that Helios expression as a measure of negative selection has only been validated for CD4 cells (Hu, D. *et al*., 2015), and thus any findings for CD8 cells may not be conclusive.

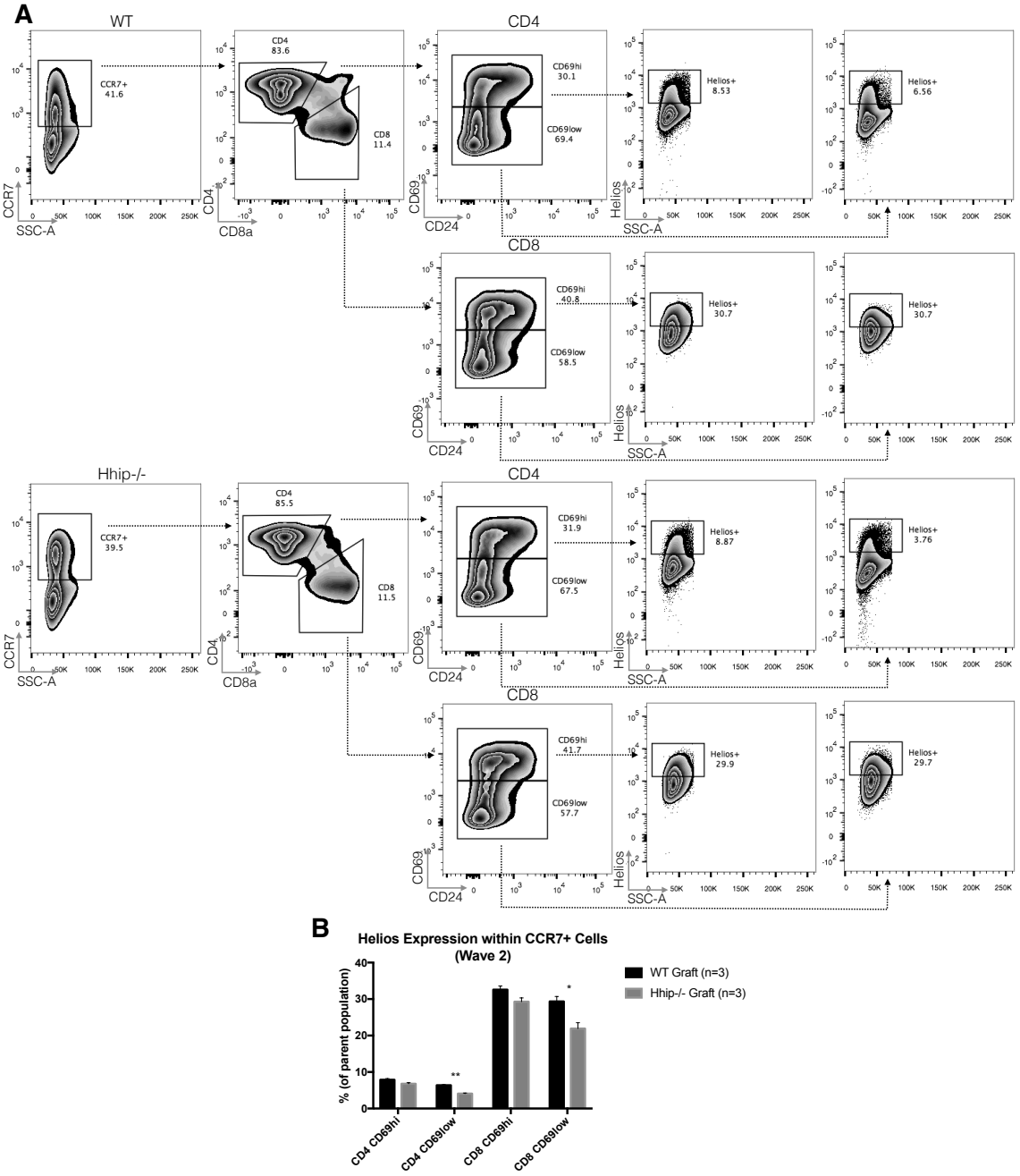

Figure 5.18: Frequencies of mature cells being negatively selected are decreased in the Hhip-/- thymus
(A) FoxP3- TCRβ+ CD45.1 donor-derived cells in both WT and Hhip-/- thymus grafts are gated on CCR7-positivity, then differentiated into CD4 and CD8 cells. Each lineage is gated on CD69 expression, and negatively selected cells are defined by Helios expression. The Helios+ gate for the CD8 lineage was gated with reference to the CD4 CD69hi population. **(B)** Helios-expressing cells as a percentage of the population of interest, for example CD4 CD69hi cells. P-values were determined by student's t test where * $p < .05$, ** $p < .01$. FACS plots and statistics are representative of 2 independent experiments.

Within the thymus there is an entire continuum of thymocytes in different maturational stages, and positive and negative selection processes are thus occurring simultaneously throughout the entire population. Consequently, while analysing positive and negative selection separately reveals valuable information, it

is difficult to attribute precisely if changes in cell surface marker expression are due solely to defects of either the positive or negative selection processes, or a combination of the two. Taken together, the results above suggest that *hhip*-deficient TECs have a defect with selection that allows relatively immature T cells with a reduced TCR affinity to survive. A positive selection defect would be consistent with the altered cTEC frequencies observed in the Hhip-/- thymus (5.11C) and the increased MHC cell surface density (5.11E), such that the increased pMHC availability allows the survival of more T cells, including those with a lower TCR affinity. *Hhip*-deficient mTECs may be competent to perform negative selection, but as negative selection eliminates cells that interact with too high affinity, the T cells with low affinity survive, thus resulting in a population of T cells with overall reduced levels of TCR affinity.

5.5 *Hhip*-deficient thymocytes migrate to the periphery

The chosen experimental design precluded the possibility to follow the emigration of host-derived CD45.1 T cells developing in the transplanted thymi out of the thymus, as the periphery also contained CD45.1 T cells that had been generated from the normal WT host thymus. However, the small proportion of donor-derived CD45.2 thymocytes that had already been seeded in the Hhip-/- E18.5 thymi at the time of transplantation were further analysed. The overall proportion of splenic T and B cells were similar for hosts grafted with either a WT or Hhip-/- thymus (5.19A). Within the T cell fraction, the proportion of CD45.2 cells was not significantly different between grafts (5.19B).

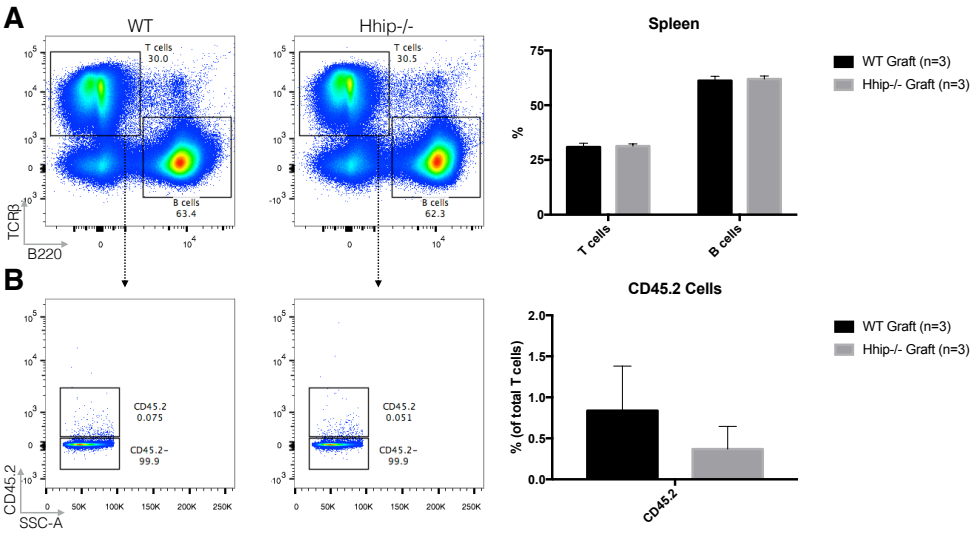

Figure 5.19: CD45.2 thymocytes originally present in the transplanted thymus emigrated to the host periphery
(A) Distribution of splenic T and B cells of host animals transplanted with either WT or Hhip-/- E18.5 thymi for 6 weeks. **(B)** Frequencies of CD45.2-positive (donor-derived) T cells in the spleen. Statistical significance was evaluated using a student's t test. Experiment shown is representative of 2 independent experiments.

Splenic CD45.2$^+$ and CD45.2$^-$ cells were analysed separately. The latter were not distinguishable between genotypes with regards to T cell subpopulation frequencies (5.20A). The majority of CD45.2$^+$ cells were T cells, and their absolute numbers were comparable for the two transplant groups (5.20A, 5.20B). Moreover, the distribution of total CD4 and CD8 cells were similar, with comparable proportions of effector, memory and naïve cells within either lineage (5.20A, 5.20C). Neither CD4 nor CD8 T cells displayed reduced TCRβ expression (data not shown).

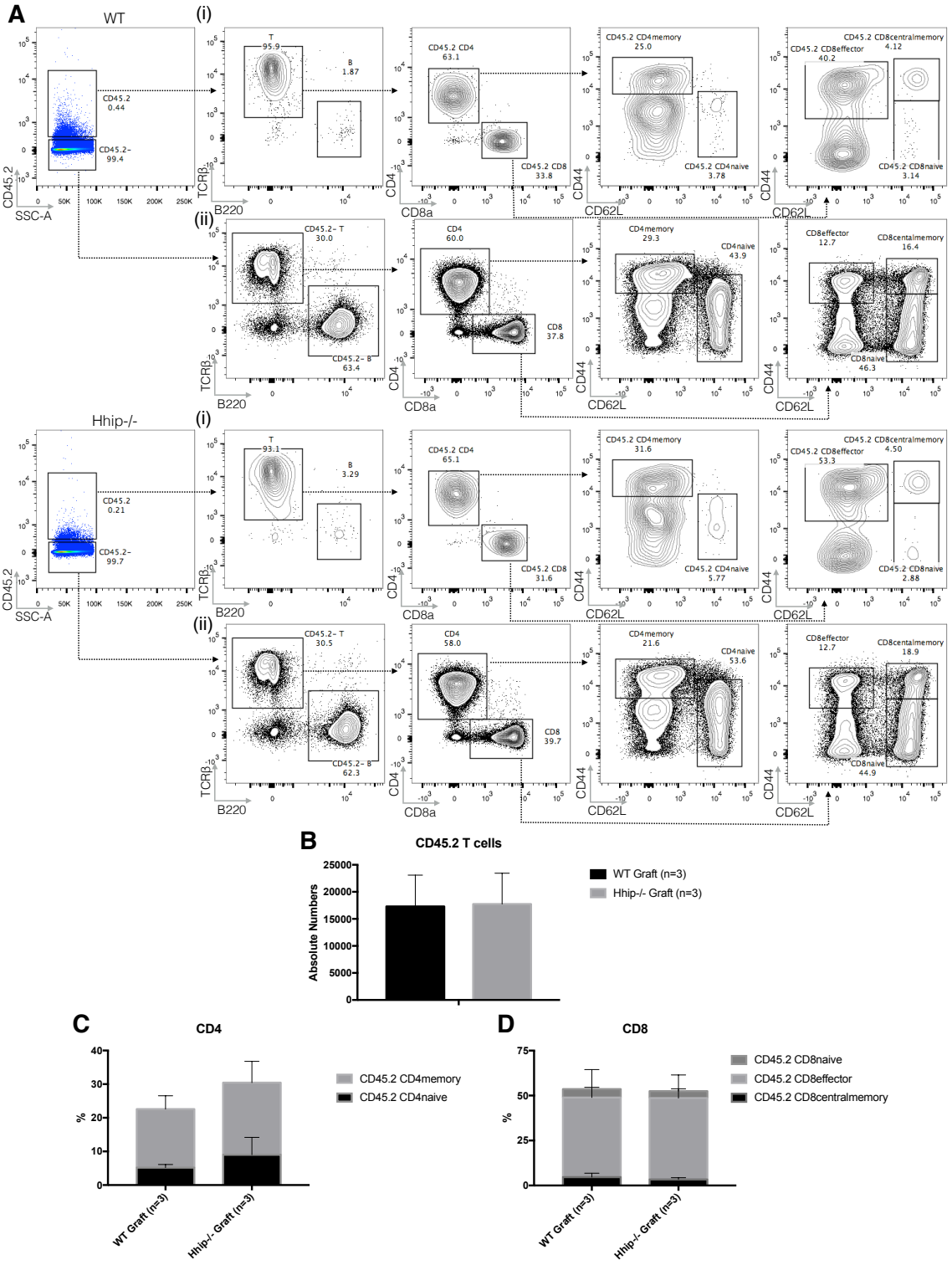

Figure 5.20: CD45.2 Hhip-/- T cell maturation is normal

(A) Splenocytes of host animals grafted with either WT or Hhip-/- E18.5 thymi for 6 weeks are gated for CD45.2 positivity. (i) CD45.2+ and (ii) CD45.2- cells are gated separately on TCRβ and B220 expression to distinguish T and B cells. T cells are divided by CD4 and CD8 expression, and each subpopulation is further characterised by CD44 and CD62L expression. **(B)** Absolute numbers of CD45.2 T cells in the spleen. **(C)** Frequencies of CD4 memory and naive cells and **(D)** CD8 naive, effector and central memory cells. Statistical significance was evaluated using a student's t test. Experiment shown is representative of 2 independent experiments.

In previous experiments, the emigration of mature Hhip-/- thymocytes to the periphery could not be analysed under unmanipulated conditions due to early lethality of the model. This transplant experiment demonstrated that Hhip-/- T cells develop normally and are able to exit the thymus to the periphery in a fashion comparable to that of WT T cells. This result supports that any developmental defects due to a lack of *hhip* expression by TECs are partial, and that despite an altered cTEC to mTEC ratio, the Hhip-deficient thymic microenvironment is still able to support thymocyte development as assessed by flow cytometry. However, the functionality of these thymocytes has not yet been tested.

5.6 Hhip-/- thymocytes have intrinsic aberrant expression of markers

Elements of the phenotype seen in the transplanted Hhip-/- thymus differed from that in the conventional *hhip*-deficient mouse model, such as altered TCRβ and CD5 expression in the transplanted model, as well as reduced frequencies of CD4 T cells in the conventional model. This raised the question of whether Hhip was relevant in cell types other than TECs. To address this issue, thymocyte progenitors were isolated from the fetal liver of E14.5 Hhip-/- embryos, and injected into lethally irradiated B6.SJL.CD45.1 WT hosts. The rationale was to observe whether *hhip*-deficient lymphoid progenitors would develop normally given a WT TEC microenvironment. In the event of regular thymocyte development of Hhip-/- lymphoid cells in a WT microenvironment, the haematopoietic changes seen so far could then be attributed as the direct consequence of a reduced capacity of Hhip-/- TECs to support development.

Five weeks after the transplantation of fetal liver-derived haematopoietic cells (CD45.2), host animals (CD45.1) were sacrificed and thymi isolated. The appearance and size of the thymus were similar regardless of whether WT or Hhip-/- progenitors were engrafted. However, the total cellularity of thymi engrafted with Hhip-/- progenitors was increased under conditions where the thymus was mechanically disrupted but not when it was enzymatically digested (5.21A). The mechanical dissociation technique is used to release thymocytes, and may thus indicate that the Hhip-/- transplanted thymi might harbour a larger amount of T cells. The rate of donor CD45.2 reconstitution was almost 100% for both experimental groups, both for the total T cell population as well as within each individual thymocyte subpopulation, demonstrating a comparable seeding of the host thymus by both Hhip-/- and WT progenitors (5.21B, 5.21C). Phenotypic analysis of intrathymic T cell development revealed a comparable maturational competence with similar frequencies of thymocyte subpopulations (5.21D), but higher absolute numbers of immature DN and DP cells were present (5.21E).

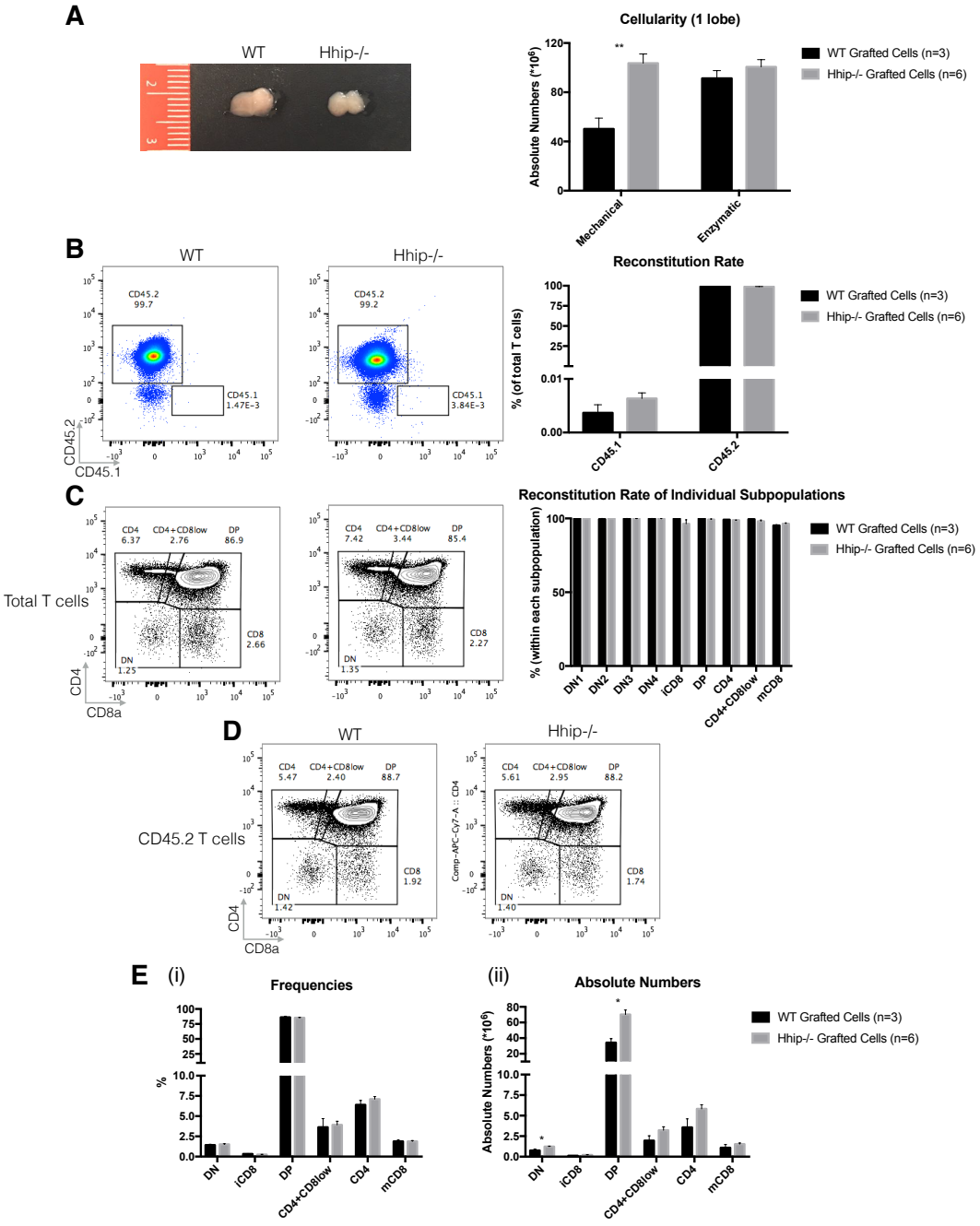

Figure 5.21: WT thymi transplanted with Hhip-/- thymocyte progenitors have altered absolute T cell numbers
(A) Representative pictures of host thymi 5-weeks post transplant, reconstituted with either WT or Hhip-/- E14.5 fetal liver cells. `graph shows overall thymic cellularity from either enzymatic or mechanical disruption. **(B)** Overall reconstitution rate of total T cells in the thymus. **(C)** Reconstitution rate of donor CD45.2 thymocytes within each individual T cell subpopulation. **(D)** Representative FACS plots showing T cell distribution of only CD45.2+ T cells. **(E)** (i) Frequencies and (ii) absolute numbers of individual thymocyte subpopulations of live single Lin- CD45.2+ T cells. Graphs and FACS plots shown are from 1 single experiment. 4 individual experiments were conducted. Total experimental size: WT n= 9, Hhip-/- n=11. P-values were determined by student's t test where * $p < .05$, ** $p < .01$.

Despite higher overall numbers of DN cells, the frequencies of Hhip-/- cells in each DN stage were similar (5.22A). The CD4 compartment, which had previously shown some phenotypic differences in the conventional Hhip-/- model as well as in the thymus transplant, was equivalent to WT with regards to CD69 and CD24

expression, the proportion of $CD25^{+}FoxP3^{+}$ T_{reg}, as well as recirculating $ICOS^{+}CD103^{+}$ T_{reg} (Barthlott, T. *et al.*, 2015) (5.22B, 5.22C). No significant differences with regards to expression of the markers CD69, CD24, TCRβ and CD5 were observed (data not shown). These results were consistent with the expectation that any haematopoietic defects previously observed were likely due to a *hhip*-deficient stromal environment. However, when the Hhip-/- CD8 population was analysed, both iCD8 and mCD8 populations displayed elevated levels of TCRβ (5.22D).

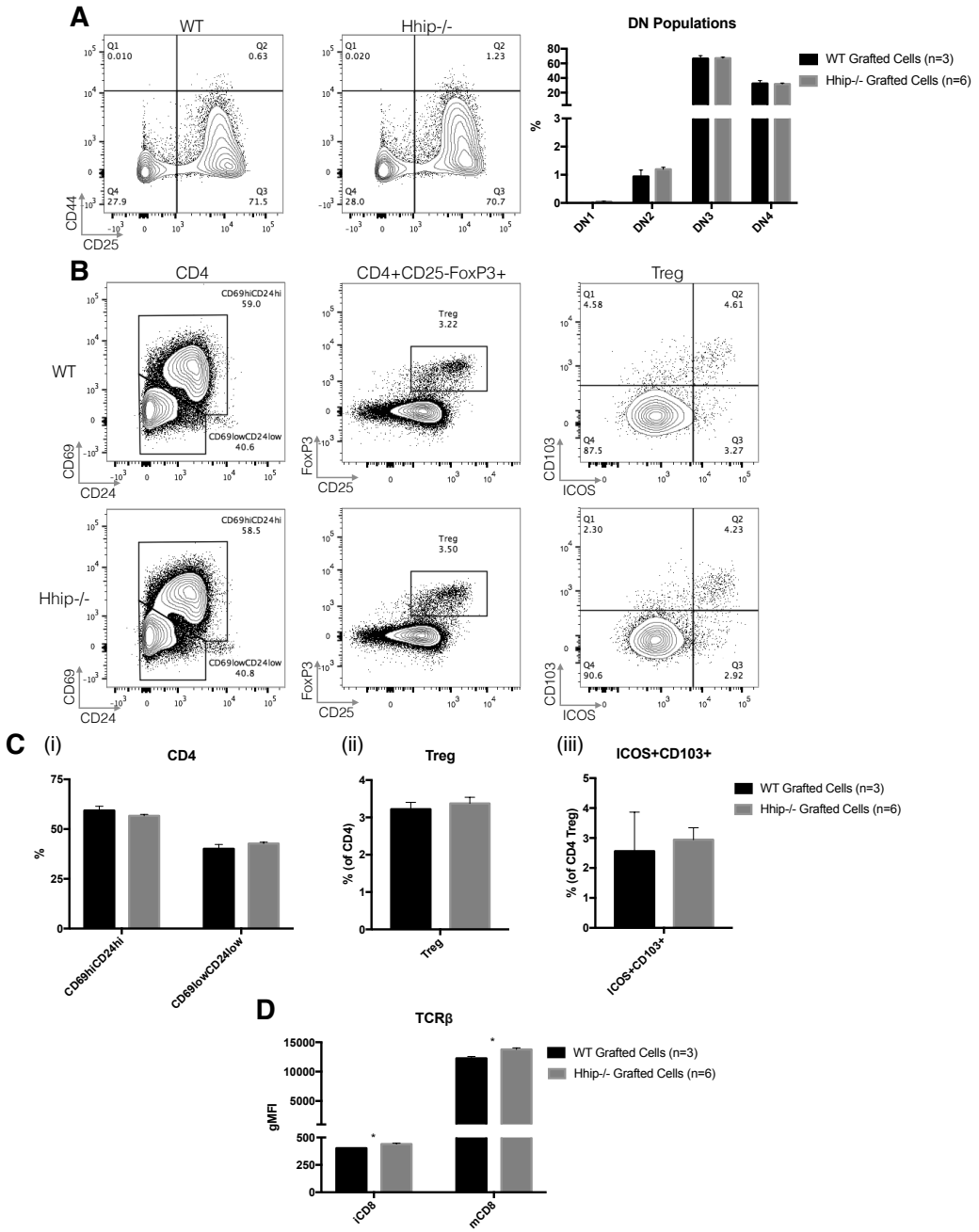

Figure 5.22: Frequencies of Hhip-/- cells in each developmental stage are normal
(A) Total live Lin- single CD45.2 donor T cells in each DN stage, distinguished as DN1 (CD44+CD25-), DN2 (CD44+CD25+), DN3 (CD44-CD25+) and DN4 (CD44-CD25-). Irradiated host animals were grafted with E14.5 WT or Hhip-/- fetal liver progenitors for 5 weeks. **(B)** Representative FACS plots demonstrating profile of CD69 and CD24 expression in CD4 T cells, frequencies of CD4 Treg and CD103+ICOS+ Tregs in the thymus. **(C)** Statistics of (i) CD4, (ii) CD4 Treg and (iii) ICOS+CD103+ Treg populations between genotypes. **(D)** TCRβ cell surface expression on iCD8 and mCD8 Hhip-/- thymocytes. P-values were determined by student's t test where * $p < .05$. Experiment is representative of at least 2 independent experiments.

Positive thymocyte selection and subsequent maturation was evaluated for the cell surface expression of CCR7, CD69, Qa2 and MHC-I. The frequencies of cells in each specific positive selection stage were comparable between WT and Hhip-/- grafted thymocytes (5.23A, 5.23B), a finding consistent with expected regular

thymocyte selection by WT TECs. However, there were slight differences in the mCD8 population, where there were more mCD8 cells in the semi-mature Hhip-/- $CCR7^{+}CD69^{+}Qa2^{low}MHC\text{-}I^{+}$ population, and fewer in the mature $CCR7^{+}CD69^{-}Qa2^{+}MHC\text{-}I^{+}$ population (5.23B), which seemed to suggest a delay or partial block in CD8 maturation.

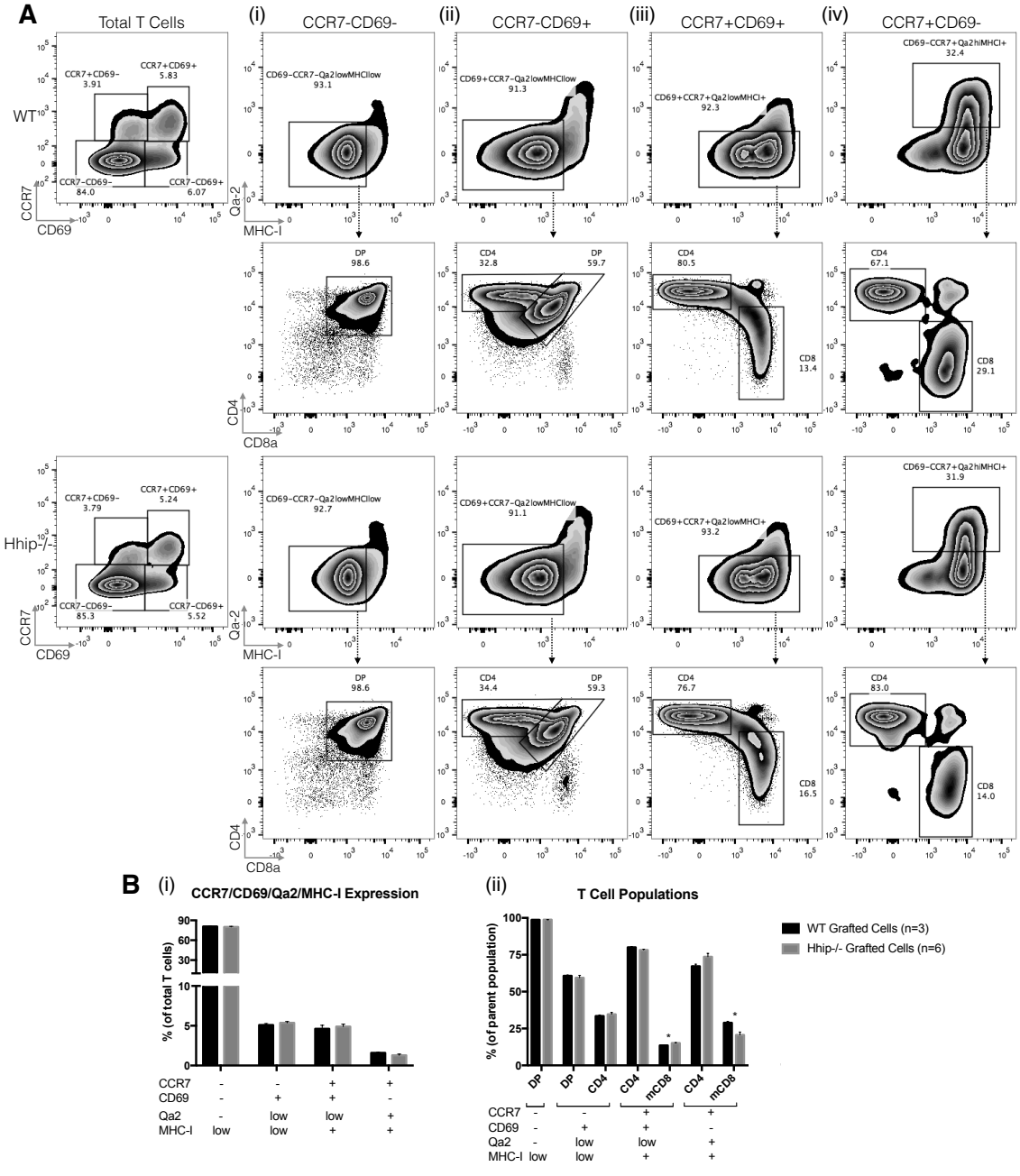

Figure 5.23: Positive selection stages for WT and Hhip-/- grafted cells
(A) Total live CD45.2 donor Lin- single T cells are divided by CCR7 and CD69 expression, and the (i) CCR7-CD69-, (ii) CCR7-CD69+, (iii) CCR7+CD69+ and (iv) CCR7+CD69- fractions shown. These are further gated by Qa2 and MHC-I expression, and the thymocyte profile by CD4 and CD8a expression in each population shown for both WT and Hhip-/- genotypes. **(B)** (i) Frequencies of total T cells in each CCR7/CD69/Qa-2/MHC-I expressing fraction between WT and Hhip-/- genotypes, and (ii) frequencies of individual thymocyte subpopulations within each fraction, where the parent population refers to the T cells with the selection phenotype of interest. P-values were determined by student's t test where * $p < .05$. Experiment is representative of at least 2 independent experiments.

Maturation of the CD4 and CD8 lineages subsequent to positive selection were analysed separately. No differences were found in the frequencies of cells in the various stages of selection, as well as their ability to mature from the DP stage (5.24A, 5.24B, 5.24C, 5.24D). However, the CD8 lineage once again presented differential expression of cell surface markers, including elevated levels of CD69 in the most immature CD8-committed cells deriving from the DP population about to undergo positive selection, as well as decreased levels of CCR7 in cells in the later post-positive stages D, E and F (5.24E). These results could imply that an intrinsic *hhip*-deficiency in lymphoid progenitors subsequently affects their ability to mature normally into the CD8 lineage, despite a WT TEC microenvironment.

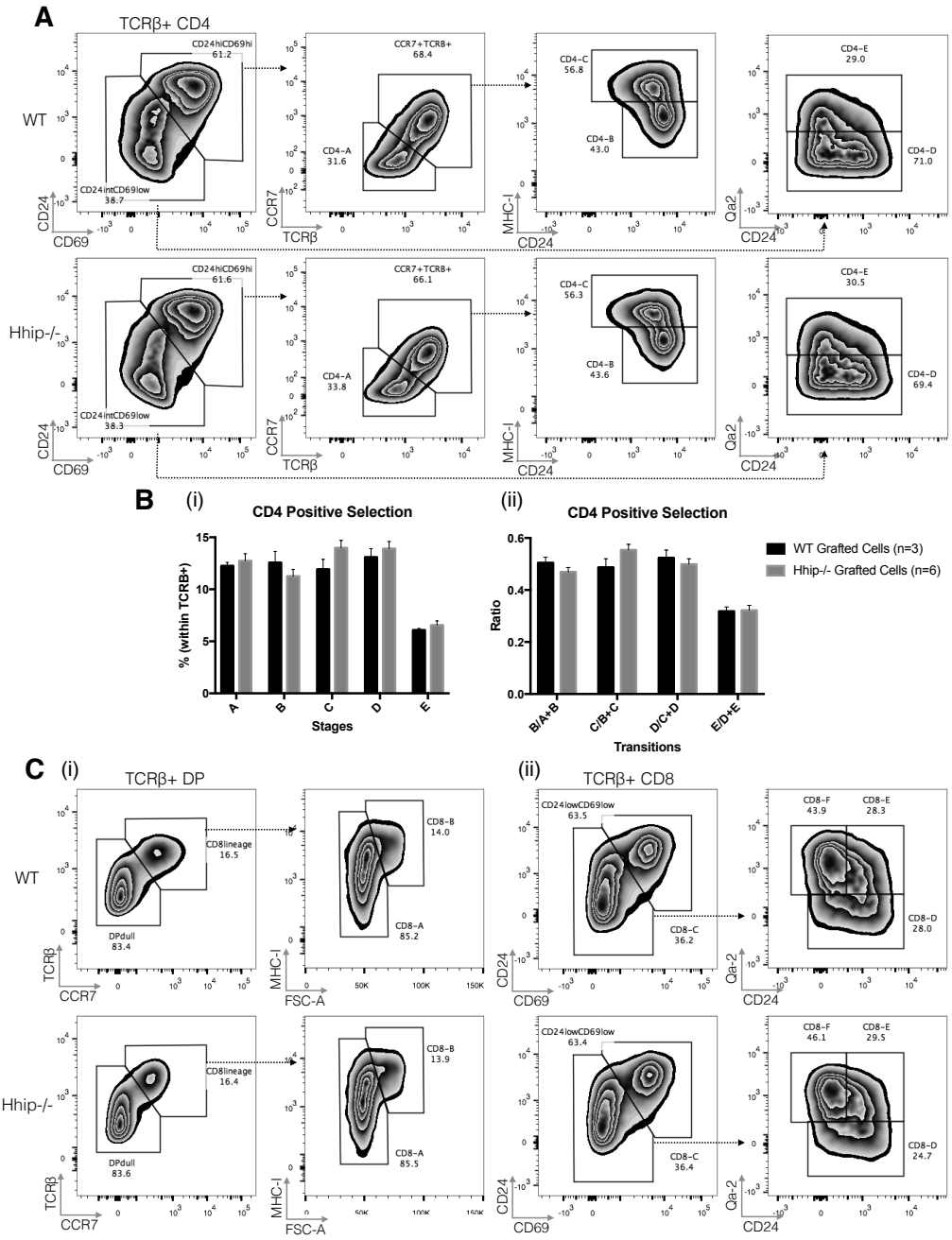

Figure 5.24: Hhip-/- cells show no overt defects in positive selection, but express markers differently
(A) Representative FACS plots show gating strategy dividing TCRβ+ CD4 donor-derived CD45.2 cells from host animals grafted with either WT or Hhip-/- E14.5 fetal liver cells into positive selection stages based on CD24, CD69, CCR7, TCRβ, Qa2 and MHC-I expression. **(B)** (i) Frequencies of cells in each selection stage and (ii) the transition between stages, calculated by taking the frequency of cells in each stage of interest divided by the total frequency of cells in that stage and the one immediately preceding, e.g B/A+B. **(C)** The CD8 lineage is divided into positive selection stages, with early CD8 committed cells gated from the (i) DP population and later stages gated from the (ii) TCRβ+ CD8 population.

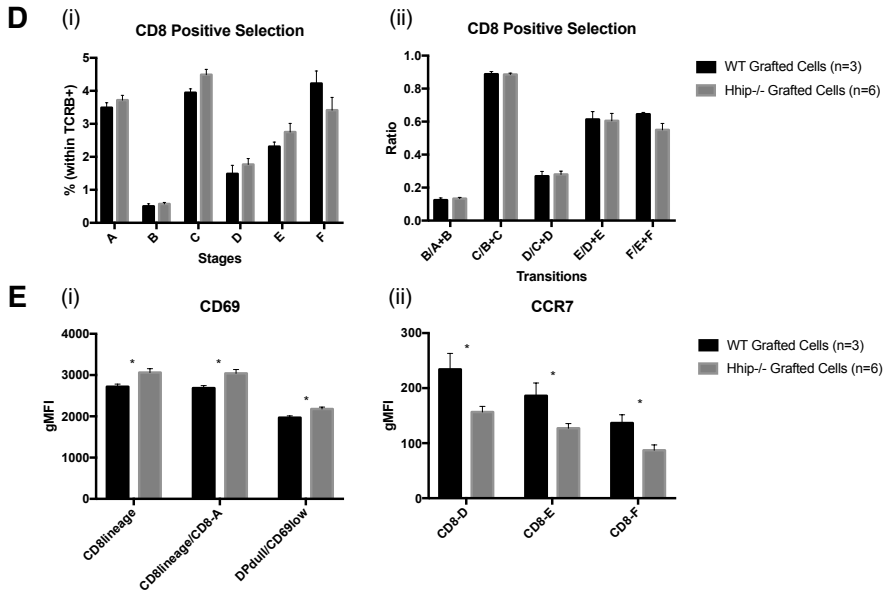

Figure 5.24: Hhip-/- cells show no overt defects in positive selection, but express markers differently
(continuation) **(D)** (i) Frequencies and (ii) transitional ability of CD45.2 TCRβ+ cells in each CD8 selection stage, defined in (B) and (C). **(E)** Statistically significant expression of (i) CD69 and (ii) CCR7 in CD8-committed cells of WT or Hhip-/- genotypes, where E14.5 fetal liver cells were grafted into irradiated hosts for 5 weeks. P-values were determined by student's t test where * $p < .05$. Experiment is representative of at least 2 independent experiments.

The results thus far suggest alterations in Hhip-/- CD8 maturation but not CD4, which may be indicative of a defect in lineage decisions possibly due to altered TCR signal strength and selection (Itano, A. *et al.*, 1996; Itano, A. & Robey, E., 2000). Hhip-/- CD8 cells developing in a WT TEC environment are less mature in comparison to WT thymocytes, yet express higher levels of cell surface TCRβ, which usually demonstrates progression along the maturation process. As negative selection is a final checkpoint in thymocyte development, this process was studied to assess whether any defects could be revealed in Hhip-/- thymocytes. As in previous analyses, the markers CCR7 and CD24 were used to identify thymocytes in different locations in the thymus, and Helios and PD-1 expression marked cells undergoing negative selection. Significant differences were not observed in the overall distribution of cell subsets based on CCR7 and CD24 expression, or in the frequencies of cells being negatively selected within those fractions (5.25A, 5.25B). In the cortical $CCR7^{-}CD24^{+}$ fraction, cells expressed higher levels of TCRβ (5.25B).

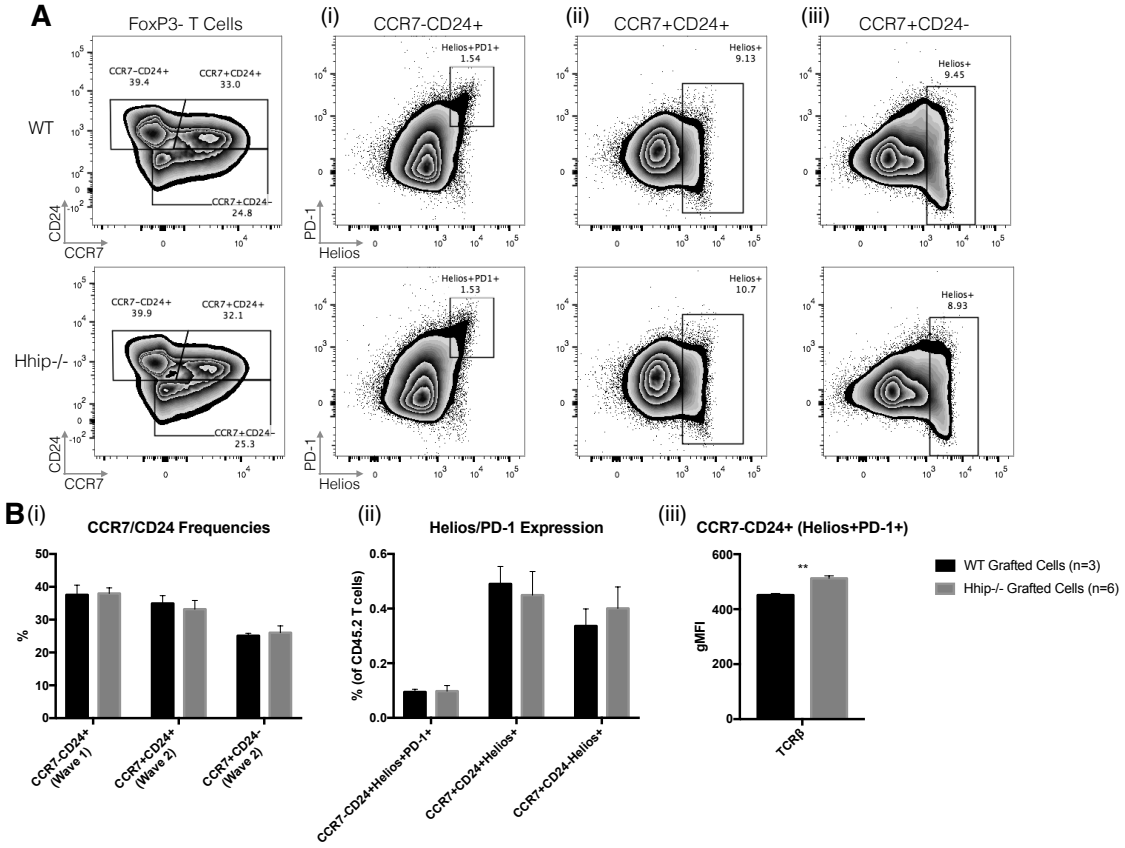

Figure 5.25: Frequencies of negatively selected cells are equivalent between WT and Hhip-/- thymocytes
(A) Total live Lin- FoxP3- single T cells are divided into negative selection stages by CCR7 and CD24 expression. The Helios and PD-1 positive fraction is gated in the (i) CCR7-CD24+ fraction (wave 1 of selection), while Helios-positive cells are gated in the (ii) CCR7+CD24+ and (iii) CCR7+CD24- fractions (wave 2 of selection) of WT and Hhip-/- grafted thymocytes. **(B)** (i) Frequencies of cells in each selection stage. (ii) Frequencies of cells expressing Helios and PD-1. **(C)** Expression of TCRβ in the CCR7-CD24+Helios+PD-1+ cell fraction. P-values were determined by student's t test where * $p < .05$, ** $p < .01$. Experiment is representative of at least 2 independent experiments.

CD4 and CD8 cells were analysed separately to identify if the elevated TCRβ cell surface expression was specific to either lineage. Neither single positive thymocyte populations displayed differences in their frequencies of negatively selected cells (5.26A, 5.26B), but CD8 cells again displayed an upregulation of TCRβ (5.26C).

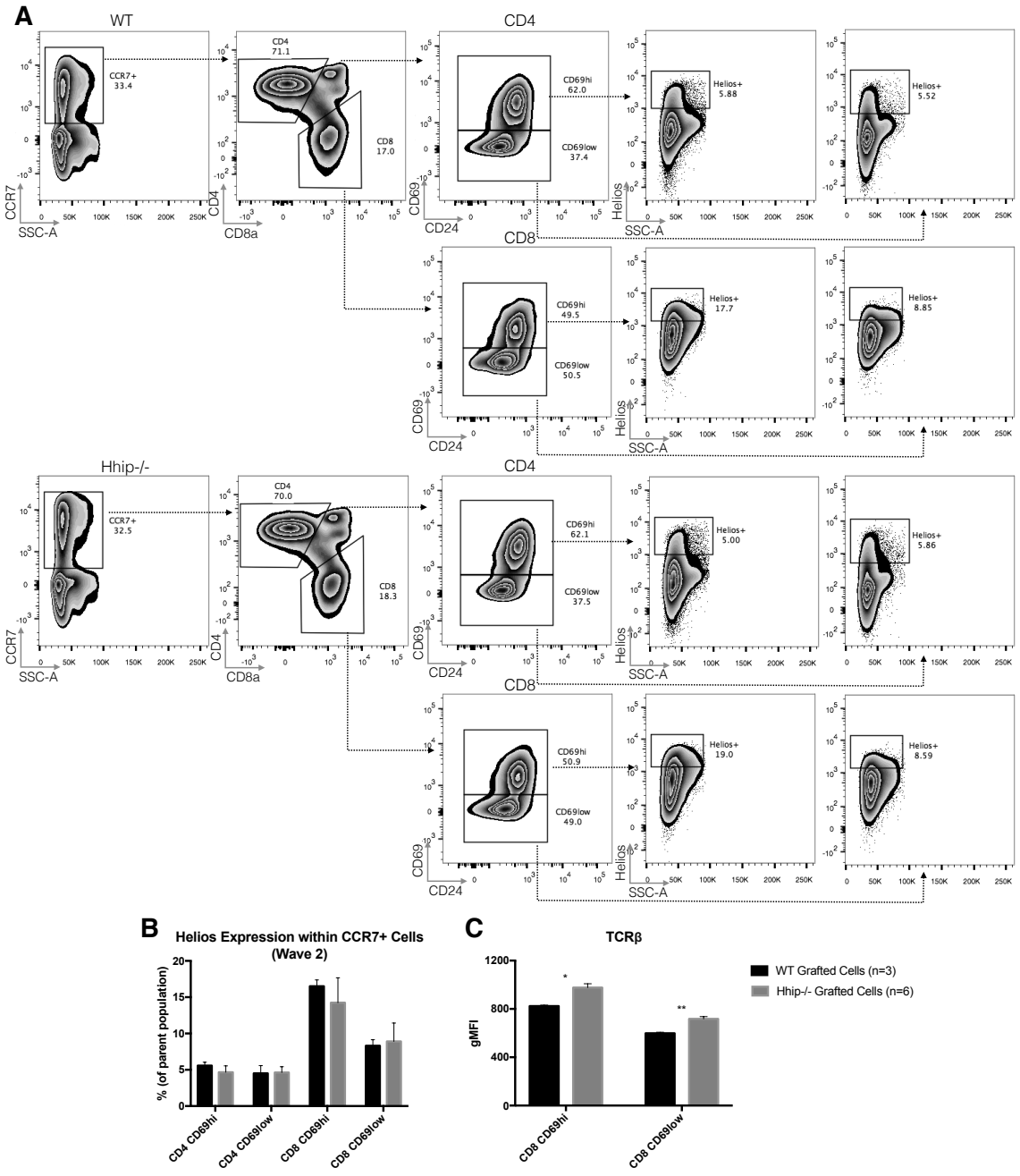

Figure 5.26: Frequencies of cells being negatively selected are comparable between grafts
(A) FoxP3- TCRβ+ CD45.2 cells in thymi grafted with either WT or Hhip-/- progenitors are gated on CCR7-positivity, then differentiated into CD4 and CD8 cells. Each lineage is gated on CD69 expression, and negatively selected cells are defined by Helios expression. Helios gates are drawn based on the CD4 population. **(B)** Helios-expressing cells as a percentage of the population of interest, for example CD4 CD69hi cells. **(C)** TCRβ expression on CD8 cells. P-values were determined by student's t test where * $p < .05$, ** $p < .01$. FACS plots and statistics are representative of 2 independent experiments.

The frequencies of cells in each of the different positive and negative selection stages in this experiment were comparable between thymi grafted with WT or Hhip-/- progenitors. As selection is effected by WT TECs under these experimental conditions, these results are consistent with the notion that the previous selection

defects observed in the transplanted Hhip-/- thymus as well as in the constitutive Hhip-/- mouse were TEC-specific. However, despite developing in a normal TEC microenvironment, *hhip*-deficient CD8 thymocytes displayed intrinsically lower cell surface expression of TCRβ and CCR7, accompanied by increased expression of CD69, which suggests that *hhip*-deficient thymocytes directed to a CD8 lineage fate may be innately less able to mature normally.

A simplistic summary of the results thus far yields three key observations. Firstly, the *hhip*-deficient TEC environment resulted in aberrant selection of normal WT progenitors, generating CD4 and CD8 cells with reduced TCRβ and CD5 expression. Secondly, *hhip*-deficient thymocyte progenitors developed in a WT stromal environment into CD8 cells with a less mature phenotype represented by increased CD69 expression, yet with increased TCRβ expression. Finally, the constitutive Hhip-/- neonatal thymus, with both *hhip*-deficient TECs and thymocytes, produced fewer and more immature CD4 cells. While CD4 and CD8 lineage fate choice is not completely understood, lineage decisions are at least partially dependent on TCR signal strength and duration (reviewed in Germain, R., 2002 and Singer, A. *et al*., 2009), such that strong TCR signals often result in the generation of more CD4 cells, although this may not reflect a switch in lineage direction (Bosselut, R. *et al*., 2001). Increased Hh signalling events reduce TCR signal strength (Rowbotham, N. *et al*., 2007). As such, the results presented thus far in this chapter are largely consistent with a loss of *hhip* expression resulting in increased Hh signalling in TECs, which consequently reduces TCR signalling on thymocytes through the TEC-thymocyte interactions. However, the thymocyte-intrinsic phenotype with increased cell surface levels of TCRβ observed in Hhip-/- CD8 cells needs to be reconciled. It is possible that a loss of Hhip in thymocyte

progenitors impairs their ability to regulate non TEC-derived Hh signals, for example from thymocyte-intrinsic Ihh signalling. Ihh is most important for the differentiation of DN cells into the DP population (Outram, S. *et al.*, 2009), but has not been thoroughly investigated in TCR signalling. It is conceivable that thymocyte-derived Ihh signals may have a mild contribution to TCR signalling, which is not observed in the context of the Hhip-deficient TEC environment given the significant contribution of TEC-derived Shh signals in the regulation of TCR signal strength. However, this will have to be studied in greater detail to draw any substantive conclusions.

5.6.1 Increased TCRβ expression is sustained in peripheral Hhip-/- T cells

The egress of Hhip-/- thymocytes (CD45.2) to the periphery was assessed to evaluate if single positive CD45.2 T cells were able to develop normally despite the apparent maturational defect of CD8 cells observed in the thymus. An equivalent frequency of WT and Hhip-/- donor cells successfully migrated to the periphery, as measured in the spleen (5.27A, 5.27B). Although the proportion of T cells from the Hhip-/- donor was increased, absolute numbers were not (5.27B). This might reflect a defect in B cell development instead, but as B cells do not develop in the thymus, this was not further investigated here. Similar ratios of effector, naïve and memory cells were observed for both lineages when comparing WT and Hhip-/- T cells. The CD8 naïve population expressed TCRβ at levels equivalent to WT (data not shown), but the central memory and effector populations had elevated levels of TCRβ expression (5.27C).

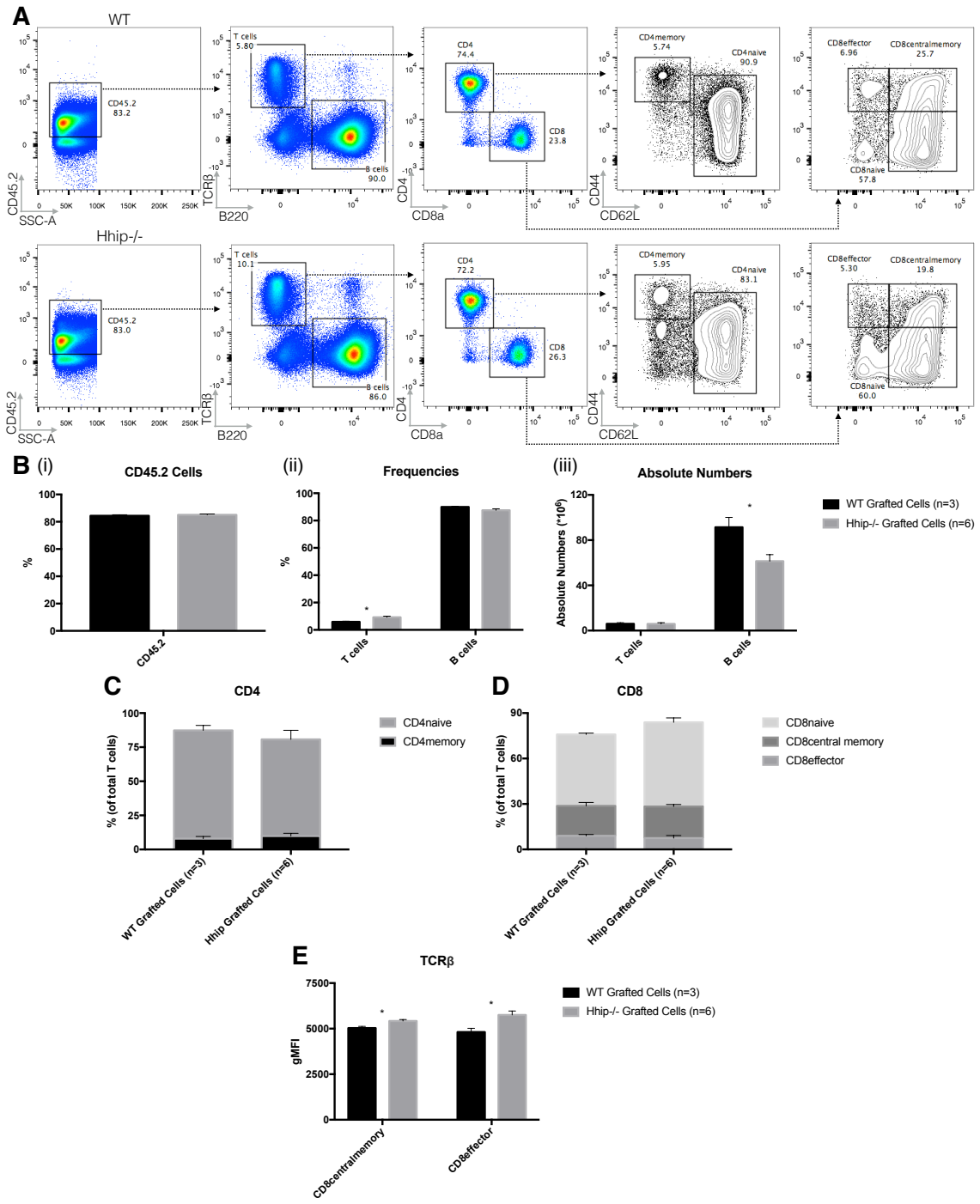

Figure 5.27: Hhip-/- T cells emigrate to the periphery, but the CD8 lineage expresses higher levels of TCRβ
(A) Live total single lymphocytes in the spleen of animals grafted with WT or Hhip-/- E14.5 fetal liver progenitors for 5 weeks are gated on CD45.2 expression, then split into T and B cells based on TCRβ and B220 expression respectively. T cells are distinguished by CD4 and CD8 expression, and effector, naive and memory cells in each lineage identified by CD44 and CD62L expression. **(B)** Statistics show (i) overall reconstitution rate of CD45.2 cells, and (ii) relative frequencies and (iii) absolute numbers of CD45.2 T and B cells. **(C)** CD4 subsets. **(D)** CD8 subsets. **(E)** TCRβ geometric mean fluorescence intensity on CD8 central memory and effector cells. P-values were determined by student's t test where * $p < .05$. Experiment is representative of at least 2 independent experiments.

The frequency of Hhip-/- mCD8 cells in the thymus and the absolute numbers in the spleen were equivalent to WT cells. Together, these results suggest that naïve Hhip-/- CD8 mature T cells develop successfully and migrate to the periphery, in

keeping with the expected normal development in a WT thymic stromal environment. However, once the Hhip-/- CD8 cells encounter antigens, they may downregulate their TCR less efficiently than WT T cells (Valitutti, S. *et al*., 1995), which could indicate altered TCR signal strength and a reduced functional competence of *hhip*-deficient thymocytes. The results also suggest that thymocyte selection by TECs may not have occurred correctly, allowing a population of T cells with altered cell surface expression of markers to survive, although this seems illogical given that development under these experimental conditions occurred within a WT thymic microenvironment.

5.6.2 Crosstalk from Hhip-/- thymocytes does not affect integrity of postnatal WT TECs

Physiological TEC development is critically dependent on physical and functional interactions with developing thymocytes, a process designated as lymphostromal crosstalk which occurs during early development and throughout life (Holländer, G. *et al*., 2006). As Hhip-/- T cells remain different from WT cells in their expression of cell surface markers even after developing within a normal thymic microenvironment, host TECs from the fetal liver transplant experiment were analysed to verify that exposure to Hhip-/- thymocytes had not induced any phenotypic changes which might affect their specific functions or maintenance. The frequencies of cTECs and mTECs, as well as the ratio of immature to mature mTECs, in the host thymi colonised by Hhip-/- thymocytes were unchanged in comparison to TECs exposed to WT thymocytes (5.28A, 5.28B). MHC-I and MHC-II expression was also unaffected (5.28C). This is not a regular physiological situation since host TECs are only exposed to transplanted thymocytes from Hhip-/- mice after they have already developed to an adult stage in normal contact with WT

thymocytes. However, this analysis excluded the possibility that Hhip-/- thymocytes affected the host thymic stromal environment despite the relatively short duration of interaction in a manner that impaired selection and development.

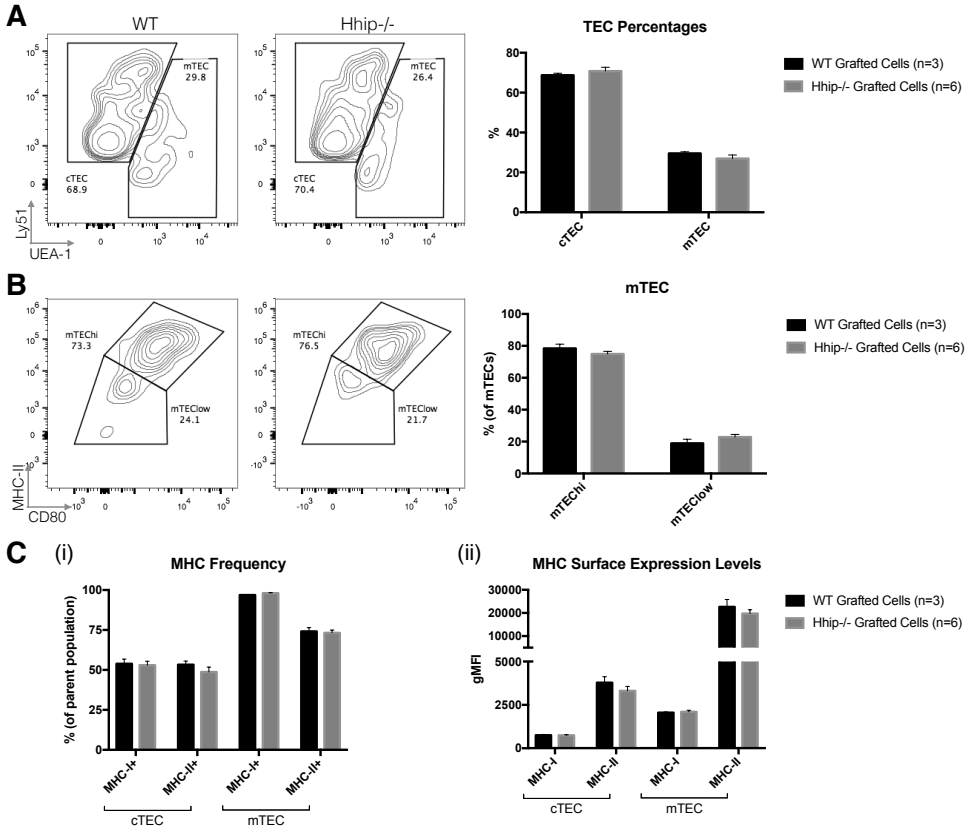

Figure 5.28: Host CD45.1 thymi reconstituted with WT or Hhip-/- progenitors display similar TEC phenotypes
(A) Frequencies of live single CD45-Epcam+ cTECs and mTECs in host thymi reconstituted with WT or with Hhip-/- E14.5 progenitors 5 weeks post-transplant. **(B)** mTEChi (MHC-IIhiCD80hi) and mTEClow (MHC-IIlowCD80low) frequencies. **(C)** (i) Frequencies of MHC-I and MHC-II highly expressing cells and (ii) levels of MHC expression in each TEC subset. Statistics were evaluated using a student's t test. Experiment is representative of at least 2 independent experiments.

5.7 A *hhip*-deficiency does not affect the lymphoid committed precursor

The results thus far indicated that fetal liver-derived Hhip-/- progenitors had an intrinsic deficiency as demonstrated by elevated TCRβ cell surface expression even when developing in a WT thymus. Counterintuitively, *hhip* expression could not be detected in WT thymocytes at E14.5, E16.5 and E18.5 (3.2F). To establish whether Hhip-/- cells had a functional disadvantage present already at the stage of the haematopoietic precursor, haematopoietic chimeras were generated either with pure thymocyte progenitors from the fetal liver of E14.5 WT mice, Hhip-/- mice, or a

mixture of equal proportions of WT and Hhip-/- fetal liver cells, designated as WT/Hhip-/- 50:50. Grafted mice were analysed 5 weeks later for the reconstitution of the bone marrow as recipient hosts were lethally irradiated. This experimental design allowed a direct evaluation of whether Hhip-/- lymphoid progenitors were less competent than their WT counterparts in a competitive environment.

The reconstitution rates of WT, WT/Hhip-/- 50:50 and Hhip-/- fetal liver progenitor cells in the bone marrow after 5 weeks were similar (5.29A, 5.29E). The $Lin^{-}Sca\text{-}1^{+}cKit^{+}$ (LSK) population, which includes haematopoietic stem cells (HSCs), was significantly reduced in Hhip-/- (0.500 ± 0.02%) as compared to WT (0.727 ± 0.04%) (5.29B, 5.29E). The multipotent progenitor (MPP) population was also reduced (WT 0.00586 ± 0.0005%, Hhip-/- 0.00256 ± 0.0007%) (5.29C, 5.29E). However, the lymphoid-primed multipotent progenitor (LMPP) fraction, which is responsible for the generation of T and B cells, was similar between WT and Hhip-/- (5.29D, 5.29E). WT/Hhip-/- 50:50 cell populations were not significantly different from WT (5.29E). As frequencies of lymphoid-committed haematopoietic precursors were unaffected by a deficiency of *hhip* expression, there is no evidence to suggest that Hhip influences the generation or colonisation of early thymocyte precursors that have not yet entered the thymus. These results imply that a loss of Hhip in thymocytes may be most relevant in the thymus, and is likely primarily important in TEC-thymocyte interactions, as previously postulated.

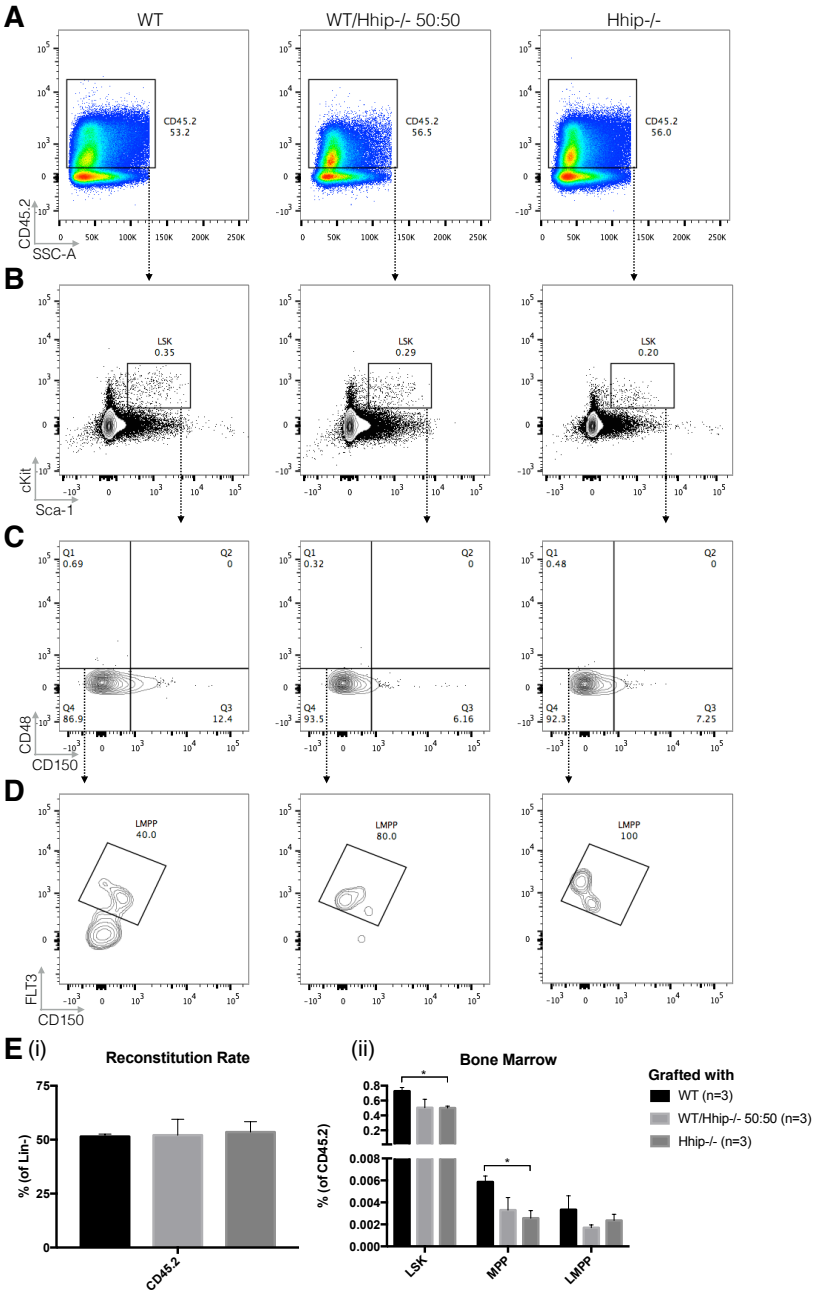

Figure 5.29: Hhip-/- lymphoid-committed precursors are at equivalent levels to WT
(A) Representative FACS plots show gating on CD45.2 cells in the bone marrow of host mice injected with a WT, WT/Hhip-/- 50:50 mix or Hhip-/- fetal liver cell suspension. **(B)** The Lin-Sca-1+cKit+ (LSK) population is gated, and **(C)** further subdivided by CD48 and CD150 expression to identify multipotent progenitors (MPP) in Q1. **(D)** Committed lymphoid-primed multipotent progenitors (LMPP) are gated on high FLT3 expression. **(E)** (i) Reconstitution rate of Lin- live single cells. (ii) Frequencies of LSK, MPP and LMPP populations, relative to total CD45.2 live Lin- single cells. A single experiment is shown, representative of 2 independent experiments. Total experimental size: WT n=6, WT/Hhip-/- 50:50 n=3, Hhip-/- n=6. P-values were determined by student's t test where * $p < .05$.

Preliminary experiments assessing the presence of *hhip* transcripts in thymocytes did not distinguish between different thymocyte stages (3.2C, 3.2F). qPCR analysis was therefore repeated to test whether *hhip* was expressed, albeit transiently, during a particular thymocyte developmental stage. Thymocytes from a 6 week old WT C57BL/6 mouse were sorted according to different phenotypes identifying

distinct developmental stages. *Rag1* expression was used as an internal reference to verify the identity of the sorted populations (5.30A). *Ptch1* and *gli2* expression were detected in all thymocyte subpopulations, in keeping with expectations that T cells express Hh signalling machinery (5.30A). Low expression of *hhip* was detected in DP cells, while *shh* was detected in DN and CD4 populations. All other thymocyte subpopulations were negative for either transcripts (5.30B). The variance of expression was very high due to low transcript copy numbers, questioning the biological relevance of any detected transcripts. Both *ihh* and *dhh* were expressed in thymocytes (5.30C). The absence of *hhip* in thymocytes correlated with an absence of Foxn1 expression and thus supported the contention that *hhip* is a target of Foxn1 in TECs. However, how a lack of Hhip in thymocytes would then affect T cell development remains unclear. It is possible that *hhip* is transiently expressed by thymocytes during a specific embryonic stage that has not been investigated here. Of note, *hhip* transcripts could be detected in all human thymocyte subsets (Sacedón, R. *et al*., 2003), although equivalent expression has not been characterised in murine cells.

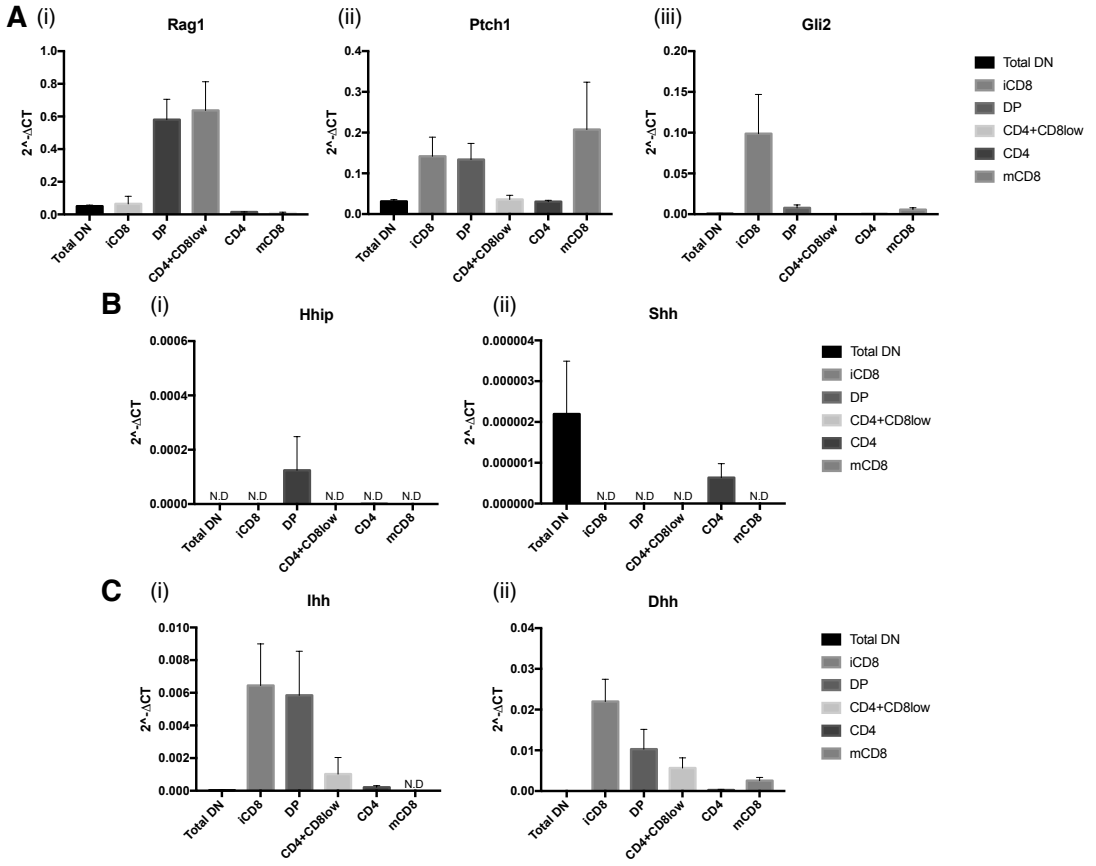

Figure 5.30: *Hhip* and Hh signal transduction genes in 6 week old thymocyte subpopulations
(A) (i) *Rag1* expression is used to verify sorted T cell subpopulations from 6 week old WT C57BL/6 mice. (ii) *Ptch1* and (iii) *gli2* expression in individual thymocyte subpopulations. **(B)** (i) *Hhip* and (ii) *shh* expression. **(C)** (i) *Ihh* and (ii) *dhh* expression. Values are normalised to *gapdh* expression. 2 independent experiments were conducted in triplicates and the results pooled.

Studies analysing conventional *hhip* knockout mice have revealed firstly that Hhip directly influences Hh signalling via *gas1* and *boc* expression, and is necessary for the maintenance of conventional cTEC/mTEC ratios in the thymus, suggesting a potential role for Hhip in TEC fate choice. Secondly, the absence of *hhip* in TECs also correlates with changes in MHC expression, which may affect TEC function and alter the repertoire of thymocytes selected, thus impairing normal T cell development. *Hhip*-deficient thymocytes also display an intrinsic differential expression of cell surface markers. This specific defect does not arise from interactions with Hhip-/- TECs as it was observed in a WT stromal environment, but could not be identified at the level of the haematopoietic precursor. However, all the experiments in this chapter were conducted using a transgenic model that has a

constitutive absence of functional Hhip protein. Specifically, in the experiments where Hhip-/- TECs or thymocyte progenitors were transplanted into a normal healthy *hhip*-sufficient environment, they had all previously developed, albeit for a short duration, from a *hhip*-deficient model. It cannot be determined if interactions during early development with other Hhip-/- cells could have affected them in a long-lasting manner that influenced their subsequent development even after transplantation. The *ex vivo* manipulation during transplantation could also have had unintended consequences on the viability of the cells, and the artificial nature of these experiments might not fully represent the true *in vivo* role of Hhip. Consequently, efforts were concentrated into developing a conditional knockout animal model, in which expression of *hhip* could be ablated on a genetic level in a specific cell type such as TECs, which will be discussed in Chapter 6.

6: A Mouse Model Exhibiting TEC-Targeted Loss of *Hhip*

Mice homozygously deficient for *hhip* expression die at birth due to respiratory failure. The premature death of these animals precludes a detailed analysis of any impact a loss of Hhip may have on TEC differentiation and function. To overcome this specific restriction, a conditional gene targeting strategy was designed to create the possibility to delete *hhip* alleles in any tissues by taking advantage of the Cre-Lox recombination system. The availability of conditional knockout mice would thus allow the examination of effects of a TEC-specific loss of *hhip.*

6.1 Overall gene targeting strategy

The general strategy developed aimed to insert loxP sites into intronic sequences of *hhip* to flank an indispensible exon within that locus. *Hhip* exon 2 was determined as an ideal target exon as this sequence encodes part of the essential Hhip ectodomain (Chuang, P. & McMahon, A., 1999). While the murine Hhip protein structure has not been resolved, it shares 94% sequence homology with human Hhip, which has been crystallised to show that exons 1 and 2 encode a Frizzled fold (Bosanac, I. *et al.*, 2009). This fold is not involved in Hh binding in humans (Bosanac, I. *et al.*, 2009; Bishop, B. *et al.*, 2009); however, deletion of *hhip* exon 1 in mice resulted in a non-functional null allele (Chuang, P. *et al.*, 2003), and thus deletion of exon 2 was expected to cause a similar outcome. This reasoning was based on the knowledge that exon 2 is early in the coding sequence, and absence was thus predicted to interfere significantly with translation and also result in the generation of a premature stop codon. Due to an uneven number of nucleotides, splicing of exon 1 to the canonical exon 3 splice acceptor site would still be unlikely to produce a functional reading frame. As such, absence of exon 2

in any *hhip* transcripts was expected to result in a complete absence of Hhip protein. As a small exon of 193 bp in size, selection of this exon also allowed for the realistic use of a single targeting vector as a template for homology directed repair (HDR) for cells to integrate the designed loxP sites flanking exon 2 of *hhip*, which would then allow the excision of exon 2 upon exposure to Cre-recombinase (6.1). The Crispr/Cas9 technology was utilised to facilitate this targeting, and specific synthetic guide RNA (sgRNA) sequences were designed to target the endonuclease Cas9 to cleave on either side of exon 2 where the loxP sites would be eventually be inserted.

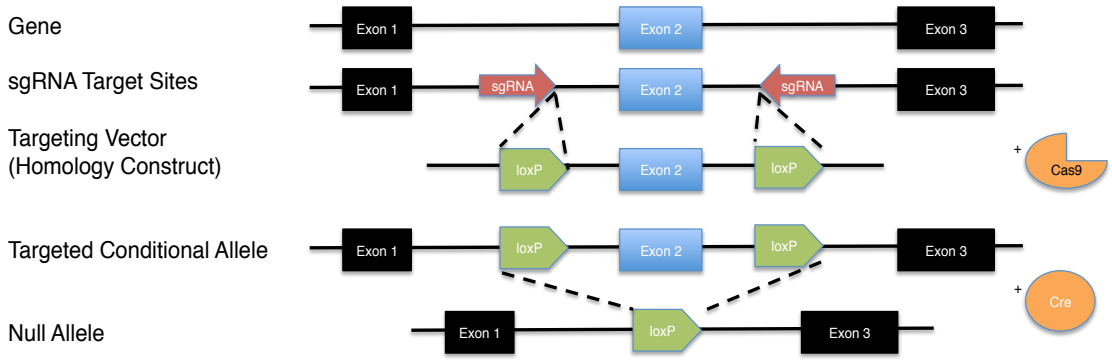

Figure 6.1: Design of gene targeting strategy to create a conditional *hhip* locus
Placement of loxP sites on the 3' and 5' sides flanking *hhip* exon 2, via homologous recombination of sites targeted by synthetic guide RNA (sgRNA) sequences for cleavage by the endonuclease Cas9. Expression of a Cre recombinase will effect recombination and deletion of exon 2, resulting in a null allele.

6.1.1 sgRNA design

Synthetic guide RNA (sgRNA) sequences were designed to target Cas9 endonuclease cleavage to the intronic regions on either side of *hhip* exon 2 (6.2A). sgRNAs were examined for off-target effects using the Crispr design algorithm (http://crispr.mit.edu) and tested for efficiency using the high-resolution melt analysis (HRMA) method (6.2B). Two sgRNAs flanking exon 2 with the highest cleavage efficiency and acceptable off-target scores of 95 and 73 were selected (Table 6.1). sgRNA2 directed Cas9 activity 472 nucleotides (nt) downstream of exon 2 on the forward strand, while sgRNA4 directed cleavage 308 nt upstream on

the reverse strand. The sgRNAs were cloned into PX459 vectors (Addgene) containing puromycin and ampicillin resistance genes for appropriate selection of successfully transfected vectors. These vectors also contained the sequences for the invariant sgRNA scaffold and Cas9 endonuclease to facilitate transfection (Ran, F. *et al*., 2013).

Table 6.1: List of designed sgRNAs targeting hhip exon 2

sgRNA Name	**sgRNA Sequence**	**Strand**	**Off-Target Score**
sgRNA1	CATTACTACGAGCCCTTGTAAGG	-	87
sgRNA2	CTGGGCCGGCTATATATTAGAGG	+	95
sgRNA3a	CAGCATAACTTTATACAGGCTGG	-	77
sgRNA3b	GTGTAAAAATTTTACCACTTAGG	+	54
sgRNA4	TACGATTCAATATATGCTCTGGG	-	73
sgRNA5	AGTAGTGAATTTTAGCGGAAAGG	+	83
sgRNA6a	AAATGAGTCTTAAGCCTATTTGG	-	71
sgRNA6b	ACATTCATTATATCTTAGCCAGG	+	66

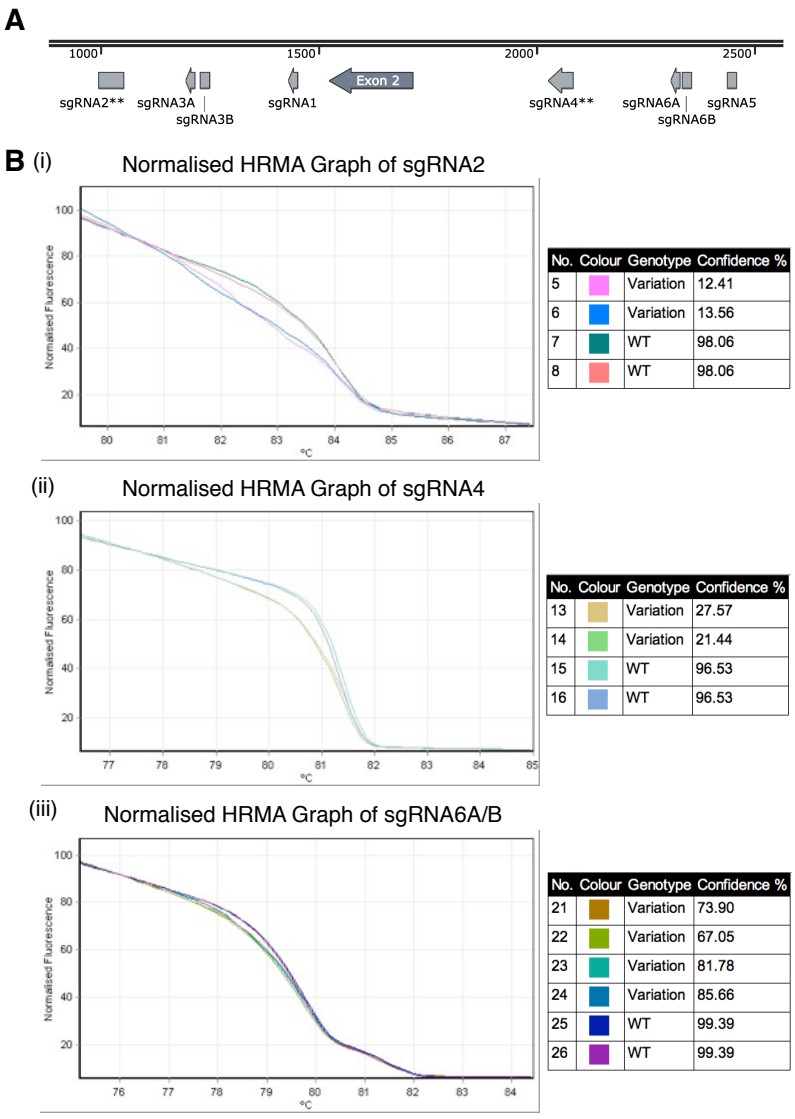

Figure 6.2: Design and verification of sgRNAs
(A) Sequence map showing positions of sgRNAs relative to *hhip* exon 2. **(B)** HRMA of N2A cells transfected with sgRNA2, sgRNA4 and sgRNA6a/b (Variation) compared with non-transfected cells (WT). Melt curves show sgRNA2 and sgRNA4 produced clear temperature shifts demonstrated by a low confidence percentage (%) compared to the initial gene sequence, indicative of successful Cas9 cleavage and subsequent nucleotide changes. sgRNA6A/B produced a modest shift.

6.1.2 Homology construct

A homology construct spanning *hhip* exon 2 and contiguous sequences of the neighbouring intronic region was designed to insert loxP sites flanking exon 2 at both 5' and 3' ends. This construct was used as a template for HDR following Cas9-directed endonuclease cleavage, allowing for modifications to be introduced via the template in lieu of correction by non-homologous end joining (NHEJ), the default DNA repair mechanism. A single construct of 2890 bp was chosen instead

of two separate loxP cassettes with the intention to enhance co-transfection and integration efficiency. The sequence of the construct encoded the original *hhip* exon 2 sequence flanked by loxP sequences replacing the sites of sgRNA2 and sgRNA4. Successful homologous recombination of the construct was expected to replace the sequences corresponding to sgRNA2 and sgRNA4 such that further Cas9 cleavage could not then take place, thus minimising the likelihood of sequence errors to be introduced. Restriction enzyme sites for BamHI, MfeI/SpeI and NotI were included at various points within the intronic sequence to allow for ease of screening and additional molecular manipulations as required (6.3A). The homology construct was synthesised in a pMA plasmid vector (Life Technologies) containing the gene for ampicillin resistance for convenient selection (6.3D).

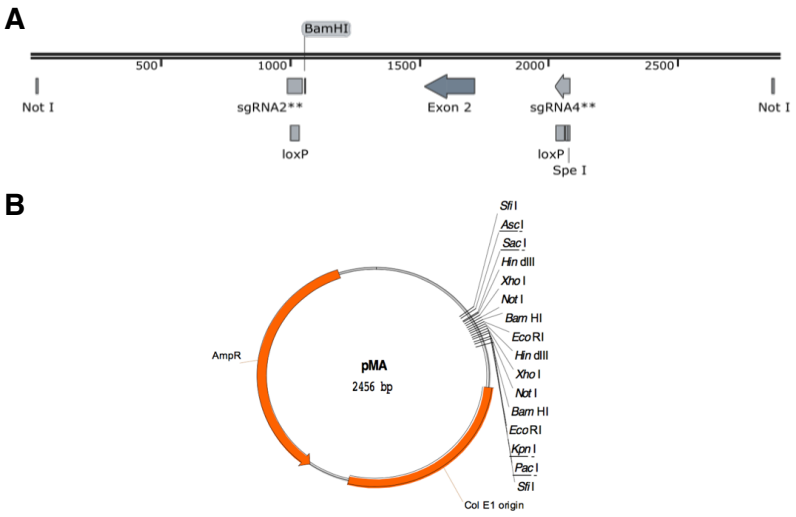

Figure 6.3: Design of targeting vector
(A) Map shows the sequence of the targeting construct and the modifications made to include loxP sequences and additional restriction enzyme sites. sgRNA2 and sgRNA4 tags are included to demonstrate where the loxP sites are inserted relative to the Cas9 cuts. **(B)** Plasmid map of the pMA vector which served as the backbone for cloning the targeting construct, showing all available restriction enzyme sites. The homology construct was cloned into the plasmid using NotI sites.

6.1.3 Transfection

sgRNA2 and sgRNA4 cloned into PX459 vectors and the homology construct were co-transfected into a C57BL/6 JM8.F6 feeder-dependent embryonic stem cell line. Successfully transfected clones were selected based on antibiotic resistance of the

plasmid vectors. Subsequently, 96 individual clones were picked and grown in a 96-well plate (Corning), labelled in alphabetical order from A1 to H12. Primers were designed to screen for presence of loxP sites and correct genomic integration by PCR (6.4A).

6.1.4 Screening

Targeted gene amplification using a primer pair directed within the 3' genomic sequence and the engineered upstream loxP site (GPB-R and Lox4F) produces a 925 bp fragment under conditions where the homology construct is successfully and precisely integrated into the 3' genomic site. In contrast, if the construct is not integrated correctly, no fragment is generated. PCR screening of all 96 clones revealed 9 ES cell clones with correct 3' integration of the homology construct (6.4B). Upon further screening for the 5' homology arm (GPA-F and Lox2R). 8 clones were identified with correct integration of the entire construct, specifically clones A3, C1, C4, E1, E3, F9, G2 and G4 (6.4C). Homozygosity for the homologous recombination was analysed using primer pairs on either side of the loxP insertion sites (S1-F and S2-R; S3-F and S4-R). Agarose gel electrophoresis revealed that all clones except E1 had both alleles correctly recombined (6.4C).

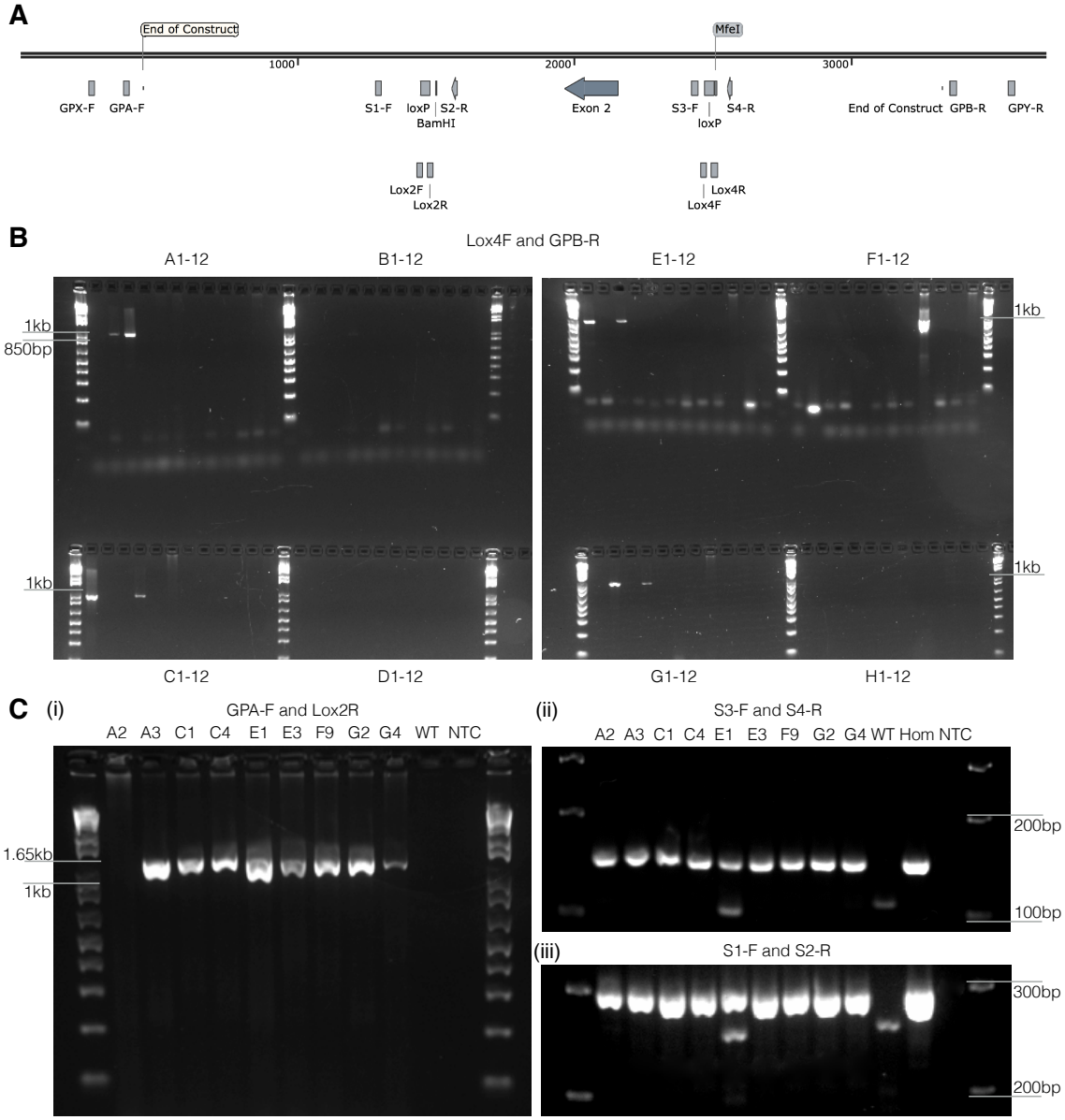

Figure 6.4: PCR screening strategy to verify correct integration of the targeting vector
(A) Sequence map of the *hhip* reverse strand shows design of PCR primers to test for correct insertion of loxP and restriction enzymes sites (S1-S4, Lox4, Lox2) and genomic integration (GPA, GPB). F indicates primers in the 5'-3' direction, R indicates primers in the 3'-5' orientation. **(B)** 96 picked clones (labelled A1-H12 based on their position in a 96-well plate) were screened for successful integration of the homology construct via a PCR reaction using the genomic primer GPB-R and the primer Lox4F which spans the 3' loxP site. The expected product is 925 bp. **(C)** (i) Clones that successfully amplified the GPB-R and Lox4F PCR product were tested for genomic integration of the 5' loxP site using the genomic primer GPA-F and the 5' loxP primer Lox2R. The expected product size is 1122 bp. (ii) S3-F and S4-R primers were used to test for homozygosity of the 3' loxP site, where successful integration gave a product of 147 bp and WT gave 111 bp. (iii) S1-F and S2-R primers were used to test for the 5' loxP site, giving a targeted product size of 297 bp and WT 263 bp. (B) and (C)(i) were run on 1.5% agarose gels, (C)(ii)(iii) were run on 2% agarose gels. The NEB 1kb+ ladder was used as reference.

PCR-amplified products from the 8 positive clones were purified and sequenced, including PCR products spanning either homology arm (GPA-F and S2-R; S3-F and GPB-R) as well as the complete genomic fragment spanning exon 2 (GPX-F and GPY-R). This analysis revealed that while most clones had at least partially

integrated the homology construct, only clones A3, C1 and G2 had integrated both loxP sites in the expected orientation with no other acquired sequence mutations, and had a fully intact and correct exon 2 sequence (6.5B, 6.5C).

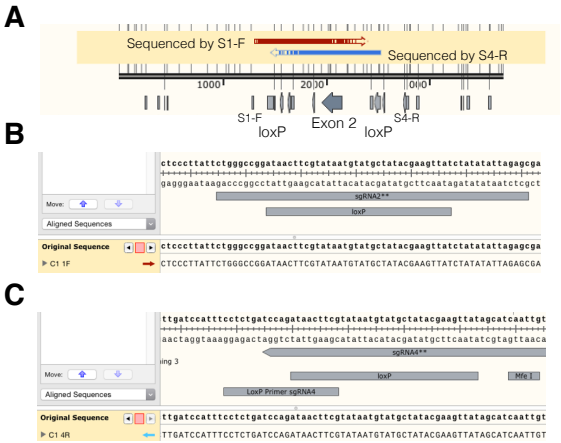

Figure 6.5: Sequencing results confirming the correct integration of loxP sites
(A) Sequence map shows alignment of the GPX-F and GPY-R genomic PCR product, sequenced by the primer S1-F in red (C1 1F), and sequenced by the S4-R primer in blue (C1 4R), where the sequenced product is largely identical to the targeted sequence. Analysis of the sequenced region at the loxP sites revealed that the targeted sequence is integrated with complete accuracy in the genomic product from the C1 clone at both the **(B)** 5' and **(C)** 3' loxP sites, as aligned with the designed homology construct sequence.

6.2 *In vitro* Cre transfection

To test the functionality of the inserted loxP sites, an expression vector containing the recombinase Cre was transfected into clones A3, C1 and G2. Individual colonies were subsequently picked to determine the successful recombination and excision of *hhip* exon 2. To demonstrate the correct recombination, primers were chosen on either external side of the loxP sites (S1-F and S4-R). The amplification product of the unaltered locus produced a wild-type fragment of 1222 bp, whereas the product of the recombined locus was only 264 bp. Twenty-four individually transfected clones of the C1 line are shown as a representative example of this screening method (6.6A).

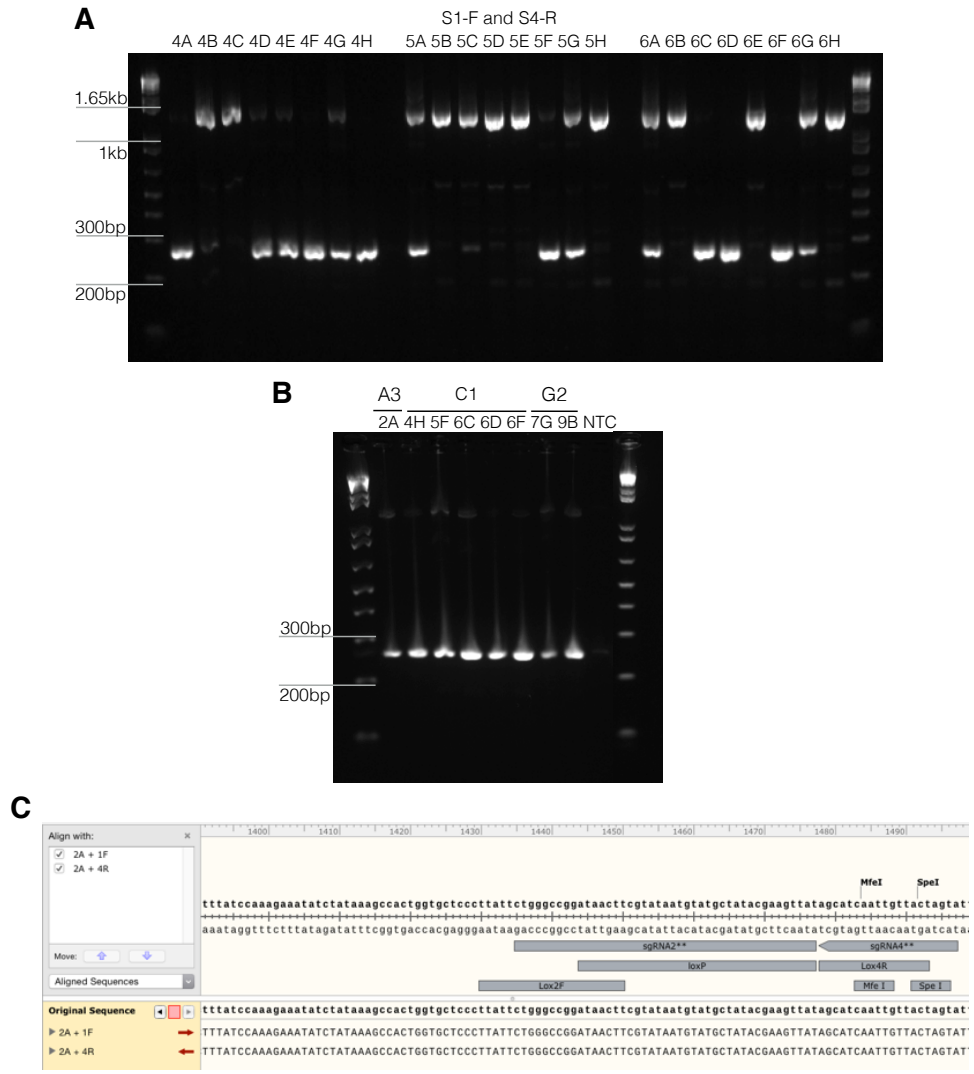

Figure 6.6: Cre-mediated recombination of the targeted *hhip* locus in ES cells
(A) The A3, C1 and G2 cell lines were transfected with the Cre recombinase plasmid and individual clones picked into a 96-well plate where A3 clones were plated successively from 1A to 3H, C1 from 4A to 6H and G2 from 7A to 9H. C1 clones (4A-6H) are shown here. PCR reactions were run using the primers S1-F and S4-R on either side on the 2 loxP sites **(B)** Clones that had demonstrated almost complete excision of *hhip* exon 2 were randomly selected and run on a gel to show a representative example. 10B did not amplify correctly. A non-template control using water (NTC) was included. 2% agarose gels were used and the NEB 1kb+ ladder was loaded as reference. **(C)** The PCR products with successful excision were sequenced for confirmation. A representative example of Clone 2A (from the original ES cell clone A3) is shown sequenced using the S1-F primer (2A + 1F) or the S4-R primer (2A + 4R), aligned against the hypothetical excised sequence which should result in a single loxP site. Sequences show perfect alignment, confirming that *hhip* exon 2 was correctly excised as expected.

A recombination efficiency of >50% was observed in all 3 clone lines analysed, with some transfected clones displaying homozygous recombination and others heterozygous recombination. Incomplete recombination was likely the consequence of suboptimal transfection efficiency or the length of transfection duration. Several successfully recombined clones from each of the different original ES cell clone lines were selected for sequencing (6.6B), which revealed that all

recombined clones had accurately excised *hhip* exon 2, leaving a single loxP site remaining. The sequencing results from transfected clone 2A (from the original clone line A3) are shown (6.6C).

6.3 Chimeras

The three positive ES cell clones, A3, C1 and G2, were expanded for blastocyst injection into host albino pseudopregnant C57BL/6 mice (C57BL/6BrdCrHsd-Tyr^{c}). Clone line A3 gave rise to 13 pups from 2 separate mothers, of which 3 were males. The degree of chimerism was determined by coat colour (6.7A). Two of these mice had high chimeric scores of 60% and 80%, but had health problems and were euthanised. 7 pups were born from a single mother from clone C1, and 4 male pups displayed a fur chimerism of 30%, 75%, 85% and 85%, designated A, B, C and D respectively. One male mouse with 50% fur chimerism died of an unknown cause. Clone line G2 yielded two litters with 3 male pups demonstrating fur chimerism of 85%, 90% and 90% (E, F, G).

Female chimeras were culled due to low possibility of transmitting the engineered mutation, since ES cells used were of an XY karyotype. Male chimeras were genotyped using DNA from ear clips and all were confirmed to harbour the desired mutation. Six male mice with a high degree of chimerism (>60%) were mated with albino C57BL/6 mice to establish germline transmission, but the breeding pairs were not successful. ES cell injections into albino host females were therefore repeated using on this occasion cell clones A3 and C1. This attempt yielded only 2 male chimeras both displaying low degrees of chimerism (30% from cell clone C1, designated H; 50% from cell clone A3, designated J). However, these animals also failed to transmit the mutation via conventional breeding.

Table 6.2: Chimeras produced

Cell Clone A3			
Embryos Implanted	26	26	36
Live Pups	6	7	8
Male Chimeras	1 (10%)	2 (80%, 60%)	1 (50%)
Female Chimeras	1 (10%)	1 (80%)	
Cell Clone C1			
Embryos Implanted	20	36	
Live Pups	7	10	
Male Chimeras	5 (85%, 85%, 70%, 50%, 30%)	1 (30%)	
Female Chimeras	1 (50%)	1 (60%)	
Cell Clone G2			
Embryos Implanted	20	20	
Live Pups	8	6	
Male Chimeras		3 (90%, 90%, 85%)	
Female Chimeras	2 (90%, 50%)		

Mouse F, derived from ES cell clone G2 and displaying a fur chimerism of 90%, was chosen as a sperm donor for *in vitro* fertilisation (IVF) treatment. For this purpose, sperm was harvested and frozen, tested for the correct genotype and assessed for mobility. Genotyping confirmed that this chimera contained the mutation of interest in the testes (6.7C). *In vitro* fertilised C57BL/6 oocytes were implanted into CD1 pseudopregnant females. Of the 6 pups, born, one male mouse (designated 1) successfully carried the desired mutation (6.7D) and was used to establish the desired transgenic mouse line.

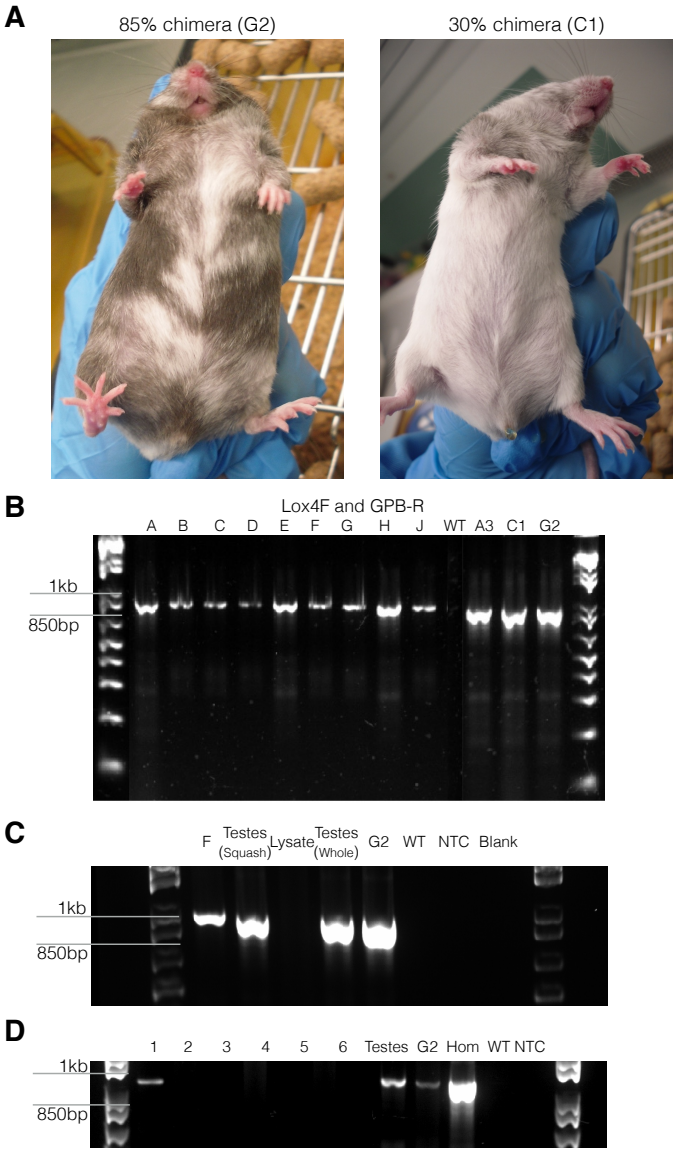

Figure 6.7: Chimeras possess the correct mutation as confirmed by coat colour and genotyping
(A) Chimeras were scored based on coat colour, where dark fur indicates contribution from the targeted black C57BL/6J ES cell, and light fur indicates contribution from the albino host mother. **(B)** Ear clips from the chimeras A-J were genotyped using the primers Lox4F and GPB-R to confirm presence of the targeted allele, with an expected band size of 925 bp. **(C)** DNA from the testes from the chimera F designated for IVF was extracted to confirm presence of the mutation in the sperm. One teste was squashed using frosted glass slides, and the other was minced whole. Lysate from the squash was also tested. PCR confirmed presence of the desired mutation using the primers Lox4F and GPB-R in the testes regardless of processing method. **(D)** Pups born from IVF, labelled 1-6, were genotyped for presence of the mutation using Lox4F and GPB-R. Pup 1 had the expected PCR product of 925 bp. A WT genomic sample and a non-template PCR control using water (NTC) were included as controls. DNA from the original ES cell clones A3, C1, and G2 were included as positive controls.

In aggregate, a fully transgenic mouse experimental system has been generated using Crispr/Cas9 technology to introduce a conditional modification of exon 2 of the *hhip* gene sensitive to Cre-mediated recombination.

6.4 Hhip$^{lox/lox}$

To ensure that off-target mutations had not occurred in the process of generating the line, homozygous gene targeted mice (designated Hhip$^{lox/lox}$) were first compared against wild-type littermates (Hhip$^{WT/WT}$). Hhip$^{lox/lox}$ mice were born at a regular Mendelian frequency and could not be distinguished by appearance from Hhip$^{WT/WT}$ mice. Thymi of 4 week old Hhip$^{WT/WT}$ and Hhip$^{lox/lox}$ mice were of equivalent gross morphology and appearance (6.8A). PCR analysis of genomic DNA confirmed presence of the targeted allele (6.8B). Overall cellularity was similar regardless of the method used to dissociate the thymi (6.8C).

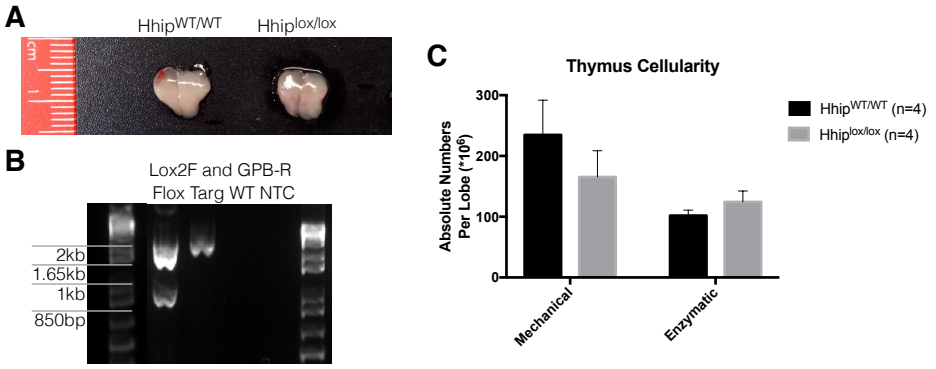

Figure 6.8: Gross anatomical appearance and cellularity of Hhip$^{lox/lox}$ thymi are similar to Hhip$^{WT/WT}$
(A) Representative pictures of 4 week old Hhip$^{WT/WT}$ thymi and Hhip$^{lox/lox}$ thymi shown next to a size measurement in cm. **(B)** A Foxn1$^{Cre+/-}$Hhip$^{flox/WT}$ mouse (Flox) produced 2 bands in the PCR reaction with the Lox2F and GPB-R primers, with an expected targeted product size of 1952 bp, and an excised product size of 957 bp. The Foxn1$^{Cre-/-}$ Hhip$^{lox/lox}$ mouse (Targ) only produced the targeted band of 1952 bp. A genomic DNA sample from a WT C57BL/6 mouse (WT) and the non-template PCR control using water (NTC) did not produce any bands. **(C)** The overall cell yield retrieved after either mechanical squash or enzymatic digestion. Statistics shown are pooled from 2 experiments and were calculated using a student's t test. At least 3 independent experiments were conducted.

6.4.1 The TEC compartment in Hhip$^{lox/lox}$ mice is not distinguishable from WT

TEC frequencies and cellularity were comparable for Hhip$^{lox/lox}$ and Hhip$^{WT/WT}$ mice (6.9A), with similar cTEC and mTEC frequencies (6.9B). Within the mTEC compartment, the distribution of immature (CD80^{-}MHC-II^{low}, designated mTEC^{low}) and mature (CD80^{+}MHC-II^{hi}, designated mTEC^{hi}) cells was also comparable (6.9C). The frequency of mature Aire-positive (MHC-II^{+}Aire^{+}) mTECs was similar for Hhip$^{WT/WT}$ and Hhip$^{lox/lox}$ at 4 weeks of age (6.9C).

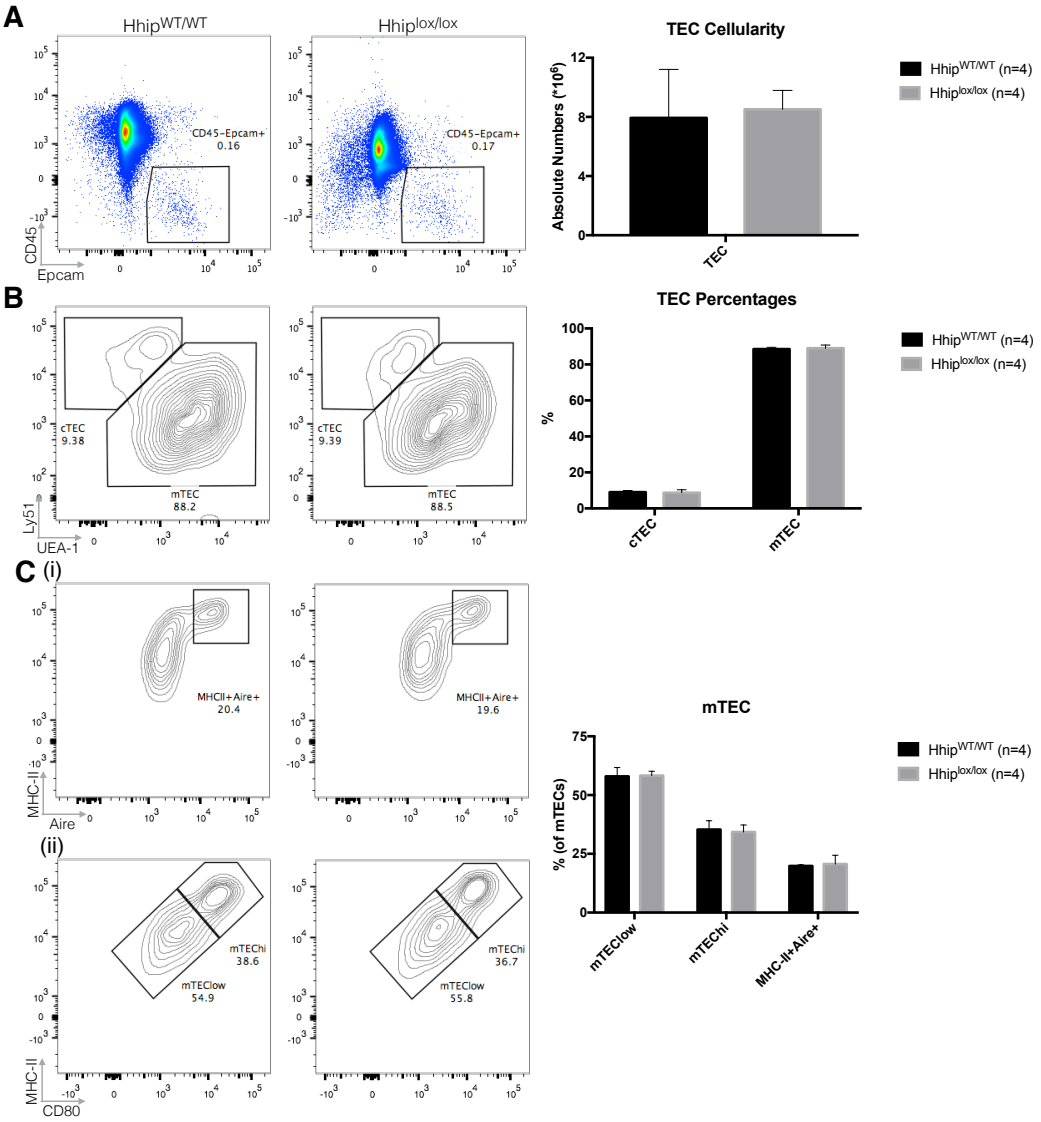

Figure 6.9: Hhip$^{lox/lox}$ mice have a comparable TEC profile to Hhip$^{WT/WT}$ mice
(A) Frequencies and absolute numbers of TECs in 4 week old Hhip$^{WT/WT}$ and Hhip$^{lox/lox}$ mice. **(B)** cTEC (Ly51+UEA-1-) and mTEC (Ly51-UEA-1+) frequencies. **(C)** (i) Frequencies of mature MHC-II+Aire+ cells, and (ii) mTEClow and mTEChi as distinguished by MHC-II and CD80 expression. Graphs shown are from 1 independent experiment, statistics are pooled from 2 experiments. Statistical validity was determined by student's t test.

cTECs and mTECs of both genotypes expressed comparable cell surface concentrations and frequencies of MHC-I, MHC-II, CD205, CD80, CD86 and Ki67, as demonstrated for MHC-II and Ki67 (6.10A, 6.10B).

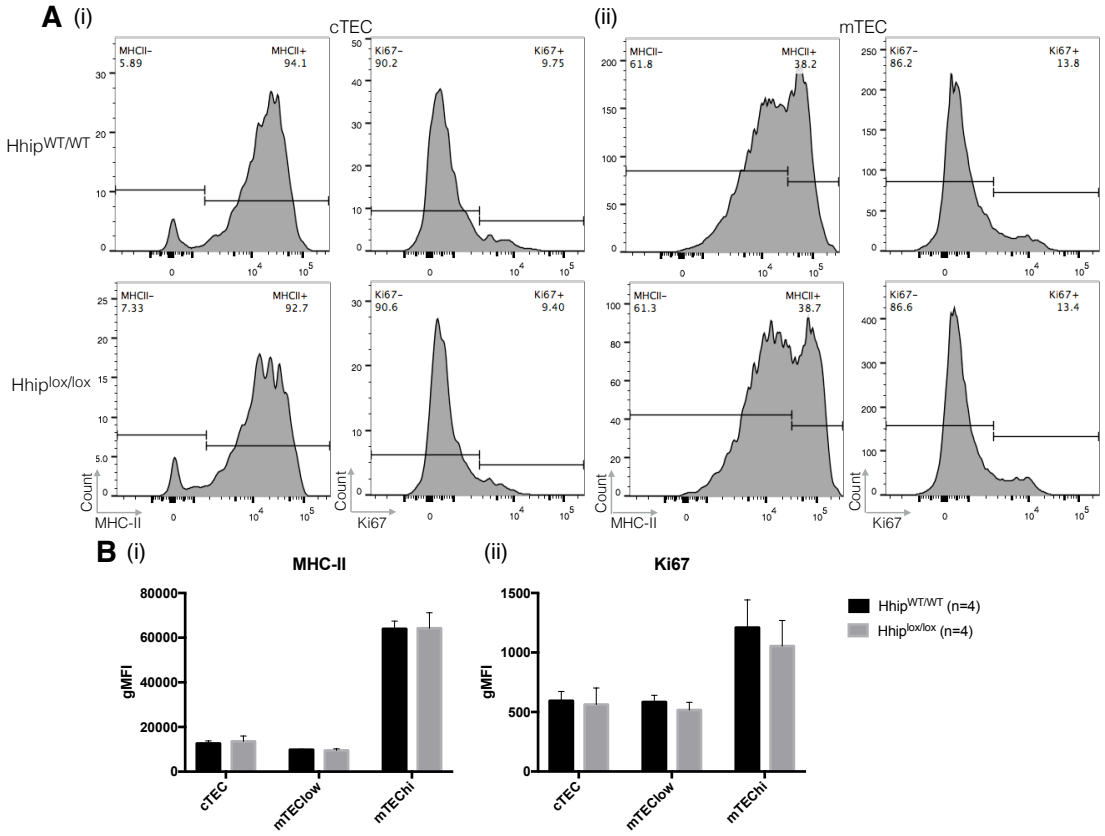

Figure 6.10: Expression of common markers in Hhip$^{lox/lox}$ TECs are similar to Hhip$^{WT/WT}$

(A) Frequencies of MHC-II+ and Ki67+ cells in (i) cTECs and (ii) mTECs of Hhip$^{lox/lox}$ and Hhip$^{WT/WT}$ 4 week old mice. **(B)** Cell surface expression levels of (i) MHC-II and (ii) Ki67. Graphs shown are from 1 independent experiment, statistics are pooled from 2 experiments. Statistical validity was determined by student's t test.

6.4.2 Thymocyte development in Hhip$^{lox/lox}$ mice is comparable to WT

Thymocyte maturation was assessed (6.11A, 6.11B, 6.11C). Analysis of the different DN stages, DP, CD4 and CD8 cells revealed a regular developmental progression in Hhip$^{lox/lox}$ mice comparable to Hhip$^{WT/WT}$ (6.11A, 6.11D, 6.11E, 6.11F). No differences in the expression of various cell surface markers (CD69, CD24, TCRβ, CD5 and CCR7) were noted in any of the T cell subpopulations in Hhip$^{lox/lox}$ compared to Hhip$^{WT/WT}$ (data not shown), suggesting that Hhip$^{lox/lox}$ thymocytes are phenotypically similar to Hhip$^{WT/WT}$ and likely develop in a comparable manner.

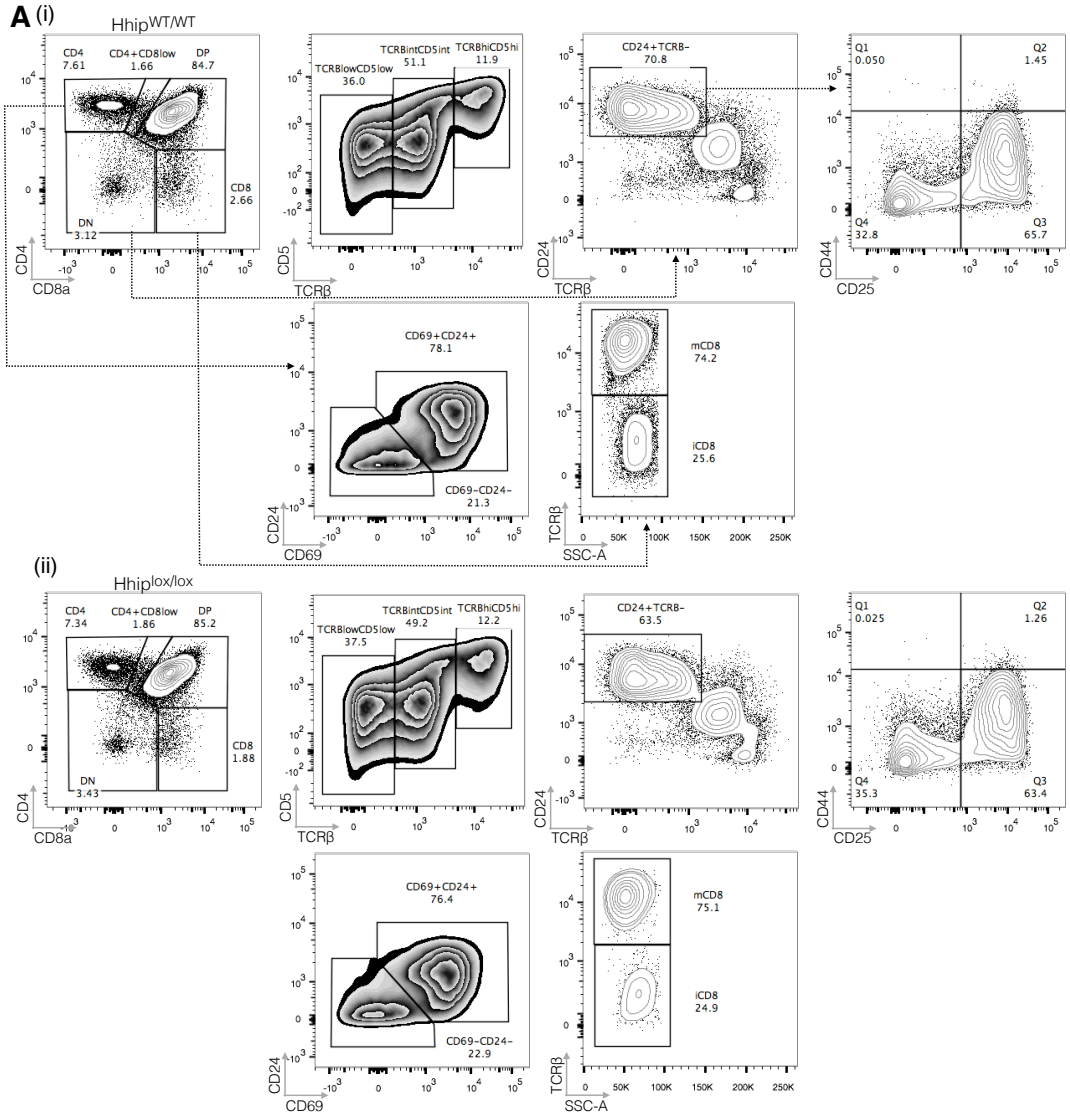

Figure 6.11: Thymocyte populations in Hhip$^{lox/lox}$ mice appear equivalent to Hhip$^{WT/WT}$
(A) Representative FACS plots showing in the first row from left to right, the distribution of live Lin- single T cells based on CD4 and CD8 expression, distribution of TCRβ and CD5 expression, gating of the true DN population using CD24 and TCRβ expression, and these cells in the various DN stages based on CD44 and CD25 expression. In the second row, CD69 and CD24 expression of CD4 single positive T cells, and distribution of mature and immature CD8 cells based on TCRβ expression. This is shown in 4 week old (i) Hhip$^{WT/WT}$ and (ii) Hhip^{loxlox} mice.

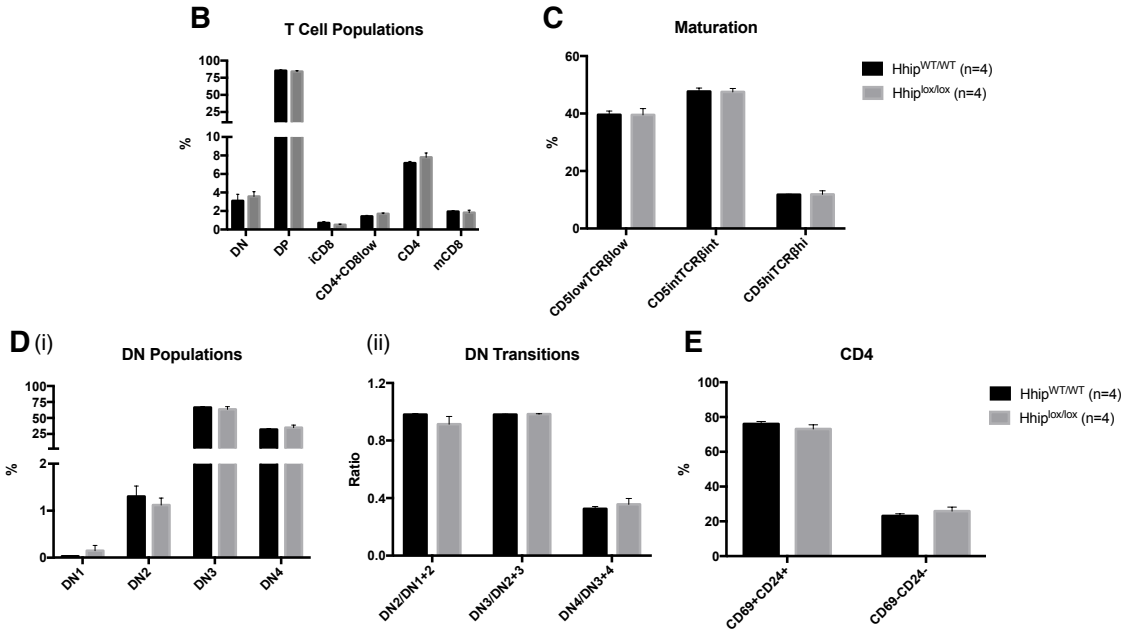

Figure 6.11: Thymocyte populations in Hhip$^{lox/lox}$ mice appear equivalent to Hhip$^{WT/WT}$
(continuation) **(B)** T cell subpopulations of live Lin- single T cells and **(C)** maturation as assessed by TCRβ and CD5 expression. **(D)** (i) Frequencies of cells in the various DN stages and (i) the ratio of cells successfully progressing through each DN stage. **(E)** CD69 and CD24 expression of CD4 cells. Graphs shown are from 1 independent experiment, statistics are pooled from 2 experiments. Statistical validity was determined by student's t test.

6.4.3 Peripheral T cell compartment of Hhip$^{lox/lox}$ mice is comparable to WT

A comparison of Hhip$^{lox/lox}$ and Hhip$^{WT/WT}$ mice demonstrated comparable numbers and frequencies of splenic B and T cells (6.12), the latter comprising similar proportions of naïve, memory and effector cells (6.12B, 6.12C).

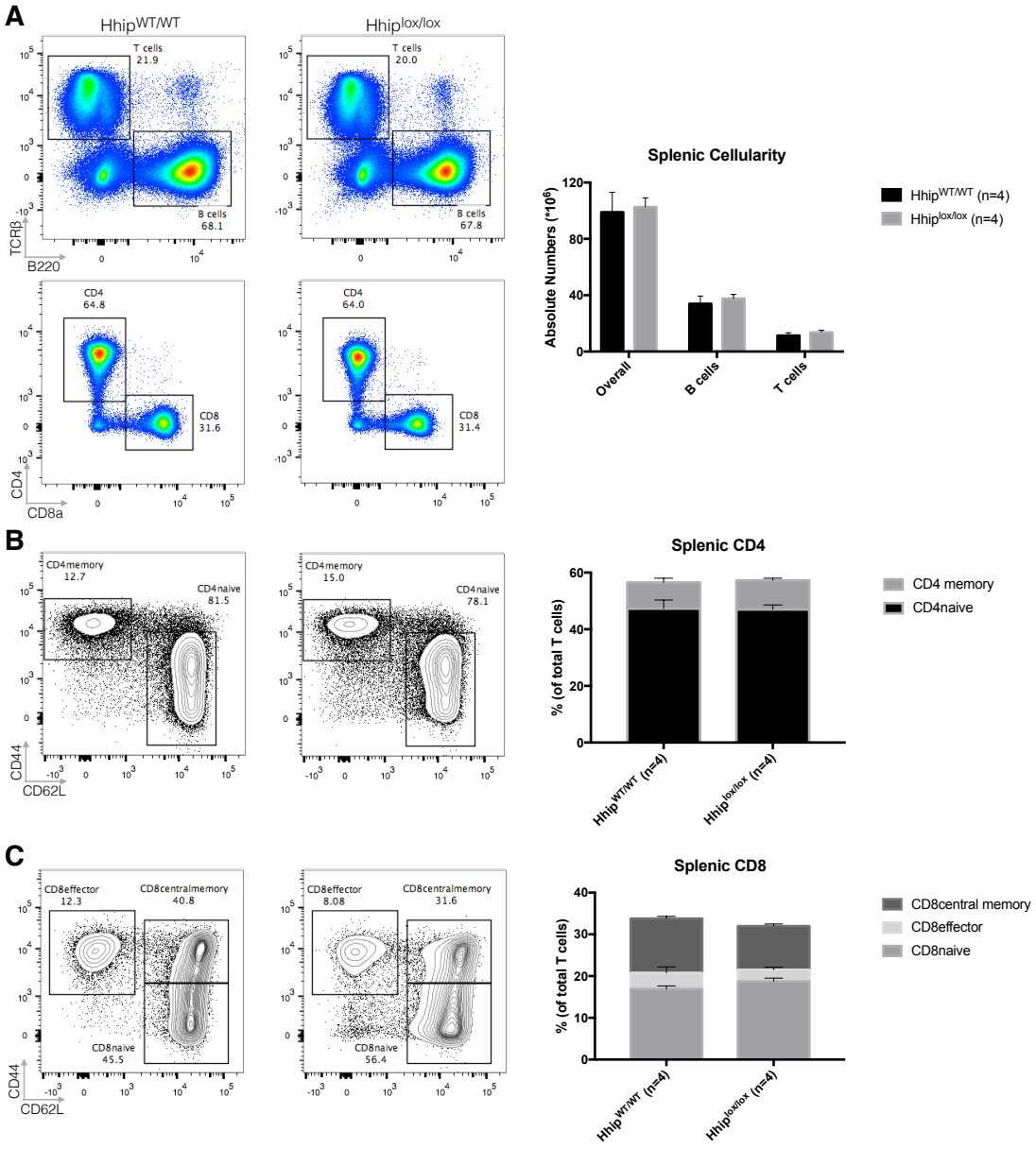

Figure 6.12: Peripheral T cells of Hhip$^{lox/lox}$ mice are phenotypically equivalent to Hhip$^{WT/WT}$
(A) Frequencies and absolute numbers of splenic T and B cells in 4 week old Hhip$^{WT/WT}$ and Hhip$^{lox/lox}$ mice. **(B)** CD4 memory and naive cells. **(C)** CD8 naive, effector and central memory cells. Graphs shown are from a single experiment, statistics are pooled from 2 experiments. Statistical validity was determined by student's t test.

In summary, this data demonstrates that the insertion of loxP and restriction enzyme sites adjacent to *hhip* exon 2 did not disrupt Hhip function and consequently neither TEC nor T cell development, validating this mouse model as a functional experimental system.

6.5 Foxn1$^{Cre+/-}$Hhip$^{flox/flox}$

The consequences of a TEC-specific loss of hhip expression were investigated. For this purpose, Hhip$^{lox/lox}$ mice were bred to heterozygous Foxn1^{Cre}-positive mice. Since Hhip$^{lox/lox}$ and Hhip$^{WT/WT}$ mice were indistinguishable in all immunological aspects investigated, the experimental genotypes Foxn1$^{Cre+/-}$Hhip$^{flox/flox}$ and Foxn1$^{Cre-/-}$Hhip$^{WT/WT}$ were compared, and are hereafter referred to as Hhip$^{flox/flox}$ and Hhip$^{+/+}$ respectively.

Four week old Hhip$^{flox/flox}$ thymi had a gross anatomical appearance identical to that of Hhip$^{+/+}$ and Hhip$^{lox/lox}$ thymi (6.13A). cTECs and mTECs were sorted from either genotype, and a PCR was conducted using primers flanking *hhip* exon 2. Hhip$^{flox/flox}$ TECs produced a shorter PCR product, confirming successful excision of exon 2, while Hhip$^{+/+}$ TECs had a larger PCR product with an intact exon 2 (6.13B). This confirmed successful excision of *hhip* exon 2 by Foxn1^{Cre} in both cTECs and mTECs. TEC cellularity was similar between Hhip$^{+/+}$ and Hhip$^{flox/flox}$, but overall T cell numbers were decreased (6.13C).

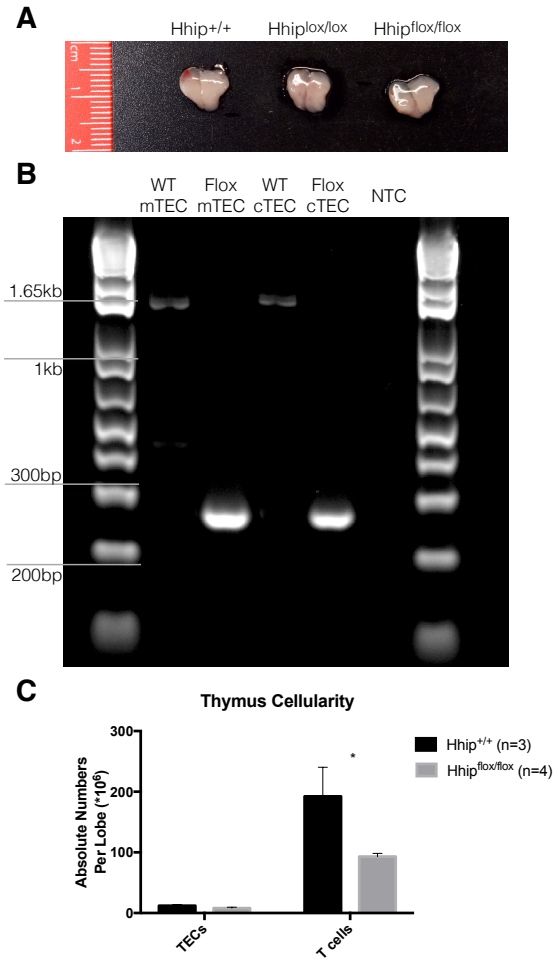

Figure 6.13: Appearance of the Hhip$^{flox/flox}$ thymus is similar to Hhip$^{+/+}$ but cellularity is different
(A) Representative pictures of Hhip$^{+/+}$, Hhip$^{lox/lox}$ and Hhip$^{flox/flox}$ thymi from 4 week old mice set next to a size measurement in cm. **(B)** Genomic excision of *hhip* exon 2 was confirmed in sorted cTECs and mTECs from Hhip$^{+/+}$ (WT) and Hhip$^{flox/flox}$ (Flox) using the S1-F and S4-R primer set, compared against a 1kb+ ladder. Expected excised product is 264 bp, intact genomic sequence is 1222 bp. **(C)** Cellularity of TECs and T cells in Hhip$^{flox/flox}$ and Hhip$^{+/+}$ thymi. Statistics shown are from a single experiment and are representative of at least 2 independent experiments. P-values were evaluated using a student's t test where * $p < .05$.

6.5.1 TEC differentiation in Hhip$^{flox/flox}$ mice is altered

The total TEC cellularity was unaffected in Hhip$^{flox/flox}$ mice at 4 weeks of age (6.14A), although the frequency of cTECs was decreased in Hhip$^{flox/flox}$ animals compared to age matched controls (7.93 ± 0.9% vs 12.2 ± 0.8%), and mTEC frequencies correspondingly increased (6.14B). Within the medullary compartment, the frequencies of the individual mTEC^{low}, mTEC^{hi} and MHC-II^{+}Aire^{+} subpopulations were identical for the two genotypes (6.14C). Of note, this phenotype was in keeping with that observed in the conventional *hhip*-deficient mice.

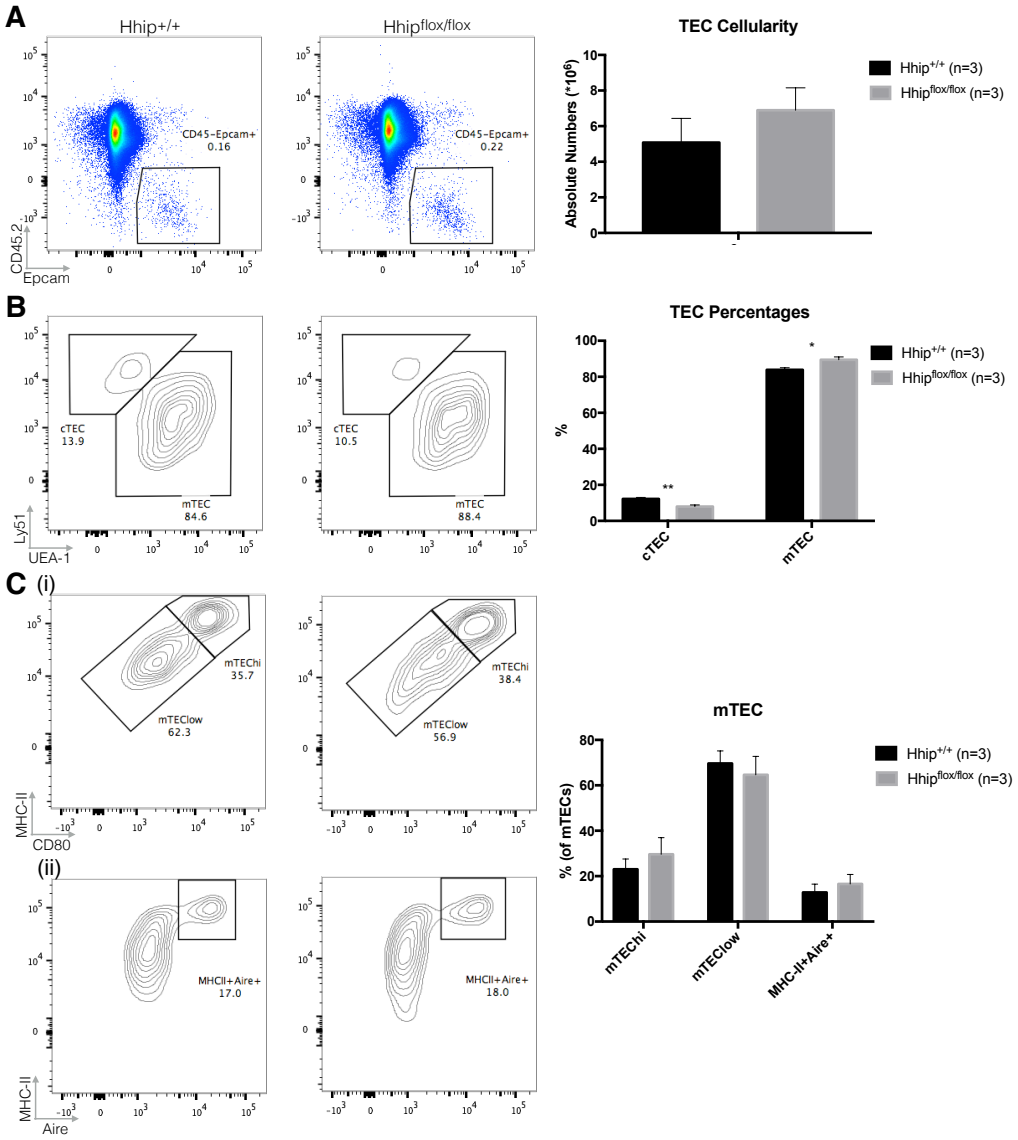

Figure 6.14: TEC differentiation is altered in Hhip$^{flox/flox}$ mice
(A) Frequencies and absolute numbers of TECs in Hhip+/+ and Hhip$^{flox/flox}$ thymi from 4 week old mice. **(B)** cTEC and mTEC frequencies. **(C)** (i) Frequencies of mTEChi and mTEClow as determined by MHC-II and CD80 expression. (ii) The mature MHC-II+Aire+ compartment. Graphs shown are from a single experiment and are representative of 2 independent experiments. Total experimental size: Hhip+/+ n=6, Hhip$^{flox/flox}$ n=7. P-values were determined by student's t test where * $p < .05$, ** $p < .01$.

TECs in both Hhip$^{+/+}$ and Hhip$^{flox/flox}$ mice displayed comparable MHC-I and MHC-II expression (6.15A, 6.15B). Spontaneous proliferation of these cells as determined by Ki67 expression was also comparable (6.15C).

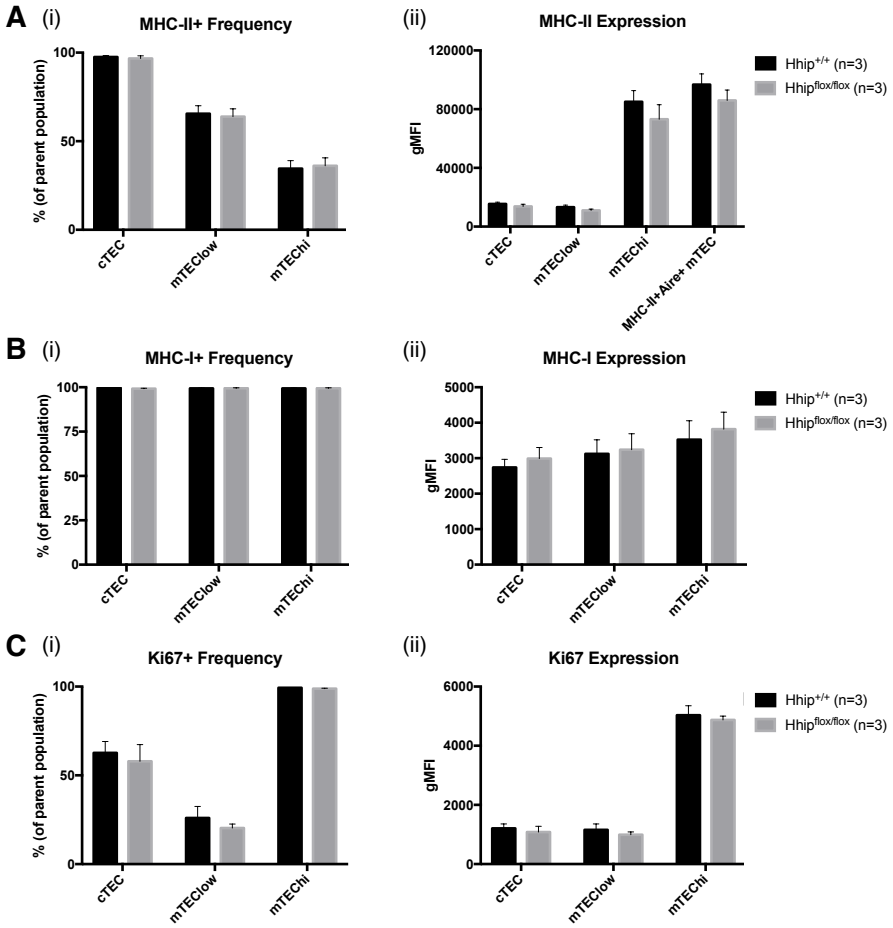

Figure 6.15: MHC and Ki67 expression are not altered in Hhip$^{flox/flox}$ TECs
(A) MHC-II and **(B)** MHC-I positive TEC subpopulation (i) frequencies in 4 week old Hhip$^{flox/flox}$ and Hhip$^{+/+}$ thymi, as well as (ii) expression levels. **(C)** (i) Ki67+ frequencies and (ii) expression. Graphs shown are from a single experiment and are representative of 2 independent experiments. Significance was evaluated by student's t test.

The altered TEC ratios in Hhip$^{flox/flox}$ mice recapitulate the results observed in conventional *hhip*-deficient mice, both at birth and after transplantation under the kidney capsule of healthy adult mice (5.1C, 5.2B, 5.11C). Hence, these results show unequivocally that the loss of Hhip expression in TECs accounted cell-autonomously for this alteration in TEC differentiation, although other stromal cells in the thymic microenvironment may still express this inhibitor. The MHC-II expression pattern did not correspond to the previous findings in embryonic and neonatal constitutive Hhip-/- thymi (4.8D, 5.1D, 5.2C). However, Hhip-/- thymi transplanted under the kidney capsule of adult WT hosts did not display differences in MHC-II cell surface expression either. Hence, differences in MHC expression

may effect changes that are only present in fetal development and early life. This notion will be verified in further experiments using neonatal Hhip$^{flox/flox}$ mice.

6.5.2 Normal thymocyte frequencies are observed in Hhip$^{flox/flox}$ mice

The impact of a lack of Hhip expression in TECs on their competence to support normal T cell development was investigated. Hhip$^{flox/flox}$ and Hhip$^{+/+}$ mice at 4 weeks of age displayed identical frequencies for each T cell subpopulation, defined by the differential expression of CD44, CD25, CD4 and CD8 (6.16A, 6.16B). Progression of DN cells through early developmental stages was comparable for both genotypes (6.16A, 6.16C). At the DP stage of development, the acquisition of high cell surface expression of both TCRβ and CD5 was mildly reduced (10.5 ± 0.1% vs 11.7 ± 0.2%) (6.16D). This could indicate a partial deficiency in the positive selection of thymocytes under these conditions where cTECs do not express Hhip.

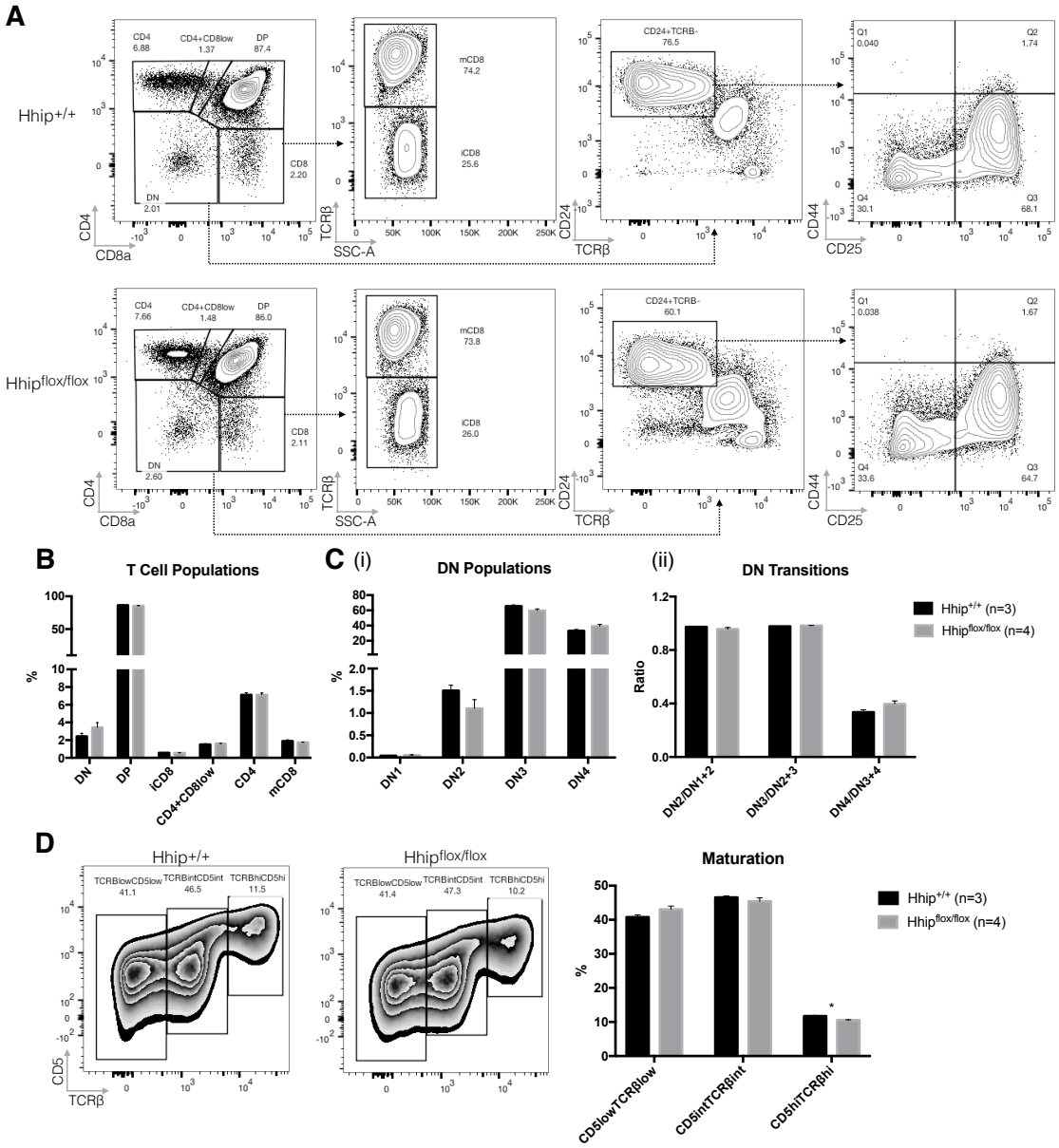

Figure 6.16: The Hhip$^{flox/flox}$ TEC environment supports thymocyte development but not proper maturation
(A) Representative FACS plots show from left to right the thymocyte profile, CD8 maturity based on TCRβ expression, DN gating on CD24+TCRβ- cells, and the different DN developmental stages in Hhip+/+ and Hhip$^{flox/flox}$ 4 week old mice. **(B)** Individual thymocyte subpopulations. **(C)** (i) Frequencies of cells in different DN stages. (ii) Ability of DN cells to transit between different stages, calculated by taking the frequency of cells in the stage of interest divided by the total frequency of cells in that stage and the preceding e.g DN2/DN1+DN2. **(D)** Maturation as assessed by CD5 and TCRβ expression. Graphs are from a single experiment, where at least 3 independent experiments were conducted. P-values were calculated by student's t test where * $p < .05$.

The single positive CD4 compartment was assessed for any phenotypic differences. The maturational progression of thymocytes expressing CD4 was examined using the cell surface expression of CD69 and CD24. Identical frequencies of the different subpopulations were observed for both genotypes (6.17A, 6.17B). Similarly, the frequencies of T_{reg} cells resident in the thymus were

comparable, including the CD103^{+}ICOS^{+} T_{reg} subpopulation that has recirculated back to the thymus from the periphery (6.17A, 6.17C, 6.17D).

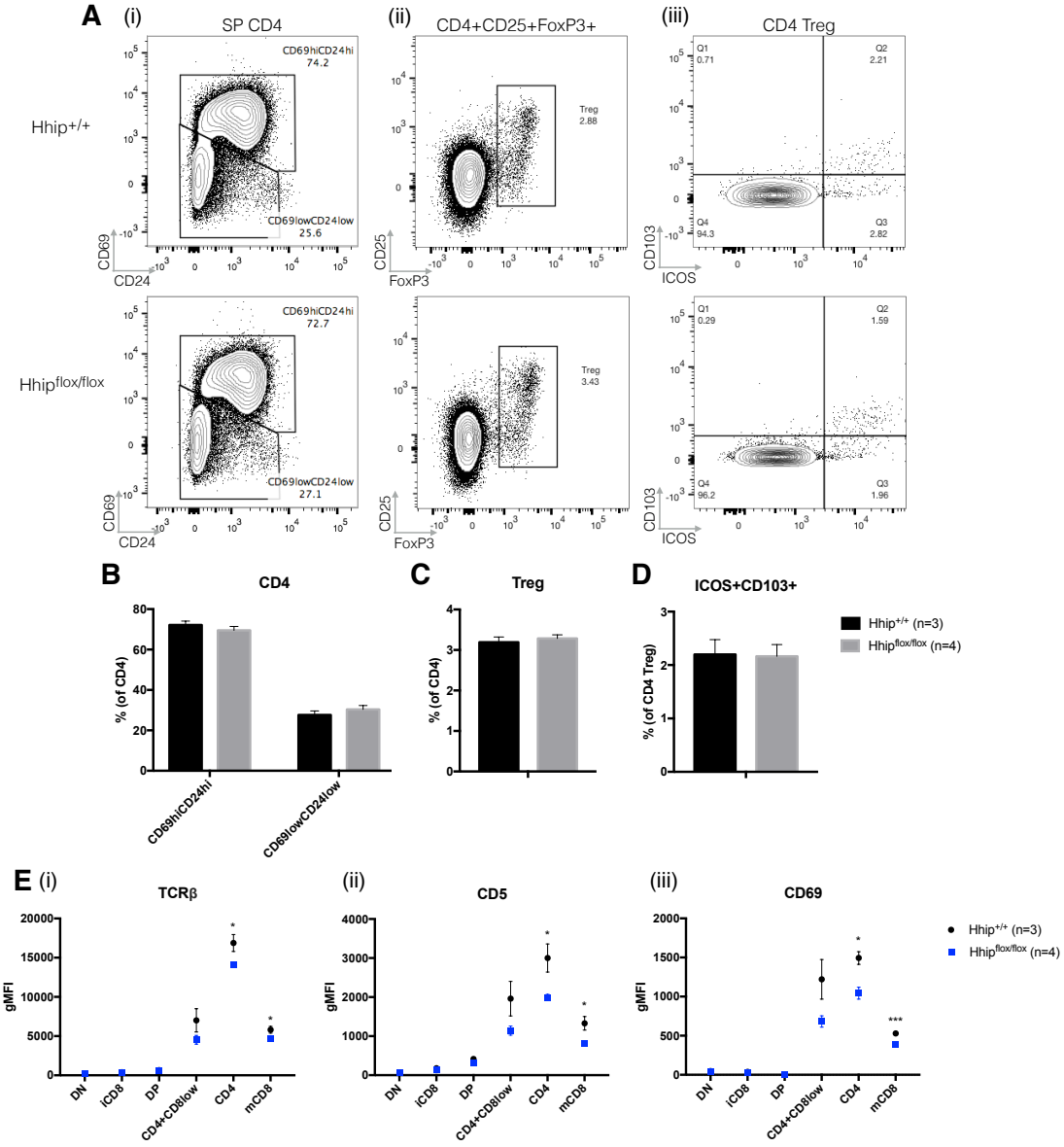

Figure 6.17: Thymocytes developing in the Hhip$^{flox/flox}$ thymus have altered expression of markers
(A) Representative FACS plots show (i) the CD69 and CD24 expression within the SP CD4 compartment, (ii) gating of Treg based on CD25 and FoxP3 expression and (iii) ICOS+CD103+ recirculating Tregs in the thymi of Hhip+/+ and Hhip$^{flox/flox}$ 4 week old mice. **(B)** SP CD4, **(C)** Treg and **(D)** ICOS+CD103+ Treg frequencies. **(E)** (i) Expression of (i) TCRβ, (ii) CD5 and (iii) CD69 in individual thymocyte subpopulations. P-values were calculated by student's t test where * $p < .05$, ** $p < .01$, *** $p < 0.001$. Graphs are from a single experiment, where at least 3 independent experiments were conducted.

Selection and consequent upregulation of TCRβ, CD5 and CD69 were, however, reduced in Hhip$^{flox/flox}$ thymi as compared to Hhip$^{+/+}$ (6.17E). This phenotype mirrored the results obtained from transplanted E18.5 Hhip-/- grafts under the

kidney capsule seeded with WT thymocyte progenitors, and highlighted that a loss of *hhip* expression allowed cells with a reduced TCR affinity to be selected.

6.5.3 Thymocyte selection in Hhip$^{flox/flox}$ mice is non-lineage specific

The ability of thymocyte selection to proceed normally in the absence of *hhip* expression in TECs was assessed. The cell surface expression of CCR7, CD69, Qa2 and MHC-I was used to identify the separate, sequential stages of thymocyte selection (6.18A). The CCR7^{-}CD69^{-}Qa2^{-}MHC-I^{-} phenotype, which represents a pre-selection stage, was reduced in Hhip$^{flox/flox}$ animals, while the most mature post-selection population (CCR7^{+}CD69^{-}Qa2^{hi}MHC-I^{hi}) was overrepresented in the Hhip$^{flox/flox}$ mice in comparison to Hhip$^{+/+}$ (6.18B). More DP cells had an immature CCR7^{-}CD69^{-}MHC-I^{-} phenotype in Hhip$^{flox/flox}$ mice, but a comparable frequency of DP cells were poised to undergo positive selection (CCR7^{-}CD69^{-}Qa2^{low}MHC-I^{low}) (6.18C, 6.18D). Most single positive CD4 cells in the cortex that had survived the process of positive selection (CCR7^{-}CD69^{+}Qa2^{low}MHC-I^{low}) had a CD69^{hi}CD24^{hi} phenotype as expected given engagement of their TCR, and were not significantly different between genotypes. After positive selection, some CD4 cells began to mature and lose expression of CD69 and CD24, and may be distinguished with a CD69^{low}CD24^{low} phenotype. In the last stage after selection (CCR7^{+}CD69^{-} Qa2^{hi}MHC-I^{hi}), there were reduced frequencies of CD69^{low}CD24^{hi} CD4 cells but an increased percentage with a CD69^{low}CD24^{low} phenotype in the Hhip$^{flox/flox}$ thymus, implying that more CD4 cells had matured and downregulated CD24 in the absence of Hhip-expressing TECs (6.18D).

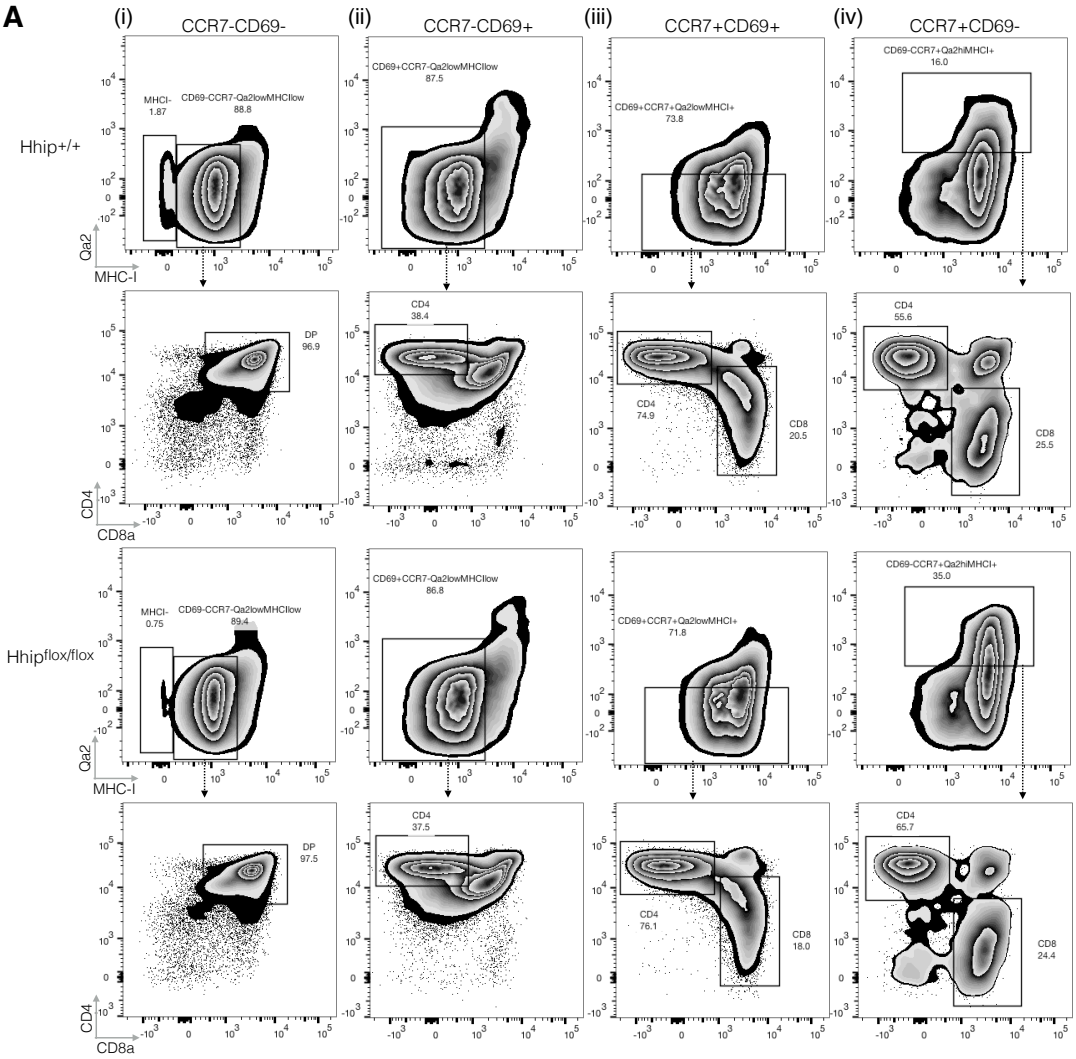

Figure 6.18: Stages of positive selection in Hhip$^{flox/flox}$

(A) Total live Lin- single T cells from 4 week old Hhip$^{+/+}$ and Hhip$^{flox/flox}$ mice are divided into positive selection stages based on CCR7 and CD69 expression, then further divided by Qa2 and MHC-I as (i) CCR7-CD69-Qa2lowMHC-I- and CCR7-CD69-Qa2lowMHC-Ilow, (ii) CCR7-CD69+Qa2lowMHC-Ilow, (iii) CCR7+CD69+Qa2lowMHC-I+ and (iv) CCR7+CD69-Qa2hiMHC-I+, and the thymocyte distribution by CD4 and CD8a expression shown below.

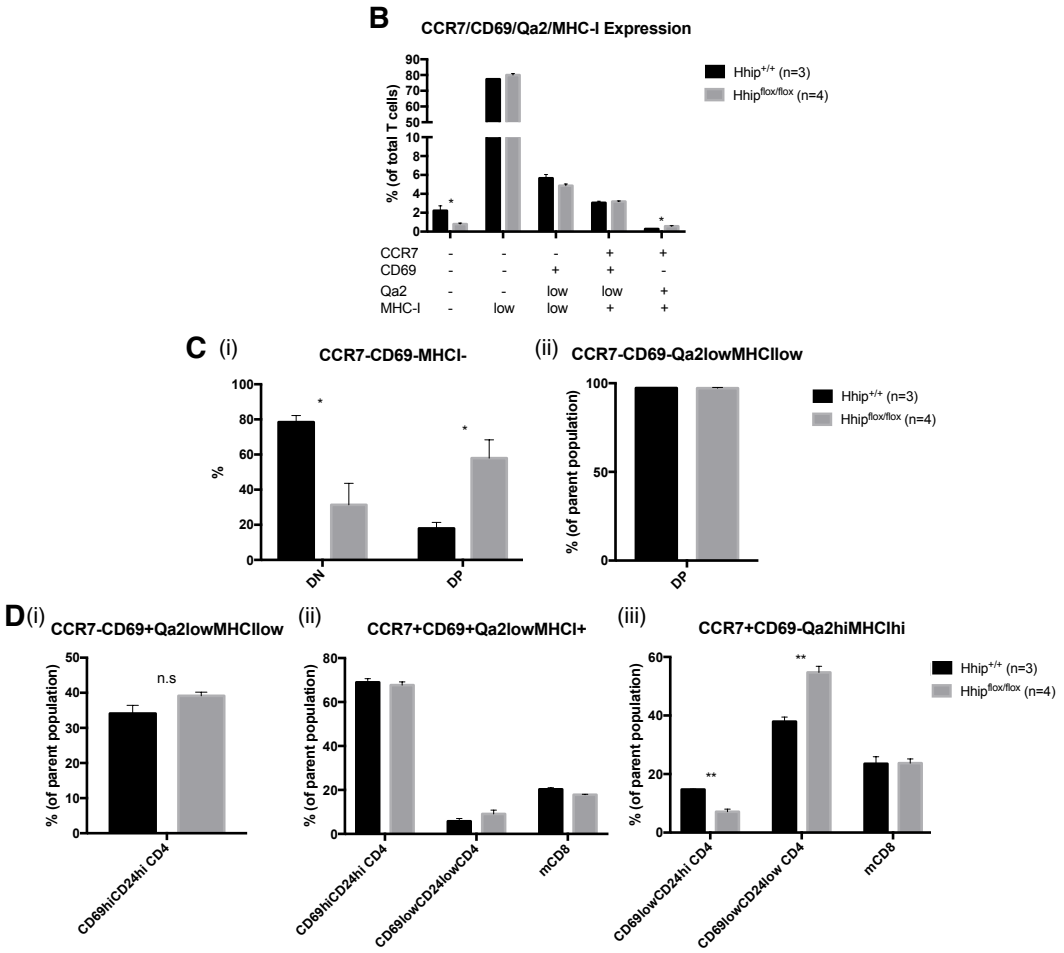

Figure 6.18: Stages of positive selection in Hhip$^{flox/flox}$
(continuation) **(B)** Frequencies of cells in each selection stage as defined in (A). **(C)** Relative frequencies of thymocytes pre-positive selection including a (i) seeming MHC-I- population and (ii) MHC-IIow. **(D)** (i) Cortical positive selection stage. (ii) First medullary positive selection stage. (iii) Final mature post-positive selection stage. P-values were calculated by student's t test where * $p < .05$, ** $p < .01$. Graphs are from a single experiment, where at least 3 independent experiments were conducted.

All nucleated cells should express MHC-I. The CCR7$^-$CD69$^-$Qa2$^-$MHC-I$^-$ compartment thus likely comprises extremely immature cells so early in development that they have yet to upregulate MHC-I to detectable levels, and may not be relevant for analysis. Frequencies of CCR7$^-$CD69$^+$Qa2^{low}MHC-I^{low} and CCR7$^+$CD69$^+$Qa2^{low}MHC-I$^+$ thymocytes did not differ between Hhip$^{flox/flox}$ and Hhip$^{+/+}$ mice, suggesting that a loss of *hhip* expression does not affect the antigen-presenting capacity of cortical and medullary TECs. However, CD4 cells in the Hhip$^{flox/flox}$ thymus present a more mature phenotype once they survive positive selection. The increased mature fraction is consistent with that seen in the

conventional Hhip-/- thymus transplant experiment (5.14B). The increased frequency of CD4 cells with a $CD69^{low}CD24^{low}$ phenotype is also in keeping with the notion that positive selection by Hhip-deficient TECs may favour CD4 thymocyte selection.

The continued maturation of CD4 lineage cells after positive selection had been initiated was assessed. Fewer $TCR\beta^{+}$ thymocytes were noted in $Hhip^{flox/flox}$ mice (6.19A). However, there were more $TCR\beta^{+}$ CD4 cells as compared to $Hhip^{+/+}$ animals, whereas the frequency of mature CD8 cells was unaffected (6.19B), which could imply that more DP cells had progressed to the CD4 lineage. $TCR\beta^{+}$ CD4 cells were divided into maturational stages as detailed previously (5.15B, 6.19C). An increased frequency of CD4 cells successfully survived positive selection and progressed to the final maturational stage ($CD69^{low}CD24^{low}Qa2^{hi}$) in $Hhip^{flox/flox}$ mice (6.19D, 6.19E). Correspondingly, there were less immature $CD24^{hi}CD69^{hi}$ CD4 cells (6.19F). However, CD5 cell surface expression levels were reduced in mature CD4 cells that had completed positive selection (6.19G). Taken together, this data suggests that Hhip-deficient thymocyte selection allows more CD4 cells to survive and mature, but with a TCR signalling ability or affinity that is altered.

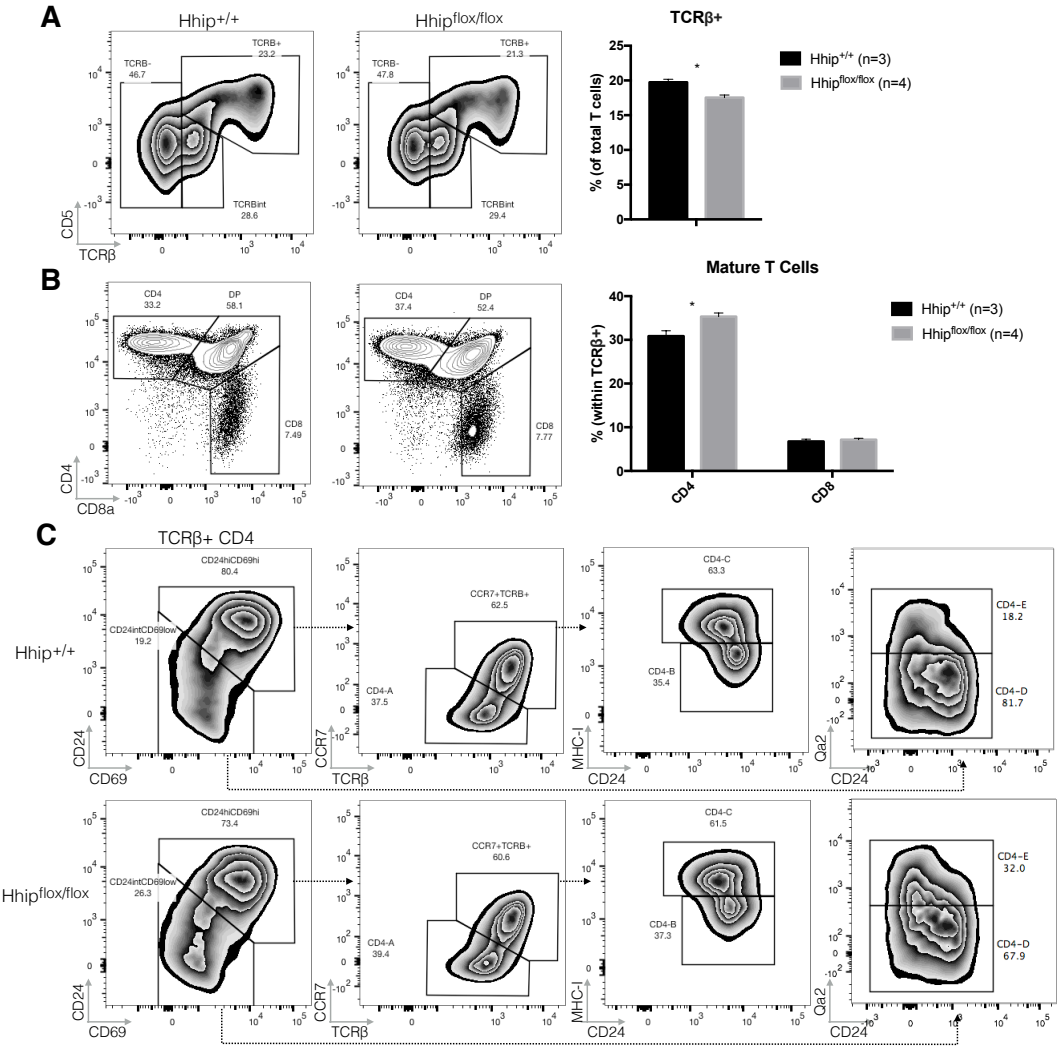

Figure 6.19: Positive selection of the CD4 lineage is altered in Hhip$^{flox/flox}$ mice
(A) Total Lin- single T cells of 4 week old mice are gated on CD5 and TCRβ expression. **(B)** TCRβ+ CD4 and CD8 thymocytes. **(C)** Gating strategy shows positive selection of the TCRβ+ CD4 population, divided by CD24, CD69, CCR7, TCRB, Qa2 and MHC-I expression.

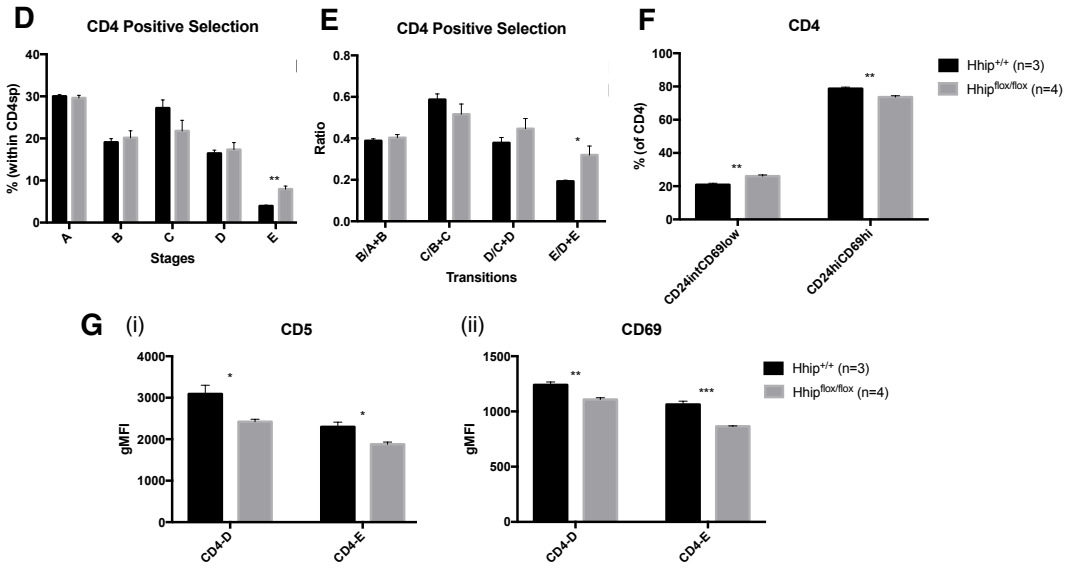

Figure 6.19: Positive selection of the CD4 lineage is altered in Hhip$^{flox/flox}$ mice
(continuation) **(D)** Frequency of cells in each stage of positive selection. **(E)** Transitions of cells between each selection stage. **(F)** Frequencies of immature and mature single positive CD4 cells, based on CD69 and CD24 expression. **(G)** CD5 and CD69 expression on cells in CD4 selection stages D and E. P-values were calculated by student's t test where * p < .05, ** p < .01. Graphs are from a single experiment, where at least 3 independent experiments were conducted.

Similar to the assessment of CD4 T cells, the CD8 lineage was probed for the efficiency by which they mature (5.16A, 6.20A). An increased frequency of mature cells successfully progressed to the final post-positive selection stage ($CD69^{low}CD24^{low}Qa2^{hi}$) (6.20B, 6.20C). Within the total $TCR\beta^{+}$ CD8 population, more $CD24^{low}CD69^{low}$ cells were found in $Hhip^{flox/flox}$ mice, which are considered phenotypically mature (6.20D). Overall, this indicates that $Hhip^{flox/flox}$ positive selection results in the generation of CD4 and CD8 single positive cells with a more mature phenotype as compared to $Hhip^{+/+}$.

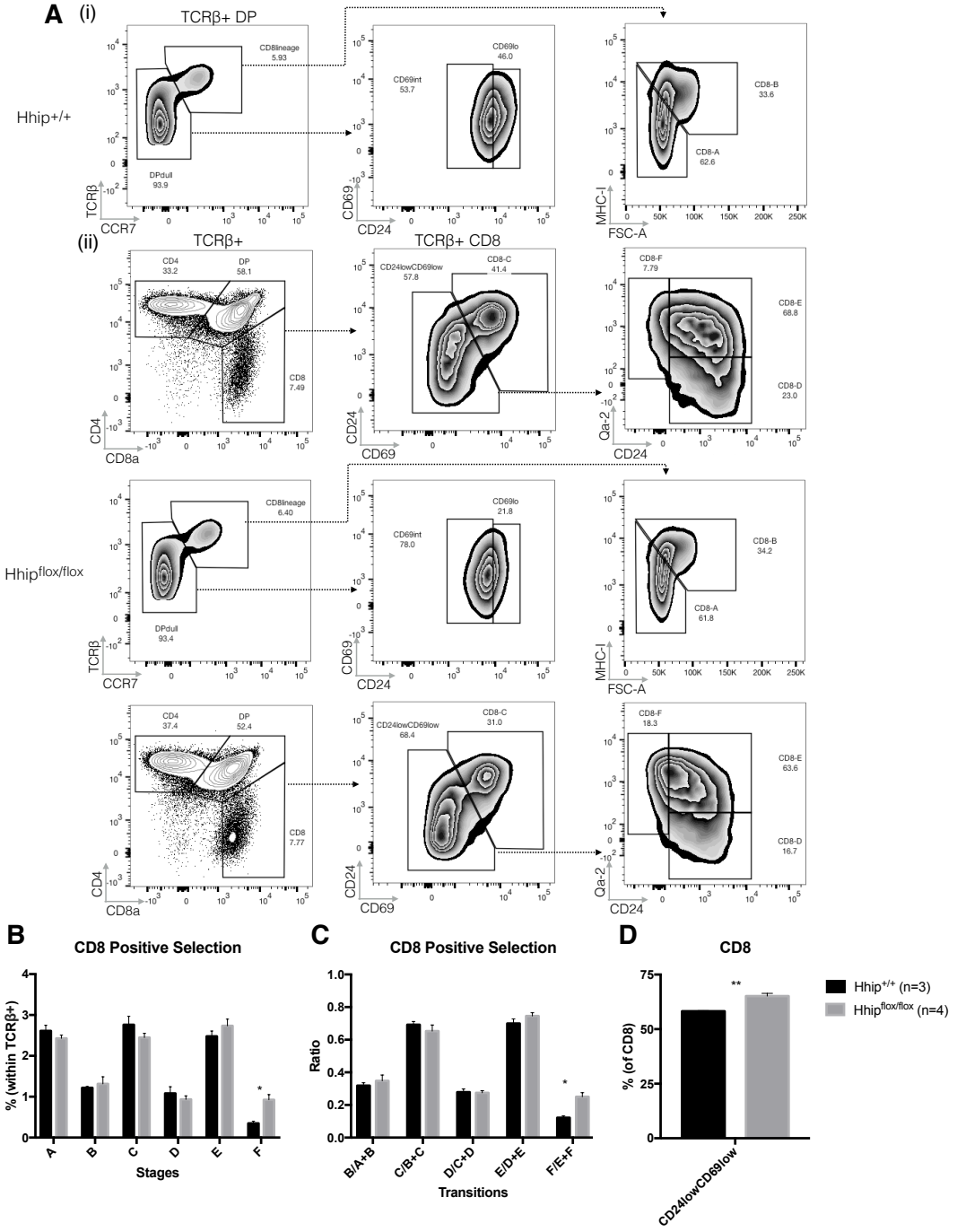

Figure 6.20: Positive selection of the CD8 lineage is altered in Hhip$^{flox/flox}$ mice
(A) CD8 committed cells from 4 week old Hhip$^{+/+}$ and Hhip$^{flox/flox}$ mice are divided into positive selection stages A-F, with early stages from (i) TCRβ+ DP, and late stages from (ii) TCRβ+ CD8 populations. **(B)** Frequencies of cells in each stage of positive selection. **(C)** Transitions of cells through each stage of selection. **(D)** Frequency of mature CD24lowCD69low CD8 cells. P-values were calculated by student's t test where * $p < .05$, ** $p < .01$. Graphs are representative of at least 3 independent experiments.

Taken together, this data analysing single positive T cell maturation demonstrates that *hhip*-deficient TECs are unable to perform positive selection in a manner comparable to normal WT TECs, corroborating with the previous findings in constitutive *hhip*-deficient mice. The results also highlighted for Hhip$^{flox/flox}$ mice a

CD4/CD8 lineage-independent change in the efficiency of selection. However, only CD4 cells presented with altered cell surface expression of markers such as CD5. This may indicate a specific additional maturational delay in the CD4 lineage, which was already observed in the conventional *hhip*-deficient mice. Changes in the expression of these specific markers were thus also monitored during the analysis of negative thymocyte selection as CD5 reflects TCR signal strength, which defines which T cells are negatively selected and directed to a T_{eff} or T_{reg} fate.

6.5.4 Hhip$^{flox/flox}$ negative selection allows T cells with lower TCR signal strength to survive

Positive selection is impaired in the Hhip$^{flox/flox}$ mouse, allowing more T cells to survive and continue with their differentiation. Yet, the overall proportion of mature (TCRβ^{hi}CD5^{hi}) thymocytes in Hhip$^{flox/flox}$ mice is reduced. Two possibilities that could explain this finding include that mature T cells in Hhip$^{flox/flox}$ exit the thymus with a greater efficiency, or that Hhip$^{flox/flox}$ TECs are more efficient in reducing cells with a mature phenotype. If the latter is indeed the case, negative selection could be one such mechanism as it effectively eliminates T cells that interact with pMHC complexes with an inappropriate level of affinity. Negative selection in Hhip$^{flox/flox}$ mice was therefore analysed, detailing the frequencies of distinct thymocyte subpopulations based on their CCR7 and CD24 phenotype (6.21A). There were more thymocytes in the medulla (CCR7^{+}CD24^{+}) of Hhip$^{flox/flox}$ mice when compared to Hhip$^{+/+}$ animals (6.21B), although the frequency of cells that had been negatively selected, as defined by Helios expression, was similar for both groups of animals. Thymocytes that had adopted a mature phenotype and thus had successfully survived negative selection expressed lower levels of CD5 (6.21C).

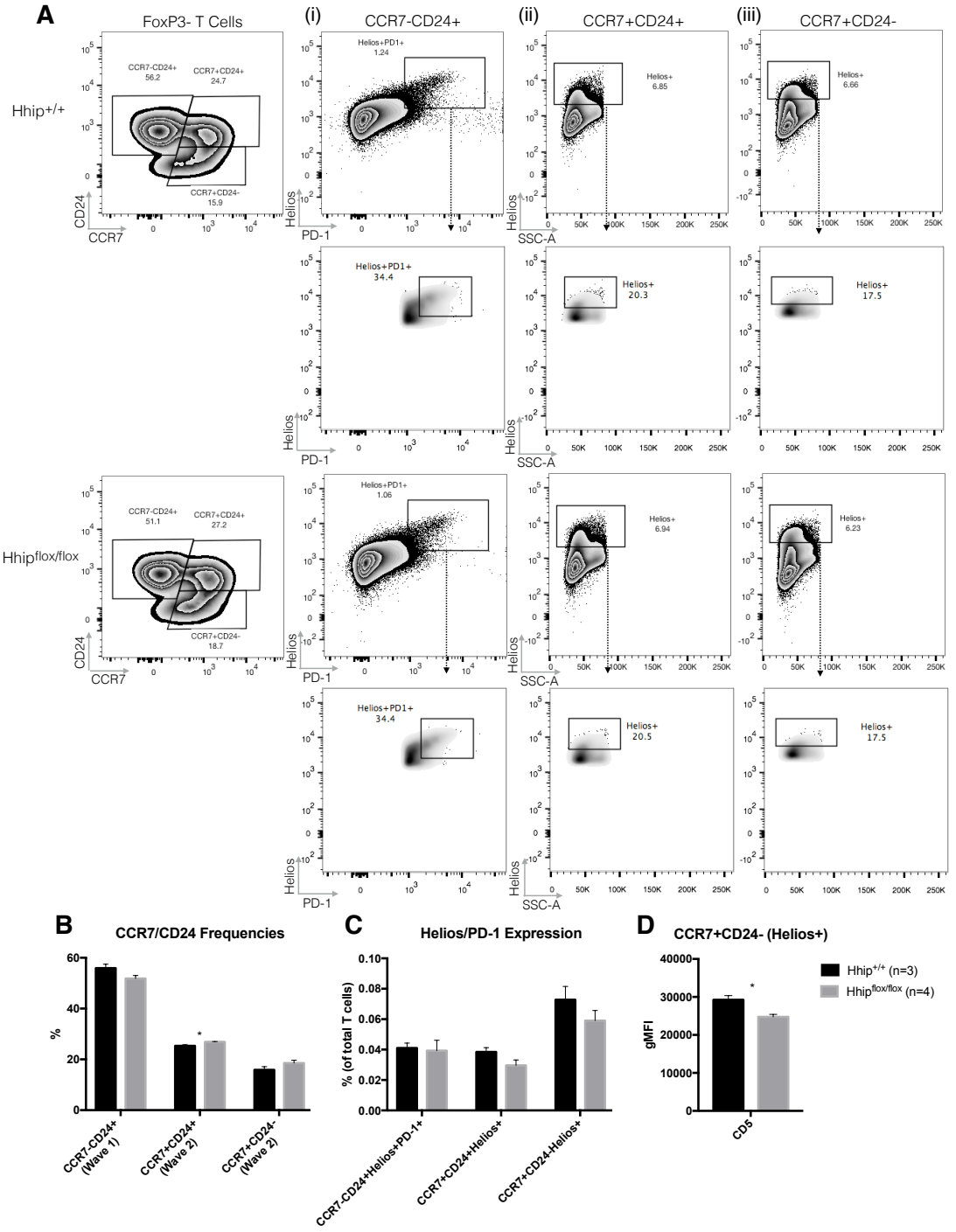

Figure 6.21: Overall negative selection is altered in Hhip$^{flox/flox}$ mice

(A) Representative FACS plots show gating of total FoxP3- single T cells from 4 week old Hhip+/+ and Hhip$^{flox/flox}$ mice into negative selection stages defined as (i) CCR7-CD24+, (ii) CCR7+CD24+ and (iii) CCR7+CD24-. Helios and PD-1 expression are first "pre-gated" using a zebra plot, and the positive population is further visualised using a density plot to gate only highly expressing cells. **(B)** Frequencies of cells in each stage. **(C)** Frequencies of cells being negatively selected in each stage. **(D)** CD5 expression on the CCR7+CD24-Helios+ fraction. P-values were calculated by student's t test where * $p < .05$. Graphs are representative of at least 3 independent experiments.

CD4 and CD8 negative selection in the medulla were assessed separately to determine if there were any lineage-specific effects. Frequencies of mature CD4 and CD8 cells undergoing negative selection in Hhip$^{flox/flox}$ animals were reduced

(6.22A, 6.22B), and cell surface expression of CD5 was diminished on mature cells of both lineages (6.22C). However, within the populations of Helios^{+} cells undergoing negative selection, CD5 expression was equivalent between genotypes, although CD69^{low} CD4 cells expressed lower levels of TCRβ (6.22D).

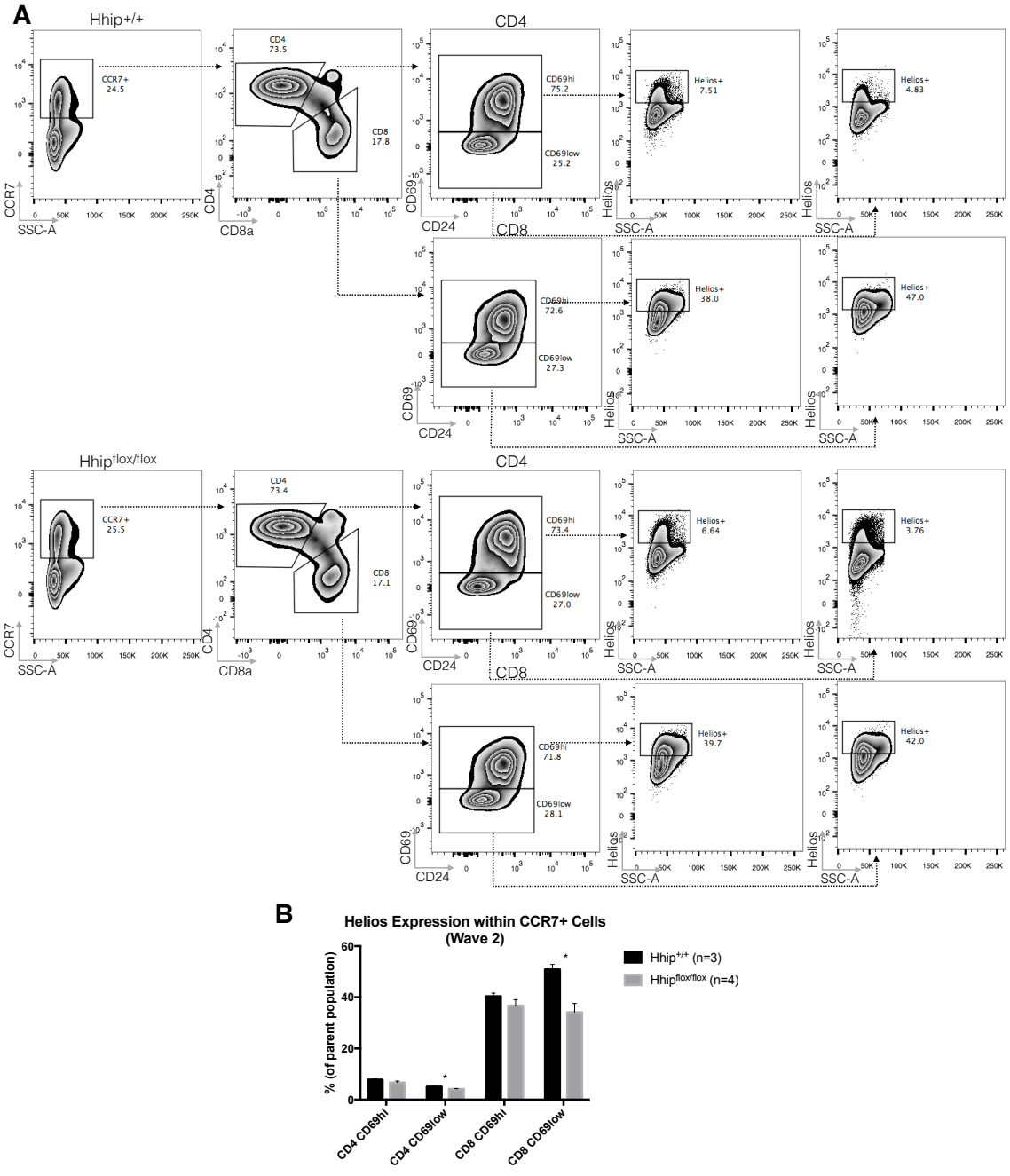

Figure 6.22: T cells with reduced TCR affinity have survived negative selection in Hhip$^{flox/flox}$ mice
(A) FoxP3- TCRβ+ cells from 4 week old Hhip$^{+/+}$ and Hhip$^{flox/flox}$ mice are gated on CCR7-positivity, then differentiated into CD4 and CD8 cells. Each lineage is gated on CD69 expression, and negatively selected cells are defined by Helios expression. The Helios+ gate for the CD8 lineage was gated with reference to the CD4 CD69hi population. **(B)** Helios-expressing cells as a percentage of the parent population of interest, e.g CD4 CD69hi cells.

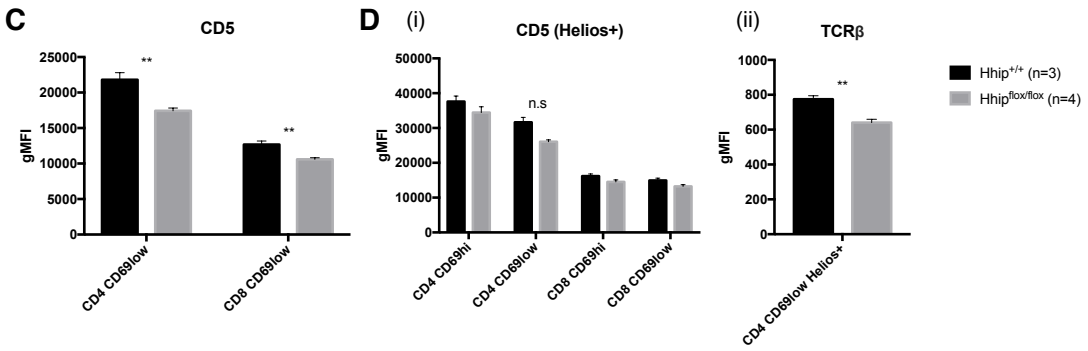

Figure 6.22: T cells with reduced TCR affinity have survived negative selection in Hhip$^{flox/flox}$ mice
(continuation) **(C)** Expression of CD5 in mature CD69low cells. **(D)** Expression of (i) CD5 and (ii) TCRβ on Helios+ cells. P-values were determined by student's t test where * p < .05, ** p < .01. FACS plots and statistics are representative of 2 independent experiments.

The increased numbers of mature T cells which survived positive selection could result in a larger proportion of cells subsequently having to undergo negative selection, evidenced by the increased frequencies of CCR7^{+}CD24^{+} T cells (6.21B). However, fewer mature Hhip$^{flox/flox}$ cells were negatively selected in the medulla (6.22B). Consequently, negative selection did not compensate for the increased frequencies of T cells generated post-positive selection by eliminating a larger proportion of these cells. Instead, the Hhip$^{flox/flox}$ negative selection machinery allowed more mature cells to survive, which could suggest a defect where Hhip$^{flox/flox}$ mTECs were unable to interact with a regular frequency of thymocytes. This is unlikely given that the frequencies of immature CD69^{hi} cells undergoing negative selection were comparable between Hhip$^{flox/flox}$ and Hhip$^{+/+}$ genotypes. Given that single positive T cells in the Hhip$^{flox/flox}$ thymus likely had a reduced TCR affinity as observed during the analysis of positive selection, it is possible that negative selection was unaffected by the absence of *hhip* expression, effecting the regular elimination of T cells with high TCR affinity, such that Hhip$^{flox/flox}$ T cells with reduced expression of TCRβ and CD5 cell surface molecules and likely lower TCR signal strength were thus able to escape negative selection and survive. This hypothesis is supported by the observation that Hhip$^{flox/flox}$ mTECs were able to

identify and target for negative selection a range of T cells with TCR signal strength comparable to those selected by $Hhip^{+/+}$ mTECs, as represented by CD5 cell surface levels. These results therefore support the concept that the absence of Hhip in TECs impairs positive but not negative selection.

6.6 Neonatal $Hhip^{flox/flox}$ TECs display normal MHC expression

Both a constitutive and a TEC-exclusive deficiency of *hhip* expression alter the frequencies of TECs and positive selection. However, neonatal constitutively *hhip*-deficient mice displayed changes in MHC-II cell surface expression, as well as a partial developmental block in the CD4 lineage. To probe whether said phenotypic changes were age-related or alternatively due to a constitutive lack of *hhip* expression in all cell types, neonatal $Hhip^{flox/flox}$ mice were analysed.

The ratio of cTECs to mTECs was changed in $Hhip^{flox/flox}$ neonates ($Hhip^{+/+}$ cTEC 54.0 ± 5.0%, $Hhip^{flox/flox}$ 33.5 ± 4.6%; $Hhip^{+/+}$ mTEC 43.1 ± 5.2%, $Hhip^{flox/flox}$ 64.6 ± 4.1%), a finding consistent with changes observed in the adult $Hhip^{flox/flox}$ mice as well as the conventional knockout mouse model (6.23A). However, frequencies of MHC-positive cells and cell surface expression levels of MHC were identical for $Hhip^{+/+}$ and $Hhip^{flox/flox}$ TECs (6.23B).

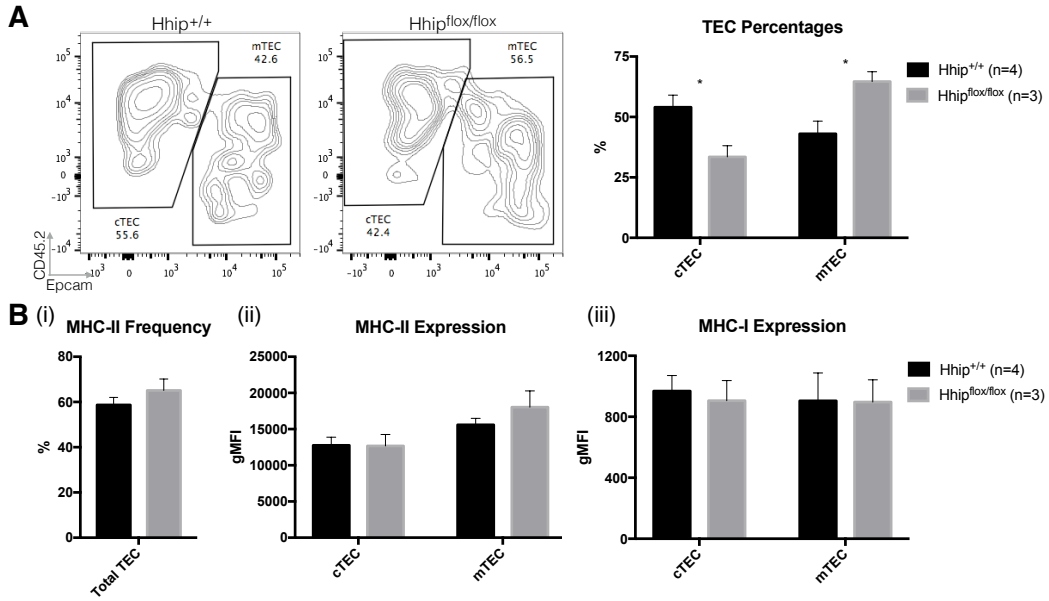

Figure 6.23: TEC lineage differentiation is altered in neonatal Hhip$^{flox/flox}$ mice
(A) cTEC and mTEC frequencies in the Hhip$^{flox/flox}$ neonate as compared to Hhip+/+. **(B)** (i) Frequencies and (ii) expression levels of MHC-II. (iii) MHC-I expression in cTECs and mTECs. Graphs are from a single experiment. At least 3 independent experiments were conducted. P-values were calculated by student's t test where * $p < .05$.

As MHC cell surface levels were unaffected in adult Hhip$^{flox/flox}$ TECs, a specific loss of *hhip* expression in TECs does not directly impact on MHC expression. A general loss of *hhip* expression and the ubiquitous addition of rShh or rHhip (as observed in FTOC experiments) appears to impact MHC expression on TECs, supporting that MHC expression is indirectly affected in TECs due to changes in Hh signalling occurring in or mediated by a different cell type. One potential option would be thymocytes, as changes in Hh signalling could affect their interactions with TECS and subsequently modify MHC levels via cell-cell crosstalk. Alternatively, changes in Hh signalling in neighbouring mesenchymal cells might affect TECs, a notion supported by the literature where impaired MHC-II expression in mice with a mesenchymal defect has been reported (Itoi, M. *et al.*, 2007). As the focus of this research was the role of *hhip* in the context of Foxn1 regulation i.e in TECs, *hhip* in other cell types were not investigated. Future work could focus on establishing a role for Hhip in thymus biology generated by cells other than TECs.

6.6.1 Neonatal Hhip$^{flox/flox}$ thymocytes are phenotypically less mature

T cell development was next analysed in neonatal Hhip$^{flox/flox}$ mice to probe whether CD4 maturation was partially blocked, as previously observed in conventional *hhip*-deficient neonates. Extensive phenotypic analysis did not uncover any significant differences between Hhip$^{flox/flox}$ and Hhip$^{+/+}$ mice for any of the individual T cell subpopulations (6.24A). Frequencies of individual DN stages were equivalent between genotypes (data not shown). The CD4 individual subpopulations defined by CD69 and CD24 expression were similar between Hhip$^{flox/flox}$ and Hhip$^{+/+}$ (6.24C). However, the proportion of CD5^{hi}TCRβ^{hi} thymocytes was reduced from 7.47 ± 0.9% in Hhip$^{+/+}$ thymi to 3.67 ± 1.1% in Hhip$^{flox/flox}$ mice (6.24B).

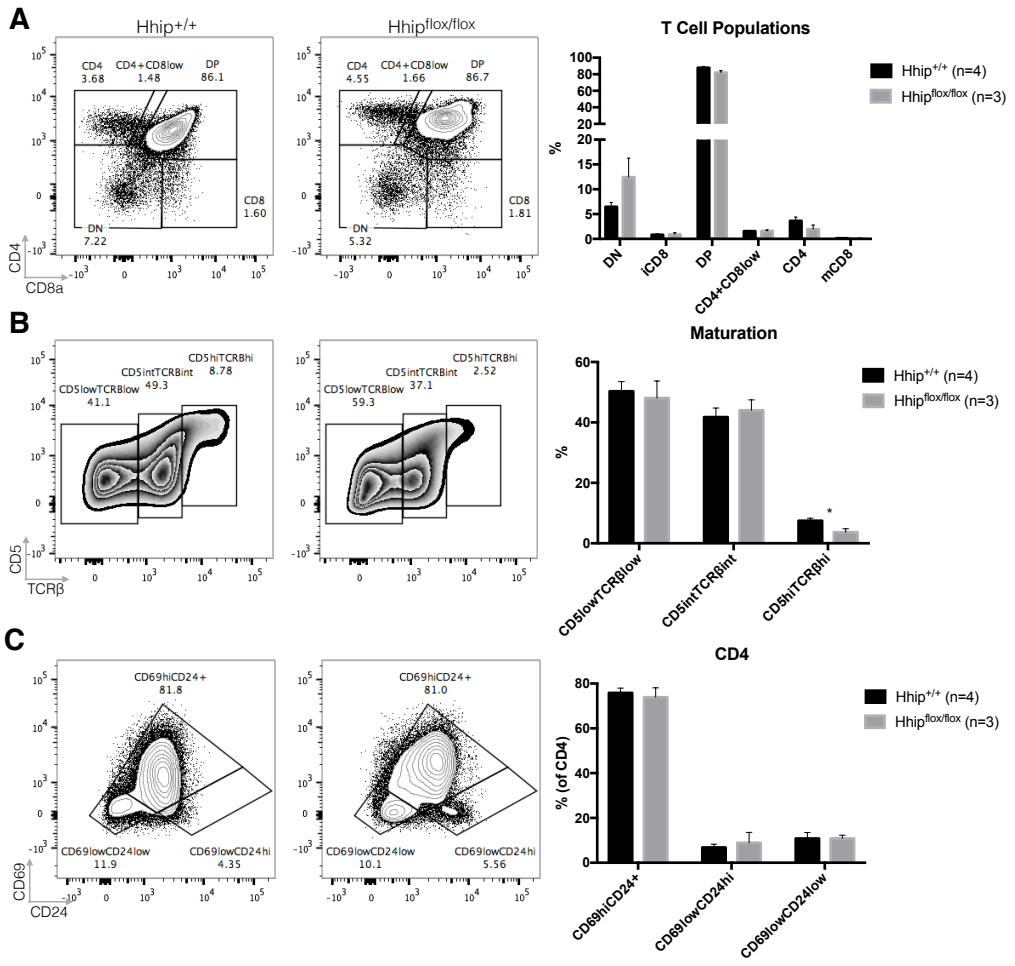

Figure 6.24: Thymocyte population frequencies are similar between neonatal Hhip$^{flox/flox}$ and Hhip$^{+/+}$ mice
(A) Individual thymocyte subpopulations in neonatal Hhip$^{flox/flox}$ and Hhip+/+ mice. **(B)** Maturation as assessed by CD5 and TCRβ expression. **(C)** Immature (CD69hiCD24+), semi-mature (CD69lowCD24hi) and mature (CD69lowCD24low) single positive CD4 frequencies. P-values were calculated by student's t test where * $p < .05$. Graphs are representative of 3 independent experiments.

CCR7 and CD69 expression were used to distinguish T cells with an immature pre-selection phenotype ($CCR7^{-}CD69^{-}$), cells undergoing positive selection in the cortex ($CCR7^{-}CD69^{+}$), and cells migrating to or already placed in the medulla ($CCR7^{+}CD69^{+}$) (6.25A). In neonates, the fraction of $CCR7^{+}CD69^{-}$ mature cells was very small as T cells at this developmental stage are nascent and have not yet been fully established, and thus was not further considered. The frequencies of total cells in each different selection stage were similar for $Hhip^{flox/flox}$ and $Hhip^{+/+}$ animals (6.25B). However, more $Hhip^{flox/flox}$ DN cells were present in the $CCR7^{-}CD69^{-}$ population, while fewer single positive CD4 thymocytes were present in both $CCR7^{-}CD69^{+}$ and $CCR7^{+}CD69^{+}$ fractions (6.25B), demonstrating a possible maturational delay.

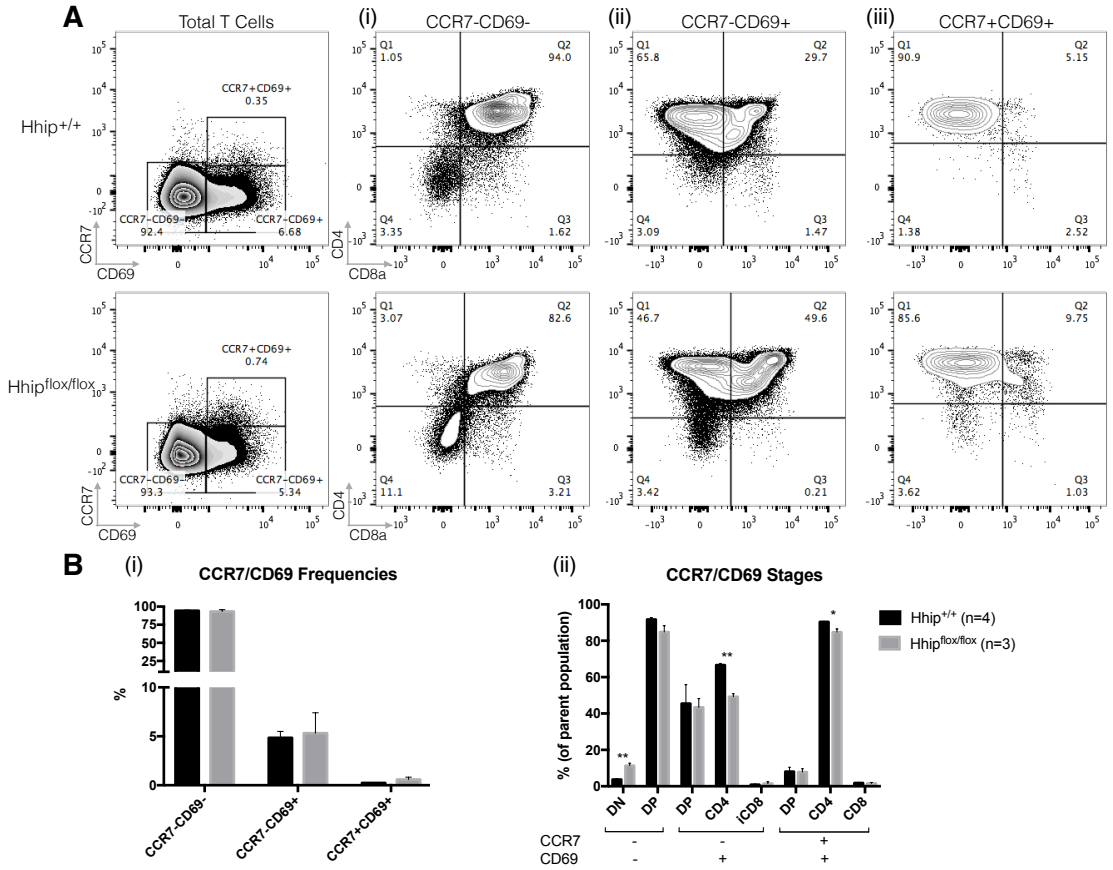

Figure 6.25: Maturation of neonatal $Hhip^{flox/flox}$ mice is impaired
(A) Total live Lin- single T cells in neonatal $Hhip^{flox/flox}$ and Hhip+/+ mice are divided into (i) CCR7-CD69-, (ii) CCR7-CD69+ and (iii) CCR7+CD69+ fractions. **(B)** Frequencies of cells in each CCR7/CD69 fraction. **(C)** Frequencies of individual thymocyte subpopulations, where the parent population refers to cells in each CCR7/CD69 fraction. P-values were calculated by student's t test where * $p < .05$, ** $p < .01$. Graphs are representative of 3 independent experiments.

Positive T cell selection was also analysed in neonatal $Hhip^{flox/flox}$ and $Hhip^{+/+}$ mice following changes in CD69 and TCRβ expression, as previously described (6.26A). Differences in frequencies of individual subpopulations were not observed (6.26B). However, fewer CD4 cells successfully progressed through selection to the $TCR\beta^{int}CD69^{+}$ stage in the $Hhip^{flox/flox}$ thymus as compared to $Hhip^{+/+}$, where thymocytes with this phenotype have engaged with pMHC complexes presented by TECs (6.26C). After selection, CD4 frequencies returned to levels comparable to that of $Hhip^{+/+}$ (6.26C).

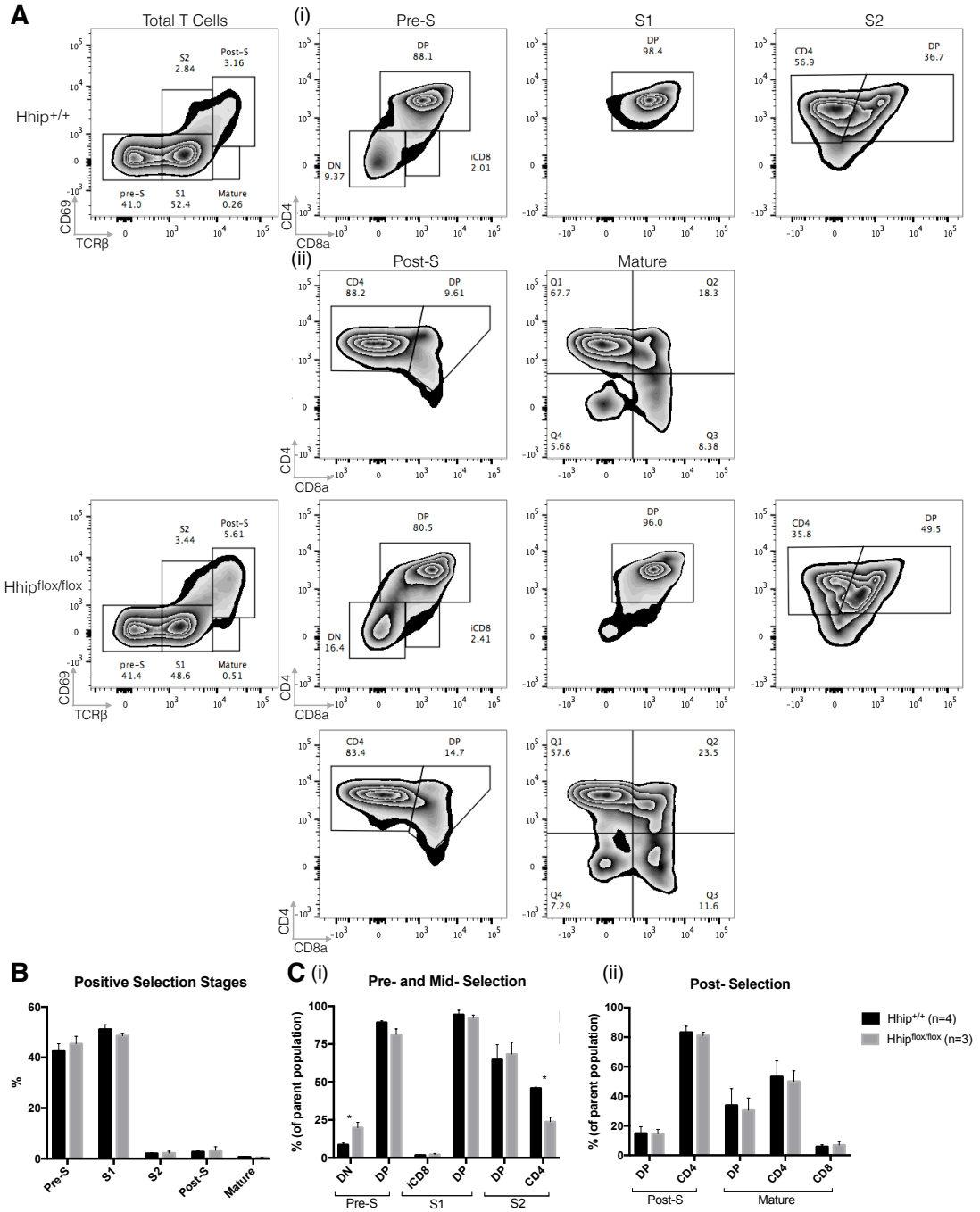

Figure 6.26: Selection of thymocytes occurs differentially between Hhip$^{flox/flox}$ and Hhip$^{+/+}$ neonates
(A) Total live Lin- single T cells in neonates are divided by TCRβ and CD69 expression into positive selection stages, including (i) pre-selection (TCRβ-CD69-), S1 (TCRβintCD69-) and S2 (TCRβintCD69+), followed by (ii) post-selection (CD69hiTCRβhi) and mature (CD69lowTCRβhi). **(B)** Frequencies of cells in each selection stage. **(C)** Thymocyte subpopulations in (i) pre- and mid- selection stages (Pre-S, S1 and S2), and (ii) post-selection (Post-S and Mature) stages, where the parent population refers to cells in each selection stage. P-values were calculated by student's t test where * $p < .05$. Graphs are representative of 3 independent experiments.

Positive selection is partially impaired in the neonatal Hhip$^{flox/flox}$ thymus as demonstrated by reduced frequencies of single positive CD4 thymocytes undergoing positive selection. However, it is unclear if this delay is lineage specific. While only CD4 cells are affected, in the young mouse, there are physiologically

very few single positive CD8 cells present in the thymi, with the majority of these being immature (0.833 ± 0.2% in $Hhip^{+/+}$). Hence, it is impossible to determine at this age whether CD8 lineage selection is also affected. This is supported by results from the 4 week old adult mouse, where selection in the $Hhip^{flox/flox}$ mouse was affected in both CD4 and CD8 lineages. As such, while an absence of genetic *hhip* expression in TECs impairs their ability to perform positive selection, the results from adult and neonatal mice together suggest that this defect is not likely to be lineage specific.

Defining the precise defect in positive selection caused by a loss of *hhip* expression is confounded by the contrasting phenotypes in neonatal and adult $Hhip^{flox/flox}$ mice. In the neonatal mouse, statistically significant changes are observed in thymocyte populations defined to be undergoing positive selection, suggesting that the positive selection machinery is less competent to perform selection in a manner or rate comparable to $Hhip^{+/+}$. In contrast, positive selection in $Hhip^{flox/flox}$ adult mice does not appear to be delayed, but rather allows more cells with an immature phenotype to survive positive selection. In the neonatal thymus, the total numbers of TECs are very low as the thymus is still developing and organogenesis not complete. Consequently, in the $Hhip^{flox/flox}$ neonatal thymus where there are significantly less cTECs than $Hhip^{+/+}$, there may simply be too few cTECs available for thymocytes to encounter, thus impacting the selection process, which would explain the partial positive selection defect observed. In contrast, the adult $Hhip^{flox/flox}$ thymus may still have sufficient absolute numbers of cTECs to effect positive selection as efficiently as $Hhip^{+/+}$ animals. It is now also evident that the reduced expression of TCRβ and CD5, which translated as a decreased fraction of

$CD5^{hi}TCR\beta^{hi}$ cells in *hhip*-deficient mice, is reflective of reduced TCR signal strength, but not delayed maturation per se.

Finally, a developmental impairment of the CD4 lineage had been observed inconsistently in various experiments. There are reports showing that Shh favours the production of CD8 cells, thus affecting the CD4/CD8 ratio, although the precise mechanism for this differential is unclear (Rowbotham, N. *et al*., 2007). Loss of *hhip* expression resulting in increased Shh signalling may thus negatively influence the normal maturation of CD4 cells, which may translate into altered expression levels of markers such as CD69. Thus, Hhip may be important to ensure the normal maturation of the CD4 lineage, although this defect seems relatively mild given that frequencies of CD4 cells produced in the thymus are comparable to WT frequencies at least when *hhip* is ablated only in TECs.

6.7 Fewer $Hhip^{flox/flox}$ T cells exit the thymus, but in normal proportions

Migration of thymocytes to the spleen was assessed to evaluate if defects in selection by TECs resulted in T cell defects sustained in the periphery. Absolute numbers of splenic B cells were equivalent between genotypes, whereas the absolute numbers of splenic T cells were reduced in $Hhip^{flox/flox}$ mice, similar to the reduced absolute numbers observed in the thymus (6.27A, 6.27B, 6.27C). The ratio of CD4 to CD8 cells was comparable to that in $Hhip^{+/+}$, as were the proportions of naïve, effector and memory cells in each lineage (6.27A, 6.27D). This suggests that the $Hhip^{flox/flox}$ thymus had a lower T cell output as compared to $Hhip^{+/+}$, but was able to generate different CD4 and CD8 T cell populations successfully.

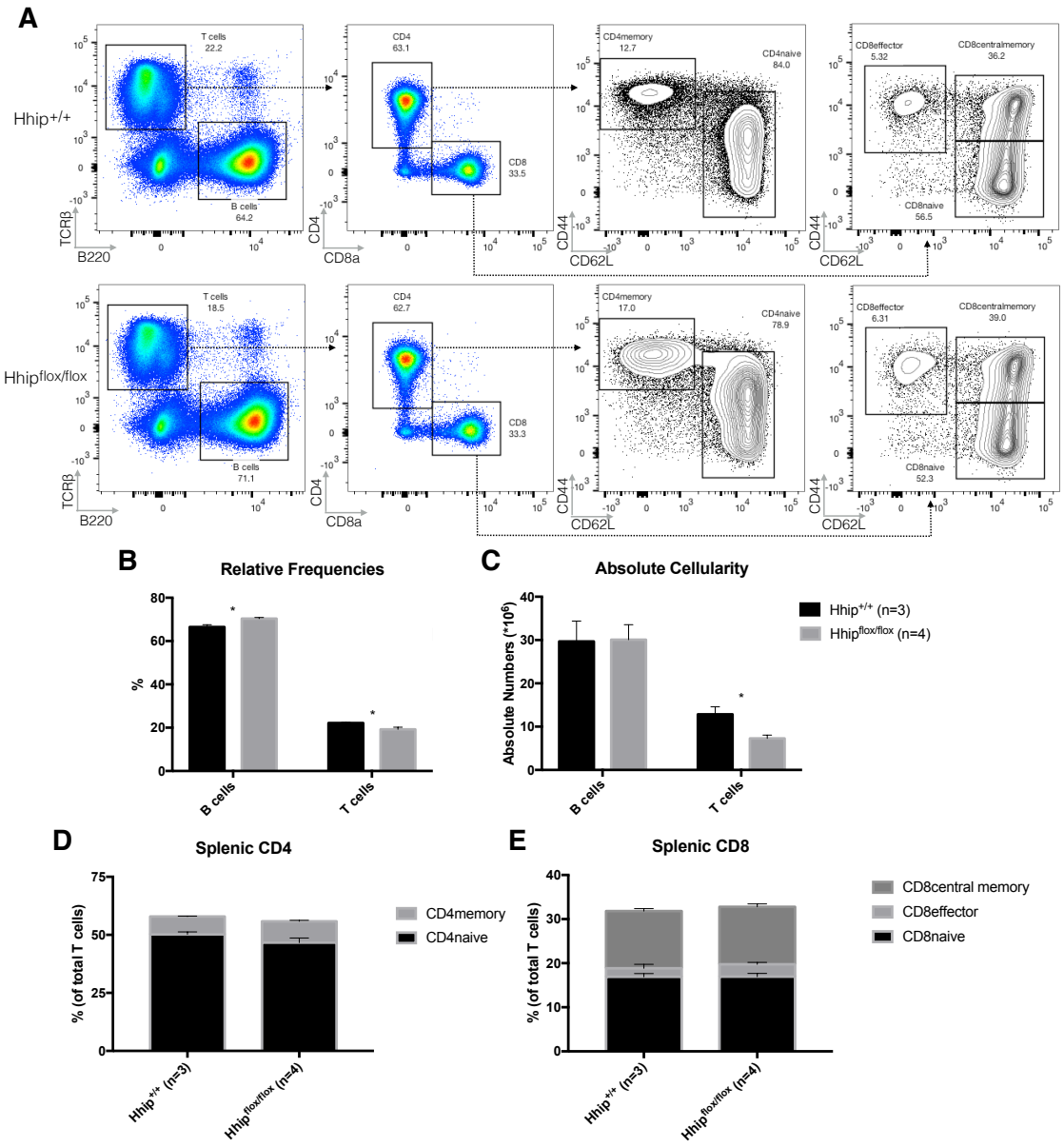

Figure 6.27: Fewer peripheral T cells in the Hhip$^{flox/flox}$ mouse

(A) Total single live splenic cells of 4 week old Hhip$^{flox/flox}$ and Hhip+/+ mice are separated into T and B cells by TCRβ and B220 expression respectively. T cells are then divided into CD4 and CD8, and effector, memory and naive populations distinguished by CD44 and CD62L expression. **(B)** Relative frequencies and **(C)** absolute numbers of B and T cells. Frequencies of naive, memory and effector **(D)** CD4 and **(E)** CD8 populations. P-values were calculated by student's t test where * $p < .05$. Graphs shown are from a single experiment and are representative of 2 independent experiments.

6.7.1 Hhip$^{flox/flox}$ CD4 naïve cells are less responsive to T cell stimulation

To investigate T cell responses to mitogenic stimuli, CD4 naïve T cells from the spleen and lymph nodes were activated *in vitro* with anti-CD3 and anti-CD28 antibodies (Frauwirth, K. & Thompson, C., 2002). Proliferation of these cells was quantified by the dilution of the membrane dye CFSE CellTrace, a well-retained dye that is diluted with each progressive cell division cycle. A consistent concentration

of anti-CD28 (1.0 µg/ml) was combined with increasing concentrations of immobilised anti-CD3 (0.1 to 5 µg/ml) and used to stimulate cells for 3 days in culture. At low anti-CD3 concentrations, such as 0.5 µg/ml, naïve CD4 $Hhip^{flox/flox}$ T cells proliferated as efficiently as their $Hhip^{+/+}$ counterparts (6.28A). At higher concentrations, such as 2.5 µg/ml, fewer $Hhip^{flox/flox}$ T cells responded to the mitogenic stimulus (21.6% vs 14.1%) (6.28A). Proliferation and expansion indices were calculated for all the different concentrations of anti-CD3 used. The former assesses the number of cell divisions elicited among responding cells, whereas the latter measures fold expansion of stimulated cells. Naïve $Hhip^{flox/flox}$ and $Hhip^{+/+}$ T cells demonstrated comparable proliferation and expansion at low levels of stimulation. In contrast, at higher stimulatory concentrations (>1.25 µg/ml), $Hhip^{flox/flox}$ cells were less able to respond to stimulation as compared to $Hhip^{+/+}$ T cells (6.28B). The differential responsiveness correlated with decreased expression of TCRβ and CD5 observed in $Hhip^{flox/flox}$ T cells in the thymus. Taken together, the loss of *hhip* expression in TECs therefore impaired the responsiveness of naïve CD4 T cells to TCR-mediated activation stimuli.

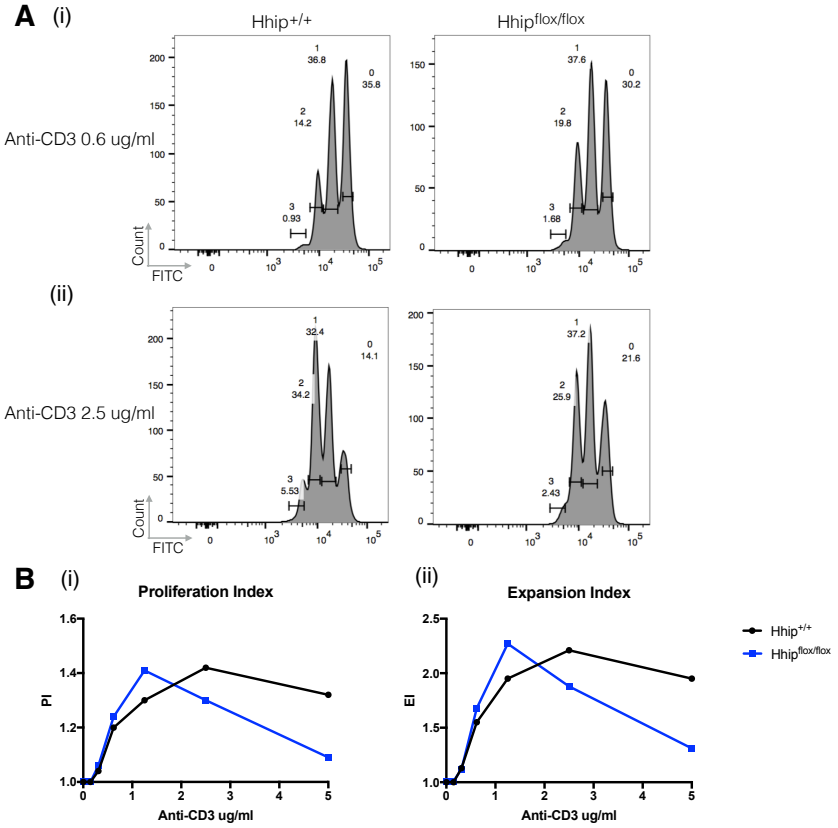

Figure 6.28: Mitogenic responsiveness of naive CD4 T cells from Hhip$^{flox/flox}$ mice
(A) CFSE (FITC channel) stain of sorted CD4 naive T cells from the periphery of 4 week old Hhip$^{+/+}$ and Hhip$^{flox/flox}$ mice. 250 000 cells were stimulated with various concentrations of anti-CD3 and a standardised concentration of anti-CD28 (1 ug/ml) and cultured for 3 days. Both cultures stimulated with (i) 0.6 and (ii) 2.5 ug/ml plated concentration of anti-CD3 underwent 3 divisions in 3 days, with the undivided peak marked as 0, the first division as 1 and so on. **(B)** (i) The proliferation index at each anti-CD3 concentration i.e the sum of all cells divided number of parent cells and (ii) expansion index i.e fold-expansion of the culture were calculated by the Flowjo Cell Cycle tool. 2 independent experiments were conducted. Graphs shown are from a single experiment.

The results in this chapter present a first look at the direct effects of a TEC-specific loss of *hhip* expression. The data presented here are consistent with findings described in previous chapters using mice with a constitutive loss of *hhip* expression, and further demonstrate the importance of Hhip in regulating the differentiation between the cortical and medullary TEC lineages. It also highlighted that MHC expression is not directly affected by the absence of Hhip specifically in TECs, but rather may be influenced by a loss of *hhip* expression in another cell type within the thymus, likely mesenchyme-derived stromal cells. Nevertheless, *hhip*-deficient TECs are impaired in their capacity to perform positive selection, allowing T cells with lower TCR signal strength to survive and to be exported to the

periphery. Finally, these results demonstrate that the abnormal positive selection performed by *hhip*-deficient TECs results in the generation of T cells that are functionally impaired and are less responsive to mitogenic stimuli possibly due to their reduced TCR signalling strength. This clearly highlights the importance of Hhip in regular TEC biology.

7: Discussion

Hedgehog (Hh) signalling in the thymus regulates multiple stages of T cell development. This has been extensively documented in mouse embryos (reviewed in Barbarulo, A. *et al.*, 2016), where Shh signalling is first necessary for the differentiation of DN1 thymocytes to the DN2 stage and their subsequent expansion (Shah, D. *et al.*, 2004). Shh signals then act as a negative regulator, controlling the pre-TCR-mediated differentiation of DN4 cells to DP thymocytes (Outram, S. *et al.*, 2000). Finally, Shh negatively regulates the DP-SP transition and TCR signal strength, thus influencing CD4 and CD8 lineage commitment (Furmanski, A. *et al.*, 2012; Rowbotham, N. *et al.*, 2007). Alongside Shh, Ihh signalling also contributes to the differentiation of early DN cells, and negatively regulates proliferation of DN3 cells after transduction of the pre-TCR signal (Outram, S. *et al.*, 2009). Clear expression of Hh signalling machinery in thymocytes complemented with studies using transgenes encoding either a Gli2 activator or repressor form which compete with endogenous Gli transcription factors in thymocytes have lead to the understanding that thymocyte-intrinsic Hh transcription regulates T cell development (Furmanski, A. *et al.*, 2012; Outram, S. *et al.*, 2000). There is however comparatively limited data on the role of Hh signalling in TECs, although transcripts for all three Hh ligands are detected in human TECs and in the murine model Shh is exclusively expressed in TECs (Outram, S. *et al.*, 2000; Sacedón, R. *et al.*, 2003), suggesting a role for Hh signalling in these cells. Recently, this concept was confirmed in adult mice where a TEC-directed loss of *shh* expression resulted in increased TCR signal strength and a higher frequency of mature single positive T cells (Saldaña, J. *et al.*, 2016). These findings demonstrate that Shh produced by

TECs modulates thymocyte development, and more generally that Hh signalling in the thymus is not solely mediated in a thymocyte-intrinsic manner.

The work presented in this thesis now extends the role of Hh signalling to a novel and direct function in TEC lineage differentiation, demonstrating that the loss of *hhip* expression in TECs favours mTEC development. Conversely, an increased availability of Hhip, experimentally achieved by the exposure of WT E18.5 thymi to rHhip protein, decreased the relative frequency of mTECs, an effect consistent with reports in gene targeted mice showing that an absence of Shh in TECs reduces the mTEC frequency in both fetal and adult thymi (Saldaña, J. *et al*., 2016). Therefore, Hhip is a non-redundant inhibitor of Hh signalling in the thymus and its presence is essential for the preservation of a normal cTEC to mTEC ratio. A loss of *hhip* expression enhances Hh signalling in TECs favouring the differentiation of the mTEC compartment, modulated by the Hh co-receptors Gas1 and Boc, which are required for Hh-dependent signal transduction (Izzi, L. *et al*., 2011).

Given that changes in Hh signalling result only in alterations of the relative frequencies of cTECs and mTECs, but not changes in the absolute numbers of TECs, I therefore propose that Hhip controls the fate choice of common bipotent TEC progenitors (Rossi, W. *et al*., 2006). This is supported by my data where experiments with reporter GBS-GFP mice demonstrated that when Hh signalling was exogenously increased in FTOC by addition of rShh, favouring mTEC differentiation, transcriptional increases in Hh signalling reflected by GFP expression were only observed in the mTEC lineage. Correspondingly, when rHhip was supplemented to inhibit Hh signalling, favouring the cTEC compartment, Gli activity was only altered in cTECs. Gene expression profiles also showed that

genes important for mTEC differentiation, including *tnfrsf11a* (Rossi, S. *et al*., 2007; Akiyama, T. *et al*., 2008) and *fgf7* (Rossi, S. *et al*., 2007; Alpdogen, O. *et al*., 2006) were upregulated in mTECs in response to heightened Hh signalling secondary to an absence of Hhip. Notedly, published literature shows that at E12, only $Foxn1^{+}$ TEC progenitors and not $Foxn1^{-}$ cells responded to RANK stimulation, which promotes mTEC differentiation (Baik, S. *et al*., 2013). This supports a requirement for Hhip as a Foxn1 target gene to modulate the development of bipotent TEC progenitors. As the presently defined bipotent progenitors concomitantly express cortical and medullary phenotypic markers, such as CD205 (cTEC) and RANK (mTEC) (Baik, S. *et al*., 2013), it is difficult to identify the precise time point at which progenitors adopt either a cTEC or mTEC fate. Moreover, the molecular pathways by which Hh signalling influences TEC differentiation remain unknown. Hence, future work should focus on the downstream effects of Hh signalling in bipotent progenitors. This could be experimentally achieved by isolating these progenitors and stimulating them with rShh or rHhip, and analysing the subsequent phenotypic and functional changes.

In addition to its impact on TEC differentiation, Hhip also controls T cell selection. A loss of *hhip* expression affects the positive selection and generation of conventional mature single positive T cells. The changes observed are a direct consequence of an absence of Hhip in TECs, as Hhip-/- thymocyte progenitors displayed a regular selection phenotype when transplanted into a WT thymic microenvironment. Although equivalent frequencies of CD4 and CD8 single positive T cells were generated in *hhip*-deficient mice when compared to WT controls, fewer T cells were recovered from $Hhip^{flox/flox}$ mice and these expressed lower cell surface levels of CD69, CD24, TCRβ and CD5. Additionally, peripheral T cells from $Hhip^{flox/flox}$ mice

were less responsive to mitogenic stimulation. These findings extend previously published data showing that Hh signalling reduces the positive selection of TCR transgenic T cells and lowers their TCR signalling strength (Rowbotham, N. *et al.*, 2007). However, these effects have been shown as a result of Hh pathway activation and repression in T-lineage cells (Rowbotham, N. *et al.*, 2008), and the role of Hh signalling in TECs and its indirect impact on thymocyte development and selection was not addressed. By specifically ablating *hhip* in TECs, I demonstrate that the loss of this inhibitor in TECs upregulates Hh signalling, impairing the ability of TECs to perform positive selection normally.

Table 7.1 provides a summary of the phenotypes observed in the two genetic models described in this thesis.

Table 7.1: Summary of phenotypes in constitutive and tissue-targeted hhip-deficient mice

	Hhip-/- (Constitutive loss of *hhip*)		**Hhip$^{flox/flox}$ (TEC-specific loss of *hhip*)**	
Age	Neonatal	Pseudo-adult (Thymus transplant)	Neonatal	Adult
cTEC frequencies	Decreased	Decreased	Decreased	Decreased
MHC-II^{+} frequencies	Decreased	Increased	Unaltered	Unaltered
Positive selection	CD4 affected	Mature compartment increased	CD4 affected	Mature compartment increased
Negative selection	Not assessed	Less mature cells selected	Not assessed	Less mature cells selected
TCRβ/CD5 expression	Decreased	Decreased	Decreased	Decreased
CD4 frequencies	Decreased	Unaltered	Unaltered	Unaltered

Absence of Hhip in TECs results in decreased cTEC frequencies at all ages. Given that positive selection is mediated by cTECs (Benoist, C. & Mathis, D., 1989), it is conceivable that the reduced presence of cTECs contributes to the observed defects in T cell selection. However, the molecular mechanism that functionally underpins the loss of effective positive selection remains unclear. Loss of *hhip* expression in TECs results in reduced TCRβ and CD5 cell surface expression on thymocytes. Decreased CD5 expression is indicative of reduced TCR signal strength and affinity (Azzam, H. *et al*., 1998). Fewer cTECs may collectively result in a reduced density of pMHC complexes and consequently lower TCR signals (Gottschalk, R. *et al*., 2011; Matis, L. *et al*., 1983). The observation that the CD4 lineage was preferentially affected may have several non-exclusive reasons. Strong TCR signals tend to favour the differentiation of CD4 single positive T cells, as Lck, the tyrosine kinase that transduces TCR signals, preferentially associates with CD4 (Bosselut, R. *et al*., 2001; Itano, A. *et al*., 1996; Wiest, D. *et al*., 1993). This would also impact the expression of TCRβ, as Lck activation regulates the expression of TCR components (Wiest, D. *et al*., 1993), and weak TCR signals could thus result in impaired upregulation of TCRβ. Expression levels of MHC-II also contribute to the selection fate of CD4 T cells (Fukui, Y. *et al*., 1997). Hence, the T cell phenotype of Hhip-/- neonatal mice could be explained by a mechanism whereby a loss of *hhip* results in decreased MHC-II expression on cTECs. Consequently, fewer TCR interactions are established, which impair the generation of a normal frequency of CD4 T cells. However, altered MHC-II expression was only observed upon a constitutive loss of *hhip* expression as well as external non-tissue specific modulation of Hh signalling by addition of rShh and rHhip protein to WT FTOC, but not as a consequence of a TEC-targeted loss of *hhip* expression. This therefore supports in addition to a TEC defect also a thymocyte-intrinsic Hh signalling defect

consequent to loss of Hhip, affecting the ability of thymocytes to interact with pMHC complexes, and thus modulating MHC-II expression.

A constitutive deficiency of *hhip* that affects both TECs and thymocytes appears to influence TCR signal strength. A theory that could resolve these phenotypes suggests that Hh signalling controls different aspects of TCR-pMHC interactions. In TECs, autocrine Hh signalling may affect availability of pMHC complexes. In thymocytes, absence of Hhip may enhance Hh signalling which in turn decreases the strength of their TCR interaction. As such, *hhip*-deficient thymocytes may collectively signal with lower TCR strength, which in the context of a WT Hhip-sufficient thymic microenvironment, such as in the transplant experiment where Hhip-/- haematopoietic progenitors were grafted into irradiated WT hosts, results in changes in the CD8 lineage. WT TECs may be able to compensate for the thymocyte-intrinsic reduced TCR signal strength by selecting from the range of thymocytes with a relatively higher TCR signal strength, which would explain the persistent increase in TCRβ cell surface expression on CD8 Hhip-/- T cells developing in a normal WT TEC scaffold. However, certain observations cannot be explained by this simplistic model, such as changes in CCR7 expression in Hhip-/- thymocytes, which could indicate a deficiency in migratory capabilities. Attempts to distinguish a Hh-related defect at the level of thymocyte progenitors were also unfruitful. Conflicting views can be found in the literature, for example where loss of Smo, a non-redundant element of Hh signalling does not impair haematopoiesis. In contrast, loss of *ptch1* and *gli1* expression alters the proliferation of haematopoietic stem cells (reviewed in Lim, Y. & Matsui, W., 2010). Moreover, Ptch1 is important for common lymphoid progenitors to commit to a T cell fate (Curtis, D. *et al*., 2008; Uhmann, A. *et al*., 2007). A constitutive loss of *hhip* may therefore have enhanced

Hh signalling in bone marrow-resident lymphocyte progenitors during early stages of their development, resulting in permanent changes in the cells' functional capacities which are apparent even upon their differentiation in a Hhip-proficient microenvironment. This hypothesis can now be directly addressed using the newly developed conditional allele to delete the expression of *hhip* in haematopoietic precursors.

A contribution by Hh ligands other than Shh to the *hhip*-deficient phenotype has not been addressed with the experiments presented here. The focus on Shh signalling was chosen given the knowledge that this member of the Hh family is the most broadly expressed throughout the body, is most abundantly expressed in TECs (Outram, S. *et al*., 2000) and has previously been noted to be involved in epithelial cell development in many tissues, for example in the dental and airway epithelium, as well as in the thymus (Watkins, D. *et al*., 2003; Gritli-Linde, A. *et al*., 2002; Saldaña, J. *et al*., 2016). In contrast, the developmental roles of Ihh and Dhh are more restricted (reviewed in Varjosalo, M. & Taipale, J., 2008). qPCR and gene expression profiles demonstrated that trace amounts of all three ligands (including *dhh*) could be found in both embryonic and adult thymi. As Hhip can inhibit any of these three ligands, it can therefore regulate signalling by any of the said ligands. Notably, Ihh signalling specifically in peripheral CD8 T lymphocytes has been studied, where it is important after TCR signalling for the expression of RAC1, a protein required for cytotoxic effector cell function (de la Roche, M. *et al*., 2013), although Ihh signalling has not been studied for its role, if any, in TCR signalling in the thymus. Additionally, the role of Dhh in TECs was not pursued due to the lack of evidence in the literature of *dhh* expression by TECs. However, given that both qPCR and sequencing results clearly demonstrated some expression of *dhh*, this

should be followed up on in order to better understand the specific contributions of each Hh ligand to thymus organogenesis.

The Hh signalling pathway interacts with many different molecules. Gli transcription factors, the main downstream modulators of the Hh pathway, are responsive to transforming growth factor β (TGF-β) and epidermal growth factor receptor (EGFR) signalling, pathways which regulate other central developmental processes including cell growth, differentiation and homeostasis in the body (Dennler, S. *et al.*, 2007; Kasper, M. *et al.*, 2006). While Hhip is primarily known as an inhibitor of Hh signalling, it also crucially modulates fibroblast growth factor (Fgf) signalling in the lungs, where *fgf10* expression in the mesenchyme is Hhip-dependent (Chuang, P. *et al.*, 2003). Fgf signalling is essential for proliferation of TECs, where Fgf10 is expressed in the thymic mesenchyme and *fgf10*-deficient mice have a hypoplastic thymus (Revest, J. *et al.*, 2001; Ohuchi, H. *et al.*, 2000). *Fgf7* expression was also altered in Hhip-/- mTECs, supporting a potential involvement of the Fgf pathway. This reinforces the need to explore the role of Hhip in the context of other relevant signalling pathways, as well as in non-TEC lineages such as the mesenchyme in order to have a truly comprehensive understanding of the importance of Hhip in the thymus.

Taken together, in addition to the importance of Hhip in TECs throughout developmental life, the results presented support an importance of Hh signalling in adult thymocyte development, which has previously been less well described in comparison to fetal development largely due to the early lethality of most transgenic knockout mouse models for elements of the Hh signalling pathway. For example, conditional deletion of the transducing molecule *smo* in adult thymocyte lineages

did not affect T cell development after initiation of pre-TCR signalling (El Andaloussi, A. *et al*., 2006). However, this study shows that loss of *hhip* expression at embryonic, neonatal and adult ages affect positive selection of thymocytes, highlighting the continuous requirement of tightly regulated Hh signalling in thymocyte development throughout life.

Finally, the relationship between thymic Foxn1 and the Hh signalling pathway can now be better explored, given our discovery that *hhip* is a target of Foxn1-regulated transcription (Žuklys, S. *et al*., 2016). Foxn1 is indispensible for TEC growth, differentiation and thymopoietic function (Blackburn, C. *et al*., 1996; Nowell, C. *et al*., 2011; Corbeaux, T. *et al*., 2010). No conclusive evidence has been found thus far demonstrating that Foxn1 regulates TEC fate choice. Concurrently, Shh signalling critically controls cell fate decisions (reviewed in Kiecker, C. *et al*., 2016), and indeed, Shh is necessary for thymus organogenesis and fate specification, and seems to play a role in TEC lineage choice (Bain, V. *et* al., 2016; Saldaña, J. *et al*., 2016). This would propose that while Foxn1 is not sufficient or solely responsible for TEC sublineage fate choice, it may nonetheless contribute to lineage fate decisions via regulation of *hhip* to affect Shh signalling, reinforcing its overarching role as a master transcriptional regulator in the thymus. My *in vitro* data also revealed that Shh seemed upstream of *foxn1*. This observation raises the possibility that Shh-mediated signals enhance *foxn1* transcription, a concept that has been proposed for the patterning of the parathyroid, with limited evidence showing that the area of pharyngeal *foxn1* expression is expanded in mice deficient for *shh*, whereas ectopic Shh suppresses *foxn1* expression, and the Shh target Tbx1 inhibits *foxn1* expression (Bain, V. *et* al., 2016; Reeh, K. *et al*., 2014). In contrast, the data presented here is not compatible with the suggestion that Shh

exerts a suppressive function of *foxn1* transcription, given that an increase of *foxn1* transcripts was observed in response to rShh exposure. One explanation for this discrepancy could be that Shh indirectly regulates *foxn1* expression via transduction pathways that are differentially expressed between the parathyroid and thymus anlagen. Taken together, the data could also propose a mechanism where Foxn1 autoregulates its own expression via a feedback loop that involves *hhip*, by inhibiting Shh signalling and its capacity to upregulate *foxn1.* Shh and Foxn1 could therefore contribute to TEC sublineage commitment choices cooperatively, emphasising the importance of Hhip as a crucial molecule in this relationship that allows Foxn1 to indirectly modulate Hh signal transduction.

There have not been any reports thus far regarding immunodeficiencies or autoimmunity as a consequence of *hhip* mutations. However, Shh signalling is important in human peripheral T cell responses, where it positively modulates T cell activation and proliferation, as well as cytokine production (Stewart, G. *et al.*, 2002; Lowrey, J. *et al.*, 2002). Additionally, Shh also regulates the survival and function of dendritic cells (Varas, A. *et al.*, 2008), highlighting the relevance of Hh signalling in the human immune system. Given our findings that Hhip is crucial for normal selection of thymocytes, the role of Hhip should be investigated in human thymocyte development to expand our understanding of the importance of the Hh signalling pathway in human immunological function and disease.

In conclusion, the data shown in this thesis has demonstrated for the first time the importance of Hhip in thymus organogenesis and function. TEC sublineage choice, function, and subsequently thymocyte development are critically dependent on a tightly regulated level of Hh signalling in TECs. The inhibition of Shh signalling via

Hhip is an integral part of the signalling network controlling thymocyte differentiation, as supported by Shh's important role as a regulator of TCR signal strength and repertoire selection (Robowtham, N. *et al*., 2007) Hence, there is a strong functional relationship between Foxn1 and Hh signalling in TECs which allows for regular TEC differentiation and function, and this is critically maintained by Foxn1's transcriptional regulation of *hhip*.

References

Adolfsson, J., Månsson, R., Buza-Vidas, N., Hultquist, A., Liuba, K., Jensen, C. T., ... & Anderson, K. (2005). Identification of Flt3+ lympho-myeloid stem cells lacking erythro-megakaryocytic potential: a revised road map for adult blood lineage commitment. *Cell*, *121*(2), 295-306.

Akira, S., & Takeda, K. (2004). Toll-like receptor signalling. *Nature Reviews Immunology*, 4(7), 499-511.

Akira, S., Uematsu, S., & Takeuchi, O. (2006). Pathogen recognition and innate immunity. *Cell*, 124(4), 783-801.

Akiyama, T., Shimo, Y., Yanai, H., Qin, J., Ohshima, D., Maruyama, Y., ... & Inoue, J. I. (2008). The tumor necrosis factor family receptors RANK and CD40 cooperatively establish the thymic medullary microenvironment and self-tolerance. *Immunity*, 29(3), 423-437.

Akiyama, N., Takizawa, N., Miyauchi, M., Yanai, H., Tateishi, R., Shinzawa, M., ... & Yagi, S. (2016). Identification of embryonic precursor cells that differentiate into thymic epithelial cells expressing autoimmune regulator. *The Journal of Experimental Medicine*, 213(8), 1441-1458.

Alpdogan, Ö., Hubbard, V. M., Smith, O. M., Patel, N., Lu, S., Goldberg, G. L., ... & Suh, D. (2006). Keratinocyte growth factor (KGF) is required for postnatal thymic regeneration. *Blood*, *107*(6), 2453-2460.

Anderson, M. S., Venanzi, E. S., Klein, L., Chen, Z., Berzins, S. P., Turley, S. J., ... & Mathis, D. (2002). Projection of an immunological self shadow within the thymus by the aire protein. *Science*, *298*(5597), 1395-1401.

Anderson, B. E., McNiff, J. M., Matte, C., Athanasiadis, I., Shlomchik, W. D., & Shlomchik, M. J. (2004). Recipient CD4+ T cells that survive irradiation regulate chronic graft-versus-host disease. *Blood*, *104*(5), 1565-1573.

Astorga, J., & Carlsson, P. (2007). Hedgehog induction of murine vasculogenesis is mediated by Foxf1 and Bmp4. *Development*, *134*(20), 3753-3761.

Aza-Blanc, P., Ramírez-Weber, F. A., Laget, M. P., Schwartz, C., & Kornberg, T. B. (1997). Proteolysis that is inhibited by hedgehog targets Cubitus interruptus protein to the nucleus and converts it to a repressor. *Cell*, *89*(7), 1043-1053.

Azzam, H. S., Grinberg, A., Lui, K., Shen, H., Shores, E. W., & Love, P. E. (1998). CD5 expression is developmentally regulated by T cell receptor (TCR) signals and TCR avidity. *Journal of Experimental Medicine*, *188*(12), 2301-2311.

Bach, E. A., Szabo, S. J., Dighe, A. S., Ashkenazi, A., Aguet, M., Murphy, K. M., & Schreiber, R. D. (1995). Ligand-induced autoregulation of IFN-gamma receptor beta chain expression in T helper cell subsets. *Science*, 270(5239), 1215-1219.

Bai, C. B., Auerbach, W., Lee, J. S., Stephen, D., & Joyner, A. L. (2002). Gli2, but not Gli1, is required for initial Shh signaling and ectopic activation of the Shh pathway. *Development*, *129*(20), 4753-4761.

Baik, S., Jenkinson, E. J., Lane, P. J., Anderson, G., & Jenkinson, W. E. (2013). Generation of both cortical and Aire+ medullary thymic epithelial compartments from CD205+ progenitors. *European Journal of Immunology*, *43*(3), 589-594.

Bain, V. E., Gordon, J., O'Neil, J. D., Ramos, I., Richie, E. R., & Manley, N. R. (2016). Tissue-specific roles for Sonic hedgehog signaling in establishing thymus and parathyroid organ fate. *Development,* 143(21), 4027-4037.

Balaskas, N., Ribeiro, A., Panovska, J., Dessaud, E., Sasai, N., Page, K. M., ... & Ribes, V. (2012). Gene regulatory logic for reading the Sonic Hedgehog signaling gradient in the vertebrate neural tube. *Cell*, *148*(1), 273-284.

Balciunaite, G., Keller, M. P., Balciunaite, E., Piali, L., Žuklys, S., Mathieu, Y. D., ... & Holländer, G. A. (2002). Wnt glycoproteins regulate the expression of FoxN1, the gene defective in nude mice. *Nature Immunology*, 3(11), 1102-1108.

Barbarulo, A., Lau, C. I., Mengrelis, K., Ross, S., Solanki, A., Saldaña, J. I., & Crompton, T. (2016). Hedgehog signalling in the embryonic mouse thymus. *Journal of Developmental Biology*, *4*(3), 22.

Barthlott, T., Bosch, A. J., Berkemeier, C., Nogales-Cadenas, R., Jeker, L. T., Keller, M. P., ... & Holländer, G. A. (2015). A subpopulation of CD103posICOSpos Treg cells occurs at high frequency in lymphopenic mice and represents a lymph node specific differentiation stage. *European Journal of Immunology*, *45*(6), 1760-1771.

Bassett, A. R., Tibbit, C., Ponting, C. P., & Liu, J. L. (2013). Highly efficient targeted mutagenesis of Drosophila with the CRISPR/Cas9 system. *Cell Reports*, *4*(1), 220-228.

Bellusci, S., Furuta, Y., Rush, M. G., Henderson, R., Winnier, G., & Hogan, B. L. (1997). Involvement of Sonic hedgehog (Shh) in mouse embryonic lung growth and morphogenesis. *Development*, *124*(1), 53-63.

Bendelac, A., Matzinger, P., Seder, R. A., Paul, W. E., & Schwartz, R. H. (1992). Activation events during thymic selection. *The Journal of Experimental Medicine*, 175(3), 731-742.

Benes, P., Vetvicka, V., & Fusek, M. (2008). Cathepsin D—many functions of one aspartic protease. *Critical Reviews in Oncology/Hematology*, 68(1), 12-28.

Benoist, C., & Mathis, D. (1989). Positive selection of the T cell repertoire: where and when does it occur?. *Cell*, *58*(6), 1027-1033.

Bishop, B., Aricescu, A. R., Harlos, K., O'callaghan, C. A., Jones, E. Y., & Siebold, C. (2009). Structural insights into hedgehog ligand sequestration by the human

hedgehog-interacting protein HHIP. *Nature Structural & Molecular Biology*, *16*(7), 698-703.

Bitgood, M. J., Shen, L., & McMahon, A. P. (1996). Sertoli cell signaling by Desert hedgehog regulates the male germline. *Current Biology*, *6*(3), 298-304.

Blackburn, C. C., Augustine, C. L., Li, R., Harvey, R. P., Malin, M. A., Boyd, R. L., ... & Morahan, G. (1996). The nu gene acts cell-autonomously and is required for differentiation of thymic epithelial progenitors. *Proceedings of the National Academy of Sciences*, *93*(12), 5742-5746.

Bleul, C. C., & Boehm, T. (2005). BMP signaling is required for normal thymus development. *The Journal of Immunology*, 175(8), 5213-5221.

Bleul, C. C., Corbeaux, T., Reuter, A., Fisch, P., Mönting, J. S., & Boehm, T. (2006). Formation of a functional thymus initiated by a postnatal epithelial progenitor cell. *Nature*, 441(7096), 992-996.

Bosanac, I., Maun, H. R., Scales, S. J., Wen, X., Lingel, A., Bazan, J. F., ... & Lazarus, R. A. (2009). The structure of SHH in complex with HHIP reveals a recognition role for the Shh pseudo active site in signaling. *Nature Structural & Molecular Biology*, *16*(7), 691-697.

Bosco, N., Swee, L. K., Bénard, A., Ceredig, R., & Rolink, A. (2010). Auto-reconstitution of the T-cell compartment by radioresistant hematopoietic cells following lethal irradiation and bone marrow transplantation. *Experimental Hematology*, *38*(3), 222-232.

Bosselut, R., Feigenbaum, L., Sharrow, S. O., & Singer, A. (2001). Strength of signaling by CD4 and CD8 coreceptor tails determines the number but not the lineage direction of positively selected thymocytes. *Immunity*, *14*(4), 483-494.

Brändle, D., Müller, S., Müller, C., Hengartner, H., & Pircher, H. (1994). Regulation of RAG-1 and CD69 expression in the thymus during positive and negative selection. *European Journal of Immunology*, 24(1), 145-151.

Brugnera, E., Bhandoola, A., Cibotti, R., Yu, Q., Guinter, T.I., Yamashita, Y., Sharrow, S.O., and Singer, A. (2000). Coreceptor reversal in the thymus: signaled CD4+8+ thymocytes initially terminate CD8 transcription even when differentiating into CD8+ T cells. *Immunity,* 13, 59-71.

Bunting, M. D., Comerford, I., Kara, E. E., Korner, H., & McColl, S. R. (2014). CCR6 supports migration and differentiation of a subset of DN1 early thymocyte progenitors but is not required for thymic nTreg development. *Immunology and Cell Biology*, *92*(6), 489-498.

Burnley, P., Rahman, M., Wang, H., Zhang, Z., Sun, X., Zhuge, Q., & Su, D. M. (2013). Role of the p63-FoxN1 regulatory axis in thymic epithelial cell homeostasis during aging. *Cell Death & Disease*, 4(11), e932.

Buttitta, L., Mo, R., Hui, C. C., & Fan, C. M. (2003). Interplays of Gli2 and Gli3 and their requirement in mediating Shh-dependent sclerotome induction. *Development*, *130*(25), 6233-6243.

Butz, E. A., & Bevan, M. J. (1998). Massive expansion of antigen-specific CD8+ T cells during an acute virus infection. *Immunity*, 8(2), 167-175.

Cai, J., Lee, J., Kopan, R., & Ma, L. (2009). Genetic interplays between Msx2 and Foxn1 are required for Notch1 expression and hair shaft differentiation. *Developmental Biology*, 326(2), 420-430.

Calderón, L., & Boehm, T. (2012). Synergistic, context-dependent, and hierarchical functions of epithelial components in thymic microenvironments. *Cell*, 149(1), 159-172.

Callejo, A., Torroja, C., Quijada, L., & Guerrero, I. (2006). Hedgehog lipid modifications are required for Hedgehog stabilization in the extracellular matrix. *Development*, *133*(3), 471-483.

Chen, L., Xiao, S., & Manley, N. R. (2009). Foxn1 is required to maintain the postnatal thymic microenvironment in a dosage-sensitive manner. *Blood*, 113(3), 567-574.

Chen, M. H., Li, Y. J., Kawakami, T., Xu, S. M., & Chuang, P. T. (2004). Palmitoylation is required for the production of a soluble multimeric Hedgehog protein complex and long-range signaling in vertebrates. *Genes & Development,* 18(6), 641-659.

Cheng, L., Guo, J., Sun, L., Fu, J., Barnes, P. F., Metzger, D., ... & Su, D. M. (2010). Postnatal tissue-specific disruption of transcription factor FoxN1 triggers acute thymic atrophy. *Journal of Biological Chemistry*, 285(8), 5836-5847.

Chuang, P. T., & McMahon, A. P. (1999). Vertebrate Hedgehog signalling modulated by induction of a Hedgehog-binding protein. *Nature*, *397*(6720), 617-621.

Chuang, P. T., Kawcak, T. N., & McMahon, A. P. (2003). Feedback control of mammalian Hedgehog signaling by the Hedgehog-binding protein, Hip1, modulates Fgf signaling during branching morphogenesis of the lung. *Genes & Development*, 17(3), 342-347.

Clark, A. M., Garland, K. K., & Russell, L. D. (2000). Desert hedgehog (Dhh) gene is required in the mouse testis for formation of adult-type Leydig cells and normal development of peritubular cells and seminiferous tubules. *Biology of Reproduction*, *63*(6), 1825-1838.

Ciofani, M., & Zúñiga-Pflücker, J. C. (2010). Determining γδ versus αβ T cell development. *Nature Reviews Immunology*, 10(9), 657-663.

Corbeaux, T., Hess, I., Swann, J. B., Kanzler, B., Haas-Assenbaum, A., & Boehm, T. (2010). Thymopoiesis in mice depends on a Foxn1-positive thymic epithelial cell lineage. *Proceedings of the National Academy of Sciences*, 107(38), 16613-16618.

Cong, L., Ran, F. A., Cox, D., Lin, S., Barretto, R., Habib, N., ... & Zhang, F. (2013). Multiplex genome engineering using CRISPR/Cas systems. *Science*, *339*(6121), 819-823.

Cote-Sierra, J., Foucras, G., Guo, L., Chiodetti, L., Young, H. A., Hu-Li, J., ... & Paul, W. E. (2004). Interleukin 2 plays a central role in Th2 differentiation. *Proceedings of the National Academy of Sciences of the United States of America*, *101*(11), 3880-3885.

Croce, J. C., & McClay, D. R. (2009). Evolution of the Wnt pathways. *Wnt Signaling*, 3-18.

Crompton, T., Outram, S. V., & Hager-Theodorides, A. L. (2007). Sonic hedgehog signalling in T-cell development and activation. *Nature Reviews Immunology*, *7*(9), 726-735.

Curtis, D. J., Siggins, S., Nguyen, N. Y., Hetherington, R., & Wainwright, B. (2008). Ptch1 Regulates the Bone Marrow Cell Niche Critical for Survival of Pre-B Cells but Not Hematopoietic Stem Cells. *Blood*, *112*(11), 3571-3571.

Daley, S. R., Hu, D. Y., & Goodnow, C. C. (2013). Helios marks strongly autoreactive CD4+ T cells in two major waves of thymic deletion distinguished by induction of PD-1 or NF-κB. *Journal of Experimental Medicine*, jem-20121458.

Daniels, M. A., Teixeiro, E., Gill, J., Hausmann, B., Roubaty, D., Holmberg, K., ... & Palmer, E. (2006). Thymic selection threshold defined by compartmentalization of Ras/MAPK signalling. *Nature*, 444(7120), 724-729.

Davis, M. M., & Bjorkman, P. J. (1988). T-cell antigen receptor genes and T-cell recognition. *Nature*, 395-402.

de la Hera, A., Marston, W., Aranda, C., Toribio, M. L., & Martinez-A, C. (1989). Thymic stroma is required for the development of human T cell lineages in vitro. *International Immunology*, 1(5), 471-478.

de la Roche, M., Ritter, A. T., Angus, K. L., Dinsmore, C., Earnshaw, C. H., Reiter, J. F., & Griffiths, G. M. (2013). Hedgehog signaling controls T cell killing at the immunological synapse. *Science*, *342*(6163), 1247-1250.

Denef, N., Neubüser, D., Perez, L., & Cohen, S. M. (2000). Hedgehog induces opposite changes in turnover and subcellular localization of patched and smoothened. *Cell*, *102*(4), 521-531.

Dennler, S., André, J., Alexaki, I., Li, A., Magnaldo, T., Ten Dijke, P., ... & Mauviel, A. (2007). Induction of sonic hedgehog mediators by transforming growth factor-β: Smad3-dependent activation of Gli2 and Gli1 expression in vitro and in vivo. *Cancer Research*, *67*(14), 6981-6986.

Depreter, M. G., Blair, N. F., Gaskell, T. L., Nowell, C. S., Davern, K., Pagliocca, A., ... & Robertson, K. (2008). Identification of Plet-1 as a specific marker of early thymic epithelial progenitor cells. *Proceedings of the National Academy of Sciences*, *105*(3), 961-966.

Derbinski, J., Schulte, A., Kyewski, B., & Klein, L. (2001). Promiscuous gene expression in medullary thymic epithelial cells mirrors the peripheral self. *Nature Immunology*, 2(11), 1032-1039.

Derbinski, J., Gäbler, J., Brors, B., Tierling, S., Jonnakuty, S., Hergenhahn, M., ... & Kyewski, B. (2005). Promiscuous gene expression in thymic epithelial cells is regulated at multiple levels. *Journal of Experimental Medicine*, *202*(1), 33-45.

Dessaud, E., Yang, L. L., Hill, K., Cox, B., Ulloa, F., Ribeiro, A., ... & Briscoe, J. (2007). Interpretation of the sonic hedgehog morphogen gradient by a temporal adaptation mechanism. *Nature*, *450*(7170), 717-720.

Di Marcotullio, L., Ferretti, E., Greco, A., De Smaele, E., Screpanti, I., & Gulino, A. (2007). Multiple ubiquitin-dependent processing pathways regulate hedgehog/gli signaling: implications for cell development and tumorigenesis. *Cell Cycle*, *6*(4), 390-393.

Ding, Q., Motoyama, J., Gasca, S., Mo, R., Sasaki, H., Rossant, J., & Hui, C. C. (1998). Diminished Sonic hedgehog signaling and lack of floor plate differentiation in Gli2 mutant mice. *Development*, *125*(14), 2533-2543.

dos Santos Reis, M. D., Csomos, K., Dias, L. P. B., Prodan, Z., Szerafin, T., Savino, W., & Takacs, L. (2015). Decline of FOXN1 gene expression in human thymus correlates with age: possible epigenetic regulation. *Immunity & Ageing*, 12(1), 1.

Duman-Scheel, M., Weng, L., Xin, S., & Du, W. (2002). Hedgehog regulates cell growth and proliferation by inducing Cyclin D and Cyclin E. *Nature*, *417*(6886), 299-304.

Dumitriu, B., Patrick, M. R., Petschek, J. P., Cherukuri, S., Klingmuller, U., Fox, P. L., & Lefebvre, V. (2006). Sox6 cell-autonomously stimulates erythroid cell survival, proliferation, and terminal maturation and is thereby an important enhancer of definitive erythropoiesis during mouse development. *Blood*, *108*(4), 1198-1207.

Egerton, M., Scollay, R., & Shortman, K. (1990). Kinetics of mature T-cell development in the thymus. *Proceedings of the National Academy of Sciences*, *87*(7), 2579-2582.

El Andaloussi, A., Graves, S., Meng, F., Mandal, M., Mashayekhi, M., & Aifantis, I. (2006). Hedgehog signaling controls thymocyte progenitor homeostasis and differentiation in the thymus. *Nature Immunology*, *7*(4), 418-426.

Erickson, M., Morkowski, S., Lehar, S., Gillard, G., Beers, C., Dooley, J., ... & Farr, A. G. (2002). Regulation of thymic epithelium by keratinocyte growth factor. *Blood*, *100*(9), 3269-3278.

Farley, A. M., Morris, L. X., Vroegindeweij, E., Depreter, M. L., Vaidya, H., Stenhouse, F. H., ... & Blackburn, C. C. (2013). Dynamics of thymus organogenesis and colonization in early human development. *Development*, 140(9), 2015-2026.

Figueiredo, M., Silva, J. C., Santos, A. S., Proa, V., Alcobia, I., Zilhão, R., ... & Neves, H. (2016). Notch and Hedgehog in the thymus/parathyroid common primordium: Crosstalk in organ formation. *Developmental Biology*, *418*(2), 268-282.

Flanagan, S. P. (1966). 'Nude', a new hairless gene with pleiotropic effects in the mouse. *Genetical Research*, 8(03), 295-309.

Frank, J., Pignata, C., Panteleyev, A. A., Prowse, D. M., Baden, H., Weiner, L., ... & Christiano, A. M. (1999). Exposing the human nude phenotype. *Nature*, 398(6727), 473-474.

Frauwirth, K. A., & Thompson, C. B. (2002). Activation and inhibition of lymphocytes by costimulation. *The Journal of Clinical Investigation*, *109*(3), 295-299.

Frost, L. S., Lopes, V. S., Stefano, F. P., Bragin, A., Williams, D. S., Mitchell, C. H., & Boesze-Battaglia, K. (2013). Loss of melanoregulin (MREG) enhances cathepsin-D secretion by the retinal pigment epithelium. *Visual Neuroscience,* 30(03), 55-64.

Fujimoto, Y., Tu, L., Miller, A. S., Bock, C., Fujimoto, M., Doyle, C., ... & Tedder, T. F. (2002). CD83 expression influences CD4+ T cell development in the thymus. *Cell*, 108(6), 755-767.

Fukui, Y., Ishimoto, T., Utsuyama, M., Gyotoku, T., Koga, T., Nakao, K., ... & Sasazuki, T. (1997). Positive and negative CD4+ thymocyte selection by a single

MHC class II/peptide ligand affected by its expression level in the thymus. *Immunity*, *6*(4), 401-410.

Furmanski, A. L., Saldana, J. I., Rowbotham, N. J., Ross, S. E., & Crompton, T. (2012). Role of Hedgehog signalling at the transition from double-positive to single-positive thymocyte. *European Journal of Immunology*, *42*(2), 489-499.

Galy, A. H., & Spits, H. (1992). CD40 is functionally expressed on human thymic epithelial cells. *The Journal of Immunology*, 149(3), 775-782.

Gay, D., Maddon, P., Sekaly, R., Talle, M. A., Godfrey, M., Long, E., ... & Marrack, P. (1987). Functional interaction between human T-cell protein CD4 and the major histocompatibility complex HLA-DR antigen. *Nature,* 328, 626-629.

Germain, R. N. (2002). T-cell development and the CD4–CD8 lineage decision. *Nature Reviews Immunology*, *2*(5), 309-322.

Gill, J., Malin, M., Holländer, G. A., & Boyd, R. (2002). Generation of a complete thymic microenvironment by MTS24+ thymic epithelial cells. *Nature Immunology*, *3*(7), 635-642.

Godfrey, D.I., Kennedy, J., Mombaerts, P., Tonegawa, S., and Zlotnik, A. (1994). Onset of TCR-beta gene rearrangement and role of TCR-beta expression during CD3-CD4-CD8- thymocyte differentiation. *The Journal of Immunology 152*, 4783-4792.

Goldrath, A. W., & Bevan, M. J. (1999). Selecting and maintaining a diverse T-cell repertoire. *Nature*, 402(6759), 255-262.

Gordon, J., Bennett, A. R., Blackburn, C. C., & Manley, N. R. (2001). Gcm2 and Foxn1 mark early parathyroid-and thymus-specific domains in the developing third pharyngeal pouch. *Mechanisms of Development*, 103(1), 141-143.

Goss, A. M., Tian, Y., Cheng, L., Yang, J., Zhou, D., Cohen, E. D., & Morrisey, E. E. (2011). Wnt2 signaling is necessary and sufficient to activate the airway smooth

muscle program in the lung by regulating myocardin/Mrtf-B and Fgf10 expression. *Developmental Biology*, *356*(2), 541-552.

Gray, D. H., Seach, N., Ueno, T., Milton, M. K., Liston, A., Lew, A. M., ... & Boyd, R. L. (2006). Developmental kinetics, turnover, and stimulatory capacity of thymic epithelial cells. *Blood*, *108*(12), 3777-3785.

Grevellec, A., Graham, A., & Tucker, A. S. (2011). Shh signalling restricts the expression of Gcm2 and controls the position of the developing parathyroids. *Developmental Biology*, *353*(2), 194-205.

Gritli-Linde, A., Lewis, P., McMahon, A. P., & Linde, A. (2001). The whereabouts of a morphogen: direct evidence for short-and graded long-range activity of hedgehog signaling peptides. *Developmental Biology*, 236(2), 364-386.

Gritli-Linde, A., Bei, M., Maas, R., Zhang, X. M., Linde, A., & McMahon, A. P. (2002). Shh signaling within the dental epithelium is necessary for cell proliferation, growth and polarization. *Development*, *129*(23), 5323-5337.

Goodrich, L. V., Milenković, L., Higgins, K. M., & Scott, M. P. (1997). Altered neural cell fates and medulloblastoma in mouse patched mutants. *Science*, 277(5329), 1109-1113.

Gottschalk, R. A., Hathorn, M. M., Beuneu, H., Corse, E., Dustin, M. L., Altan-Bonnet, G., & Allison, J. P. (2012). Distinct influences of peptide-MHC quality and quantity on in vivo T-cell responses. *Proceedings of the National Academy of Sciences*, *109*(3), 881-886.

Guo, J., Rahman, M., Cheng, L., Zhang, S., Tvinnereim, A., & Su, D. M. (2011). Morphogenesis and maintenance of the 3D thymic medulla and prevention of nude skin phenotype require FoxN1 in pre-and post-natal K14 epithelium. *Journal of Molecular Medicine*, 89(3), 263-277.

Guo, J., Feng, Y., Barnes, P., Huang, F. F., Idell, S., Su, D. M., & Shams, H. (2012). Deletion of FoxN1 in the thymic medullary epithelium reduces peripheral T cell responses to infection and mimics changes of aging. *PLoS One*, 7(4), e34681.

Gurlo, T., & von Grafenstein, H. (2003). Antigen-independent cross-talk between macrophages and CD8+ T cells facilitates their cooperation during target destruction. *International Immunology*, 15(9), 1063-1071.

Hager-Theodorides, A. L., Furmanski, A. L., Ross, S. E., Outram, S. V., Rowbotham, N. J., & Crompton, T. (2009). The Gli3 transcription factor expressed in the thymus stroma controls thymocyte negative selection via Hedgehog-dependent and-independent mechanisms. *The Journal of Immunology*, 183(5), 3023-3032.

Hamazaki, Y., Fujita, H., Kobayashi, T., Choi, Y., Scott, H. S., Matsumoto, M., & Minato, N. (2007). Medullary thymic epithelial cells expressing Aire represent a unique lineage derived from cells expressing claudin. *Nature Immunology*, *8*(3), 304-311.

Harfe, B. D., Scherz, P. J., Nissim, S., Tian, H., McMahon, A. P., & Tabin, C. J. (2004). Evidence for an expansion-based temporal Shh gradient in specifying vertebrate digit identities. *Cell*, *118*(4), 517-528.

Hebrok, M., Kim, S. K., St Jacques, B., McMahon, A. P., & Melton, D. A. (2000). Regulation of pancreas development by hedgehog signaling. *Development,* 127(22), 4905-4913.

Holländer, G. A., Wang, B., Nichogiannopoulou, A., & Platenburg, P. P. (1995). Developmental control point in induction of thymic cortex regulated by a subpopulation of prothymocytes. *Nature*, *373*(6512), 350.

Holländer, G., Gill, J., Zuklys, S., Iwanami, N., Liu, C., & Takahama, Y. (2006). Cellular and molecular events during early thymus development. *Immunological Reviews*, *209*(1), 28-46.

Holtz, A. M., Griffiths, S. C., Davis, S. J., Bishop, B., Siebold, C., & Allen, B. L. (2015). Secreted HHIP1 interacts with heparan sulfate and regulates Hedgehog ligand localization and function. *Journal of Cell Biology*, *209*(5), 739-758.

Horikawa, T., Nakayama, T., Hikita, I., Yamada, H., Fujisawa, R., Bito, T., ... & Morita, A. (2002). IFN-γ-inducible expression of thymus and activation-regulated chemokine/CCL17 and macrophage-derived chemokine/CCL22 in epidermal keratinocytes and their roles in atopic dermatitis. *International Immunology*, *14*(7), 767-773.

Hrycaj, S. M., Dye, B. R., Baker, N. C., Larsen, B. M., Burke, A. C., Spence, J. R., & Wellik, D. M. (2015). Hox5 genes regulate the Wnt2/2b-Bmp4-signaling axis during lung development. *Cell Reports*, *12*(6), 903-912.

Hu, B., Lefort, K., Qiu, W., Nguyen, B. C., Rajaram, R. D., Castillo, E., ... & Dotto, G. P. (2010). Control of hair follicle cell fate by underlying mesenchyme through a CSL–Wnt5a–FoxN1 regulatory axis. *Genes & Development*, 24(14), 1519-1532.

Hu, D. Y., Yap, J. Y., Wirasinha, R. C., Howard, D. R., Goodnow, C. C., & Daley, S. R. (2015). A timeline demarcating two waves of clonal deletion and Foxp3 upregulation during thymocyte development. *Immunology and Cell Biology*.

Hu, Q., Nicol, S. A., Suen, A. Y., & Baldwin, T. A. (2012). Examination of thymic positive and negative selection by flow cytometry. *JoVE (Journal of Visualized Experiments)*, (68), e4269-e4269.

Hugo, P., Waanders, G.A., Scollay, R., Shortman, K., and Boyd, R.L. (1990). Ontogeny of a novel CD4+CD8-CD3- thymocyte subpopulation: a comparison with CD4-CD8+CD3- thymocytes. *International Immunology*, 2, 209-218.

Hutchinson, I. V., & Zola, H. (1978). Antigen-reactive cell opsonization: a mechanism of antibody-mediated immune suppression. *Cellular Immunology*, 36(1), 161-169.

Incardona, J. P., Lee, J. H., Robertson, C. P., Enga, K., Kapur, R. P., & Roelink, H. (2000). Receptor-mediated endocytosis of soluble and membrane-tethered Sonic hedgehog by Patched-1. *Proceedings of the National Academy of Sciences*, *97*(22), 12044-12049.

Ingham, P. W., & McMahon, A. P. (2001). Hedgehog signaling in animal development: paradigms and principles. *Genes & Development*, 15(23), 3059-3087.

Irving, B. A., Alt, F. W., & Killeen, N. (1998). Thymocyte development in the absence of pre-T cell receptor extracellular immunoglobulin domains. *Science*, 280(5365), 905-908.

Itano, A., Salmon, P., Kioussis, D., Tolaini, M., Corbella, P., & Robey, E. (1996). The cytoplasmic domain of CD4 promotes the development of CD4 lineage T cells. *Journal of Experimental Medicine*, *183*(3), 731-741.

Itano, A., & Robey, E. (2000). Highly efficient selection of CD4 and CD8 lineage thymocytes supports an instructive model of lineage commitment. *Immunity*, *12*(4), 383-389.

Itoi, M., Tsukamoto, N., & Amagai, T. (2007). Expression of Dll4 and CCL25 in Foxn1-negative epithelial cells in the post-natal thymus. *International Immunology*, 19(2), 127-132.

Itoi, M., Tsukamoto, N., Yoshida, H., & Amagai, T. (2007). Mesenchymal cells are required for functional development of thymic epithelial cells. *International Immunology*, *19*(8), 953-964.

Izzi, L., Lévesque, M., Morin, S., Laniel, D., Wilkes, B. C., Mille, F., ... & Charron, F. (2011). Boc and Gas1 each form distinct Shh receptor complexes with Ptch1 and are required for Shh-mediated cell proliferation. *Developmental Cell*, *20*(6), 788-801.

Jackson, B. C., Carpenter, C., Nebert, D. W., & Vasiliou, V. (2010). Update of human and mouse forkhead box (FOX) gene families. *Human Genomics*, 4(5), 345.

Janas, M. L., Varano, G., Gudmundsson, K., Noda, M., Nagasawa, T., & Turner, M. (2010). Thymic development beyond β-selection requires phosphatidylinositol 3-kinase activation by CXCR4. *The Journal of Experimental Medicine*, 207(1), 247-261.

Jenkinson, W. E., Rossi, S. W., Jenkinson, E. J., & Anderson, G. (2005). Development of functional thymic epithelial cells occurs independently of lymphostromal interactions. *Mechanisms of Development*, *122*(12), 1294-1299.

Jeong, J., & McMahon, A. P. (2005). Growth and pattern of the mammalian neural tube are governed by partially overlapping feedback activities of the hedgehog antagonists patched 1 and Hhip1. *Development*, *132*(1), 143-154.

Jerome, L. A., & Papaioannou, V. E. (2001). DiGeorge syndrome phenotype in mice mutant for the T-box gene, Tbx1. *Nature Genetics*, 27(3), 286-291.

Kagi, D., Vignaux, F., Ledermann, B., Burki, K., Depraetere, V., Nagata, S., … & Golstein, P. (1987). Fas and perforin pathways as major mechanisms of T cell-mediated cytoxicity. *Science*, 235, 458.

Karp, S. J., Schipani, E., St-Jacques, B., Hunzelman, J., Kronenberg, H., & McMahon, A. P. (2000). Indian hedgehog coordinates endochondral bone growth and morphogenesis via parathyroid hormone related-protein-dependent and-independent pathways. Development, 127(3), 543-548.

Kasper, M., Schnidar, H., Neill, G. W., Hanneder, M., Klingler, S., Blaas, L., ... & Aberger, F. (2006). Selective modulation of Hedgehog/GLI target gene expression by epidermal growth factor signaling in human keratinocytes. *Molecular and Cellular Biology*, *26*(16), 6283-6298.

Kawahira, H., Ma, N. H., Tzanakakis, E. S., McMahon, A. P., Chuang, P. T., & Hebrok, M. (2003). Combined activities of hedgehog signaling inhibitors regulate pancreas development. *Development*, 130(20), 4871-4879.

Kawakami, T., Kawcak, T. N., Li, Y. J., Zhang, W., Hu, Y., & Chuang, P. T. (2002). Mouse dispatched mutants fail to distribute hedgehog proteins and are defective in hedgehog signaling. *Development*, *129*(24), 5753-5765.

Kiecker, C., Graham, A., & Logan, M. (2016). Differential Cellular Responses to Hedgehog Signalling in Vertebrates—What is the Role of Competence?. *Journal of Developmental Biology*, *4*(4), 36.

Kim, C. H., Pelus, L. M., White, J. R., & Broxmeyer, H. E. (1998). Differential chemotactic behavior of developing T cells in response to thymic chemokines. *Blood*, *91*(12), 4434-4443.

Kim, D., Langmead, B., & Salzberg, S. L. (2015). HISAT: a fast spliced aligner with low memory requirements. *Nature Methods*, *12*(4), 357-360.

Kim, I., Saunders, T. L., & Morrison, S. J. (2007). Sox17 dependence distinguishes the transcriptional regulation of fetal from adult hematopoietic stem cells. *Cell*, *130*(3), 470-483.

Kim, J., Kato, M., & Beachy, P. A. (2009). Gli2 trafficking links Hedgehog-dependent activation of Smoothened in the primary cilium to transcriptional activation in the nucleus. *Proceedings of the National Academy of Sciences*, *106*(51), 21666-21671.

Kishi, H., Borgulya, P., Scott, B., Karjalainen, K., Traunecker, A., Kaufman, J., & von Boehmer, H. (1991). Surface expression of the beta T cell receptor (TCR) chain in the absence of other TCR or CD3 proteins on immature T cells. *The EMBO Journal*, 10(1), 93.

Kishimoto, H., & Sprent, J. (1997). Negative selection in the thymus includes semimature T cells. *Journal of Experimental Medicine*, *185*(2), 263-272.

Koch, U., Fiorini, E., Benedito, R., Besseyrias, V., Schuster-Gossler, K., Pierres, M., ... & Radtke, F. (2008). Delta-like 4 is the essential, nonredundant ligand for Notch1 during thymic T cell lineage commitment. *The Journal of Experimental Medicine*, 205(11), 2515-2523.

Kondo, M., Weissman, I. L., & Akashi, K. (1997). Identification of clonogenic common lymphoid progenitors in mouse bone marrow. *Cell,* 91(5), 661-672.

Kopf, M., Le Gros, G., Bachmann, M., Lamers, M. C., Bluethmann, H., & Köhler, G. (1993). Disruption of the murine IL-4 gene blocks Th2 cytokine responses. *Nature*, *362*(6417), 245-248.

Kwan, J., & Killeen, N. (2004). CCR7 directs the migration of thymocytes into the thymic medulla. *The Journal of Immunology*, *172*(7), 3999-4007.

Kwong, L., Bijlsma, M. F., & Roelink, H. (2014). Shh-mediated degradation of Hhip allows cell autonomous and non-cell autonomous Shh signaling. *Nature Communications*, *5*, 4849.

Lai, K., Robertson, M. J., & Schaffer, D. V. (2004). The sonic hedgehog signaling system as a bistable genetic switch. *Biophysical Journal*, *86*(5), 2748-2757.

Lanzavecchia, A. (1984). Antigen-specific interaction between T and B cells. *Nature*, 314(6011), 537-539.

Lau, C. I., Outram, S. V., Saldaña, J. I., Furmanski, A. L., Dessens, J. T., & Crompton, T. (2012). Regulation of murine normal and stress-induced erythropoiesis by Desert Hedgehog. *Blood*, *119*(20), 4741-4751.

Le Gros, G., Ben-Sasson, S. Z., Seder, R., Finkelman, F. D., & Paul, W. E. (1990). Generation of interleukin 4 (IL-4)-producing cells in vivo and in vitro: IL-2 and IL-4 are required for in vitro generation of IL-4-producing cells. *Journal of Experimental Medicine*, 172(3), 921-929.

Lee, C. S., Buttitta, L., & Fan, C. M. (2001). Evidence that the WNT-inducible growth arrest-specific gene 1 encodes an antagonist of sonic hedgehog signaling in the somite. *Proceedings of the National Academy of Sciences*, *98*(20), 11347-11352.

Lee, D., Prowse, D. M., & Brissette, J. L. (1999). Association between mouse nude gene expression and the initiation of epithelial terminal differentiation. *Developmental Biology*, 208(2), 362-374.

Lee, J., Platt, K. A., Censullo, P., & i Altaba, A. R. (1997). Gli1 is a target of Sonic hedgehog that induces ventral neural tube development. *Development*, *124*(13), 2537-2552.

Li, S., Chen, Y., Shi, Q., Yue, T., Wang, B., & Jiang, J. (2012). Hedgehog-regulated ubiquitination controls smoothened trafficking and cell surface expression in Drosophila. *PLoS Biol*, *10*(1), e1001239.

Lim, Y., & Matsui, W. (2010). Hedgehog signaling in hematopoiesis. *Critical Reviews in Eukaryotic Gene Expression*, *20*(2).

Lin, J., Yang, L., Silva, H. M., Trzeciak, A., Choi, Y., Schwab, S. R., ... & Lafaille, J. J. (2016). Increased generation of Foxp3+ regulatory T cells by manipulating antigen presentation in the thymus. *Nature Communications*, 7.

Lind, E. F., Prockop, S. E., Porritt, H. E., & Petrie, H. T. (2001). Mapping precursor movement through the postnatal thymus reveals specific microenvironments supporting defined stages of early lymphoid development. *The Journal of Experimental Medicine*, 194(2), 127-134.

Lobach, D. F., & Haynes, B. F. (1987). Ontogeny of the human thymus during fetal development. *Journal of Clinical Immunology,* 7(2), 81-97.

Lowrey, J. A., Stewart, G. A., Lindey, S., Hoyne, G. F., Dallman, M. J., Howie, S. E., & Lamb, J. R. (2002). Sonic hedgehog promotes cell cycle progression in activated peripheral CD4+ T lymphocytes. *The Journal of Immunology*, *169*(4), 1869-1875.

Ma, D., Wang, L., Wang, S., Gao, Y., Wei, Y., & Liu, F. (2012). Foxn1 maintains thymic epithelial cells to support T-cell development via mcm2 in zebrafish. *Proceedings of the National Academy of Sciences*, 109(51), 21040-21045.

Makki, N., & Capecchi, M. R. (2011). Cardiovascular defects in a mouse model of HOXA1 syndrome. *Human Molecular Genetics*, *21*(1), 26-31.

Mallick, C. A., Dudley, E. C., Viney, J. L., Owen, M. J., & Hayday, A. C. (1993). Rearrangement and diversity of T cell receptor β chain genes in thymocytes: a critical role for the β chain in development. *Cell*, 73(3), 513-519.

Manley, N. R., & Capecchi, M. R. (1995). The role of Hoxa-3 in mouse thymus and thyroid development. *Development*, 121(7), 1989-2003.

Martí, E., Takada, R., Bumcrot, D. A., Sasaki, H., & McMahon, A. P. (1995). Distribution of Sonic hedgehog peptides in the developing chick and mouse embryo. *Development*, *121*, 2537-2537.

Marinov, G. K., Williams, B. A., McCue, K., Schroth, G. P., Gertz, J., Myers, R. M., & Wold, B. J. (2014). From single-cell to cell-pool transcriptomes: stochasticity in gene expression and RNA splicing. *Genome Research*, *24*(3), 496-510.

Matis, L. A., Glimcher, L. H., Paul, W. E., & Schwartz, R. H. (1983). Magnitude of response of histocompatibility-restricted T-cell clones is a function of the product of the concentrations of antigen and Ia molecules. *Proceedings of the National Academy of Sciences*, *80*(19), 6019-6023.

Maun, H. R., Wen, X., Lingel, A., de Sauvage, F. J., Lazarus, R. A., Scales, S. J., & Hymowitz, S. G. (2010). Hedgehog pathway antagonist 5E1 binds hedgehog at the pseudo-active site. *Journal of Biological Chemistry*, *285*(34), 26570-26580.

McDermott, A., Gustafsson, M., Elsam, T., Hui, C. C., Emerson, C. P., & Borycki, A. G. (2005). Gli2 and Gli3 have redundant and context-dependent function in skeletal muscle formation. *Development*, *132*(2), 345-357.

McCaughtry, T. M., Baldwin, T. A., Wilken, M. S., & Hogquist, K. A. (2008). Clonal deletion of thymocytes can occur in the cortex with no involvement of the medulla. *Journal of Experimental Medicine*, *205*(11), 2575-2584.

McKeithan, T. W. (1995). Kinetic proofreading in T-cell receptor signal transduction. *Proceedings of the National Academy of Sciences*, 92(11), 5042-5046.

Mecklenburg, L., Nakamura, M., Sundberg, J. P., & Paus, R. (2001). The Nude mouse skin phenotype: The role of Foxn1 in hair follicle development and cycling. *Experimental and Molecular Pathology*, 71(2), 171-178.

Medema, J. P., Toes, R. E., Scaffidi, C., Zheng, T. S., Flavell, R. A., Melief, C. J., ... & Krammer, P. H. (1997). Cleavage of FLICE (caspase-8) by granzyme B during cytotoxic T lymphocyte-induced apoptosis. *European Journal of Immunology*, 27(12), 3492-3498.

Méthot, N., & Basler, K. (1999). Hedgehog controls limb development by regulating the activities of distinct transcriptional activator and repressor forms of Cubitus interruptus. *Cell*, *96*(6), 819-831.

Mingueneau, M., Kreslavsky, T., Gray, D., Heng, T., Cruse, R., Ericson, J., ... & Von Boehmer, H. (2013). The transcriptional landscape of [alpha][beta] T cell differentiation. *Nature Immunology*, *14*(6), 619-632.

Moore-Scott, B. A., & Manley, N. R. (2005). Differential expression of Sonic hedgehog along the anterior–posterior axis regulates patterning of pharyngeal pouch endoderm and pharyngeal endoderm-derived organs. *Developmental Biology*, 278(2), 323-335.

Mori, K., Itoi, M., Tsukamoto, N., Kubo, H., & Amagai, T. (2007). The perivascular space as a path of hematopoietic progenitor cells and mature T cells between the blood circulation and the thymic parenchyma. *International Immunology*, 19(6), 745-753.

Motoyama, J., Takabatake, T., Takeshima, K., & Hui, C. C. (1998). Ptch2, a second mouse Patched gene is co-expressed with Sonic hedgehog. *Nature Genetics*, *18*(2), 104-106.

Müller-Eberhard, H. J., & Schreiber, R. D. (1980). Molecular Biology and Chemistry of the Alternative Pathway of Complement 1–3. *Advances in Immunology*, *29*, 1-53.

Mulroy, T., McMahon, J. A., Burakoff, S. J., McMahon, A. P., & Sen, J. (2002). Wnt-1 and Wnt-4 regulate thymic cellularity. *European Journal of Immunology*, 32(4), 967-971.

Nakagawa, T., Roth, W., Wong, P., Nelson, A., Farr, A., Deussing, J., ... & Rudensky, A. Y. (1998). Cathepsin L: critical role in Ii degradation and CD4 T cell selection in the thymus. *Science*, 280(5362), 450-453.

Nakano, Y., Guerrero, I., Hidalgo, A., Taylor, A., Whittle, J. R. S., & Ingham, P. W. (1989). A protein with several possible membrane-spanning domains encoded by the Drosophila segment polarity gene patched. *Nature*, *341*, 508-513.

Nehls, M., Pfeifer, D., Schorpp, M., Hedrich, H., & Boehm, T. (1994). New member of the winged-helix protein family disrupted in mouse and rat nude mutations. *Nature*, 372(6501), 103-107.

Noelle, R., Krammer, P. H., Ohara, J., Uhr, J. W., & Vitetta, E. S. (1984). Increased expression of Ia antigens on resting B cells: an additional role for B-cell growth factor. *Proceedings of the National Academy of Sciences*, 81(19), 6149-6153.

Nowell, C. S., Bredenkamp, N., Tetélin, S., Jin, X., Tischner, C., Vaidya, H., ... & Blackburn, C. C. (2011). Foxn1 regulates lineage progression in cortical and medullary thymic epithelial cells but is dispensable for medullary sublineage divergence. *PLoS Genetics*, 7(11), e1002348.

Oettinger, M. A., Schatz, D. G., Gorka, C., & Baltimore, D. (1990). RAG-1 and RAG-2, adjacent genes that synergistically activate V (D) J recombination. *Science*, *248*(4962), 1517.

Ohigashi, I., Zuklys, S., Sakata, M., Mayer, C. E., Zhanybekova, S., Murata, S., ... & Takahama, Y. (2013). Aire-expressing thymic medullary epithelial cells originate from β5t-expressing progenitor cells. *Proceedings of the National Academy of Sciences*, *110*(24), 9885-9890.

Ohigashi, I., Zuklys, S., Sakata, M., Mayer, C. E., Hamazaki, Y., Minato, N., ... & Takahama, Y. (2015). Adult thymic medullary epithelium is maintained and regenerated by lineage-restricted cells rather than bipotent progenitors. *Cell Reports*, *13*(7), 1432-1443.

Ohlmeyer, J. T., & Kalderon, D. (1998). Hedgehog stimulates maturation of Cubitus interruptus into a labile transcriptional activator. *Nature*, *396*(6713), 749-753.

Ohuchi, H., Hori, Y., Yamasaki, M., Harada, H., Sekine, K., Kato, S., & Itoh, N. (2000). FGF10 acts as a major ligand for FGF receptor 2 IIIb in mouse multi-organ

development. *Biochemical and Biophysical Research Communications*, *277*(3), 643-649.

O'Neill, K. E., Bredenkamp, N., Tischner, C., Vaidya, H. J., Stenhouse, F. H., Peddie, C. D., ... & Blackburn, C. C. (2016). Foxn1 is dynamically regulated in thymic epithelial cells during embryogenesis and at the onset of thymic involution. *PloS One*, *11*(3), e0151666.

Outram, S. V., Varas, A., Pepicelli, C. V., & Crompton, T. (2000). Hedgehog signaling regulates differentiation from double-negative to double-positive thymocyte. *Immunity*, *13*(2), 187-197.

Outram, S., Hager-Theodorides, A. L., & Crompton, T. (2007). Hedgehog signalling in T lymphocyte development. *In Shh and Gli Signalling and Development* (pp. 107-115). Springer New York.

Outram, S. V., Hager-Theodorides, A. L., Shah, D. K., Rowbotham, N. J., Drakopoulou, E., Ross, S. E., ... & Crompton, T. (2009). Indian hedgehog (Ihh) both promotes and restricts thymocyte differentiation. *Blood*, *113*(10), 2217-2228.

Owens, T., de St Groth, B. F., & Miller, J. F. (1987). Coaggregation of the T-cell receptor with CD4 and other T-cell surface molecules enhances T-cell activation. *Proceedings of the National Academy of Sciences*, 84(24), 9209-9213.

Pagán-Westphal, S. M., & Tabin, C. J. (1998). The transfer of left-right positional information during chick embryogenesis. *Cell*, *93*(1), 25-35.

Palamaro, L., Romano, R., Fusco, A., Giardino, G., Gallo, V., & Pignata, C. (2014). FOXN1 in organ development and human diseases. *International Reviews of Immunology*, 33(2), 83-93.

Pampliega, O., Orhon, I., Patel, B., Sridhar, S., Díaz-Carretero, A., Beau, I., ... & Cuervo, A. M. (2013). Functional interaction between autophagy and ciliogenesis. *Nature*, *502*(7470), 194-200.

Pan, Y., Bai, C. B., Joyner, A. L., & Wang, B. (2006). Sonic hedgehog signaling regulates Gli2 transcriptional activity by suppressing its processing and degradation. *Molecular and Cellular Biology*, *26*(9), 3365-3377.

Pantelouris, E. M., & Hair, J. (1970). Thymus dysgenesis in nude (nu nu) mice. *Journal of Embryology and Experimental Morphology*, 24(3), 615-623.

Pasqual, N., Gallagher, M., Aude-Garcia, C., Loiodice, M., Thuderoz, F., Demongeot, J., ... & Jouvin-Marche, E. (2002). Quantitative and Qualitative Changes in VJ α Rearrangements During Mouse Thymocytes Differentiation Implication For a Limited T Cell Receptor α Chain Repertoire. *The Journal of Experimental Medicine*, *196*(9), 1163-1174.

Patro, R., Duggal, G., Love, M. I., Irizarry, R. A., & Kingsford, C. (2017). Salmon provides fast and bias-aware quantification of transcript expression. *Nature Methods*.

Pearse, G. (2006). Normal structure, function and histology of the thymus. *Toxicologic Pathology*, 34(5), 504-514.

Perrimon, N., Pitsouli, C., & Shilo, B. Z. (2012). Signaling mechanisms controlling cell fate and embryonic patterning. *Cold Spring Harbor Perspectives in Biology*, *4*(8), a005975.

Peters, C., Wolf, A., Wagner, M., Kuhlmann, J., & Waldmann, H. (2004). The cholesterol membrane anchor of the Hedgehog protein confers stable membrane association to lipid-modified proteins. *Proceedings of the National Academy of Sciences*, 101(23), 8531-8536.

Peters, H., Neubüser, A., Kratochwil, K., & Balling, R. (1998). Pax9-deficient mice lack pharyngeal pouch derivatives and teeth and exhibit craniofacial and limb abnormalities. *Genes & Development*, 12(17), 2735-2747.

Peters, P. J., Borst, J., Oorschot, V., Fukuda, M., Krähenbühl, O., Tschopp, J., ... & Geuze, H. J. (1991). Cytotoxic T lymphocyte granules are secretory lysosomes, containing both perforin and granzymes. *Journal of Experimental Medicine*, *173*(5), 1099-1109.

Petersen, S. V., Thiel, S., & Jensenius, J. C. (2001). The mannan-binding lectin pathway of complement activation: biology and disease association. *Molecular immunology*, *38*(2), 133-149.

Picelli, S., Faridani, O. R., Björklund, Å. K., Winberg, G., Sagasser, S., & Sandberg, R. (2014). Full-length RNA-seq from single cells using Smart-seq2. *Nature Protocols*, *9*(1), 171-181.

Pissarra, L., Henrique, D., & Duarte, A. (2000). Expression of hes6, a new member of the Hairy/Enhancer-of-split family, in mouse development. *Mechanisms of Development*, *95*(1), 275-278.

Ploegh, H. L., Orr, H. T., & Strominger, J. L. (1981). Major histocompatibility antigens: the human (HLA-A,-B,-C) and murine (H-2K, H-2D) class I molecules. *Cell*, 24(2), 287-299.

Podack, E. R. (1984). Molecular composition of the tubular structure of the membrane attack complex of complement. *Journal of Biological Chemistry*, *259*(13), 8641-8647.

Prinz, I., Sansoni, A., Kissenpfennig, A., Ardouin, L., Malissen, M., & Malissen, B. (2006). Visualization of the earliest steps of γδ T cell development in the adult thymus. *Nature Immunology*, 7(9), 995-1003.

Prowse, D. M., Lee, D., Weiner, L., Jiang, N., Magro, C. M., Baden, H. P., & Brissette, J. L. (1999). Ectopic expression of the nude gene induces hyperproliferation and defects in differentiation: implications for the self-renewal of cutaneous epithelia. *Developmental Biology*, 212(1), 54-67.

Pui, J. C., Allman, D., Xu, L., DeRocco, S., Karnell, F. G., Bakkour, S., ... & Pear, W. S. (1999). Notch1 expression in early lymphopoiesis influences B versus T lineage determination. *Immunity*, 11(3), 299-308.

Ramalho-Santos, M., Melton, D. A., & McMahon, A. P. (2000). Hedgehog signals regulate multiple aspects of gastrointestinal development. *Development*, *127*(12), 2763-2772.

Ran, F. A., Hsu, P. D., Wright, J., Agarwala, V., Scott, D. A., & Zhang, F. (2013). Genome engineering using the CRISPR-Cas9 system. *Nature Protocols*, *8*(11), 2281-2308.

Reeh, K. A., Cardenas, K. T., Bain, V. E., Liu, Z., Laurent, M., Manley, N. R., & Richie, E. R. (2014). Ectopic TBX1 suppresses thymic epithelial cell differentiation and proliferation during thymus organogenesis. *Development*, *141*(15), 2950-2958.

Revest, J. M., Suniara, R. K., Kerr, K., Owen, J. J., & Dickson, C. (2001). Development of the thymus requires signaling through the fibroblast growth factor receptor R2-IIIb. *The Journal of Immunology*, 167(4), 1954-1961.

Ripen, A. M., Nitta, T., Murata, S., Tanaka, K., & Takahama, Y. (2011). Ontogeny of thymic cortical epithelial cells expressing the thymoproteasome subunit β5t. *European Journal of Immunology*, *41*(5), 1278-1287.

Rock, K. L., Gramm, C., Rothstein, L., Clark, K., Stein, R., Dick, L., ... & Goldberg, A. L. (1994). Inhibitors of the proteasome block the degradation of most cell proteins and the generation of peptides presented on MHC class I molecules. *Cell*, *78*(5), 761-771.

Rode, I., Martins, V. C., Küblbeck, G., Maltry, N., Tessmer, C., & Rodewald, H. R. (2015). Foxn1 protein expression in the developing, aging, and regenerating thymus. *The Journal of Immunology*, 195(12), 5678-5687.

Rodewald, H. R., Paul, S., Haller, C., Bluethmann, H., & Blum, C. (2001). Thymus medulla consisting of epithelial islets each derived from a single progenitor. *Nature*, *414*(6865), 763-768.

Rohatgi, R., Milenkovic, L., & Scott, M. P. (2007). Patched1 regulates hedgehog signaling at the primary cilium. *Science*, *317*(5836), 372-376.

Ross, J. O., Melichar, H. J., Au-Yeung, B. B., Herzmark, P., Weiss, A., & Robey, E. A. (2014). Distinct phases in the positive selection of CD8+ T cells distinguished by intrathymic migration and T-cell receptor signaling patterns. *Proceedings of the National Academy of Sciences*, *111*(25), E2550-E2558.

Rossbacher, J., & Shlomchik, M. J. (2003). The B cell receptor itself can activate complement to provide the complement receptor 1/2 ligand required to enhance B cell immune responses in vivo. *Journal of Experimental Medicine*, 198(4), 591-602.

Rossi, F. M., Corbel, S. Y., Merzaban, J. S., Carlow, D. A., Gossens, K., Duenas, J., ... & Ziltener, H. J. (2005). Recruitment of adult thymic progenitors is regulated by P-selectin and its ligand PSGL-1. *Nature Immunology*, 6(6), 626-634.

Rossi, S. W., Jenkinson, W. E., Anderson, G., & Jenkinson, E. J. (2006). Clonal analysis reveals a common progenitor for thymic cortical and medullary epithelium. *Nature*, *441*(7096), 988-991.

Rossi, S. W., Jeker, L. T., Ueno, T., Kuse, S., Keller, M. P., Zuklys, S., ... & Holländer, G. A. (2007). Keratinocyte growth factor (KGF) enhances postnatal T-cell development via enhancements in proliferation and function of thymic epithelial cells. *Blood*, *109*(9), 3803-3811.

Rossi, S. W., Kim, M. Y., Leibbrandt, A., Parnell, S. M., Jenkinson, W. E., Glanville, S. H., ... & Anderson, G. (2007). RANK signals from CD4+ 3– inducer cells regulate development of Aire-expressing epithelial cells in the thymic medulla. *The Journal of Experimental Medicine*, 204(6), 1267-1272.

Rowbotham, N. J., Hager-Theodorides, A. L., Furmanski, A. L., & Crompton, T. (2007). A novel role for Hedgehog in T-cell receptor signaling: implications for development and immunity. *Cell Cycle*, *6*(17), 2138-2142.

Rowbotham, N. J., Hager-Theodorides, A. L., Cebecauer, M., Shah, D. K., Drakopoulou, E., Dyson, J., ... & Crompton, T. (2007). Activation of the Hedgehog signaling pathway in T-lineage cells inhibits TCR repertoire selection in the thymus and peripheral T-cell activation. *Blood*, 109(9), 3757-3766.

Rowbotham, N. J., Furmanski, A. L., Hager-Theodorides, A. L., Ross, S. E., Drakopoulou, E., Koufaris, C., ... & Crompton, T. (2008). Repression of hedgehog signal transduction in T-lineage cells increases TCR-induced activation and proliferation. *Cell Cycle*, *7*(7), 904-908.

Rowbotham, N. J., Hager-Theodorides, A. L., Furmanski, A. L., Ross, S. E., Outram, S. V., Dessens, J. T., & Crompton, T. (2009). Sonic hedgehog negatively regulates pre-TCR–induced differentiation by a Gli2-dependent mechanism. *Blood*, *113*(21), 5144-5156.

Ruan, L., Zhang, Z., Mu, L., Burnley, P., Wang, L., Coder, B., ... & Su, D. M. (2014). Biological significance of FoxN1 gain-of-function mutations during T and B lymphopoiesis in juvenile mice. *Cell Death & Disease*, 5(10), e1457.

Rus, H., Cudrici, C., & Niculescu, F. (2005). The role of the complement system in innate immunity. *Immunologic Research*, *33*(2), 103-112.

Sacedón, R., Varas, A., Hernández-López, C., Gutiérrez-deFrías, C., Crompton, T., Zapata, A. G., & Vicente, A. (2003). Expression of hedgehog proteins in the human thymus. *Journal of Histochemistry & Cytochemistry*, *51*(11), 1557-1566.

Saldaña, J. I., Solanki, A., Lau, C. I., Sahni, H., Ross, S., Furmanski, A. L., ... & Crompton, T. (2016). Sonic Hedgehog regulates thymic epithelial cell differentiation. *Journal of Autoimmunity*, *68*, 86-97.

Santambrogio, L., Sato, A. K., Carven, G. J., Belyanskaya, S. L., Strominger, J. L., & Stern, L. J. (1999). Extracellular antigen processing and presentation by immature dendritic cells. *Proceedings of the National Academy of Sciences*, *96*(26), 15056-15061.

Sant'Angelo, D. B., & Janeway, C. A. (2002). Negative selection of thymocytes expressing the D10 TCR. *Proceedings of the National Academy of Sciences*, 99(10), 6931-6936.

Sansom, S. N., Shikama-Dorn, N., Zhanybekova, S., Nusspaumer, G., Macaulay, I. C., Deadman, M. E., ... & Holländer, G. A. (2014). Population and single-cell genomics reveal the Aire dependency, relief from Polycomb silencing, and distribution of self-antigen expression in thymic epithelia. *Genome Research*, 24(12), 1918-1931.

Sasaki, H., Nishizaki, Y., Hui, C. C., Nakafuku, M., & Kondoh, H. (1999). Regulation of Gli2 and Gli3 activities by an amino-terminal repression domain: implication of Gli2 and Gli3 as primary mediators of Shh signaling. *Development*, *126*(17), 3915-3924.

Scherz, P. J., McGlinn, E., Nissim, S., & Tabin, C. J. (2007). Extended exposure to Sonic hedgehog is required for patterning the posterior digits of the vertebrate limb. *Developmental Biology*, *308*(2), 343-354.

Schlake, T., Schorpp, M., Nehls, M., & Boehm, T. (1997). The nude gene encodes a sequence-specific DNA binding protein with homologs in organisms that lack an anticipatory immune system. *Proceedings of the National Academy of Sciences*, *94*(8), 3842-3847.

Seder, R. A., Germain, R. N., Linsley, P. S., & Paul, W. E. (1994). CD28-mediated costimulation of interleukin 2 (IL-2) production plays a critical role in T cell priming

for IL-4 and interferon gamma production. *Journal of Experimental Medicine*, *179*(1), 299-304.

Senoo, M., Pinto, F., Crum, C. P., & McKeon, F. (2007). p63 Is essential for the proliferative potential of stem cells in stratified epithelia. *Cell*, 129(3), 523-536.

Shah, D. K., Hager-Theodorides, A. L., Outram, S. V., Ross, S. E., Varas, A., & Crompton, T. (2004). Reduced thymocyte development in sonic hedgehog knockout embryos. *The Journal of Immunology*, 172(4), 2296-2306.

Shakib, S., Desanti, G. E., Jenkinson, W. E., Parnell, S. M., Jenkinson, E. J., & Anderson, G. (2009). Checkpoints in the development of thymic cortical epithelial cells. *The Journal of Immunology*, *182*(1), 130-137.

Shin, M. L., Rus, H. G., & Niculescu, F. I. (1996). Membrane attack by complement: assembly and biology of terminal complement complexes. *Biomembranes: A Multi-Volume Treatise*, *4*, 123-149.

Shores, E. W., Van Ewijk, W., & Singer, A. (1991). Disorganization and restoration of thymic medullary epithelial cells in T cell receptor-negative scid mice: evidence that receptor-bearing lymphocytes influence maturation of the thymic microenvironment. *European Journal of Immunology*, *21*(7), 1657-1661.

Singer, A., Adoro, S., & Park, J. H. (2008). Lineage fate and intense debate: myths, models and mechanisms of CD4-versus CD8-lineage choice. *Nature Reviews Immunology*, *8*(10), 788-801.

Smith, K. M., Pottage, L., Thomas, E. R., Leishman, A. J., Doig, T. N., Xu, D., ... & Garside, P. (2000). Th1 and Th2 CD4+ T cells provide help for B cell clonal expansion and antibody synthesis in a similar manner in vivo. *The Journal of Immunology*, 165(6), 3136-3144.

Smits, P., Li, P., Mandel, J., Zhang, Z., Deng, J. M., Behringer, R. R., ... & Lefebvre, V. (2001). The transcription factors L-Sox5 and Sox6 are essential for cartilage formation. *Developmental Cell*, *1*(2), 277-290.

Soza-Ried, C., Bleul, C. C., Schorpp, M., & Boehm, T. (2008). Maintenance of thymic epithelial phenotype requires extrinsic signals in mouse and zebrafish. *The Journal of Immunology*, 181(8), 5272-5277.

Stewart, G. A., Lowrey, J. A., Wakelin, S. J., Fitch, P. M., Lindey, S., Dallman, M. J., ... & Howie, S. E. (2002). Sonic hedgehog signaling modulates activation of and cytokine production by human peripheral CD4+ T cells. *The Journal of Immunology*, *169*(10), 5451-5457.

Stritesky, G. L., Xing, Y., Erickson, J. R., Kalekar, L. A., Wang, X., Mueller, D. L., ... & Hogquist, K. A. (2013). Murine thymic selection quantified using a unique method to capture deleted T cells. *Proceedings of the National Academy of Sciences*, *110*(12), 4679-4684.

Su, D. M., Ellis, S., Napier, A., Lee, K., & Manley, N. R. (2001). Hoxa3 and Pax1 Regulate Epithelial Cell Death and Proliferation during Thymus and Parathyroid Organogenesis. *Developmental Biology*, 236(2), 316-329.

Sun, L., Guo, J., Brown, R., Amagai, T., Zhao, Y., & Su, D. M. (2010). Declining expression of a single epithelial cell□autonomous gene accelerates age-related thymic involution. *Aging Cell*, 9(3), 347-357.

Takahama, Y. (2000). Differentiation of mouse thymocytes in fetal thymus organ culture. *T Cell Protocols: Development and Activation*, 37-46.

Takahama, Y. (2006). Journey through the thymus: stromal guides for T-cell development and selection. *Nature Reviews Immunology*, 6, 127-135.

Tarakhovsky, A., Kanner, S. B., Hombach, J., & Ledbetter, J. A. (1995). A role for CD5 in TCR-mediated signal transduction and thymocyte selection. *Science*, *269*(5223), 535.

Tenzen, T., Allen, B. L., Cole, F., Kang, J. S., Krauss, R. S., & McMahon, A. P. (2006). The cell surface membrane proteins Cdo and Boc are components and targets of the Hedgehog signaling pathway and feedback network in mice. *Developmental Cell*, *10*(5), 647-656.

Trapnell, C., Williams, B. A., Pertea, G., Mortazavi, A., Kwan, G., Van Baren, M. J., ... & Pachter, L. (2010). Transcript assembly and quantification by RNA-Seq reveals unannotated transcripts and isoform switching during cell differentiation. *Nature Biotechnology*, *28*(5), 511-515.

Trinchieri, G., Pflanz, S., & Kastelein, R. A. (2003). The IL-12 family of heterodimeric cytokines: new players in the regulation of T cell responses. *Immunity*, 19(5), 641-644.

Tsukamoto, N., Itoi, M., Nishikawa, M., & Amagai, T. (2005). Lack of Delta like 1 and 4 expressions in nude thymus anlages. *Cellular Immunology*, 234(2), 77-80.

Tukachinsky, H., Kuzmickas, R. P., Jao, C. Y., Liu, J., & Salic, A. (2012). Dispatched and scube mediate the efficient secretion of the cholesterol-modified hedgehog ligand. *Cell Reports*, *2*(2), 308-320.

Ueno, T., Saito, F., Gray, D. H., Kuse, S., Hieshima, K., Nakano, H., ... & Takahama, Y. (2004). CCR7 signals are essential for cortex–medulla migration of developing thymocytes. *The Journal of Experimental Medicine*, 200(4), 493-505.

Uhmann, A., Dittmann, K., Nitzki, F., Dressel, R., Koleva, M., Frommhold, A., ... & Heller, T. (2007). The Hedgehog receptor Patched controls lymphoid lineage commitment. *Blood*, *110*(6), 1814-1823.

Ulyanchenko, S., O'Neill, K. E., Medley, T., Farley, A. M., Vaidya, H. J., Cook, A. M., ... & Blackburn, C. C. (2016). Identification of a bipotent epithelial progenitor population in the adult thymus. *Cell Reports*, *14*(12), 2819-2832.

Valitutti, S., Muller, S., Cella, M., Padovan, E., & Lanzavecchia, A. (1995). Serial triggering of many T-cell receptors by a few peptide-MHC complexes. *Nature*, *375*(6527), 148.

van Vliet, E., Jenkinson, E. J., Ton, R. K., Owen, J. J., & van Ewrjk, W. (1985). Stromal cell types in the developing thymus of the normal and nude mouse embryo. *European Journal of Immunology*, *15*(7), 675-681.

Varas, A., Hernández-López, C., Valencia, J., Mattavelli, S., Martínez, V. G., Hidalgo, L., ... & Vicente, A. (2008). Survival and function of human thymic dendritic cells are dependent on autocrine Hedgehog signaling. *Journal of Leukocyte Biology*, *83*(6), 1476-1483.

Varjosalo, M., & Taipale, J. (2008). Hedgehog: functions and mechanisms. *Genes & Development*, *22*(18), 2454-2472.

Vestergaard, C., Deleuran, M., Gesser, B., & Larsen, C. G. (2004). Thymus-and activation-regulated chemokine (TARC/CCL17) induces a Th2-dominated inflammatory reaction on intradermal injection in mice. *Experimental Dermatology*, *13*(4), 265-271.

Vicari, A. P., Figueroa, D. J., Hedrick, J. A., Foster, J. S., Singh, K. P., Menon, S., ... & Zlotnik, A. (1997). TECK: a novel CC chemokine specifically expressed by thymic dendritic cells and potentially involved in T cell development. *Immunity*, 7(2), 291-301.

von Boehmer, H., & Fehling, H. J. (1997). Structure and function of the pre-T cell receptor. *Annual Review of Immunology*, 15(1), 433-452.

von Boehmer, H., Aifantis, I., Feinberg, J., Lechner, O., Saint-Ruf, C., Walter, U., Buer, J., and Azogui, O. (1999). Pleiotropic changes controlled by the pre-T-cell receptor. *Current Opinion in Immunology*, 11, 135-142.

Vortkamp, A., Lee, K., Lanske, B., & Segre, G. V. (1996). Regulation of rate of cartilage differentiation by Indian hedgehog and PTH-related protein. *Science*, *273*(5275), 613.

Wallin, J., Eibel, H., Neubüser, A., Wilting, J., Koseki, H., & Balling, R. (1996). Pax1 is expressed during development of the thymus epithelium and is required for normal T-cell maturation. *Development*, 122(1), 23-30.

Wang, C., Rüther, U., & Wang, B. (2007). The Shh-independent activator function of the full-length Gli3 protein and its role in vertebrate limb digit patterning. *Developmental Biology*, *305*(2), 460-469.

Wang, H., Pierce, L. J., & Spangrude, G. J. (2006). Distinct roles of IL-7 and stem cell factor in the OP9-DL1 T-cell differentiation culture system. *Experimental Hematology*, 34(12), 1730-1740.

Watkins, D. N., Berman, D. M., Burkholder, S. G., & Wang, B. (2003). Hedgehog signalling within airway epithelial progenitors and in small-cell lung cancer. *Nature*, *422*(6929), 313.

Weed, M., Mundlos, S., & Olsen, B. R. (1997). The role of sonic hedgehog in vertebrate development. *Matrix Biology*, 16(2), 53-58.

Wiest, D. L., Yuan, L., Jefferson, J., Benveniste, P., Tsokos, M., Klausner, R. D., ... & Singer, A. (1993). Regulation of T cell receptor expression in immature CD4+ CD8+ thymocytes by p56lck tyrosine kinase: basis for differential signaling by CD4 and CD8 in immature thymocytes expressing both coreceptor molecules. *Journal of Experimental Medicine*, *178*(5), 1701-1712.

Whaley, K., & Schwaeble, W. (1997). Complement and complement deficiencies. In *Seminars in Liver Disease* (Vol. 17, No. 04, pp. 297-310). © 1997 by Thieme Medical Publishers, Inc..

Wheatley, D. N. (1995). Primary cilia in normal and pathological tissues. *Pathobiology*, *63*(4), 222-238.

Xing, Y., Wang, X., Jameson, S. C., & Hogquist, K. A. (2016). Late stages of T cell maturation in the thymus involve NF-[kappa] B and tonic type I interferon signaling. *Nature Immunology*, *17*(5), 565-573.

Yamasaki, S., Ishikawa, E., Sakuma, M., Ogata, K., Sakata-Sogawa, K., Hiroshima, M., Wiest, D.L., Tokunaga, M., and Saito, T. (2006). Mechanistic basis of pre-T cell receptor-mediated autonomous signaling critical for thymocyte development. *Nature Immunology*, 7, 67-75.

Yamashita, I., Nagata, T., Tada, T., & Nakayama, T. (1993). CD69 cell surface expression identifies developing thymocytes which audition for T cell antigen receptor-mediated positive selection. *International immunology*, *5*(9), 1139-1150.

Yang, S. J., Ahn, S., Park, C. S., Holmes, K. L., Westrup, J., Chang, C. H., & Kim, M. G. (2006). The quantitative assessment of MHC II on thymic epithelium: implications in cortical thymocyte development. *International Immunology*, *18*(5), 729-739.

Yang, Y., Drossopoulou, G., Chuang, P. T., Duprez, D., Marti, E., Bumcrot, D., ... & Tickle, C. (1997). Relationship between dose, distance and time in Sonic Hedgehog-mediated regulation of anteroposterior polarity in the chick limb. *Development*, *124*(21), 4393-4404.

Yao, H. H. C., Whoriskey, W., & Capel, B. (2002). Desert Hedgehog/Patched 1 signaling specifies fetal Leydig cell fate in testis organogenesis. *Genes & Development*, *16*(11), 1433-1440.

Yin, Y., White, A. C., Huh, S. H., Hilton, M. J., Kanazawa, H., Long, F., & Ornitz, D. M. (2008). An FGF–WNT gene regulatory network controls lung mesenchyme development. *Developmental Biology*, *319*(2), 426-436.

Zamisch, M., Moore-Scott, B., Su, D. M., Lucas, P. J., Manley, N., & Richie, E. R. (2005). Ontogeny and regulation of IL-7-expressing thymic epithelial cells. *The Journal of Immunology*, 174(1), 60-67.

Zhang, Q., Zhang, L., Wang, B., Ou, C. Y., Chien, C. T., & Jiang, J. (2006). A hedgehog-induced BTB protein modulates hedgehog signaling by degrading Ci/Gli transcription factor. *Developmental Cell*, *10*(6), 719-729.

Zhang, X. M., Ramalho-Santos, M., & McMahon, A. P. (2001). Smoothened mutants reveal redundant roles for Shh and Ihh signaling including regulation of L/R asymmetry by the mouse node. *Cell*, *105*(6), 781-792.

Zook, E. C., Krishack, P. A., Zhang, S., Zeleznik-Le, N. J., Firulli, A. B., Witte, P. L., & Le, P. T. (2011). Overexpression of Foxn1 attenuates age-associated thymic involution and prevents the expansion of peripheral CD4 memory T cells. *Blood*, 118(22), 5723-5731.

Zou, D., Silvius, D., Davenport, J., Grifone, R., Maire, P., & Xu, P. X. (2006). Patterning of the third pharyngeal pouch into thymus/parathyroid by Six and Eya1. *Developmental Biology*, 293(2), 499-512.

Žuklys, S., Gill, J., Keller, M. P., Hauri-Hohl, M., Zhanybekova, S., Balciunaite, G., ... & Amagai, T. (2009). Stabilized β-catenin in thymic epithelial cells blocks thymus development and function. *The Journal of Immunology*, 182(5), 2997-3007.

Žuklys, S., Handel, A., Zhanybekova, S., Govani, F., Keller, M., Maio, S., ... & Barthlott, T. (2016). Foxn1 regulates key target genes essential for T cell development in postnatal thymic epithelial cells. *Nature Immunology*, 17(10), 1206-1215.

Supplementary

Table S1: Primer sequences

Name/Gene	Strand	Sequence	Product Size (bp)	Purpose
Actn3	F	CCTCAGTTCGCAGGACATC	114	qPCR
	R	CGGAGCCTCTCGTTCACCT		
Aire	F	TGTGCCACGACGGAGGTGAG	144	qPCR
	R	GGTTCTGTTGGACTCTGCCCTG		
Akap12	F	CGAAGACTCCGGTGCAGAG	169	qPCR
	R	GTCGTCCTCATTGATCTCTCC		
Arhgef101	F	CTGCCTATCCTCGGACCAG	97	qPCR
	R	CTCAGCAGTGTTCGAATCGG		
Boc	F	CTGATGCAGTCAATGAGACCAC	175	qPCR
	R	TGGCTGATGGAGTGCCAGT		
Ccl25	F	GCGATGAGAATCTTGACAGCTA	167	qPCR
	R	GGCATCATCACCATCCTG		
CD45 (KpnI)	F	TAGTATGGAGGAGAGCTTTATTGAG	301	Genotyping
	R	TCCACTTGCACCATCAGACACC		
CD45 (XhoI)	F	TGTGATAATCCTTTTTGCAGTCTTCTT	489	Genotyping
	R	GTTTTAGTTCCTCACATTTTACATTCCTTA		
Cdon	F	GTGTGTGGAGTTTGAGCATCC	179	qPCR
	R	CCTGAGGATAAGAGGCTACCAC		
Cecr6	F	TGTCTGGACCTGCTGGACA	114	qPCR
	R	GGCAAGAGTGAGGAAGTAGACG		
Cstb	F	GCCGACCAGGTGAAGTCC	101	qPCR
	R	AGGTTGGTGCCAGCCACTAT		
Dhh	F	CGACTGGGTCTACTACGAGTCC	160	qPCR
	R	CCAGTCACCACGATGTAGTTCC		
Dll4	F	CAGTGACAAGAGCTTAGGAGAGAAG	150	qPCR
	R	GTGGCAATCACACACTCGTTC		
Dtx4	F	CATCCGGACTGCAAGACC	130	qPCR
	R	CGCTGTCTGGAAGGTAACAATG		
Ednrb	F	CCTAAGGGTCTGCATGCTTAATC	149	qPCR

	R	GCATTTCGCAGGTCATCAG		
Epcam	F	CGCTGTCATTGTGGTGGTGT	128	qPCR
	R	GCTCTCTGTGGATCTCACCCA		
Fabp5	F	GACGACTGTGTTCTCTTGTAACC	118	qPCR
	R	CCATTGCTGGTGCTGGAC		
Foxn1	F	TCTACAATTTCATGACGGAGCACT	109	qPCR
	R	TCCACCTTCTCAAAGCACTTGTT		
Gapdh	F	GGTGAAGGTCGGTGTGAACG	123	qPCR
	R	ACCATGTAGTTGAGGTCAATGAAGG		
Gas1	F	CCTGGCCTACTGCGGCAA	114	qPCR
	R	CACACGCAGTCGTTGAGCA		
Gcat	F	GCCCTACCTCTTCTCCAACA	151	qPCR
	R	AGTAAAACCAGCAGCTTCCAT		
Gli1	F	GGAGAACCTTAGGCTGGATCAG	171	qPCR
	R	ACTGTGTAAGCAGAGCTCATGC		
Gli2	F	CCCGCTTGGACTGACACA	179	qPCR
	R	CGTGGATGTGTTCATTGTTG		
Gli3	F	GCCAACTCAGGGAGCATTTG	139	qPCR
	R	GCATGAAGACTGACCACCAG		
GPA	F	CACTTTGTGTTGAGGAATGCG		Screening
GPB	R	GACCCTTGTGATGTTGTAGTCCAG		Screening Genotyping
GPX	F	GAAGATGCCAAGCGCTGGTAT		Screening
GPY	R	CTTGGACCATTTAGTCACTTGTCAC		Screening
Hes6	F	CCTGGTGGAGAAGAAGCGA	123	qPCR
	R	CTCACGGTCAGCTCCAGAAC		
Hhip$^{tm1Amc/J}$ (WT Allele)	F	ATCCTCCCGCGTCCTGCCCTTG	150	Genotyping
	R	TCAGGCACCGTCTCCTTCTCGC		
Hhip$^{tm1Amc/J}$ (Mutant Allele)	F	CCGGATTGATGGTAGTGGTC	1000	Genotyping
	R	TGGATGTGGAATGTGTGCGAG		
Hhip	F	ATTCAAGCCATTCAGTAACGG	149	qPCR
	R	CTTGCCATTGCTTGGTCAC		
Human U6 Promoter	F	GAGGGCCTATTTCCCATGATTCC		Sequencing
iCre (Foxn1)	F	TCTGATGAAGTCAGGAAGAACC	500	Genotyping
	R	GAGATGTCCTTCACTCTGATTC		
Ihh	F	CCTCAGACCGTGACCGAA	148	qPCR
	R	AAGCAGCCACCTGTCTTGG		
Lox4	F	CCTCTGATCCAGATAACTTCG		Screening

				Genotyping
Lox4	R	AGTAACAATTGATGCTATAACTTCG		Screening
Lox2	F	TTATTCTGGGCCGGATAACTT		Screening Genotyping
Klhdc7a	F	GCGGGAGCTGATTCTCCA	181	qPCR
	R	GAATAGGGTACAGAGTGCACAACC		
Mreg	F	GTTGTGGACCGGCTCATTG	140	qPCR
	R	CAGGGGCTTGGAAATGGA		
Ndrg3	F	CTGCTGTGGAGGCTGTGG	129	qPCR
	R	ACTTGAAGGCCTCGGTGAG		
Nefm	F	GTCATTTGCGAGAATACCAGGA	167	qPCR
	R	GGATATTGTGACTGAGGGCTGT		
Npnt	F	GGATGAGGAAGTAAAGGACGA	197	qPCR
	R	CGAGACGTAACACCAAGCGA		
Pkhd1l1	F	GCCCTTGTGTCTTCACTCTCA	190	qPCR
	R	TTCCACTAAGGCCACCAACT		
Plekhb1	F	AACGCACATGAAGCCACA	165	qPCR
	R	AAGTGAACCAAGAGCAGCAC		
Psmb11	F	AACAAACAAACTCCCAAACC	202	qPCR
	R	CTCTCCTCATTTGCTTCTTCAG		
Ptch1	F	GACGGTGCTGTGTCCACTC	198	qPCR
	R	CAGTCGGTTTAGGCCATTG		
Ptch2	F	GGCATTGGTGTTGAATTCACAG	122	qPCR
	R	ACAGCTCCATCAGTCACAGG		
Ptprn2	F	GGCTGTGCTGACCTATGACC	196	qPCR
	R	AATGACTGCACAGCCGCTT		
PX330	R	CACCTCGACCATGGTAATAGCG		Sequencing
Rag1	F	TGCAGACATTCTAGCACTCTGG	174	qPCR
	R	TTCAAAGGATCTCACCCTAAACAG		
S1	F	AGAGGACAGGACTTCAGCAT		Screening Genotyping
S2	R	CCAGCATCAACAGACATTTC		Screening
S3	F	GACATTTATAGACTGTGGGATGC		Screening
S4	R	CACACTTTGGACACACTTGG		Screening Genotyping
Shh	F	CGACTGGGTCTACTATGAATCCA	159	qPCR
	R	CGGTCTCCGGGACGTAAG		
Sipall2	F	AACGACATTCTGTTTAGCACGAC	145	qPCR
	R	CAGGATCTGCACACTTGGAC		

		T		
Slc46a2	F	TTGCGCTTATTCCGATCAC	161	qPCR
	R	CTTGTCCAGCGTAAGCTGATAG		
Slco2b1	F	CACACCTTCCTTCATGCTCAT	152	qPCR
	R	CCCAGTGAACACAGGTGGTAT		
Smo	F	TCTGCCTGGGCTCAGCAT	163	qPCR
	R	CCAAACGCTTCTCTAACTCTGG		
Snap91	F	CGGAAGTGACCTTGACTCGT	124	qPCR
	R	GTTGGCTCCACCAGTCAGC		
Trpm2	F	AAGGATGGTCAGCAGGATGT	160	qPCR
	R	CATCGGTGAAGATCTCACTGC		
Tspan18	F	CTGACGCTGGACACTGAGG	154	qPCR
	R	CGAAGGTGTTGAGGATCACTG		
Tusc5	F	CATTGCCTCTTGCTTCTGC	137	qPCR
	R	TGCTGAGTAGCCGTGCCA		
WT (Hhip)	F	CTGACCCAGAGCATATATTGAATCG		Genotyping

Table S2: List of candidate Foxn1 target genes

Gene	Gene Expression Profile in 1 Week Old WT cTECs (fpkm)
Actn3	52
Akap12	53
Arhgef10l	37
Cecr6	-
Cstb	1688
Cth	29
Dtx4	20
Ednrb	19
Fabp5	646
Gcat	17
Hes6	156
Hhip	11
Klhdc7a	15
Mreg	190
Ndrg3	68
Nefm	22
Npnt	48
Pithd1	178
Pkhd1l1	24
Plekhb1	34
Ptprn2	5
Sipa1l2	24
Slco2b1	15
Slc46a2	191
Snap91	16
Tspan18	4
Trpm2	25
Tusc5	8

Data demonstrating the identification of these target genes and gene expression profiles can be found in Žuklys, S. *et al.*, 2016 and Sansom, S. *et al.*, 2014.

Figure S1: Basic T cell gating strategy

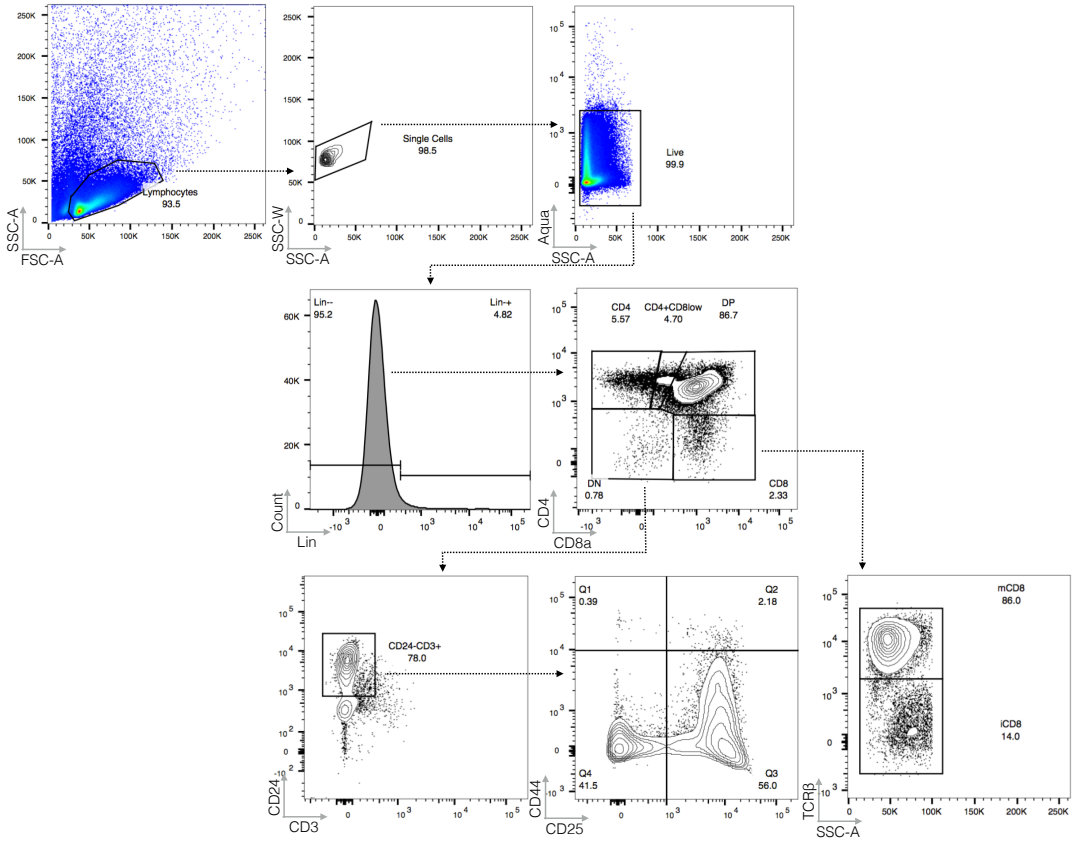

Figure S1: Basic gating strategy for T cells
Total cells are first gated by size for lymphocytes, then for single cells. Live cells are gated based on either Aqua live/dead negativity. Lineage-negative cells are then selected, where the Lineage-positive "dump" channel includes markers for non-T cells such as B220 (B cells), NK1.1 (NK cells), CD11b and CD11c (dendritic cells), Ter119 (erythrocytes), GR-1 (myeloid cells) and so on. T cells are then distinguished by CD4 and CD8a expression. DN cells are further gated as CD24+CD3-, and differentiated into stages by CD44 and CD25. CD8 cells are divided into immature (iCD8) and mature (mCD8) populations by TCRβ expression. The representative example shown above is from a 6 week old WT C57BL/6 mouse.

Figure S2: Basic TEC gating strategy

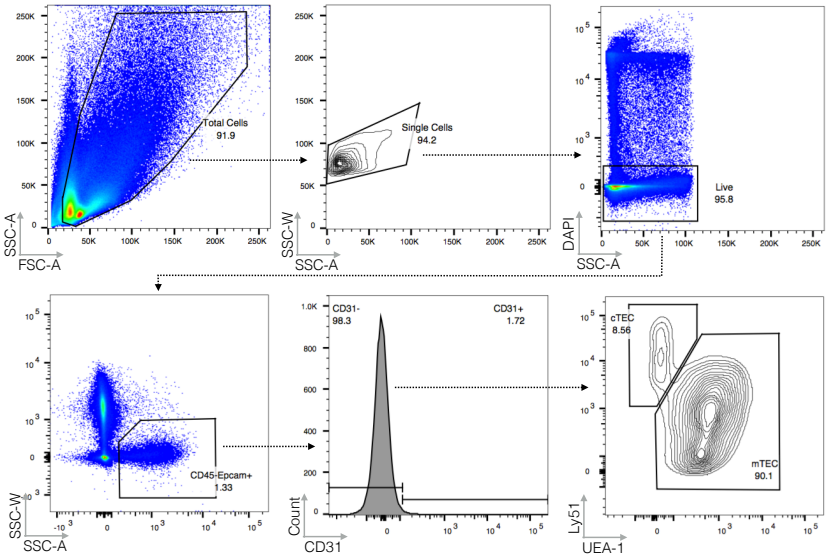

Figure S1: Basic gating strategy for TECs
Total cells are first gated, followed by single cells. Live cells are gated based on DAPI negativity. CD45-Epcam+ cells are selected, and gated on CD31 negative cells. TECs are then differentiated as cTECs and mTECs by Ly51 and UEA-1 expression respectively. The representative example shown above is from a 6 week old WT C57BL/6 mouse.